University of Stavanger

Faculty of Science and Technology

MASTER'S THESIS

Study program/Specialization: Petroleum Geosciences Engineering	Semester 4, 2015 Open
Writer: SARASI DAS	_____ (Writer's signature)

Faculty supervisor:
SYLVIA NORDFJORD
External supervisor(s): -

Title of thesis:
Seismic Stratigraphy and Geomorphology of the Chalk Group of the Central Graben, North Sea

Credits (ECTS): 30

Keywords: Chalk Seismic Stratigraphy Geomorphology Central Graben	Pages: +enclosure: 1CD Stavanger, 29 June, 2015

Seismic Stratigraphy and Geomorphology of the Chalk Group of the

Central Graben, North Sea

by

Sarasi Das

Thesis

Presented to the Faculty of Science and Technology

The University of Stavanger

The University of Stavanger

June 2015

Acknowledgements

Abstract

3D Seismic Stratigraphy and Geomorphology of the Chalk Group of the Central Graben, North Sea

Sarasi Das, MS

The University of Stavanger, 2015

Supervisor: Sylvia Nordfjord

The Ekofisk Field in the Southern part of the North Sea has been producing oil since its discovery in 1969 from naturally fractured chalk of the Late Cretaceous to Early Paleocene ages. This Chalk Group of the Norwegian Central Graben eventually became well known to be rich in hydrocarbon reserves. Chalk is a strongly lithified, calcareous sedimentary fill in the North Sea, showing stratigraphic successions. The primary objective of this study is to subdivide the Central Graben Chalk Group into stratigraphic units to provide a framework for the depositional setting using 3D seismic data and fifteen well data from the block 2/4 of the Norwegian Continental Shelf. In addition, the geomorphological studies using stratal slices, explain the specific seismic facies present in these stratigraphic units. The 3D seismic stratigraphy and the geomorphology together led to paleogeographic reconstructions of the study area. The Chalk Group in this study is divided into five major seismic sequences bounded by six sequence boundaries. The well data integrated with the interpreted seismic sequence characteristics and the geomorphological features led to identification of three different tectonic phases under which the Central Graben Chalk Group deposited. In the pre-tectonic phase, initial draping and infilling processes prevailed. The syn-tectonic depositional phase experienced extensive tectonic inversions and halokinetic uplifts. These uplifts led to formation of several channels and gravity flows due to destabilization of the slope sediments. As a result extensive erosional surfaces formed representing unconformities within the seismic sequences. The post tectonic phase was dominated by bottom currents leading to redistribution and redeposition of sediments in the study area. The bottom currents were also responsible for creation of several straight-sinuous channels, channel valleys, channel scours, slides and mega slides. As a result allochthonous sediments became common during the post tectonic phase. Overall the Central Graben Chalk Group deposition was influenced by sea-level fluctuations, halokinetic and inversion tectonic activities, and bottom current circulations.

Table of Contents

List of Figures

xiv

1.   Introduction

The giant Ekofisk field, since its discovery in 1969 in the Norwegian sector of the Central Graben, has been producing hydrocarbons from the Upper Cretaceous Chalk sediments (Surlyk et al., 2003). This area is mostly dominated by chalk from the Upper Cretaceous to Early Paleocene ages. Chalk is a biogenic sediment primarily deposited from the slow settlement of coccoliths below the wave-base marine settings, with secondary inputs of foraminifers and calcispheres (Gennaro et al., 2013; Surlyk et al., 2003) (Figure 1). The chalk deposition in the Central Graben seems to have occurred below the photic zone where the water depth varies from one hundred meters to hundreds of meters over the deepest parts and produces volatile oil accumulated in the Maastrichtian Tor and Danian Ekofisk formations.

Figure 1: Upper Cretaceous Facies Model showing chalk depositional setting from the basin margin on the Baltic Shield across the Danish Basin to the Central Graben with a south-west trending dip section (Surlyk et al., 2003).

The Upper Cretaceous to lower Paleogene Chalk Group in the Central Graben of North Sea represents a period of high eustatic sea level and low detrital influx leading to pelagic sedimentation on the continental shelves (van der Molen et al., 2005). The North Sea area underwent tectonic evolutions during the Middle to Late Jurassic which was followed by a relatively tectonically calm period with pulses of compressions in the Late Cretaceous. This calm period lead to the initiation of the deposition of the Chalk Group

16

while the compressional pulses reactivating several structural elements, lead to mass movement of chalk deposits which were then redeposited as slumps, slides and turbidites. The bottom currents also play a very important role on the deposited chalks sculpting the sea-floor relief to important topographic features like channels, drifts, valleys, ridges and mounds (Gennaro et al., 2013; Surlyk et al., 2003; van der Molen et al., 2005).

Structurally the Ekofisk field lies between the Lindesnes Ridge to the south and Albuskjell – Tor anticlines in the north trending east-west. Deeper stratigraphic levels beneath the Ekofisk Field are related to a combination of tilted fault blocks and salt diapirism (Surlyk et al., 2003). The uplift of the Lindesnes Ridge and the Albuskjell anticline changed the physiography of the Norwegian Central Graben basin affecting the style of the chalk sedimentation, and thus are important with respect to the distribution of the Upper Cretaceous and Danian chalks (Gennaro et al., 2013; Surlyk et al., 2003). Figure 2 highlights in red the location of the study area while Figure 3 displays a regional seismic cross section illustrating the different structural styles influenced by the halokinetic deformations in the Norwegian Continental Shelf and also shows the approximate location of this study. Figure 4 is a structural map of the Norwegian Central Graben showing the major structural and halokinetic features that were active during the Late Cretaceous as well as the relative positions of the chalk fields.

The deeply buried Cretaceous Chalk sediments in the Central Graben of North Sea are mainly chalk, limestone, marly chalk, marl and calcareous shale. The Chalk Group is subdivided into Hidra, Blodøks, Hod, Tor and Ekofisk formations. Figure 5 shows the lithostratigraphic column tied to a type seismic section from the study area. The majority of the chalks in the Tor and Ekofisk formations are allochthonous, formed by the mass movement of pelagic chalk. The Chalk Group also experienced syndepositional tectonics and halokinesis in the Central Graben, North Sea (Surlyk et al., 2003).

17
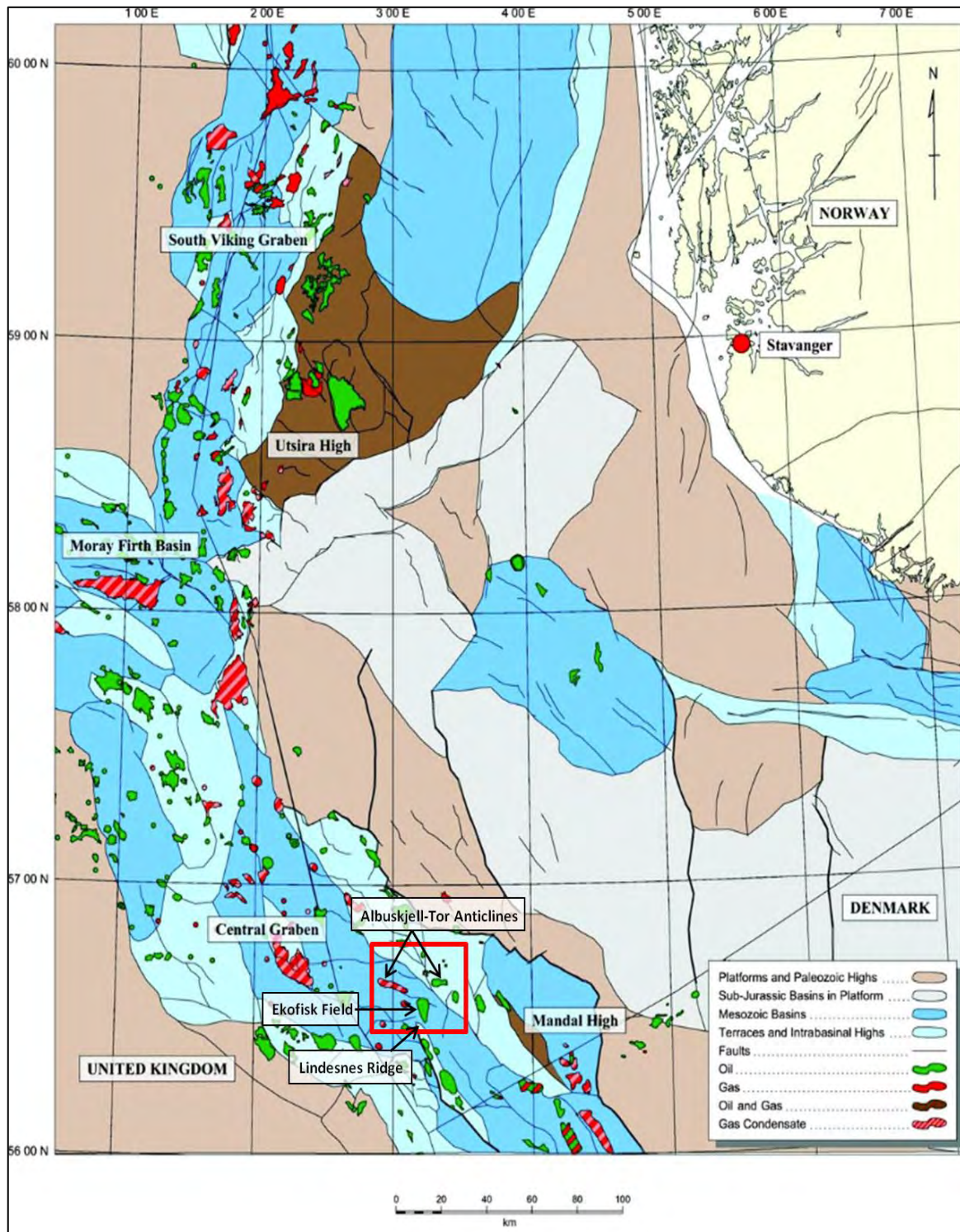
Figure 2: The geographic location of the study area situated in the North Sea region is shown here in relation to the main geologic structural elements. The study area is highlighted as a red square in the map (modified from Rossland et al., 2013).
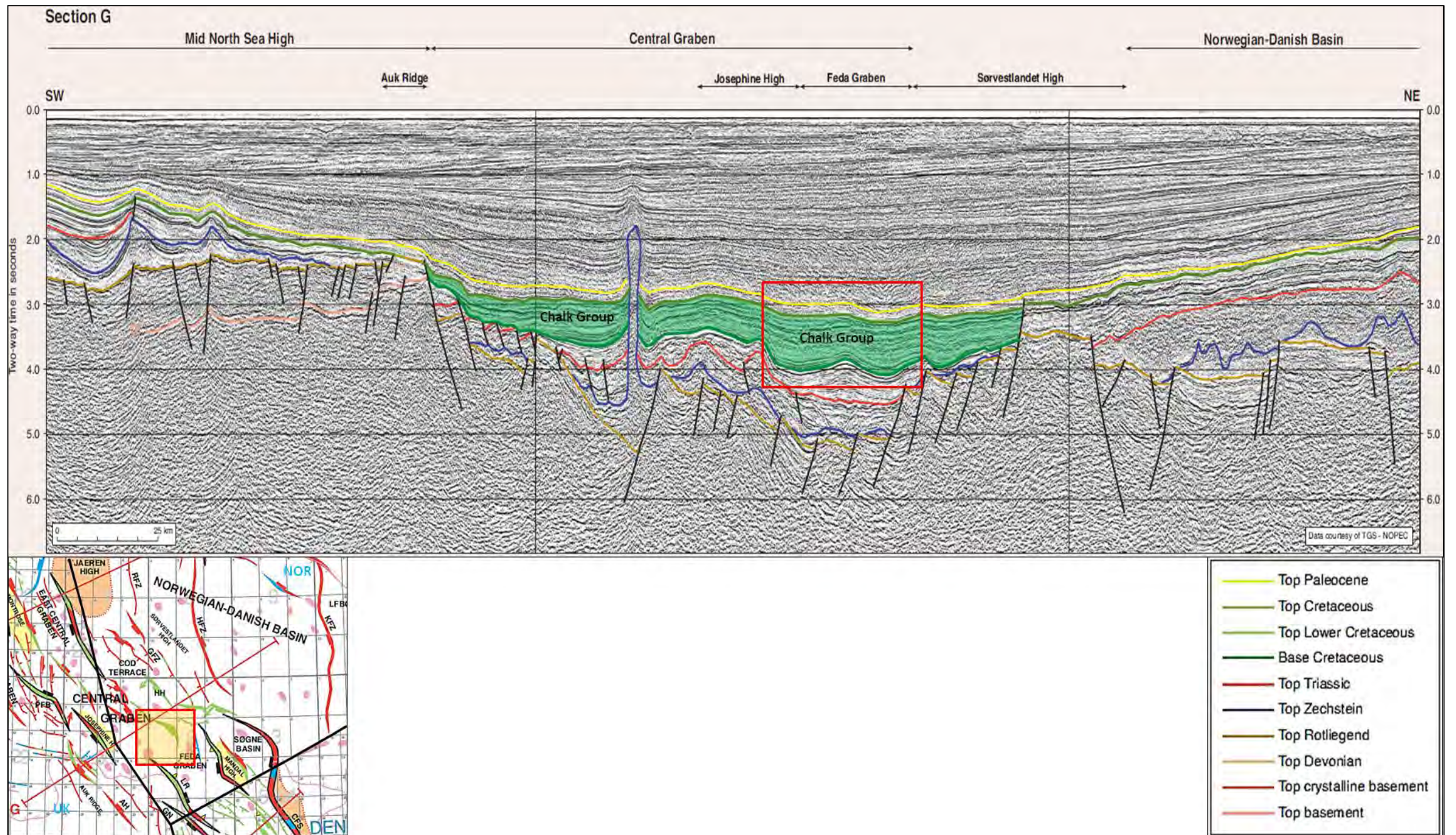
Figure 3: A regional seismic cross-section displaying the different structural styles of the central North Sea characterized by halokinetic deformations due to the Zechstein salt movements, active from early Triassic to the Cenozoic in some areas (Surlyk et al., 2003). The location of the cross section is shown by the red line 'G' in the inset map. The areas highlighted within the red squares show the approximate study area in the inset map and the seismic profile.
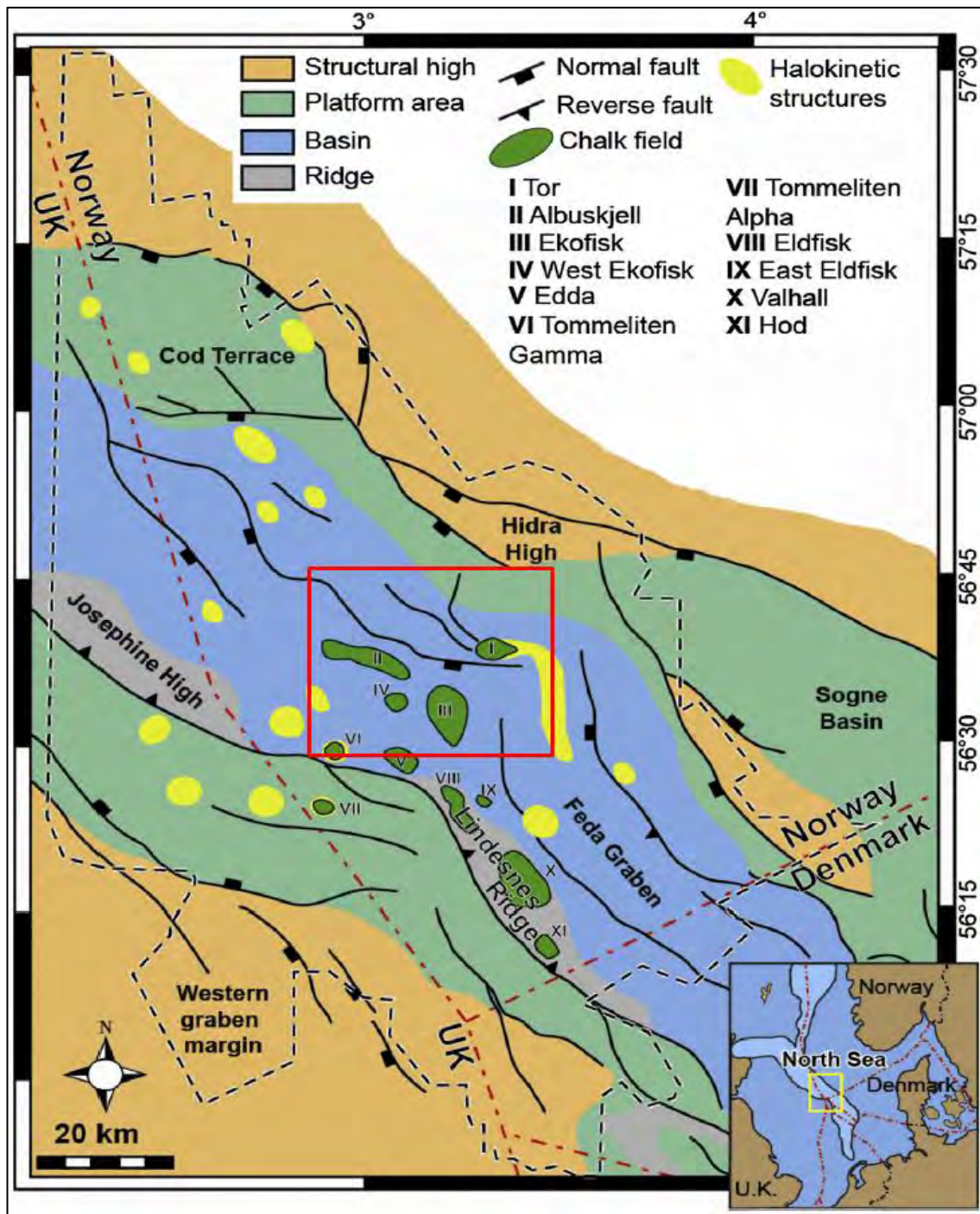
Figure 4: A structural map of the Norwegian Central Graben illustrating the dominant structural and halokinetic features which were active during the Late Cretaceous and the relative positions of the chalk fields from (modified from Gennaro et al., 2013). The highlighted area in red is the study area of this project.
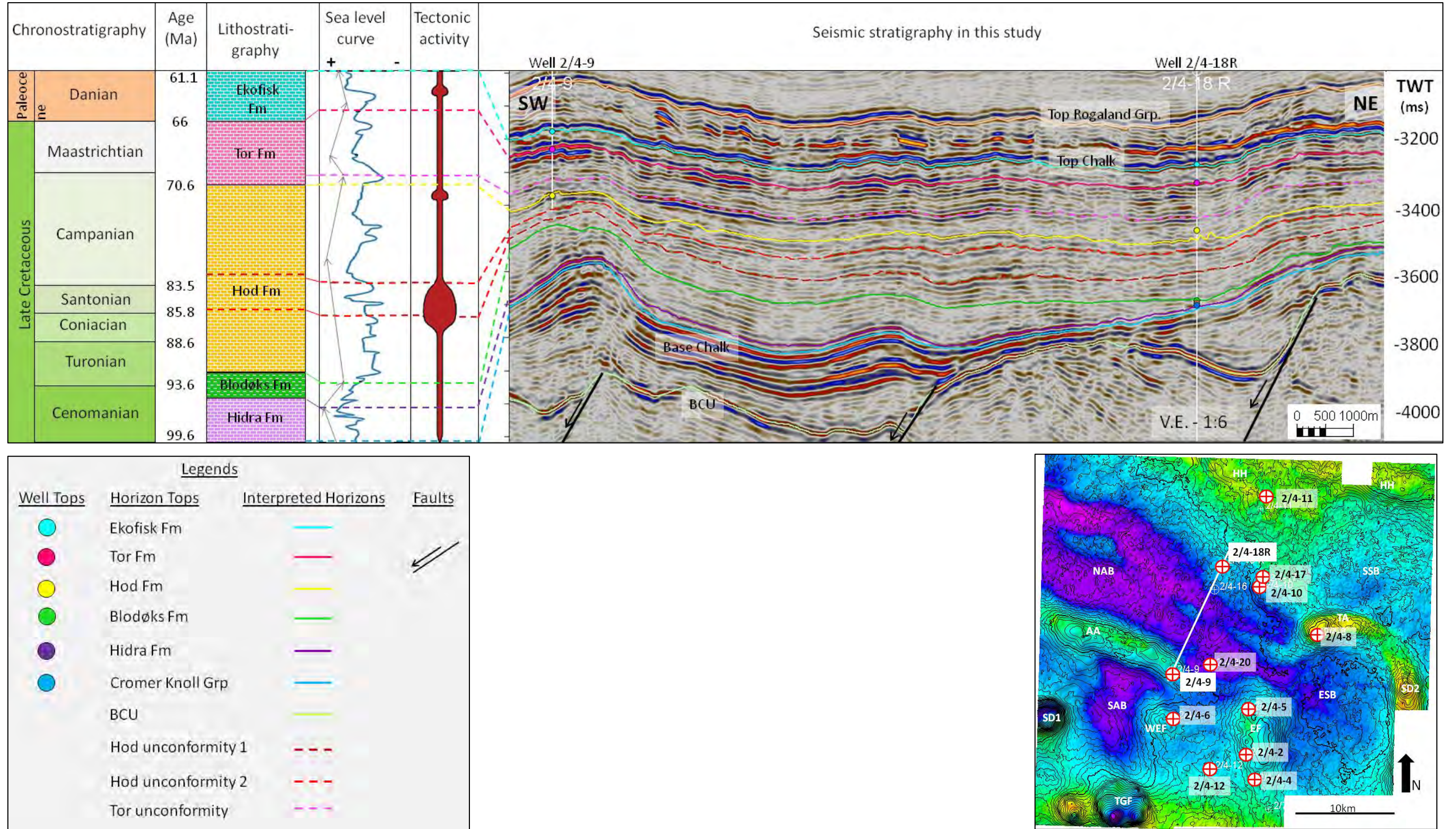
Figure 5: Lithostratigraphic chart illustrating the subdivisions of the chalk group in the study area along with their correlation to a type seismic section passing through the wells 2/4-9 and 2/4-18R. The locations of the wells and the seismic line are shown in the inset map. The inset map is TWT map of the top of the Ekofisk Formation. V.E. stands for vertical exaggeration. The sea level curve is based on Kominz et al., (2008). The tectonic activity curve is from Gennaro et al., (2013). The lithostratigraphy follows Deegan et al., (1977).

1.1. PREVIOUS STUDIES

The Chalk Group of Central Graben, southern North Sea, is well studied for understanding the chalk play, especially in particular, with respect to the sedimentology and diagenesis of the chalk reservoirs. In addition, the technological innovations in drilling for example, horizontal drilling, water and gas injection, and well stimulation by fracturing has led to advances in field developments (Surlyk et al., 2003). The aspects of deposition, re-deposition, diagenesis and reservoir characteristics of chalk despite being studied in details are under constant research and investigation (Surlyk et al., 2003).

Several studies on the Chalk Group have been conducted in the Danish North Sea. Esmerode et al., (2008) suggests that the pelagic chalk deposits were affected by powerful bottom currents which led to formation of several channels and drifts on the chalk layers in the Danish Central Graben, North Sea. Several mass transport systems also dominated the sea floor during the Late Cretaceous to early Paleocene times. Back et al., (2011) also presents similar concepts of pelagic depositional environment along with mass transport processes prevailing on the Danish North Sea floor during this time. The study proposes that the intra-chalk discontinuities were developed due to the gravity driven processes influenced by the syndepositional tectonics and halokinesis and also suggests that the contour parallel bottom currents helped developing the intra-chalk channels with drift and mound features. Another study by van der Molen et al., (2005) discuss about the influence of the tectonic regimes on chalk deposition in the Netherlands offshore area. The study also highlights the concept that locally, the tilting of the sea floor resulted in mass-movements of chalk at scales varying from decimeter thick turbidites to slumps and slide sheets of hundreds of meters of thickness implying syn-depositional tectonic control on the chalk facies. van der Molen et al., (2007) published another study which discusses a more detailed lithostratigraphic subdivision of the Netherlands North Sea area using 2D and 3D seismic dataset.

A seismic stratigraphic study by Gennaro et al., (2013) of the Chalk Group in the Norwegian Central Graben, North Sea, explains the process of the prevailing bottom currents and large scale gravity flows forming the syndepositional geomorphological

features. The study also gives an insight into the tectonostratigraphic evolution of the chalk deposits in the Norwegian Central Graben which was largely influenced by the inversion tectonics and halokinesis. Another study by Gennaro et al., (2013) characterizes the dense zones within the Danian Chalks of the Ekofisk Field explaining that the Ekofisk Formation of Danian age and the Tor Formation of the Maastrichtian age form the main reservoir units in the Ekofisk Field.

A robust regional model for chalk prospectivity was developed by Bramwell et al., (1999) covering the entire chalk basin of the Norwegian Continental Shelf and was based on the sequence stratigraphic analysis of regional seismic and well databases, integrated with petrophysical, hydrodynamic, geochemical and other key technical studies. This study identifies seven principal factors controlling the chalk stratigraphic play which includes burial depth, original depositional facies, early hydrocarbon migration, structural development concurrent with hydrocarbon migration, fracture definition, timing of chalk over pressure and the effectiveness of the top, bottom and lateral seals. Fontaine et al., (1987) explains the key ideas of seismic interpretation for carbonate depositional environments. The study points out that the chalk deposits display continuous high-amplitude reflections at the top and base with almost an internal reflection-free zone, and also shows the seismic characteristics of the pelagic deposits and carbonate debris flows. Jones et al., (2014) characterized the fractures and faults of the Ekofisk reservoir which aids in improving the technological innovations for increased and advanced field developments.

The Chalk Group of Central Graben, North Sea is an important hydrocarbon play in the Norwegian continental shelf. Since the discovery of the giant Ekofisk field in 1969, a huge number of studies have been carried out in the fields of sedimentology, petrophysics, mechanical properties like faults and fractures leading to enhanced oil recovery techniques and many more as discussed above. It is quite noticeable that the application of sequence stratigraphy on chalk and similar sediments of the Norwegian Central Graben, North Sea has been rarely published.

The primary objective of this study is to subdivide the Central Graben Chalk Group into stratigraphic units to provide a framework for the depositional setting using 3D seismic data and fifteen well data from the block 2/4 of the Norwegian Continental Shelf. Further, this project also aims to study the geomorphology of the chalk deposits using stratal slices explaining the specific seismic facies present in these stratigraphic units. The 3D seismic stratigraphy and the geomorphological studies together lead to paleogeographic reconstructions of the study area. The final objective is to explain the known hydrocarbon presences within this sequence stratigraphic framework.

2. Geological Setting

In the Late Cretaceous in the North Sea region the climate was warm-temperate to subtropical and had pronounced greenhouse character (Surlyk et al., 2003). The highly diverse faunas show that the salinity of the sea water was normal and the water temperatures were comparatively high. These favourable temperatures and salinity conditions lead to the great thickness of the chalk deposits which indicates a very high rate of production of the algae in this environment. The chalk commonly shows pronounced cyclicity on a decimeter scale in the form of marl-chalk, chalk-flint or laminated bioturbated beds (Surlyk et al., 2003).

The Late Cretaceous North Sea depositions were preceded by a Mid-Late Jurassic rifting event followed by local oblique-slip movements creating transpression/transtension in the Early Cretaceous (Surlyk et al., 2003). As an effect of these events, pronounced tilt-block topographic relief was created in this region. In the following Late Cretaceous to Danian periods this region became relatively tectonically calm encouraging huge chalk deposition which draped the tilted block relief. These draping insitu chalks are referred to as the autochthonous chalks in the Chalk Group. However, during this period, there were pulses of compression and inversion related to the early phases of the Alpine orogeny along with halokinetic activities creating a lot of accommodation space. These tectonic and halokinetic activities caused widespread mass movement of the chalk deposits in the form of slumps, debris flows and turbidity currents, which were then redeposited in the

created accommodation spaces on the slopes and the basinal areas (Surlyk et al., 2003). These re-deposited pelagic chalks, referred to as allochthonous chalks, constitute much of the chalk of the Tor and Ekofisk formations (Bramwell et al., 1999; Isaksen et al., 1989; Surlyk et al., 2003).

From previous findings and studies, the first unit of the Chalk Group, the Hidra Formation deposited in open marine environments as pelagic, coccolith oozes and is typically about 170 m thick in the Central Graben (Isaksen et al., 1989). It is absent over some structural highs, possibly due to local erosions (Surlyk et al., 2003). The Blodøks Formation lying above Hidra Formation on the other hand is widely distributed in the North Sea and is upto 120 m thick in the Norwegian Sector (Surlyk et al., 2003). Anoxic bottom conditions prevailed during its deposition, but some presence of carbonates may indicate periods of more oxic environments or supply of allochthonous limestones and chalks (Isaksen et al., 1989).

The heterogeneous Hod Formation overlies the Blodøks Formation and is the thickest unit of the Chalk Group containing high amount of clay with intervals of pure chalk in its basal parts. Two major unconformities divide the formation into lower, middle and upper units (Surlyk et al., 2003). Laminated and burrowed chalk with very low clay content is found in the lower unit where the bioturbation increases upwards. The middle unit shows cyclicity and has higher content of clay while the upper unit also shows cyclicity but has lower clay content (Surlyk et al., 2003). The formation may reach more than 700 m in the north western part of the Central Graben and is 515 m thick in type well (Isaksen et al., 1989).

The Tor Formation lying above is a homogenous and most wide spread unit of the Chalk Group with a type well thickness of 474 m and 208 m in well 1/9-1, close to the area for this study (Isaksen et al., 1989). The formation thickness may also exceed 600 m in the north western part of the Central Trough. The basal part of the formation consists of bioturbated pelagic chalk showing an upwards transition into laminated bioturbated cycles. These are commonly replaced in the uppermost part of the formation by allochthonous deposits formed by downslope mass movement of primary pelagic or older re-sedimented chalks. The top of this formation represents a regional unconformity at the

Cretaceous-Paleogene boundary. The Tor formation has very good reservoir properties and thus contains most important reservoir intervals of the Chalk Group (Surlyk et al., 2003).

The Ekofisk Formation is the final unit of the Chalk Group deposited in the Danian and extends throughout the Central Graben of the North Sea. The units of reworked chalk are locally found in the southern part of the Central Graben. The preserved sediments are upto 180 m thick in the basinal depocenters while they are 10-60 m thick on the structural highs (Surlyk et al., 2003).

Chalk deposition was finally extinguished at the end of the Danian when Paleocene siliciclastic sediments were introduced to the basin as a result of uplift of landmasses adjacent to the North Sea (Surlyk et al., 2003).

3. Database

3.1. 3D SEISMIC

The 3D seismic survey, VGCNS05 in Quad 30 in the central North Sea, used in this study is a Multi-Client Survey acquired by Veritas DGC Ltd., using the M.V. Veritas Viking vessel. This survey is situated in the northern Central Graben and covers an area of approximately 5035.3 km^2. Figure 6 shows the extent of the acquired data in pink, while the area within the red square highlights the data used for this study covering an area of ~1307.28 km^2. The dataset consisting of 6.25x25 grid size was acquired in 2004 in a north-south direction using a configuration of two sources and eight streamers. Each streamer of 6km length used 480 channels with 12.5m of constant spacing for the inlines and crosslines. This dataset used for this study is a zero phase, full offset migrated seismic cube.
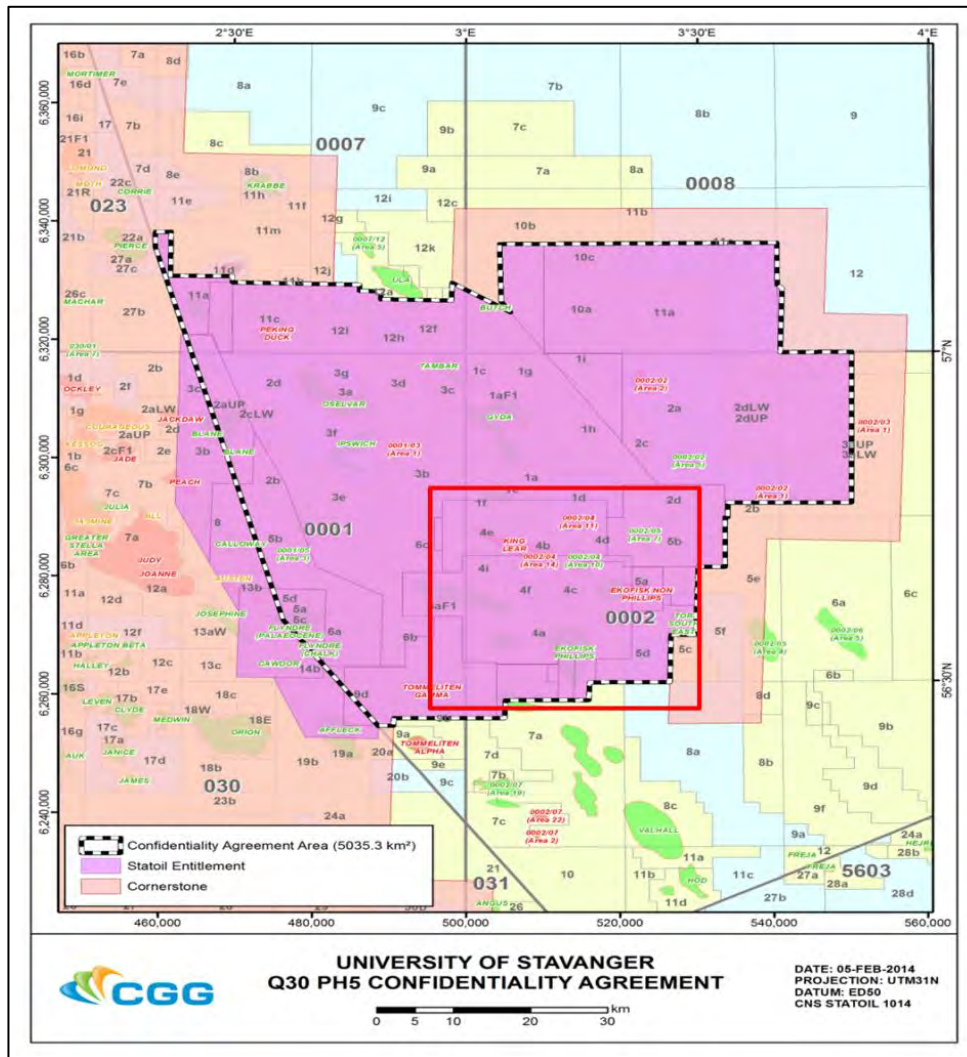
Figure 6: The acquired dataset VGCNS05 is marked in pink. The study area covering ~1307.28 km^2 is located in the area highlighted in red in the Norwegian Continental Shelf of North Sea.

3.2. WELLS

Fifteen exploration wells from block 2/4 of Norwegian continental shelf were used in this study. The well data consisted of the conventional well logs among which the gamma ray, sonic, density, and resistivity logs were most used for this study (Figure 7). The wells with most complete set of sonic and density logs were used for the well ties. The biostratigraphic and lithostratigraphic logs from some wells (2/4-2, 2/4-4, 2/4-5, 2/4-6, and 2/4-8) were also used to identify the stratigraphic markers in the study area.

4. Methodology

4.1. TOOLS

Petrel E&P Software Platform 2014 is the software mainly used to conduct this study. The dataset, VGCNS05 and the wells from the above mentioned block were loaded into this software to perform the seismic to well tie, well correlations and seismic interpretations. The products such as the TWT-structure (two-way travel time), total stratigraphic thickness (TST) and seismic attribute (amplitude and variance) maps were used as basic tools to interpret and analyse the study area. Time slices, the proportional slices between the interpreted surfaces as well as 3D seismic displays were used for detailed understanding of the chalk deposition in this area.

4.2. WELL TIES

The provided wells were divided into different formations within the Shetland Group, which is the interval of interest in this study. This was carried out using the formation information provided in the Norwegian Petroleum Directorate, as well as the gamma ray, sonic, density and acoustic impedance logs from the wells (Figure 7).

Synthetic seismograms were produced for wells 2/4-2, 2/4-4, 2/4-5, 2/4-6, 2/4-8, 2/4-9, 2/4-10, 2/4-11, 2/4-17 and 2/4-18R by extracting wavelets from the relevant windows of the seismic and using the sonic and density logs of the wells. Figure 8 shows the synthetic seismogram generated for a type well, 2/4-18R, in the study area along with the extracted wavelets used in the process. The generated time depth ratios were then applied to the wells and if necessary, small time shifts were also applied to tie the seismic and the wells together. Figure 7 shows the generated synthetic seismogram of the well 2/4-18R after applying the time depth conversions. The vertical resolution of the seismic was also measured to be ~30m as shown in Figure 7.

This step was performed to bridge the gap between the well data (measured in depth domain) and the seismic data (measured in two-way travel time, TWT) while the well ties are also important in identifying which reflectors to interpret. Figure 9 shows the seismic

lines connecting the key wells in the study area which displays the horizons picked based on the synthetic seismograms and the time depth conversions.

4.3. WELL AND SEISMIC INTERPRETATIONS

The different formation tops in the Shetland Group of Late Cretaceous age were interpreted in the seismic, keeping the well data as references (Figure 5). The Chalk Group is divided into five different formations namely Hidra, Blodøks, Hod, Tor and Ekofisk. The base of the Chalk is marked by the top of Cromer Knoll Group while the top Chalk is identified by the Ekofisk Formation top. The base of the Cromer Knoll Group is also interpreted to be the Base Cretaceous Unconformity (BCU). The Rogaland Group lies atop Ekofisk Formation and the Group top is also interpreted for this study.

This immediate overlying Rogaland Group top was used for flattening and a simplified restoration of the chalk interval, since it is a slightly younger surface than the top chalk and was nearly flat during its deposition. Moreover, the Rogaland Group top lies in a zone with parallel layering and uniform thickness between the layers and thus it was preferred for flattening and simplified restoration of the chalk interval. The simplified restoration process was carried out to visualize and identify the nature and direction of the sediment deposited and transported. The seismic profiles displayed in the Results chapter are all flattened on the Rogaland Group top for the reasons mention above. The vertical scales in these profiles are displayed as TWT in ms (milliseconds) but are not the exact representations of the actual TWT since the profiles are flattened. Instead the scales represent the relative time differences in ms on the vertical scales.
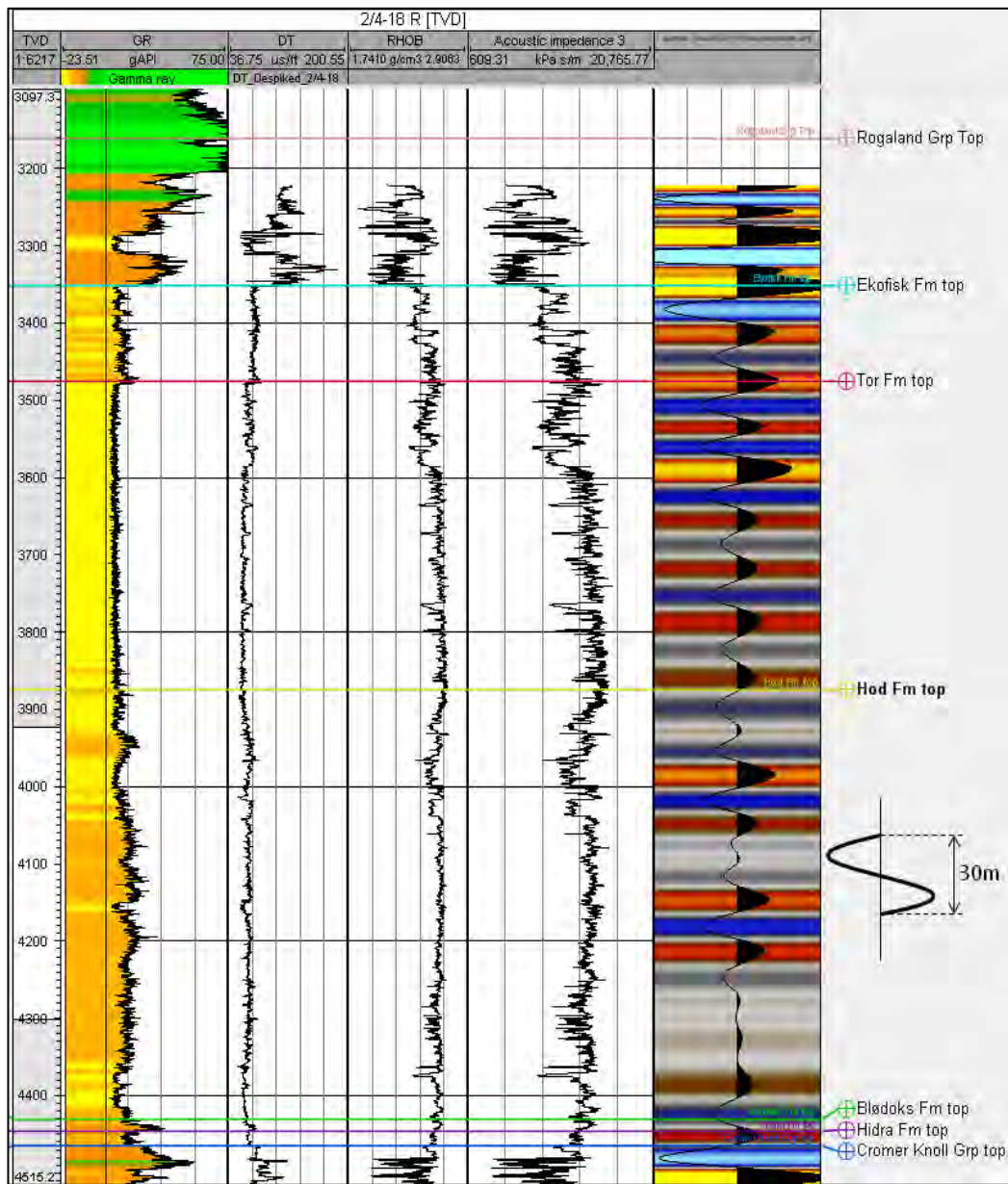
Figure 7: A type well, 2/4-18R in the study area, illustrating different interpreted formation tops of the Chalk Group based on the gamma ray log (GR), sonic log (DT), density log (RHOB) and acoustic impedance log (AI). The AI log is calculated by multiplying DT and RHOB logs. The synthetic seismogram generated to tie the well and the seismic together is also shown in the rightmost column. The Ekofisk, Tor, Hod and Hidra formation tops are picked on the peaks (red) while Blodøks and Cromer Knoll Group tops are picked on the troughs (blue). The red peaks correlate to an upward increase in DT while the blue troughs correlate to an upward decrease in DT. The changes in DT control the AI in most of the well logs in the study area.

4.4. MAPPING

The TWT structure, time TST and seismic attribute maps for all the formation tops were generated. The seismic attribute maps of amplitude and variance were created for all the

30

formations. Interval averages were created using root mean square (RMS) method for both amplitude and variance attribute maps. The amplitude attribute maps are used for identifying the acoustic impedance contrast. The compact sediment packages exhibit high amplitude reflectors indicating an undisturbed deposition, while the loose and less compacted sediment packages exhibit lower amplitude reflectors indicating deposition by mass movements related to tectonism or halokinesis. The amplitude attribute maps can also be used for identifying oil or gas filled reservoirs. The variance attribute maps were used to identify the discontinuities along the surfaces in order to map the faults and erosional features within the study area.
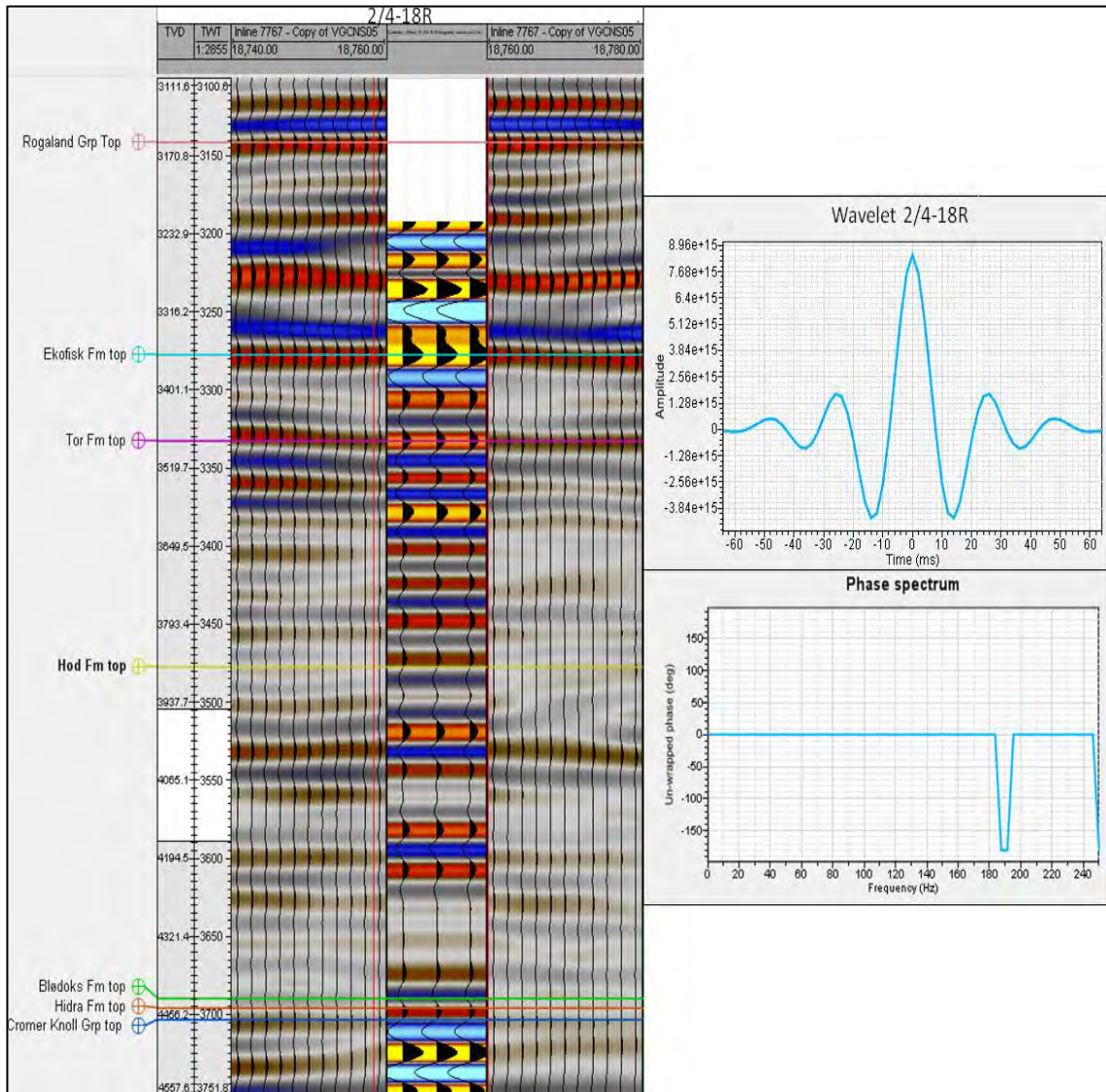
Figure 8: The generated synthetic seismogram for well 2/4-18R along with the extracted wavelets used for the process.
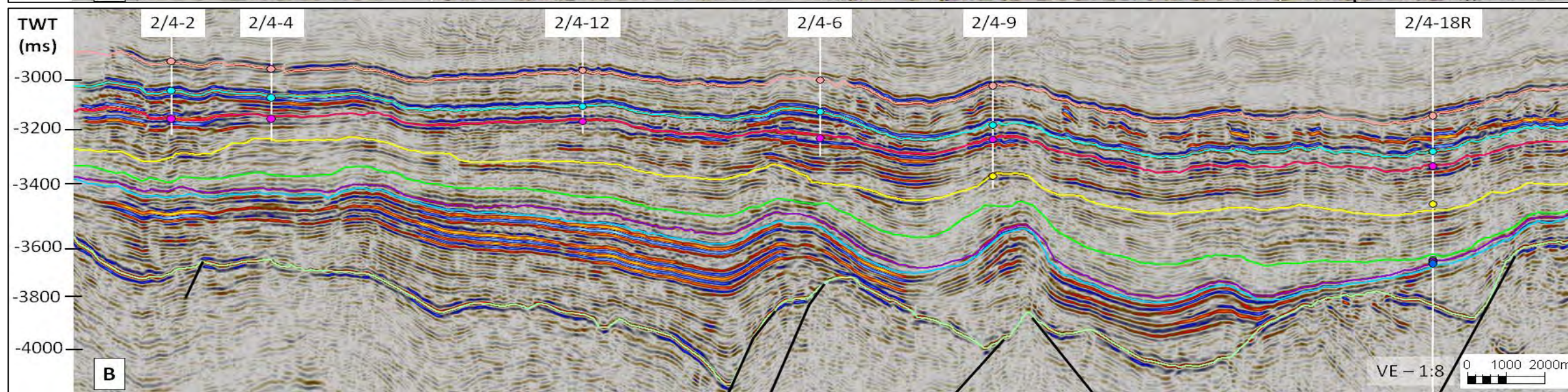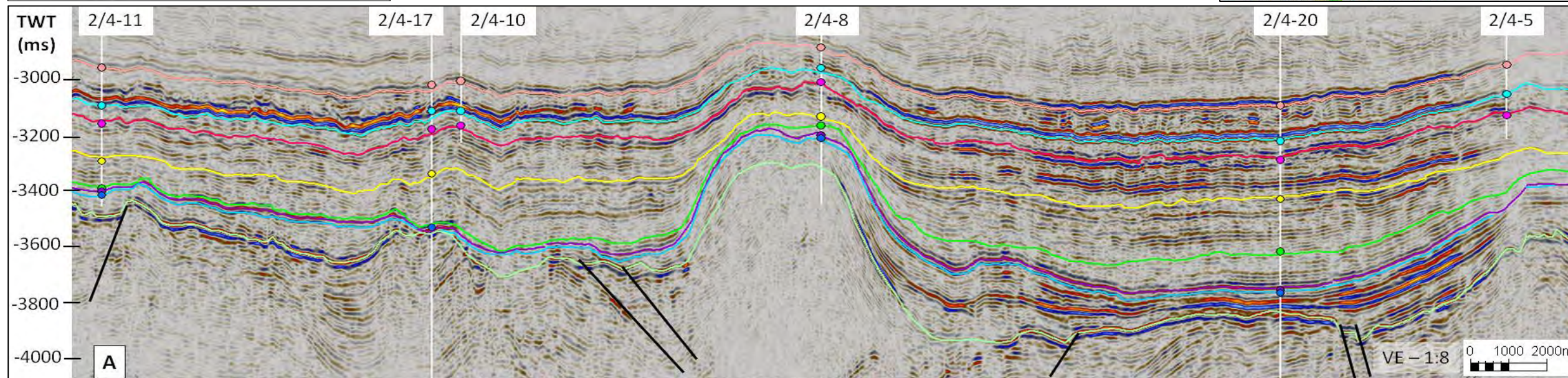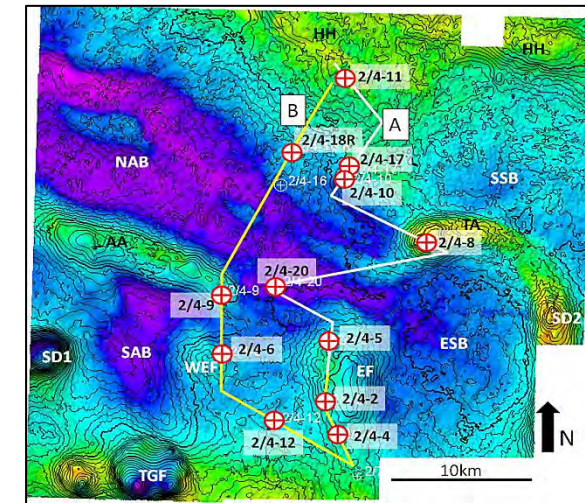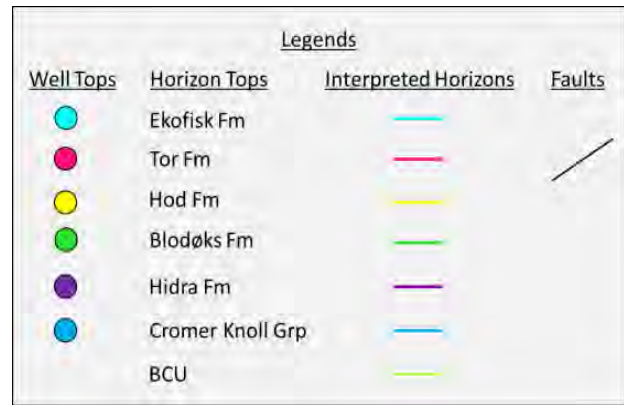
Figure 9: Seismic sections connecting the key wells in the study area displaying the wells to seismic ties after applying the time depth conversions based on the generated synthetic seismograms. The location is shown in the TWT inset map of the Ekofisk Formation top.

5. Results

5.1. SUBDIVISIONS AND SEISMIC STRATIGRAPHY ON THE CHALK INTERVAL

The Chalk Group is divided into five major stratigraphic units – Hidra, Blodøks, Hod, Tor and Ekofisk formations. Apart from the mentioned five units within the Chalk Group three more major unit tops were also identified, namely the Rogaland Group top (overlying the chalk), Cromer Knoll Group top (Base Chalk) and the BCU (base Cromer Knoll Group). The top chalk is represented by the Ekofisk Formation top while the base chalk is marked by the Cromer Knoll Group top. These eight prominent unit tops were interpreted in the seismic based on the seismic to well ties and the reflection terminations. Furthermore, several unconformities and intra formation reflectors were interpreted for understanding the depositional, non-depositional and erosional patterns in the study area. The chalk units can be identified in the seismic by the strong reflectors separating them and in some cases these strong reflectors represent unconformities (Figure 5).

Figure 10 illustrates the time-structure (TWT) maps of the top Chalk (Ekofisk Formation top) and the base Chalk (Cromer Knoll Group top) which shows the topographic variations of the top and base of the Chalk Group in the study area. The structural highs in the area, such as the Hidra High (HH), Albuskjell Anticline (AA), Tor Anticline (TA), Ekofisk Field (EF), West Ekofisk Field (WEF), Lindesnes Ridge (LR) and Tommeliten Gamma Field (TGF) along with a couple of Salt Diapirs, SD1 and SD2 (also see Figure 4) can be easily identified on these maps (nomenclature based on Bramwell et al., 1999; Gennaro et al., 2013). The deepest areas indicate the main depocenters namely the North Albuskjell Basin (NAB), South Albuskjell Basin (SAB), Epsilon Sub Basin (ESB) and Steinbit Sub Basin (SSB) (nomenclature based on Bramwell et al., 1999; Gennaro et al., 2013). Figure 11 shows the TWT maps for the different formations within the chalk group where the main depocenters of NAB, SAB, ESB and SSB remain the same for all the formations. Both the Figures 10 and 11 show that the NAB is located in the NW part of the study area and has a general trend of NW-SW; to the SW of the study area lies the SAB which is surrounded by the structural highs of the

AA, SD1, TGF and WEF; ESB lies in the SE of the study area and is surrounded by TA, EF and SD2 while, the SSB is situated in the NE of the study area between the TA and HH.

In the base Chalk, the topographic relief differences between the highs and the basins are higher compared to that in the top Chalk. Thus the base Chalk TWT map shows the structural highs as more prominent compared to that of the top Chalk map. The deepest depocenters are the NAB and SAB from the base until the top of the Chalk Group. The isolated depocenters at the base Chalk displays some level of connectivity developed between them at the top Chalk.

Figure 12 displays the chalk interval in several seismic profiles and illustrates the highs and the basins within the major interpreted horizons. The BCU underlying the chalk group is highly faulted and the Lower Cretaceous deposits of the Cromer Knoll Group onlapping on to the BCU fills up the faulted half grabens. The overall varying thickness of the group in the seismic lines infers to syn-sedimentary tectonics in the area. Most of the formations within the Chalk Group are well distributed over the study area and they also display varying thicknesses, especially near the structural highs. This hints on the prevailing syn-sedimentary activities in the area. The highlighted area in the Figure 12A, on the other hand, shows a uniform and preserved thickness of the Blodøks Formation over the structural high TA. This indicates that this part of the TA was a depocenter during the deposition of the Blodøks Formation and was tectonically inverted to be a structural high during the deposition of the Hod Formation. The seismic imaging is generally good apart from the areas near to the salt structures, some structural highs and in the areas known for presence of gas.

Figure 13 displays well correlations across EF-TA and WEF-AA-NAB. The Chalk Group is clearly identified by the lower GR log values in these wells. The cyclic depositional pattern of the Chalk deposits is also identified and shown by the red arrows in Figure 13. Most of the wells are located on the structural highs and are relatively shallow except the wells 2/48, 2/4-11 and 2/4-18R. The thickest units of the Chalk Group are observed to be the Hod and the Tor Formations in the study area.
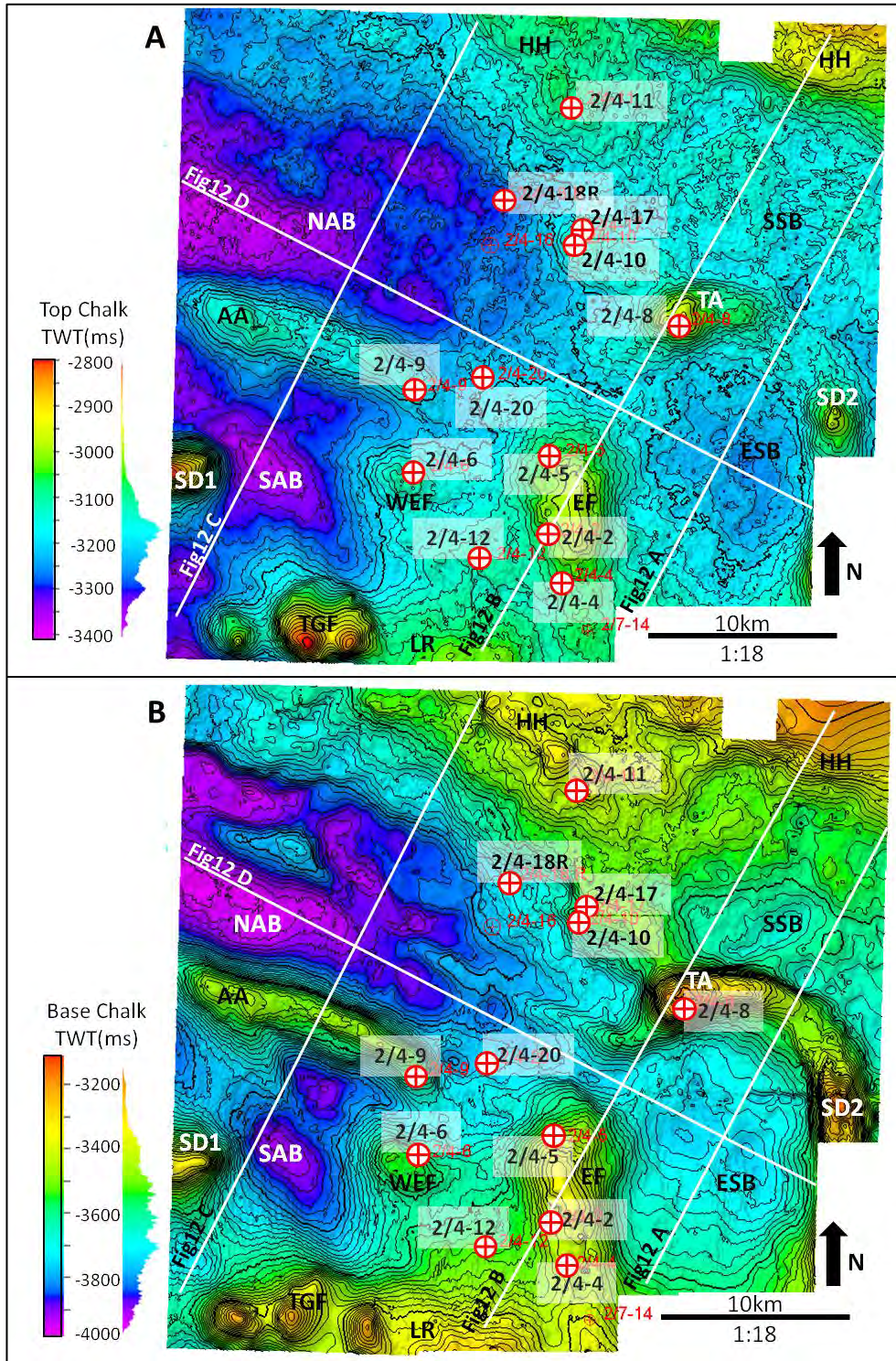
Figure 10: TWT structure maps of (A) Top Chalk and (B) Base Chalk. The prominent structural highs are AA-Albuskjell Anticline, TA-Tor Anticline, EF-Ekofisk Field, WEF-West Ekofisk Field, TGF-Tommeliten Gamma Field, LR-Lindesnes Ridge, HH-Hidra Highs, SD1-Salt Diapir 1 and SD2-Salt Diapir 2. The depocenters present in the area are NAB-North Albuskjell Basin, SAB-South Albuskjell Basin, ESB-Epsilon Sub Basin and SSB-Steinbit Sub Basin (based on Gennaro et al., 2013).

35
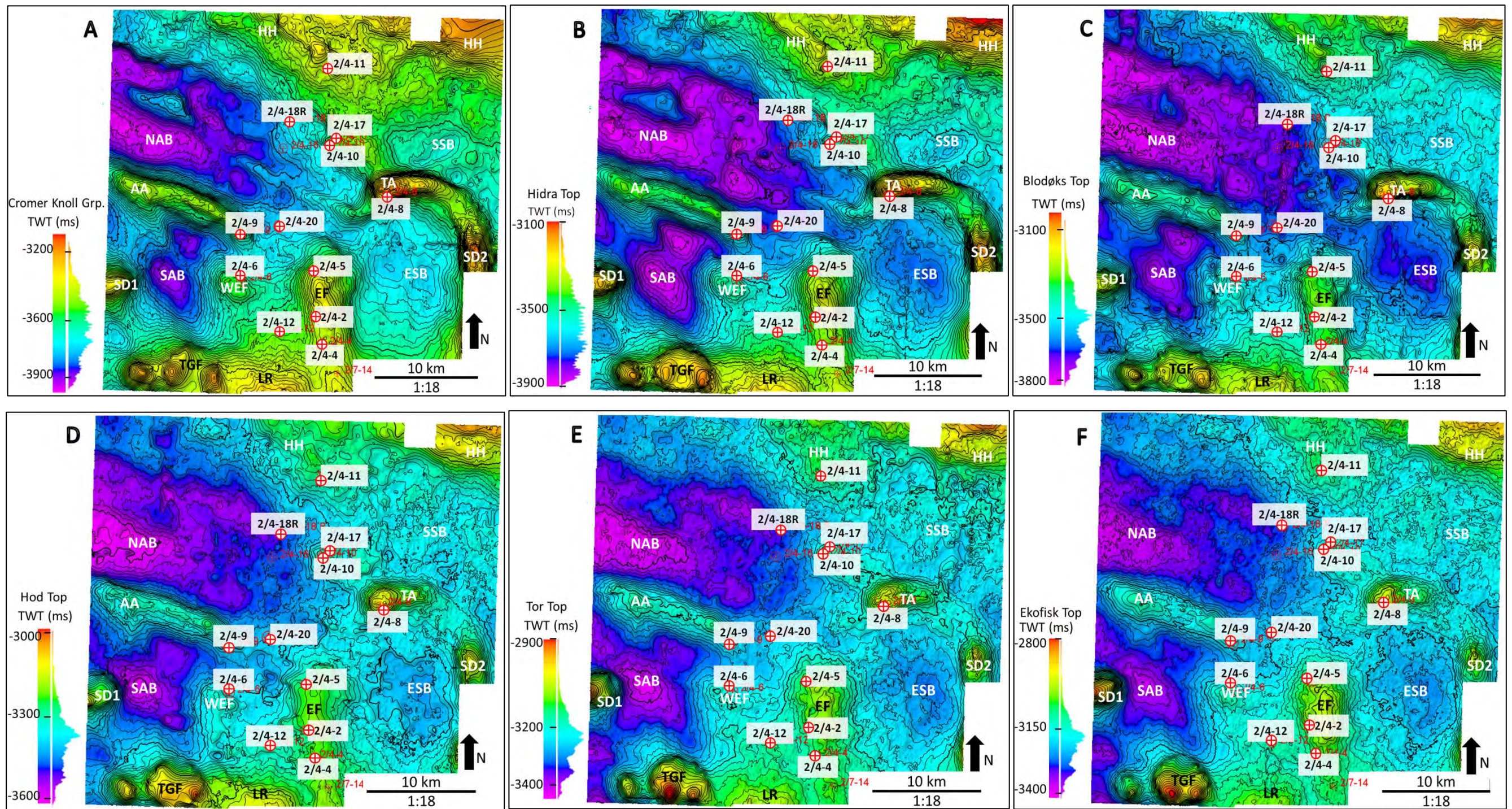
Figure 11: TWT maps of all the formation tops from Base to the Top Chalk. Four major depocenters of NAB, SAB, ESB and SSB persist through time during the Chalk Group deposition. Comparing the TWT maps from A-F of the different formation tops the initially isolated basins display development of connectivity between themselves through geological time. The deepest depocenters are the NAB and SAB throughout the Chalk Group.
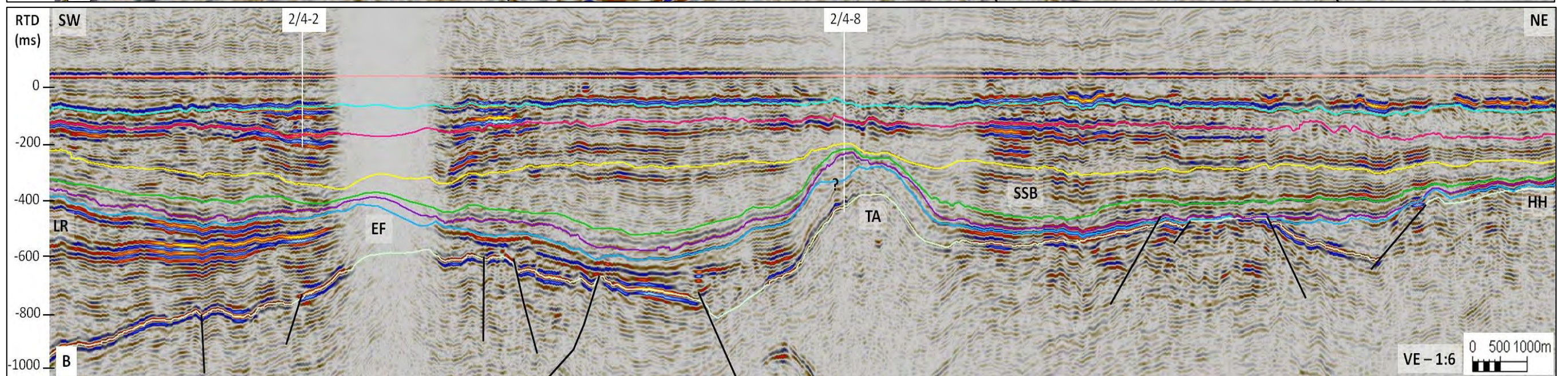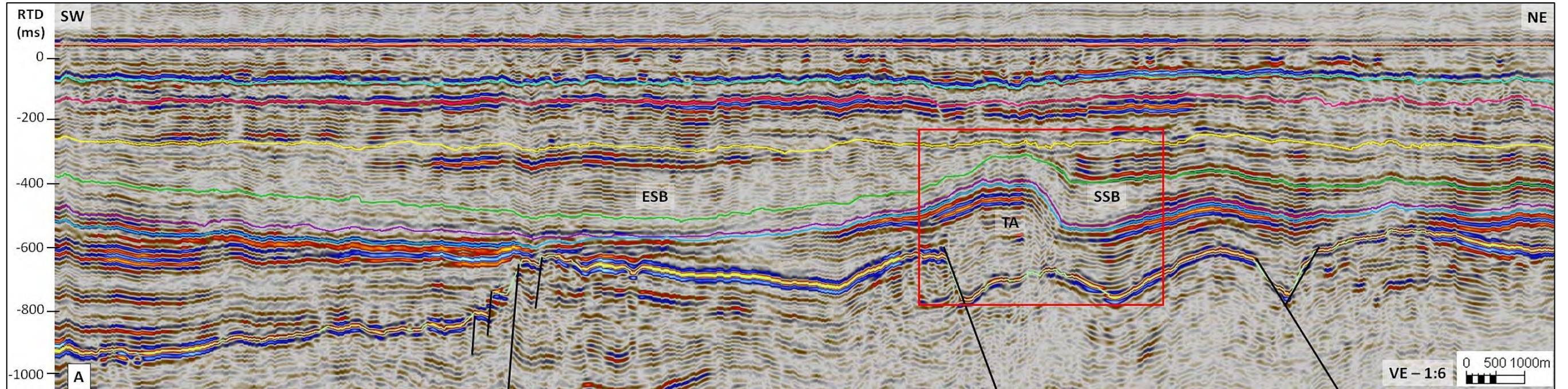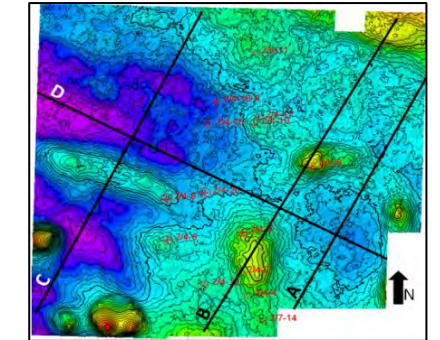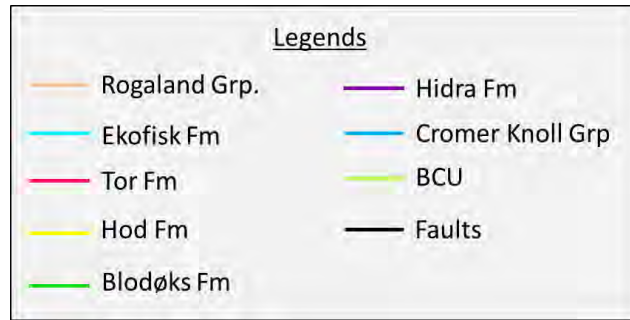
Figure 12: Seismic sections in the study area with the interpreted formation tops within the Chalk Group as well as the top of Rogaland Group and the BCU. The structural features in the study area are indicated, ESB-Epsilon Sub Basin, SSB-Steinbit SUB Basin, TA-Tor Anticline LR-Lindesnes Ridge and EF-Ekofisk Field. The area within the red square highlights the uniform and preserved thickness of the Blodøks Formation indicating tectonic inversion during the deposition of the Hod Formation. The seismic sections A-D are flattened on the Rogaland Group top. RTD-Relative Time Difference is measured in ms. The locations of the seismic sections are shown in the TWT inset map of the top Ekofisk Formation. The '?' mark in figure B represents uncertainty in interpretation at the crest of the TA.

37
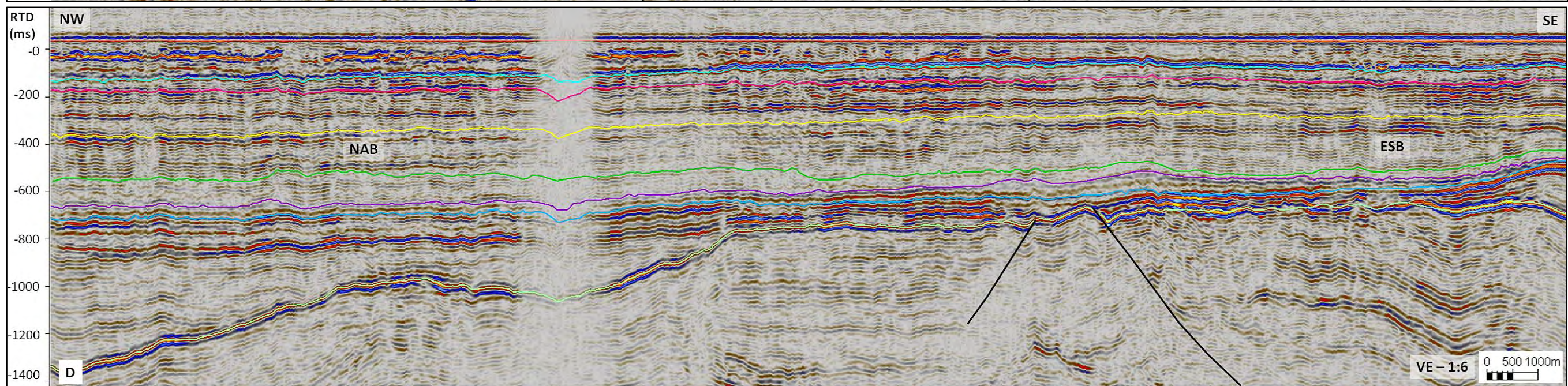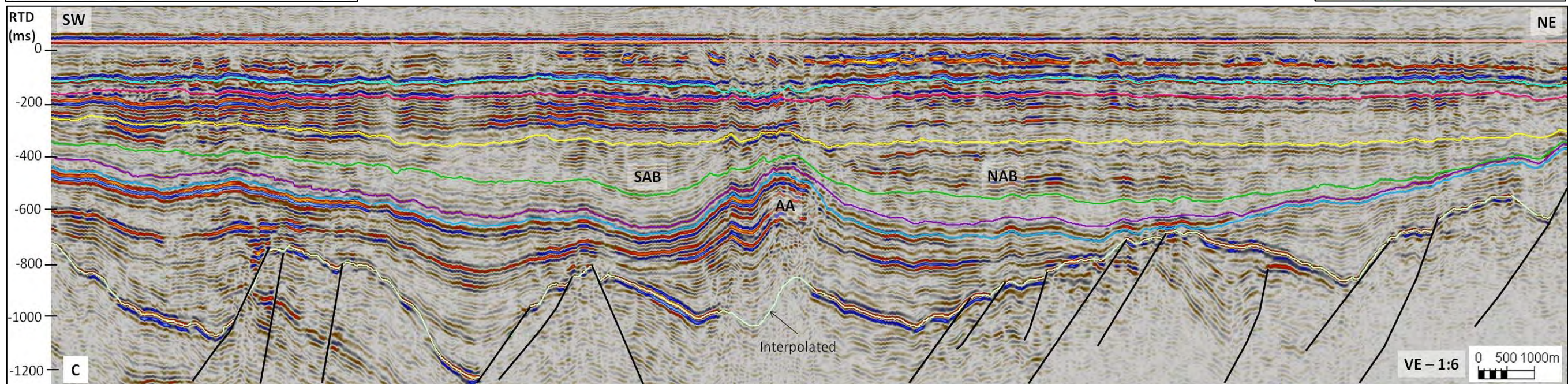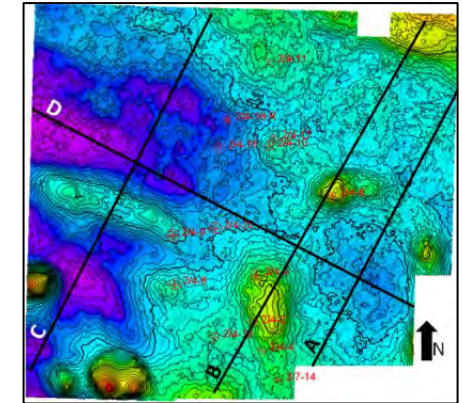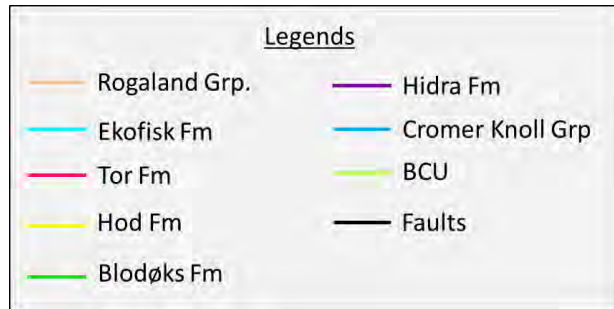
Figure 12 continued: SAB-South Albuskjell Basin, NAB-North Albuskjell Basin, and AA-Albuskjell Anticline. Figure D is displayed along the dip direction of the study area.
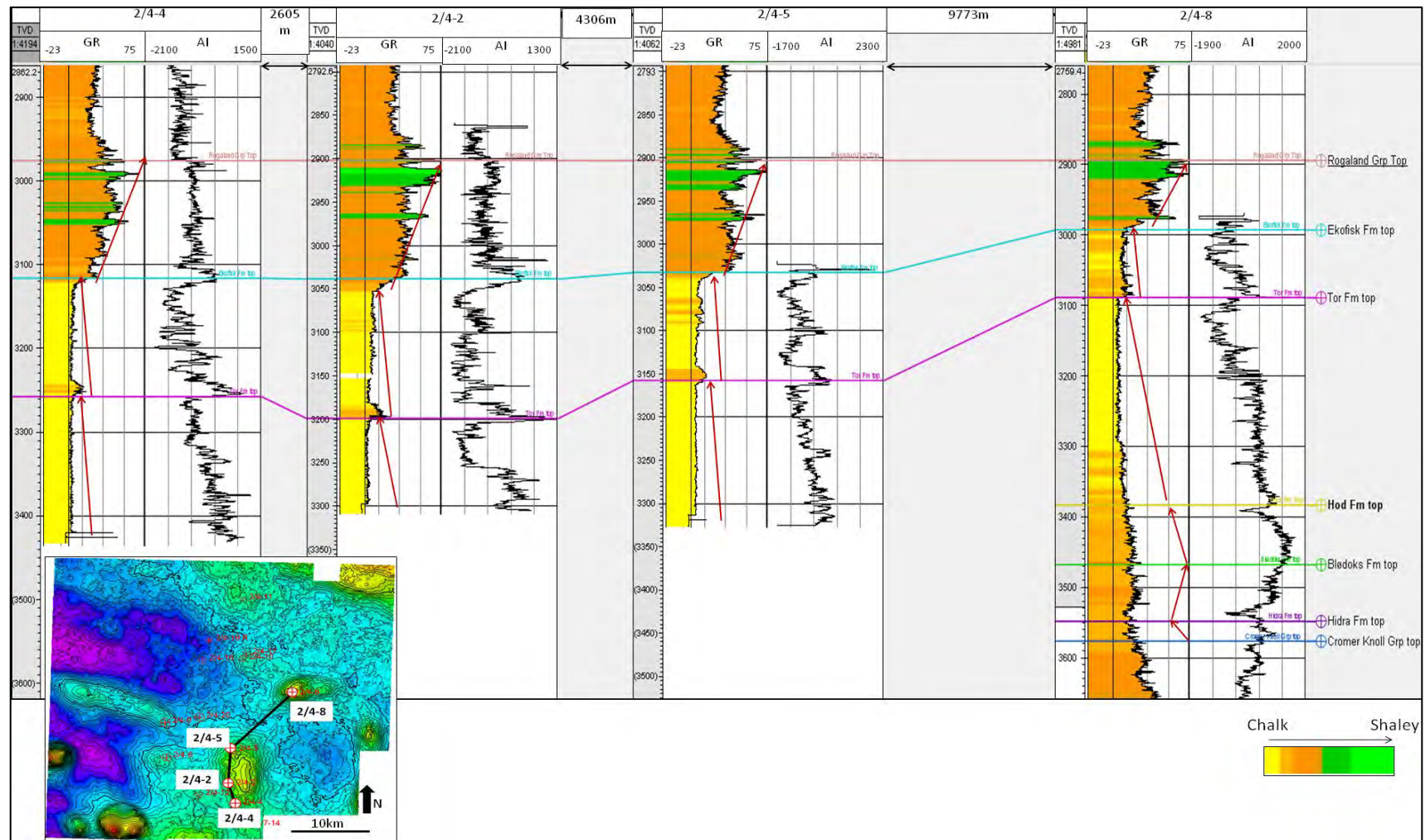
Figure 13: Well correlation across Ekofisk Field and Tor Anticline. The logs are flattened on Rogaland Group Top. The logs displayed are GR- Gamma Ray log (gAPI), AI-Acoustic Impedance log (kPa.s/m). The blue arrows show the general trends of the GR log and represent the cyclic depositional pattern of the Chalk Group. Well locations are shown in the TWT top Ekofisk inset map.
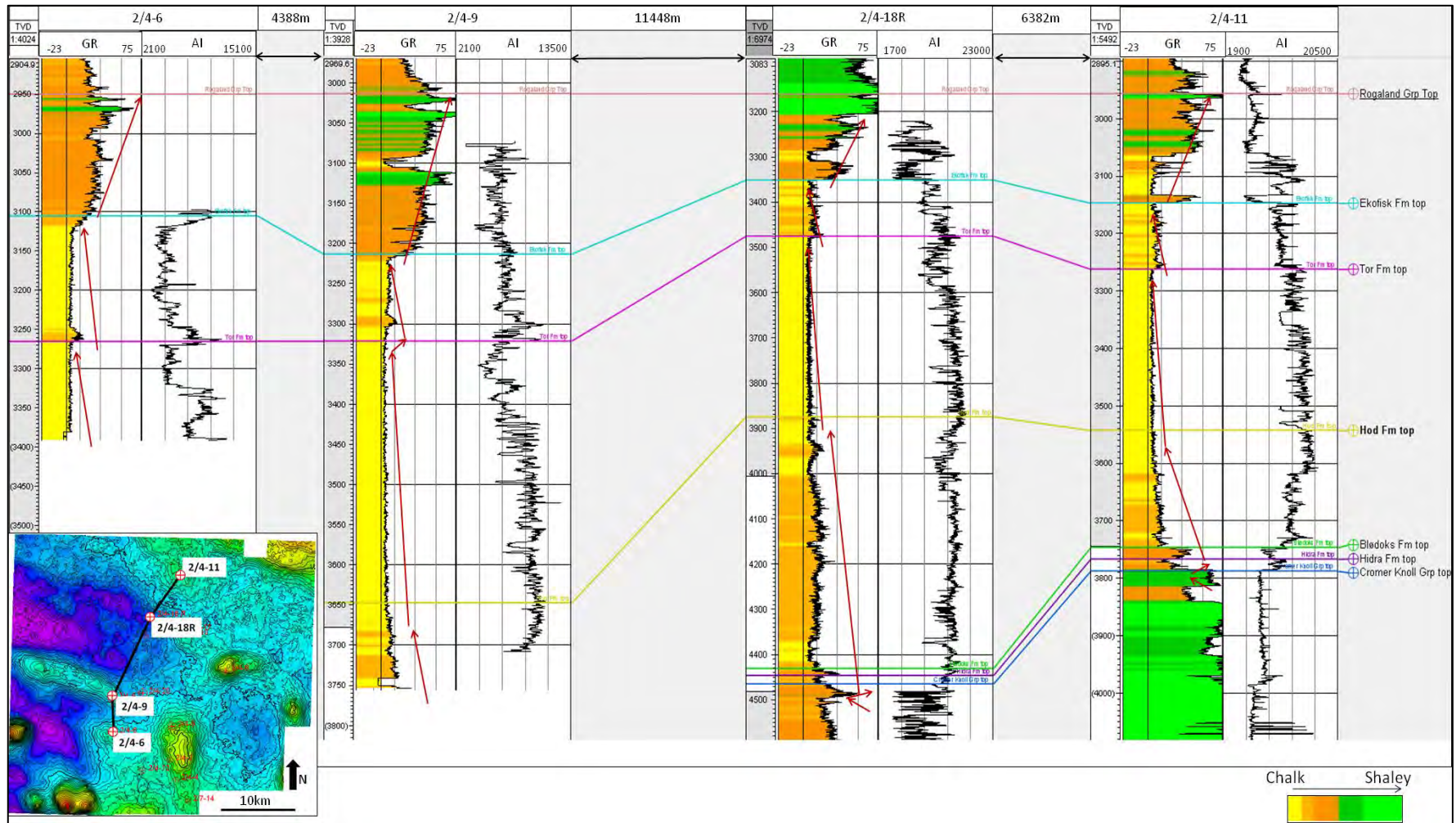
Figure 13 (continued): Well correlation across West Ekofisk Field, Albuskjell Anticline and NAB. The logs are flattened on Rogaland Group Top. The logs displayed are the GR-Gamma Ray log (gAPI), AI-Acoustic Impedance log (kPa.s/m). The red arrows show the general trends of the GR log representing the cyclicity in depositional pattern. Well locations are shown in the TWT top Ekofisk inset map.

5.1.1 Hidra Formation

The Hidra Formation is bounded by the Cromer Knoll Group below and by the Blodøks Formation above (Figures 5 and 7) and is of the Cenomanian age (Isaksen et al., 1989).

5.1.1.1. *Well Logs and cores*

<u>Lithology from cores</u>: This is a highly bioturbated formation comprising of white to light grey, hard chalks with thin interbeddings of grey to black shale in the lower part of the formation (Isaksen et al., 1989). On a local scale, the unit is marlier with interbedded marly chalk and marl (Isaksen et al., 1989).

<u>GR, DT, RHOB characteristics</u>: The gamma ray response shifts constantly to lower values with increasing acoustic impedance moving from the underlying Cromer Knoll Group to the base of the overlying Hidra Formation (Figure 13). Towards the top of this formation the boundary is characterized by a change from chalk lithology to mudstones of the Blodøks Formation (Isaksen et al., 1989) resulting in a jump to higher gamma ray values with lowered acoustic impedance (Figure 13).

5.1.1.2. *Seismic observations*

The Cromer Knoll Group top reflector representing the Base Chalk is generally a weak-medium trough and is relatively continuous in nature (Figures 5 and 7). The top reflector of the Hidra Formation is a weak to medium peak which is also relatively continuous over the entire study area (Figures 5, 7 and 12). The formation in the study area is a very thin unit (Figures 14-22). At places where the formation is relatively thicker especially in the NAB and in the SAB, the reflectors can be characterized as parallel and slightly irregular in nature with low to medium amplitudes (Figures 14, 15 and 16).

In the NAB, the formation reflectors onlap onto the Base Chalk in both the northern and the southern flanks of the NAB and have varying thickness (Figures 14 C and D). On the other hand, along the basin the formation has a relatively uniform thickness and displays no stratal terminations (Figure 15). The basal seismic facies in NAB show good continuity in all directions (Figure 14 and 15) while the reflectors

towards the top are of low amplitudes, transparent and are truncated at the Hidra Formation top in SW-NE direction (Figure 14C).

In the SAB the overall thickness of the formation is relatively uniform (Figures 16 and 17) apart from on the top of the AA where it slightly reduces (Figures 14C and 16). Stratal terminations are not clear in this basin with mostly transparent and low amplitude reflectors. Instead, a discontinuous nature is observed on the flanks of the TGF and AA (Figure 16) and SD1 and WEF (Figure 17). Similar discontinuous nature is also present on the flanks of the WEF and EF (Figure 18). These discontinuous layers convert to continuous layers at a lateral distance away from the flanks towards the basin centers (Figures 16, 17 and 18). In the rest of the area the reflectors are relatively continuous in nature with medium amplitudes.

In the ESB, the formation thins out towards the SE and NE while it is comparatively thicker towards its NW, west and SW (Figures 18, 19 and 20). In this basin on the eastern flank of the EF, the reflectors show discontinuity which becomes continuous towards the basin center (Figure 18). Few progradational features and downlap of sediments also occur in the center of the basin (Figures 19 and 20). The formation is very thin towards the north of the basin but drapes over the TA to reach the SSB. In the SSB the formation is also very thin, as well as on top of the TA. Further north it potentially merges with the BCU (Figures 21 and 22).

Overall the Hidra formation shows a draping nature with relatively continuous and parallel layers and tends to merge with the BCU towards the north and NE of the area.

5.1.1.3. Maps and observations

TWT structures: The time structure map (Figure 11B) of Top Hidra Formation prominently shows two major basins, NAB in the west and SAB in the SW. Two minor basins are also identified as SSB in the NE and ESB in the SE. The basins are the same ones as for the Cromer Knoll Group (Lower Cretaceous) deposits (Figure 11A). The depth of the deepest parts of the NAB and SAB vary between 4460-4780m (3700-3900ms), while in the ESB, it varies between 4195-4460m (3600-3700ms). In the SSB, the depth is comparatively shallow as is in the ESB, ~4195-4321m (~3600-

3650ms). The basins generally are isolated from each other except for the NAB and the ESB which seem to be connected (Figures 11A and B).

TST isochron maps: The isochron map for Hidra Formation (Figure 23) shows the thickest deposition occurring in the NAB. This depocenter trends NW-SE and the formation thickness varies from ~150-250m (60 to ~100ms). In the SAB and ESB the thickness varies from ~75-112m (~30-45ms). In the SSB, although there is a relative structural low (Figure 11B), there is a negligible amount of sedimentation here approximately ~ 38m (~15ms). The connecting area between the NAB and ESB basin also have chalk deposition of ~75m (~30ms) thickness.

Distribution: The distribution of the Hidra sediments from Figure 23 is limited within the NW, SW and in the SE where the main depocenters are located. The sediment distribution is minimal towards the northeastern parts and shows a general thickness of ~38m (~15ms). Generally the depocenters are isolated from each other but the NAB and ESB do have a narrow connectivity trending NW-SE. Overall the formation has a draping nature and drapes all the structural highs in the area.

5.1.1.4. Interpretations

The overall parallel and continuous seismic facies along with a draping nature of the formation indicate an open marine, pelagic depositional environment for the Hidra sediments which is in accordance with the previous studies by Surlyk et al., (2003), Isaksen et al., (1989) based on core and well log interpretations.

The onlapping features observed on the northern and southern flanks of the NAB indicate an increasing water depth leading to an aggradational depositional pattern in the basin. The center of this basin is dominated by undisturbed chalk deposition indicated by the continuous basal reflectors. However, the upper reflectors of the formation are transparent and slightly chaotic indicating possible sediment transportation and redeposition

In the SAB the transition of the discontinuous reflectors on the flanks of the structural highs to continuous reflectors towards the center of the basin also indicate sediment redeposition possibly as turbidites from the highs towards the basin center. This also implies that the structural highs of the SD1, TGF, WEF and AA were active and were uplifting leading to sediment redeposition along their flanks. Although no

stratal terminations are identified, the uniformity in the thickness in the basin also indicates an increasing water depth in the area leading to an overall aggradational seismic facies. Similar behavior of discontinuous reflectors converting to continuous reflectors in the eastern and western flanks of WEF and EF respectively indicates that this area also underwent similar sediment redeposition processes along their slopes (Figure 18). Sediment flows also occurred along the eastern flank of the EF and the sediments ran off to the ESB center towards the ESE as indicated by prograding layers in Figure 18. Studying the distance between the discontinuous reflectors until they become continuous, the run out distance of these sediment flows are short (~3500m in WEF and ~1500m in EF) indicating smaller uplifts of the structural highs. The ESB towards its west and SW are fed with sediments from these redeposition processes and thus show a relatively thicker sediment package. The thickness diminishes to its east and NE indicating low sedimentation rates which also prevails in the SSB.

The isochron map (Figure 23) of the formation indicates a moderate sedimentation rate in the NAB in a NW-SE direction. In the SAB the sediment deposition showing an outwards radiating pattern from the TGF and SD1 confirms that they were active and uplifting during this time. This pattern is due to the halokinetic activity of the SD1 and below the TGF. The very little deposition in the SSB indicate that the depositional conditions are not as preferable as in the other basinal areas possibly due to the relatively higher relief and lower water depths leading to creation of less accommodation space. Breaking the general isolation between the basins, the ESB is connected to the NAB through a confined area (Figure 10) through which sediments are transported from NW to SE into the ESB.

Overall the formation indicates an open marine, pelagic depositional environment with occasional gravity and turbidity flows in the south. Due to the rising sea levels the accommodation space is enough to sustain an aggradational depositional pattern in most of the areas except in the north-eastern parts where the low accommodation space affected the deposition negatively.
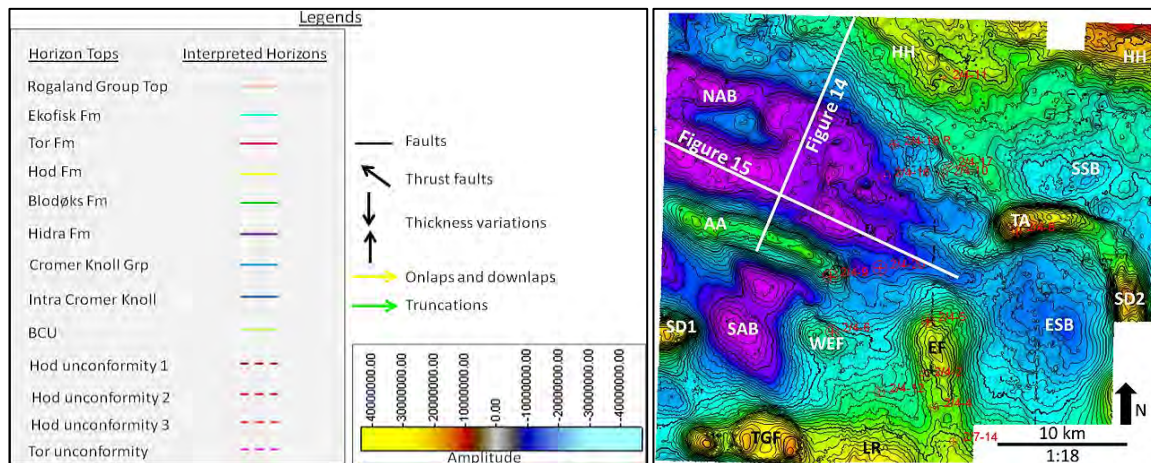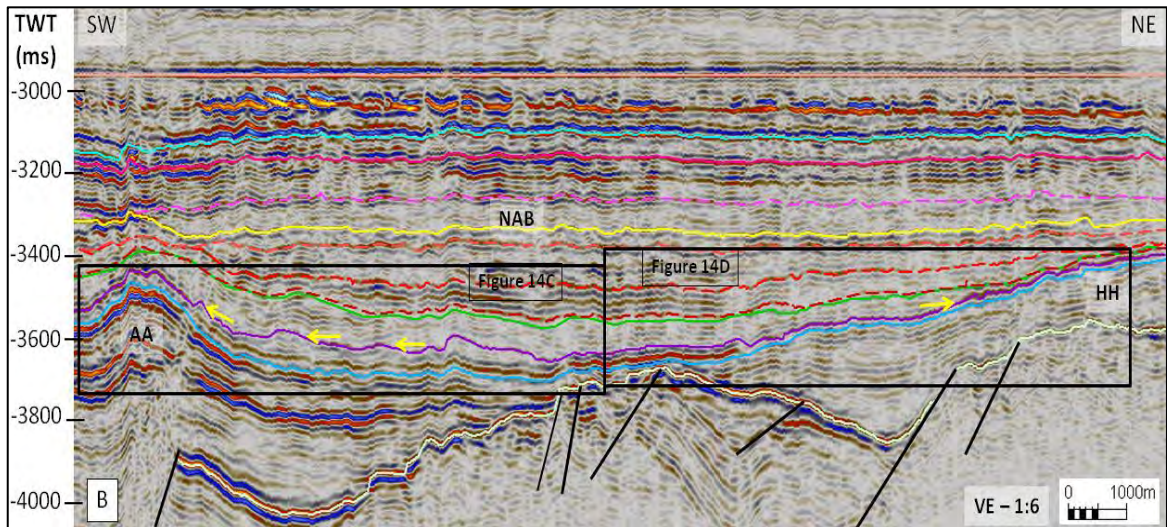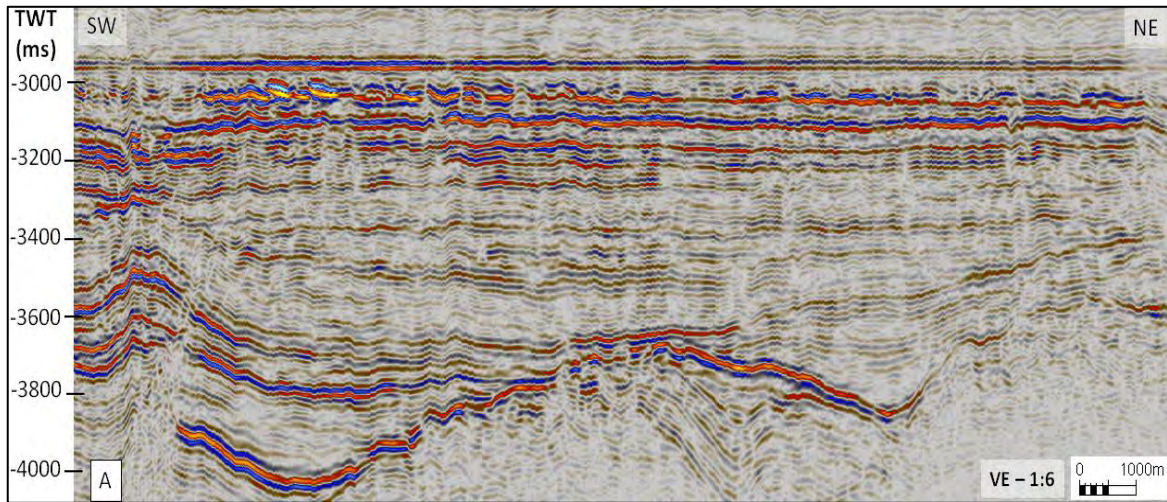
Figure 14: (A) Uninterpreted and (B) Interpreted 3D seismic line flattened on Rogaland Group top taken across the NAB. The location is shown in the inset TWT map of the top Hidra Formation. The formation drapes the structural highs of AA and HH. Overall the formation pinches out towards the NNE of the study area. Closer views of the areas within the rectangles are shown in the Figures 14 C and D.

45
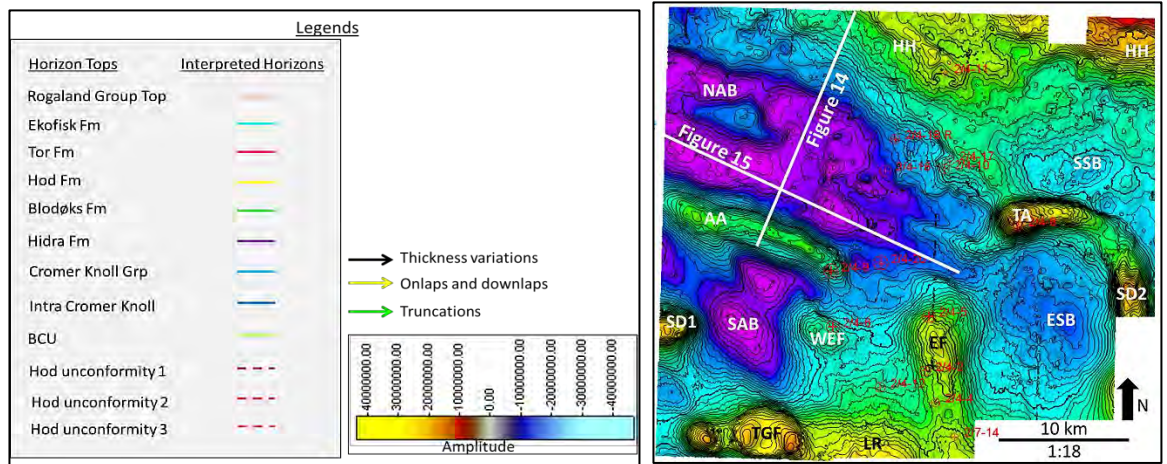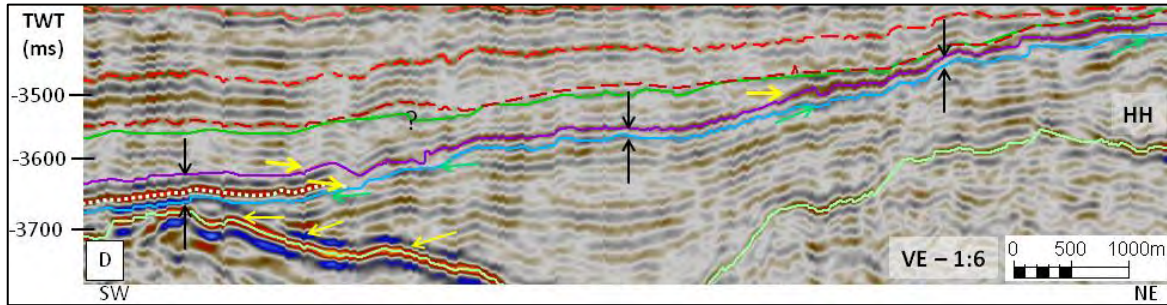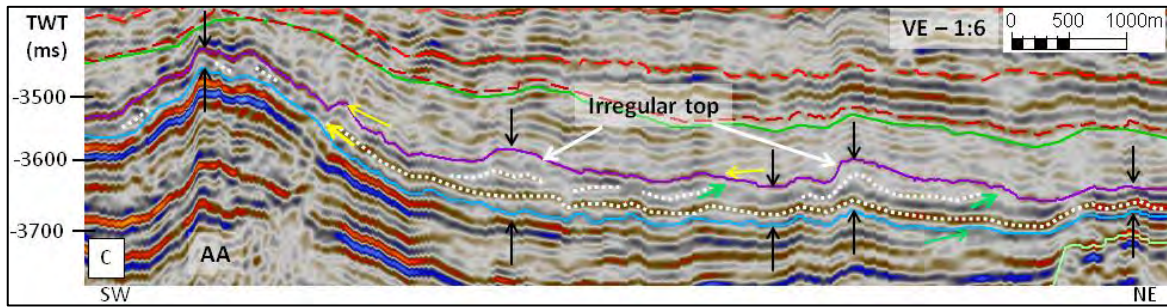
Figure 14 continued: Seismic lines across NAB, illustrating basal continuous layer with medium amplitude onlapping onto the AA and HH and on the base Chalk. The upper layers show discontinuities (white dotted lines) and sometimes truncate at the top of the Hidra Formation. The formation is thicker towards the basin center with an irregular top and tends to thin out towards the structural highs AA and HH (indicated by the black arrow pairs). In figure C the formation pinches out towards the Hidra High (HH). The '?' mark indicates a low confidence area of interpretation. The legend is as shown above. The locations are shown in the inset TWT map of the top Hidra Formation and in figure B.
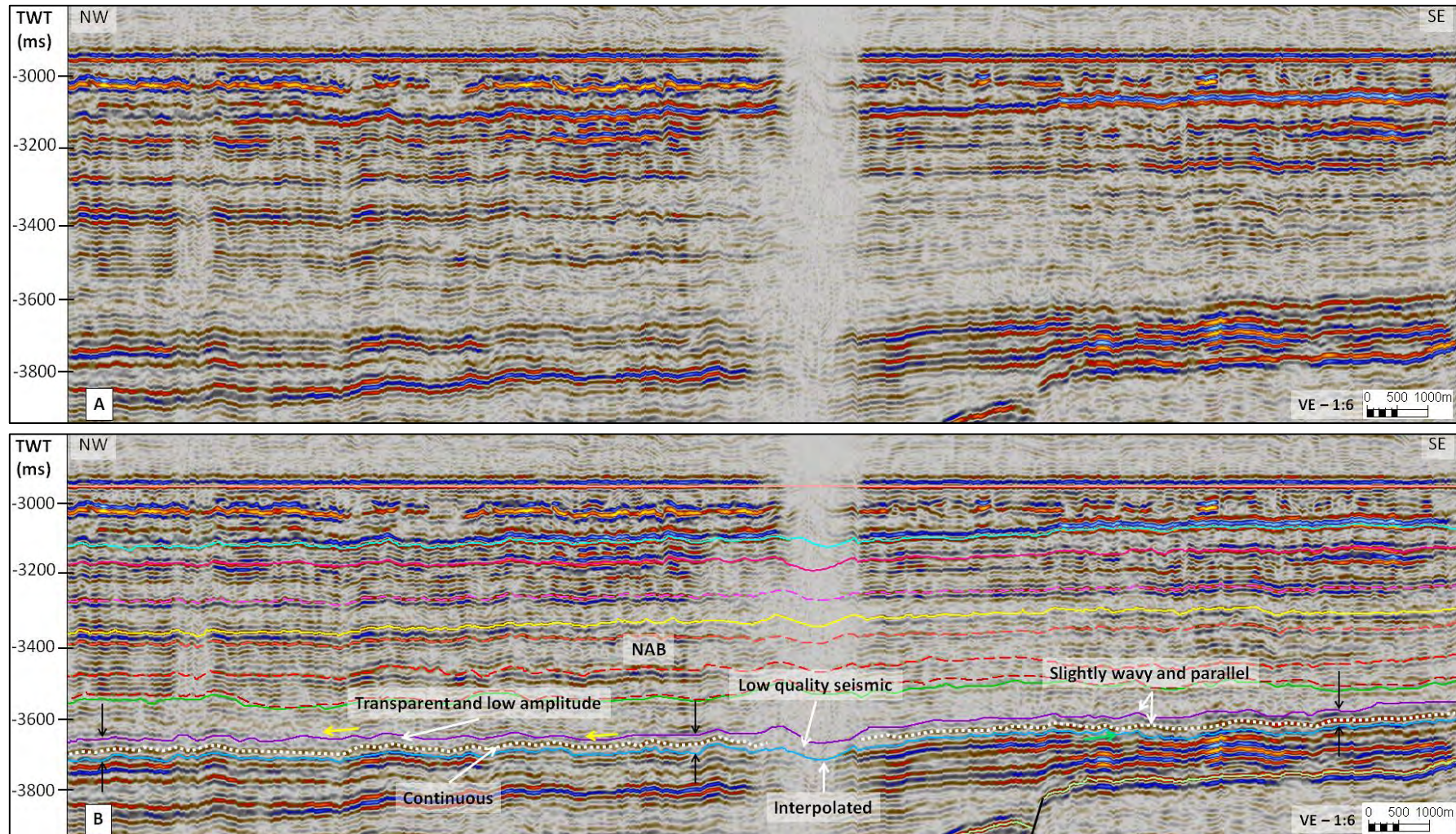
Figure 45: (A) Uninterpreted and (B) Interpreted 3D seismic line flattened on Rogaland Group top taken along the NAB as shown in the inset map of Figure 14. The formation is thin and shows relatively uniform thickness along the basin. The basal reflector shows good continuity apart from the area of poor quality seismic. The reflectors towards the top are very irregular and have low amplitudes. The Hidra Formation top reflector is of weak to medium amplitude and is slightly wavy in nature. The legend is as given in Figure 14.
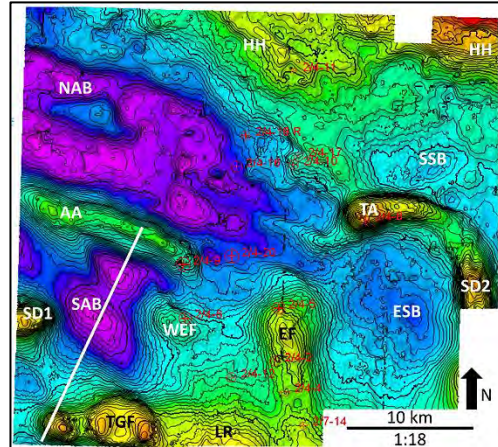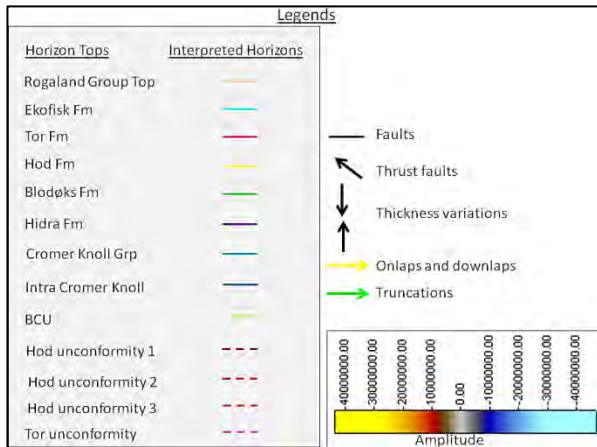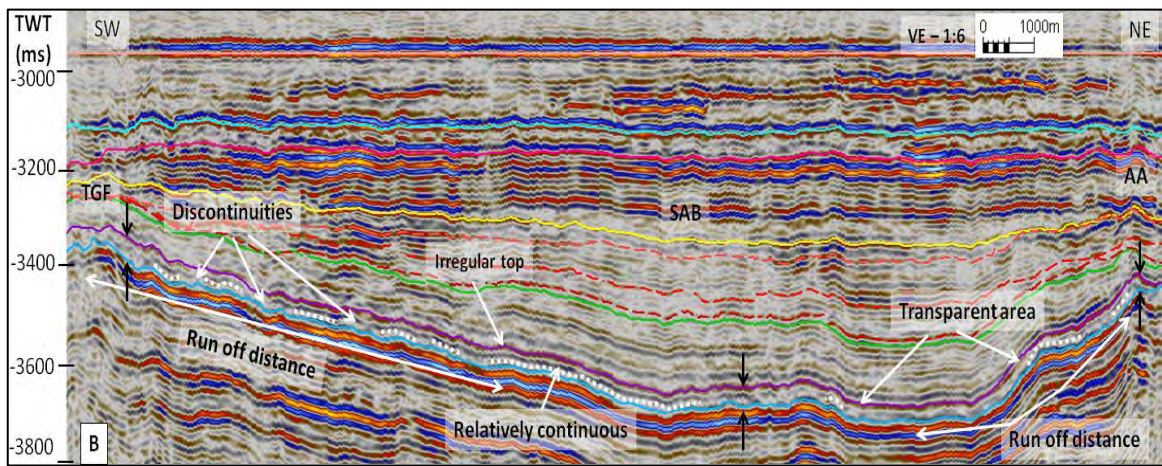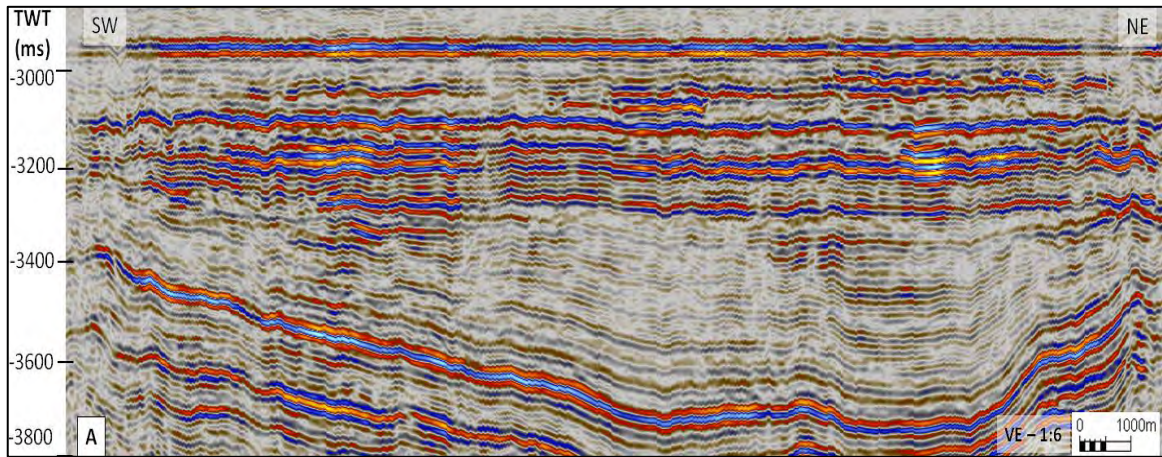
Figure 16: (A) Uninterpreted and (B) Interpreted 3D seismic line flattened on Rogaland Group top in the SAB. In this section the Hidra Formation has uniform thickness (black arrow pairs) although the thickness slightly reduces on the top of the AA. The formation clearly drapes the AA and TGF in this section. The transition of discontinuous layer to a continuous layer is shown indicating the run out distances of the sediments from the flanks of the TGF and AA towards the basin center. This indicates the presence of sediment redeposition processes during the Hidra deposition. Stratal terminations are not clearly observed in this seismic profile. Location of the seismic line is shown in the inset TWT map of the top Hidra Formation.
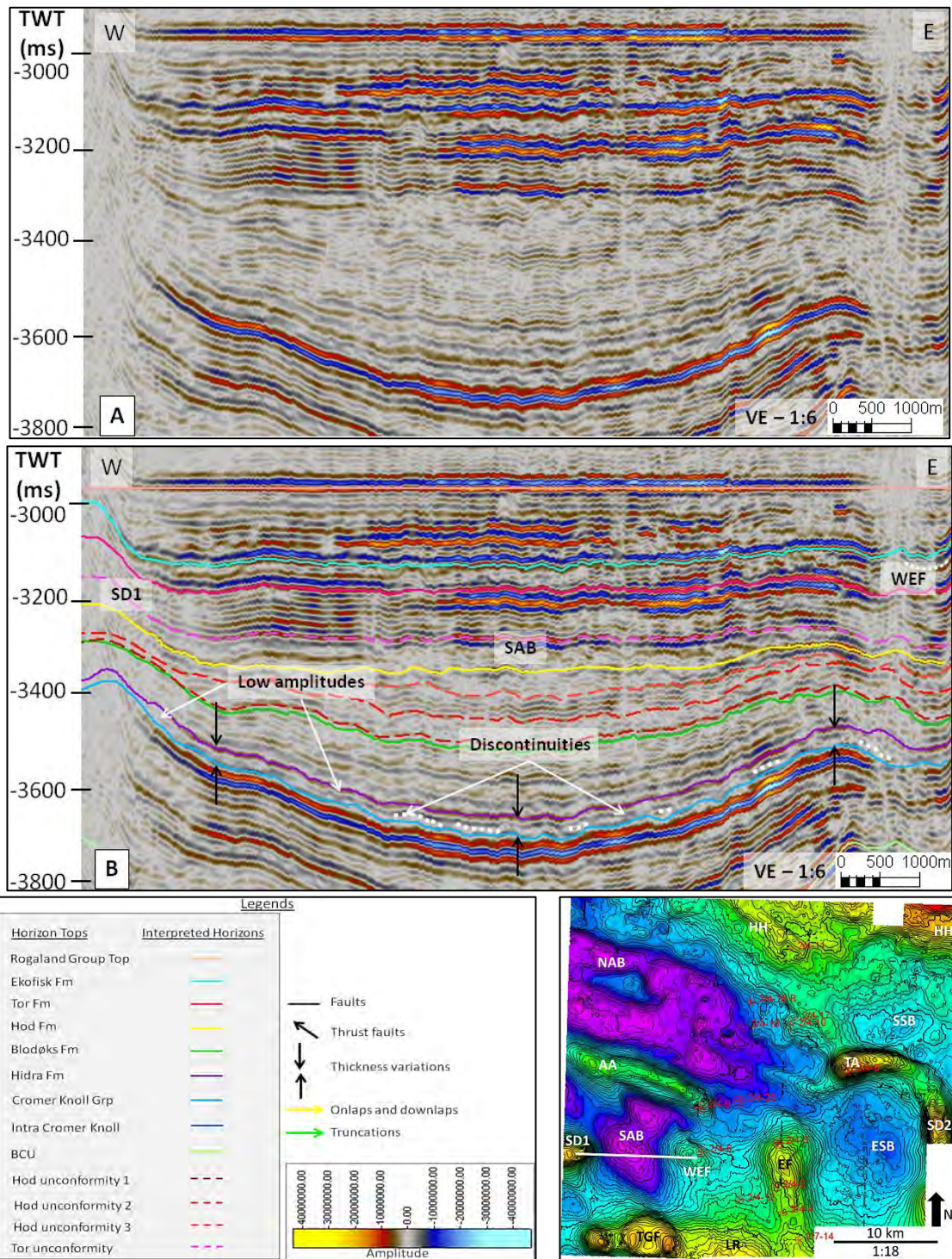
Figure17: (A) Uninterpreted and (B) Interpreted 3D seismic line flattened on Rogaland Group top in the SAB. This section also shows uniform thickness of the formation as shown by the black arrows suggesting draping. The seismic facies is highly discontinuous and have low amplitudes on the flanks of the SD1 and WEF. In the basin center the facies is better in continuity compared to that on the flanks. These might represent redeposited sediments in the basin center from elsewhere and/or from the highs SD1 and WEF. The location is shown in the inset TWT map of the top Hidra Formation.
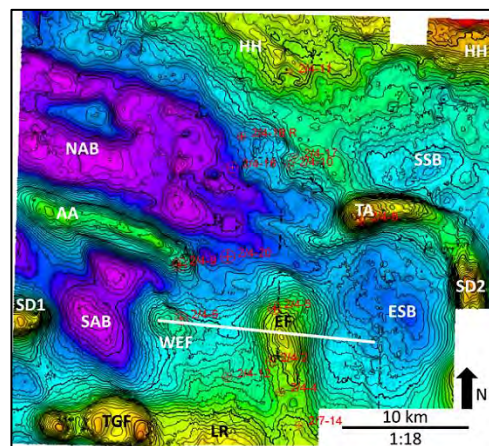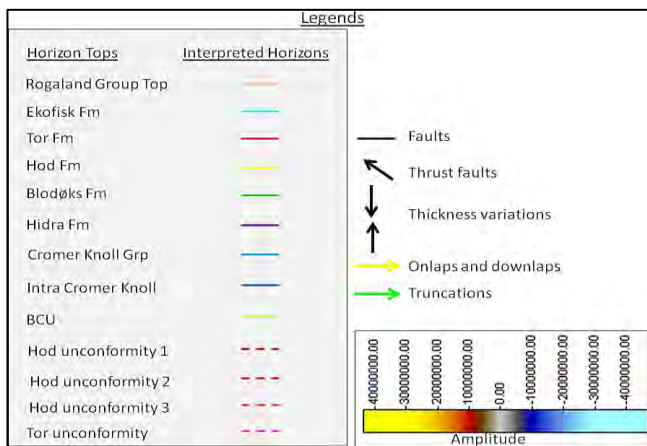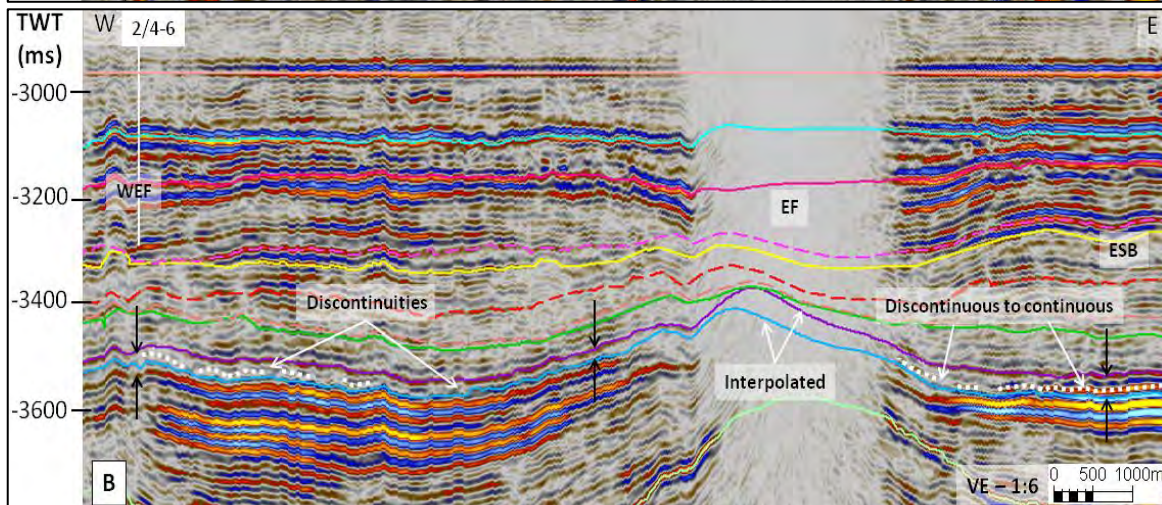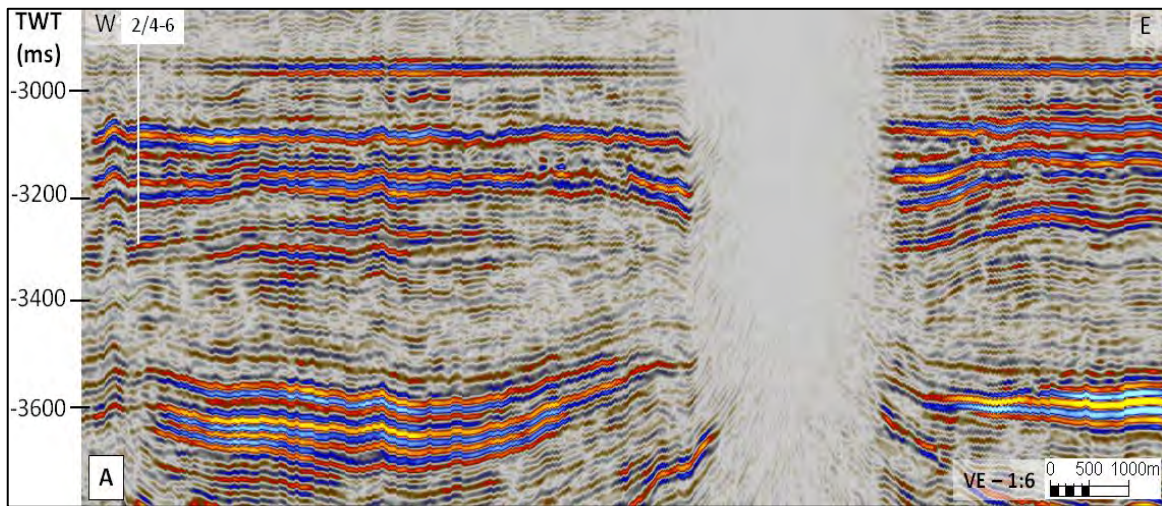
Figure 18: (A) Uninterpreted and (B) Interpreted 3D seismic line flattened on Rogaland Group top between WEF and EF. The section shows a thin but uniform thickness of the Hidra Formation although a slight thinning occurs on the western flank of the EF. The transition of the discontinuous to continuous reflectors especially in the eastern flank of the EF may indicate redeposition of loose sediments towards the ESB center. A similar process likely occurs on the eastern flank of the WEF in west of this profile. In the EF area the interpretations are interpolated. The location is shown in the inset TWT map of the top Hidra Formation

50
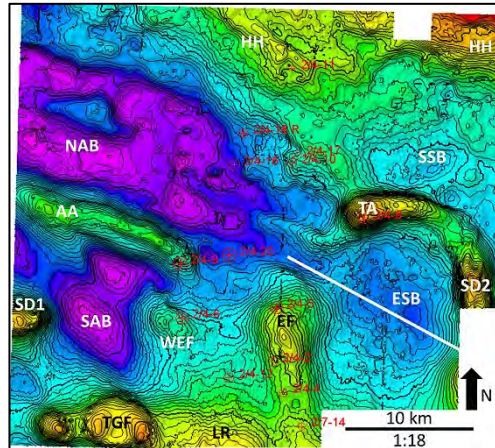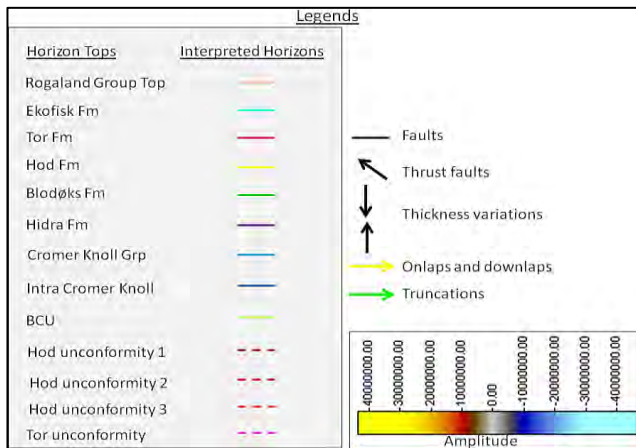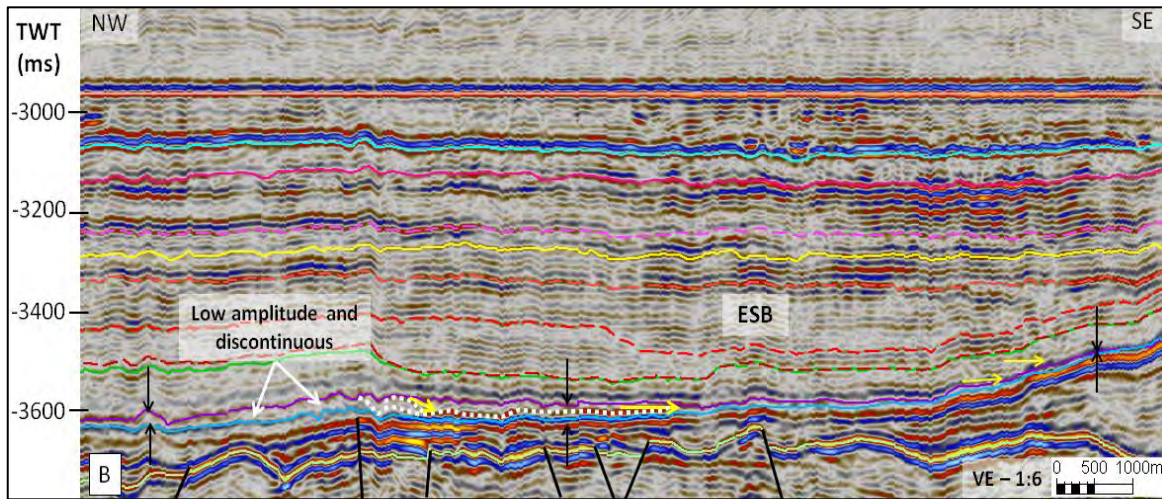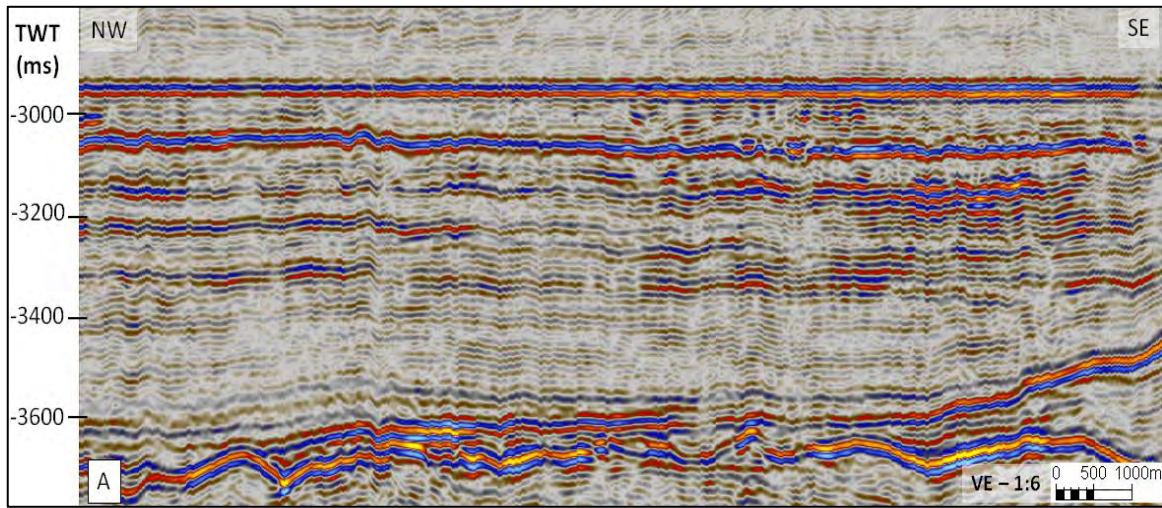
Figure19: (A) Uninterpreted and (B) Interpreted 3D seismic line flattened on Rogaland Group top in the ESB. The formation pinches out towards the SE as pointed out by the black arrow pairs. The Hidra Formation reflectors onlap on the Base Chalk towards the SE as shown by the yellow arrows. Towards the NW the seismic facies is generally discontinuous and chaotic but might display few basinward prograding layers as shown by the downlapping yellow arrow. This possibly indicates sediment transport from the NW towards the SE where the facies becomes continuous in nature. The location is shown in the inset TWT map of the top Hidra Formation.
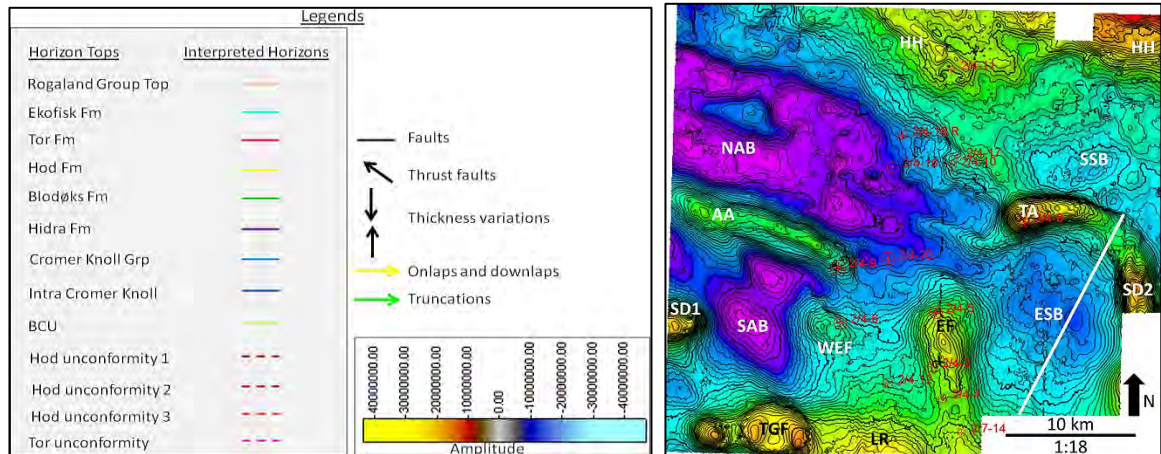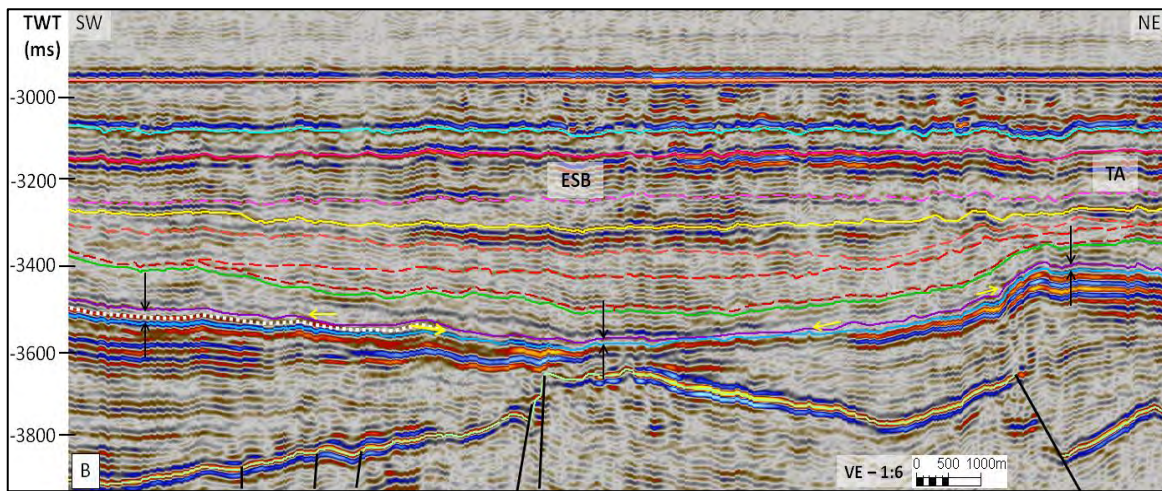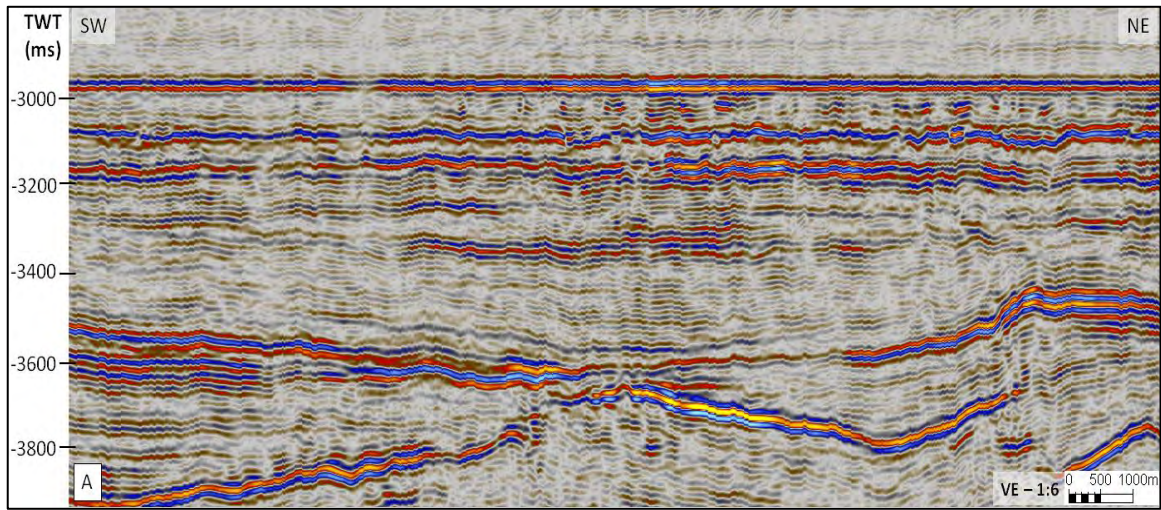
Figure 50: (A) Uninterpreted and (B) Interpreted 3D seismic line flattened on Rogaland Group top in the ESB. The Hidra Formation is very thin in this basin and pinches out further towards the TA in the NE. A continuous reflector in the SW downlaps on the Base Chalk towards the center of the basin as marked in the figure. This indicates a possible sediment source to the basin is from the SW during this time. The location is shown in the inset TWT map of the top Hidra Formation.
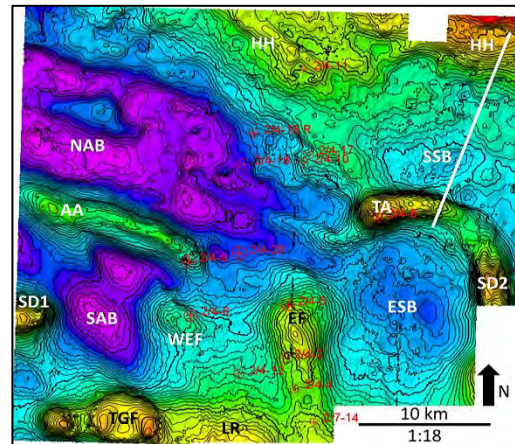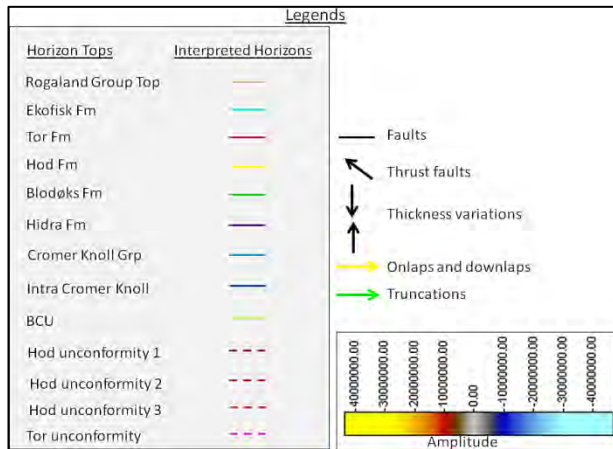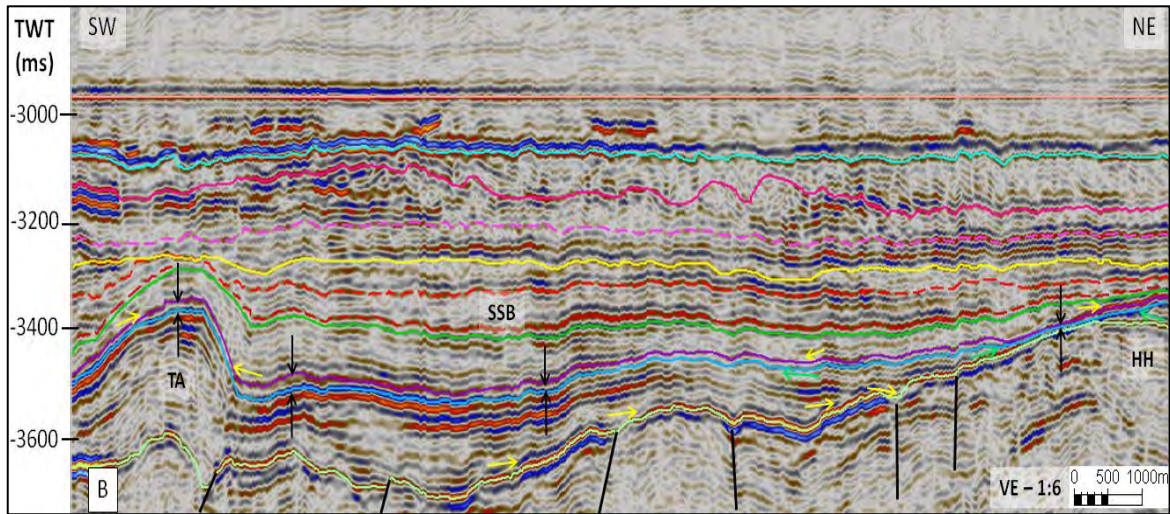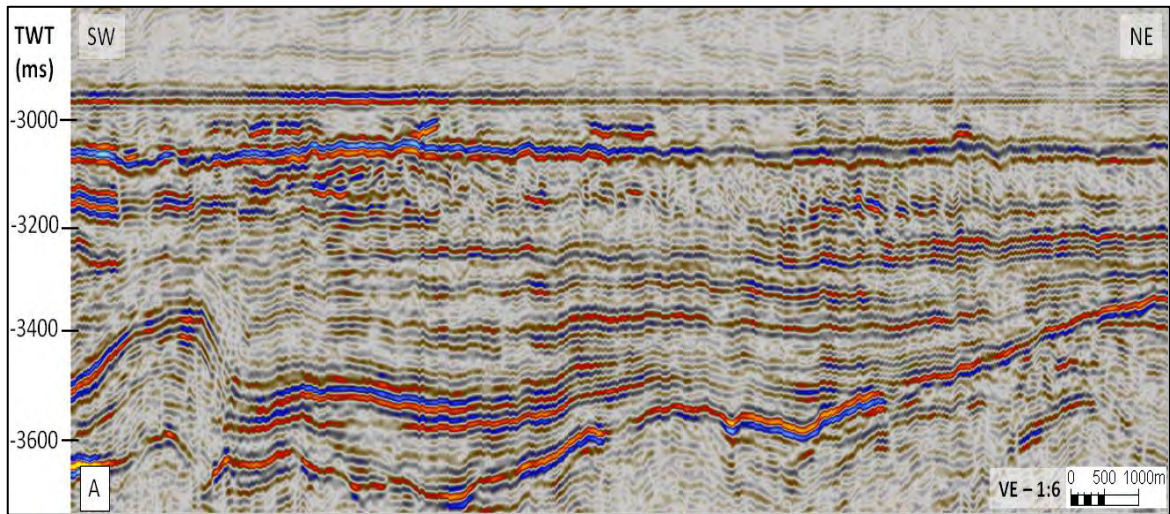
Figure 21: (A) Uninterpreted and (B) Interpreted 3D seismic line flattened on Rogaland Group top in the SSB. The formation is very thin in this basin. Thinning out further towards the HH in the NE, the Hidra Formation potentially mergers with the BCU as shown by the black arrow pairs. Although thin, the formation drapes over the TA in the SW. A slight increase in thickness occurs at the foot of the TA as pointed out (black arrow pairs). The location is shown in the inset TWT map of the top Hidra Formation.

53
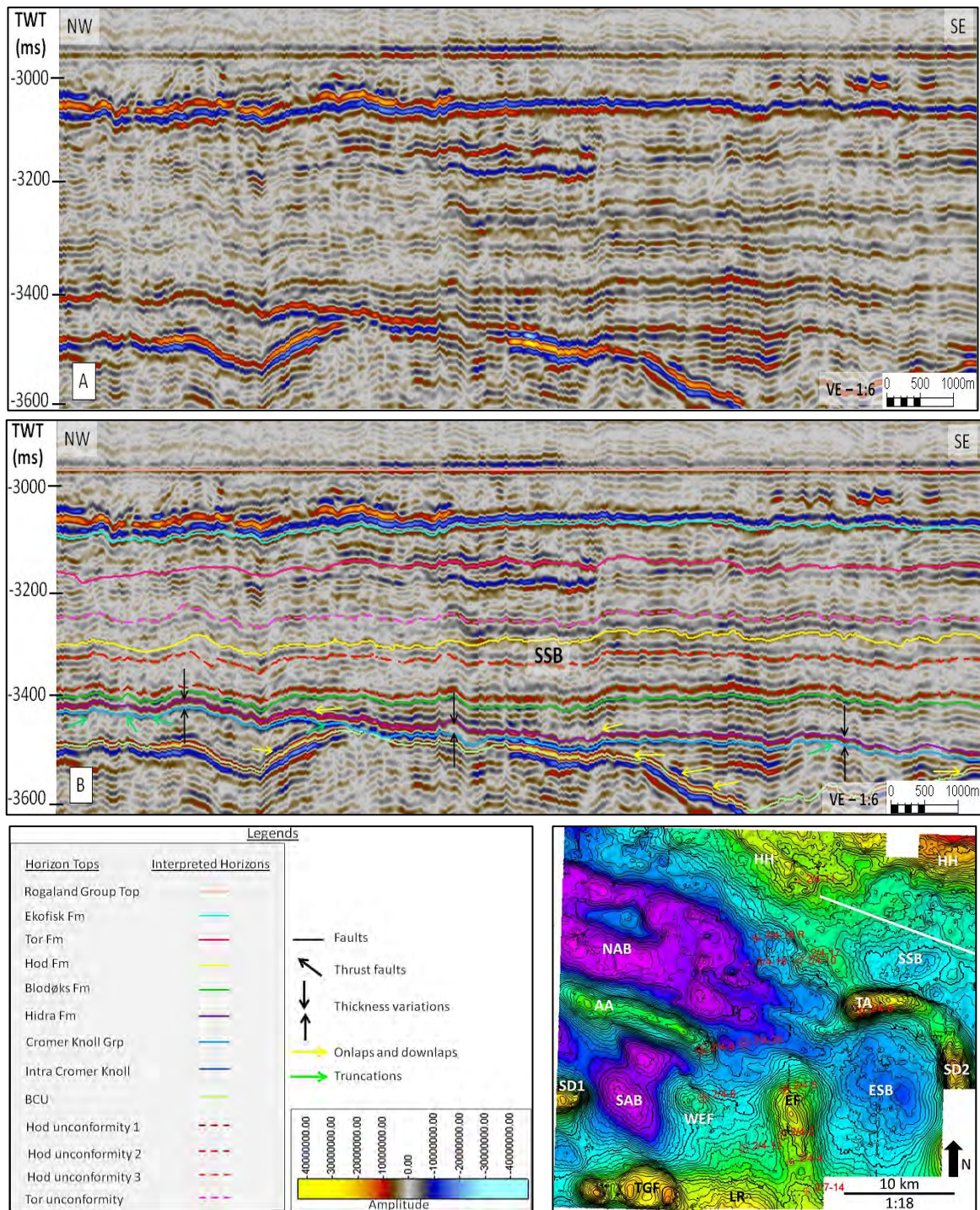
Figure 22: (A) Uninterpreted and (B) Interpreted 3D seismic line flattened on Rogaland Grp. Top in the SSB. The formation is very thin across this basin in an E-W direction. The formation nearly mergers with the BCU in this basin. The BCU has a higher relief in this basin compared to the other basins and thus might be a cause for the thin deposits. The location is shown in the inset TWT map of the top Hidra Formation.
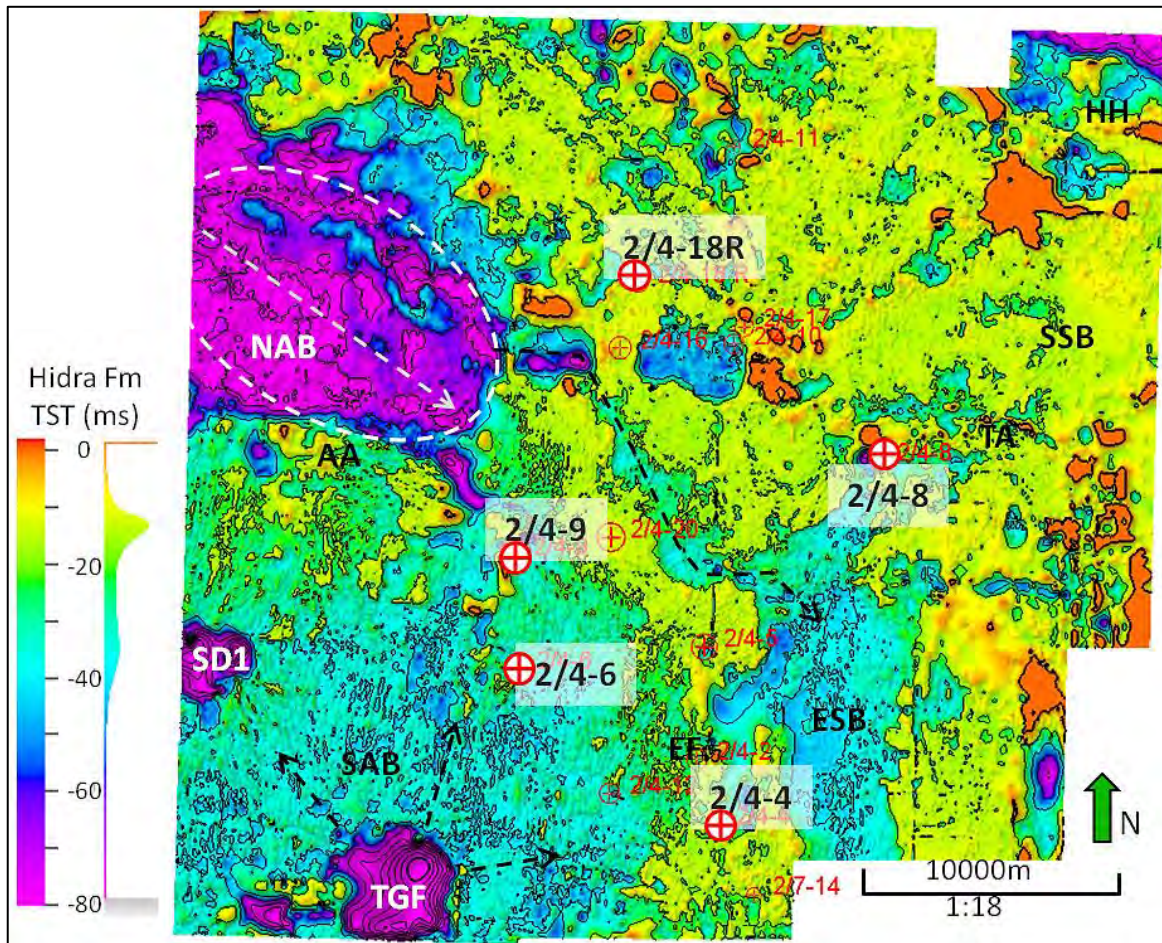
Figure 26: Isochron map of Hidra Formation in the study area. NAB displays thickest deposition of the Hidra deposits especially in the NW of the basin. In SAB and ESB the sediment thickness is equivalent to each other and is second to that in the NAB. The white arrow in the NAB shows that the general thickness trend is NW-SE. The winding black arrow points out the connectivity of sediments between the NAB and ESB running NW-SE as well. This also indicates that NAB acts as a sediment source for the ESB. The black arrows radiating outwards from TGF indicates possible sediment flow directions into the SAB. Noteworthy is that SSB has a minimal sediment thickness although the Hidra TWT map (Figure 11B) shows a relative structural low in the area. The depocenters at the TGF and SD1 are the artifacts of interpolated interpretations and represent a low confidence zone.

5.1.2   Blodøks Formation

The Blodøks Formation is bounded by the Hidra Formation below and by the Hod Formation above (Figures 5 and 7). The formation spans in age from the latest Cenomanian to early Turonian (Isaksen et al., 1989).

5.1.2.1. Well Logs and cores

Lithology from cores: The formation comprises of red, green, grey and black shales and mudstones which are non-calcareous to moderately calcareous in nature (Isaksen et al., 1989).

GR, DT, RHOB characteristics: At the base of the formation, the gamma ray values show a sharp increase moving into Blodøks Formation from the underlying Hidra Formation accompanied by a decrease in acoustic impedance within the formation (Figure 13). This is due to the lower content of carbonate in the Blodøks Formation compared to that in the Hidra Formation (Isaksen et al., 1989). The upper boundary shows a decrease in the gamma ray values and an increase in acoustic impedance moving into a chalkier Hod Formation (Figure 13).

5.1.2.2. Seismic observations

The top of the Blodøks Formation is represented by a generally weak trough while the base of the formation is represented by the relatively continuous, weak to medium peak reflector of the top Hidra Formation (Figures 5 and 7). The formation drapes the whole study area (Figures 24-32) and is identified as an unconformity where several stratal terminations are observed (Figures 24, 25 and 28). This formation is also a relatively thin formation in the study area.

The top reflector of the formation is slightly irregular in nature (Figure 24) and it is continuous on the northern flank of NAB, in the SAB and in the SSB and further north (Figures 24, 26 and 31 and 32). The seismic facies shows discontinuity and truncations in the ESB (Figures 28, 29 and 30), near and around the EF (Figure 28) and towards the southern flank and central part of the NAB (Figures 24 and 25).

In the NAB, the basal reflectors onlap on the Hidra Formation top on both its northern and southern flanks while the layers above drape the area and at places are truncated by the top reflector of the formation (Figure 24). Along the basin, trending NW-SE, the formation reflectors show discontinuities in the central parts of NAB especially in the NW and in the SE as shown in Figure 25. In this figure, in the central part of the basin

a prograding pattern is also observed in the northwesterly direction. In the SE of NAB no such pattern is identified since the reflectors are very chaotic here.

In the SAB the basal reflectors are slightly wavy, continuous and parallel to each other with medium amplitudes, while the upper layers are slightly transparent and have low amplitudes (Figures 26 and 27). The reflectors onlap onto the flank of TGF in the south and drape over the AA in the north (Figure 26). The formation is truncated on the tops of the TGF and AA as pointed out in the Figure 26. In Figure 27, the reflectors show aggradational stacking pattern with good continuity. They drape the structural highs, SD1 and WEF but are truncated on their tops as shown in this figure.

Around the WEF and EF the basal reflectors are relatively continuous while the upper ones are very wavy, discontinuous and are also truncated in this area (Figure 28). On the eastern flank of the EF, in the ESB, the basal reflectors are parallel and continuous while the upper layers show low amplitudes and seem to lie one after another as shown in Figure 28. From Figures 29 and 30 the reflectors of the formation show an overall aggradational stacking pattern. Figure 29 also shows an eroded area in the basin center. Few reflectors in Figure 30 are observed to downlap towards the center of the basin while several onlap and truncate on the flank and on the crests of the TA.

In the SSB, the seismic facies have aggradational stacking pattern and onlaps on the top of the Hidra Formation on the HH, while in the northern flank of the TA the reflectors are not traceable due to their chaotic nature (Figure 31). Figure 32 shows reflectors onlapping on the top of the Hidra Formation towards the NW of the SSB. Few reflectors also hints on possible progradation in the upper part of the formation. The formation becomes relatively thinner towards the north, NE and NW of the SSB where the BCU has a higher relief (Figures 31 and 32).

5.1.2.3. Maps and observations

TWT structures: The time structure map (Figure 11C) of the top Blodøks Formation shows that the NAB and SAB are still the deepest basins while the ESB maintained its depth at ~4460m (~3700ms) becoming comparatively deeper during the Cenomanian until

early Turonian ages. The SSB expanded further towards the north and NE with depths of ~3940-4160m (~3500-3600ms).

TST isochron map: The isochron map (Figure 33) of the formation shows the thickest parts of the formation lie in the depocenters of NAB, SAB, ESB and SSB (~325-400m or ~130-160ms). A shift in depocenter is observed from NW to SE direction in the central part of NAB and the sediment packages pinch out towards the north, NW and SE directions. Comparing this fact in the isochron map with the seismic profiles in this area, a mismatch is observed and points out a low confidence zone.

In the SAB, the formation has an increased thickness of ~325-375m (~130-150ms) in the depocenter compared to ~100m (~40ms) in the Hidra Formation. The center of SAB has the thickest deposition. In the ESB the sediment deposition is more widely distributed in the SE direction and is ~175-250m (~70-100ms) thick. The deposition in the connecting area to NAB is the same as in its surrounding area (~175-225m or ~70-90ms thick). A prominent package of Blodøks sediments of ~250-375m (~100-150ms) thickness is observed in the SSB radially pinching out towards the NE and NW (Figure 33).

Distribution: The overall sediment distribution from Figure 33 indicates that major deposition occurred in the depocenters of NAB, SAB, SSB and ESB (~250-400m or ~100-160ms thick) and the structural highs were draped with sediments of ~25-125m (~10-50ms) thickness. The sediments are further distributed in the NE developing a thick sediment package in the SSB area. The ESB deposits also distributed further towards the SE (~100-250m or ~40-100ms) compared to that in the Hidra Formation (Figure 33). Although the deposition radially widened thickening towards the NE, the HH experienced very low amounts of sedimentation (~25-38m or ~10-15ms). In the SAB the deposition is now bounded and restricted between the AA in the north, SD1 in the west, TGF in the south and WEF in the east.

Figure 27: (A) Uninterpreted and (B) Interpreted 3D seismic line flattened on Rogaland Group top in the NAB. An irregular Blodøks Formation top drapes the AA in the SW while onlaps onto the northern flank of the basin as shown by the yellow arrows. Truncations of several internal reflectors at the formation top and several stratal terminations of the overlying layers indicate that it represents an erosional unconformity in the NAB. Small truncations at the crest of AA indicate its slow uplift during the deposition. The reflectors show moderate continuity in this section. The formation is thin on the structural highs and is thick at the center of the basin. The location is shown in the inset TWT map of the top the Hidra Formation.

59
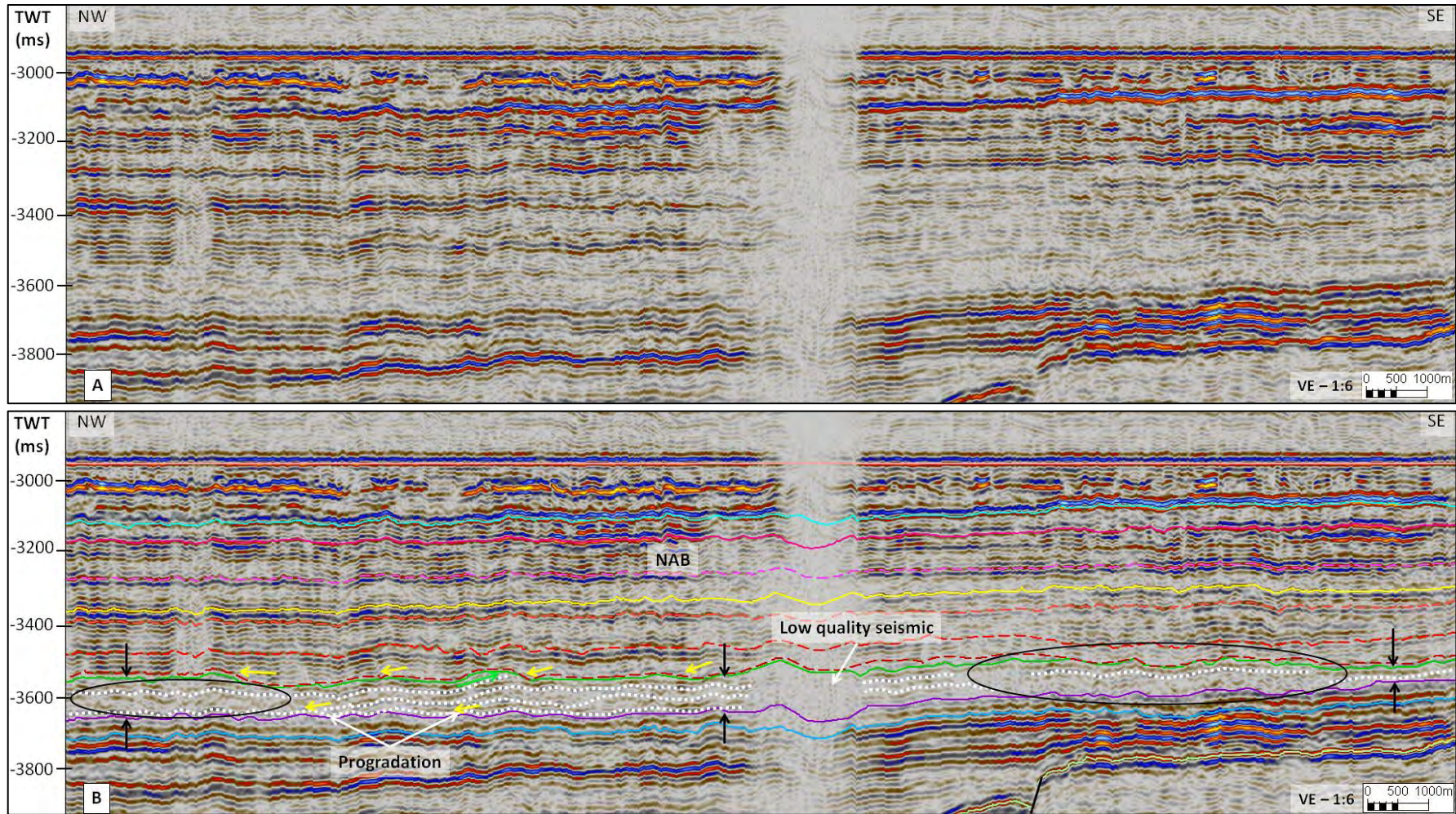
Figure 28: (A) Uninterpreted and (B) Interpreted 3D seismic line flattened on Rogaland Group top in the NAB. The continuous basal reflectors downlap on the Hidra Formation top while the whole formation progrades towards the NW indicating a possible subsidence in the NW. The encircled areas point out the discontinuous and chaotic seismic facies in the Blodøks Formation indicating possible sediment flows from different directions. The downlaps of the overlying formation reflectors confirm the Blodøks Formation top as an unconformity in this basin. The formation is thick towards the NW and becomes thin towards the SE of the basin shown by the black arrow pairs. The Legend and the location are as shown in Figure 24.
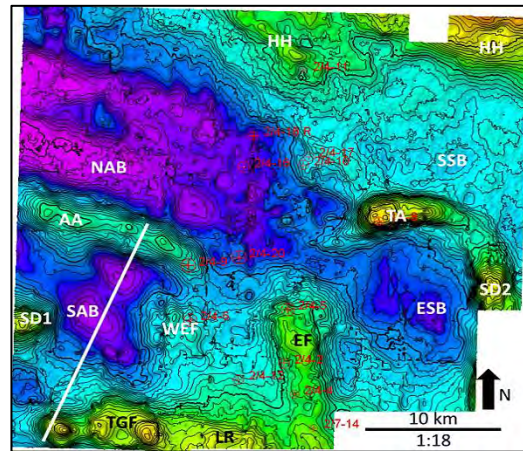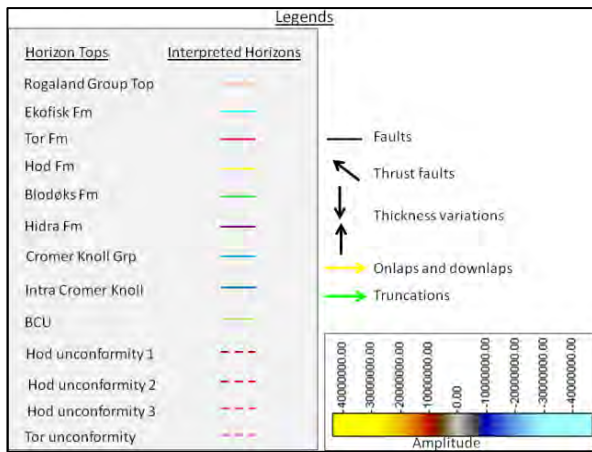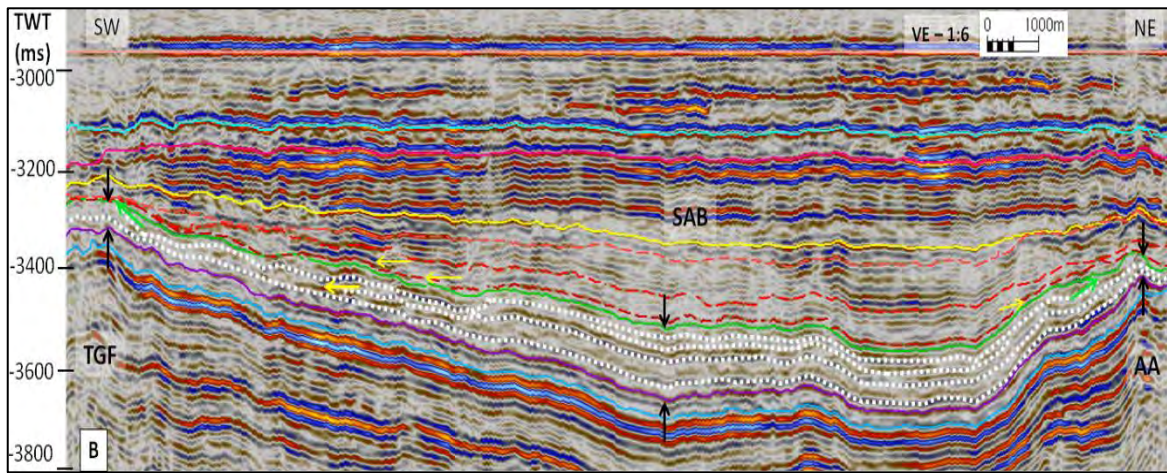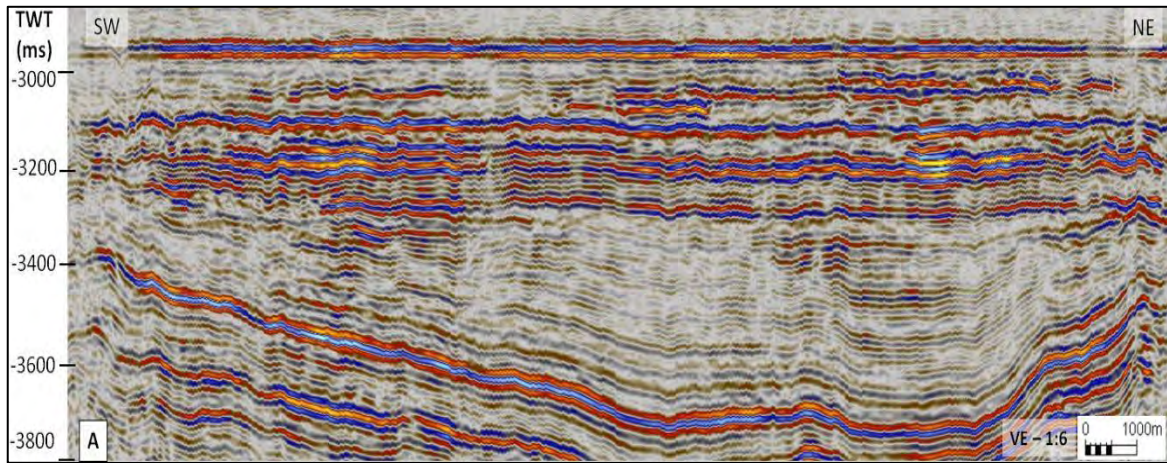
Figure 29: (A) Uninterpreted and (B) Interpreted 3D seismic line flattened on Rogaland Group top in the SAB. A continuous and parallel seismic facies is observed in this profile. The base of the Blodøks Formation show draping characteristics over the TGF and the AA. The upper reflectors of the formation are truncated at the top of the TGF and AA as shown by the green arrows. As a result the thicknesses of the formation on the top of these structural highs are thinner than that in the basin center. A few reflectors show onlapping onto the TGF flank. The location of the seismic line is in the inset TWT map of the top Blodøks Formation.
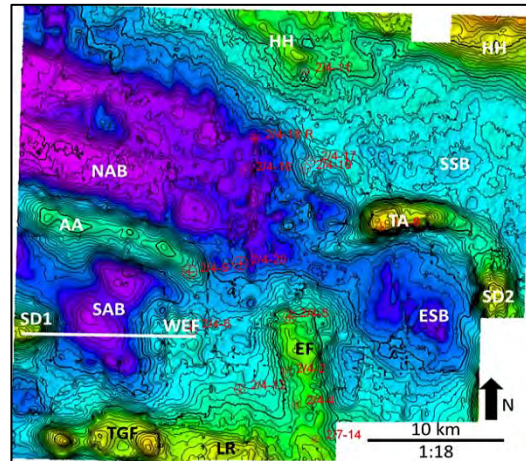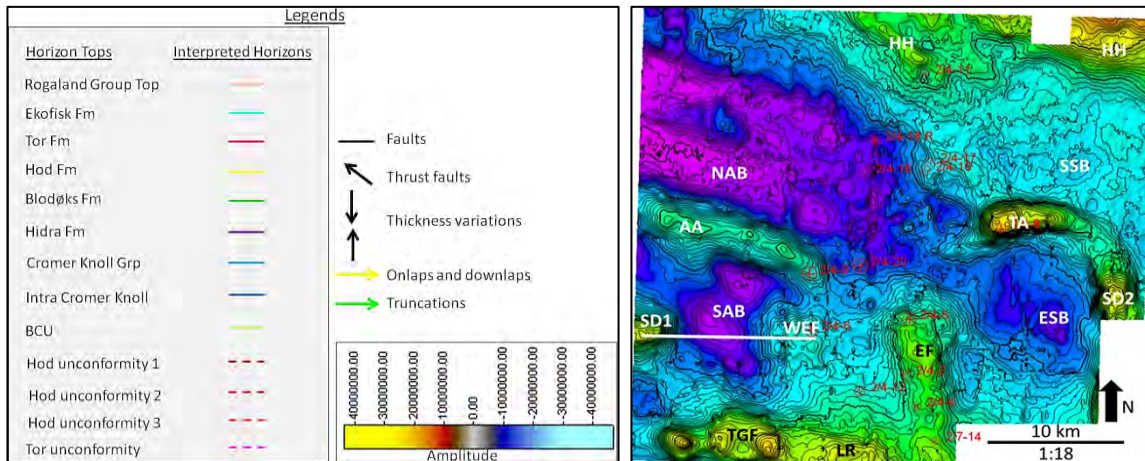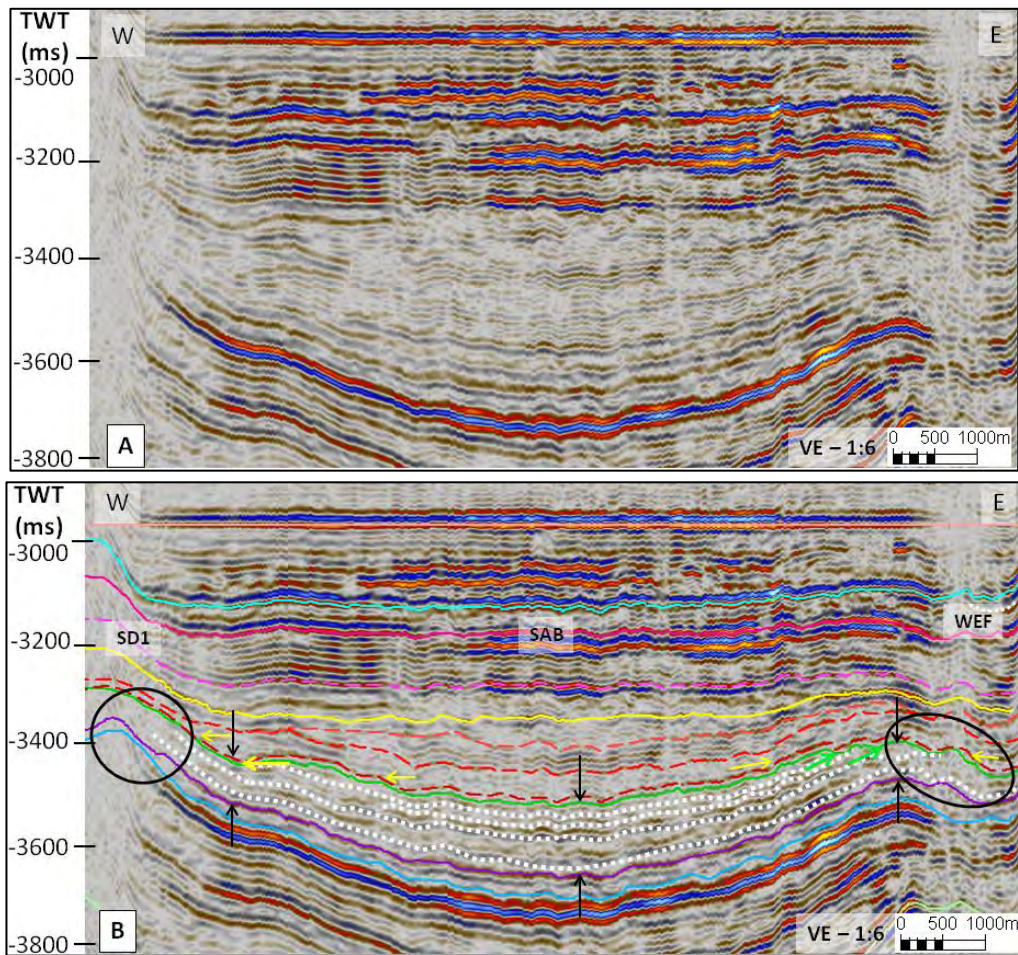
Figure 210: (A) Uninterpreted and (B) Interpreted 3D seismic line flattened on Rogaland Group top in the SAB. The reflectors have good continuity and the basal reflectors show draping characteristics as they cover the structural high WEF. The upper reflectors of the formation are however truncated by the formation top reflector (marked by the green arrows) in WEF. The encircled area in the WEF shows chaotic seismic facies indicating possible gravity flows towards its eastern flank. The encircled area in the SD1 shows low seismic resolution and thus the reflectors could not be traced further. The thickness of the formation is less on the structural highs as a result of erosion while the basin center shows thick sediment package. The location is shown in the inset TWT map of the top Blodøks Formation.
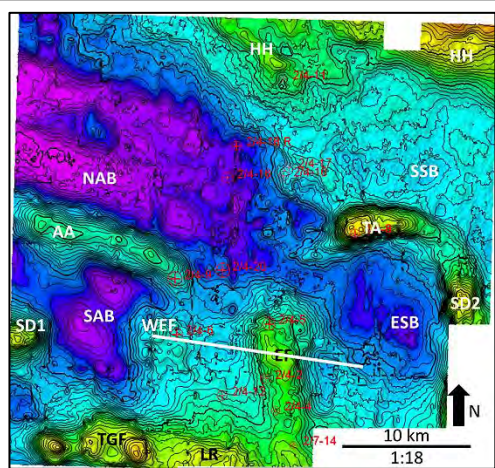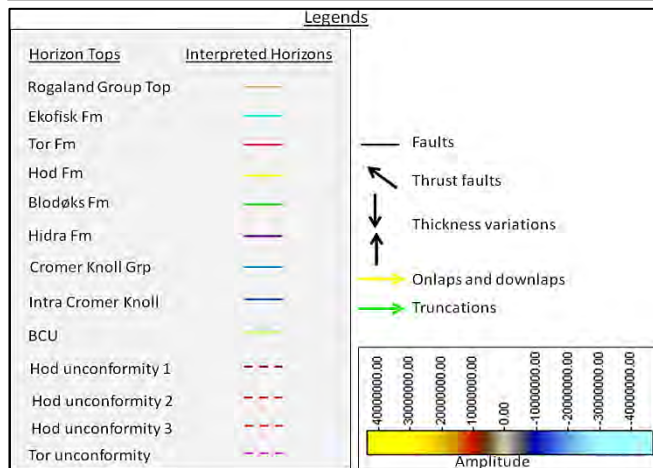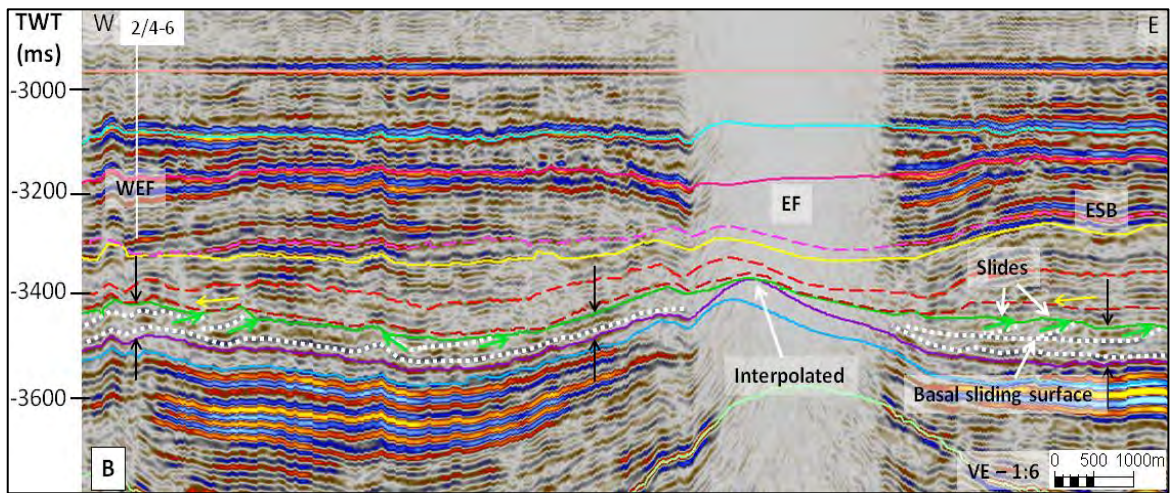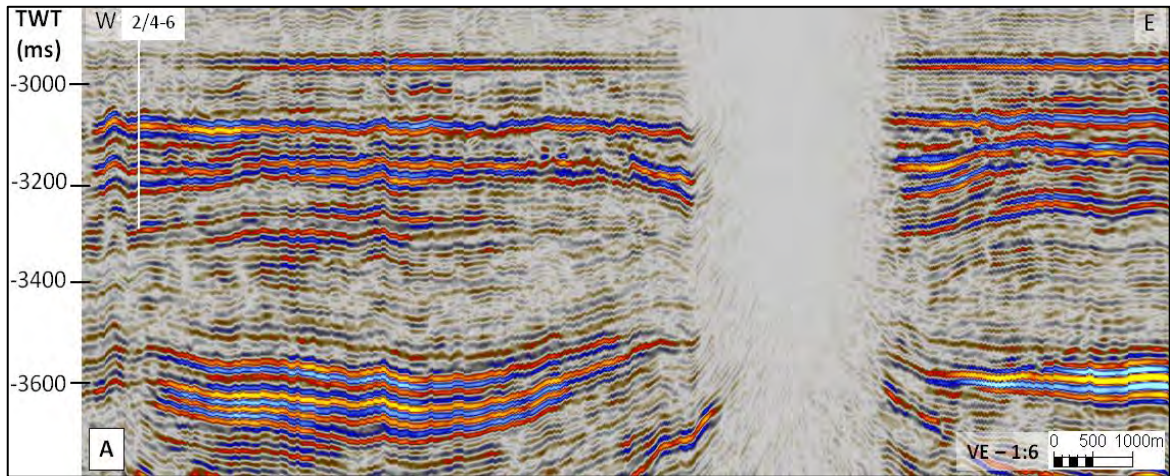
Figure 211: (A) Uninterpreted and (B) Interpreted 3D seismic line flattened on Rogaland Group top in the SAB. The formation shows relatively uniform thickness between WEF and EF while it shows slightly varying thickness towards the ESB. In between the WEF and the EF, the basal reflectors are continuous in nature and have medium amplitudes while the upper reflectors are weak and discontinuous and are truncated by the formation top. In the east, in the ESB, possible sediment slides occurred in phases which were then truncated on their tops by the formation top as pointed out by the green arrows. This indicates possible uplift of the EF in phases during this time. The location is in the inset TWT map of the Blodøks Formation top.
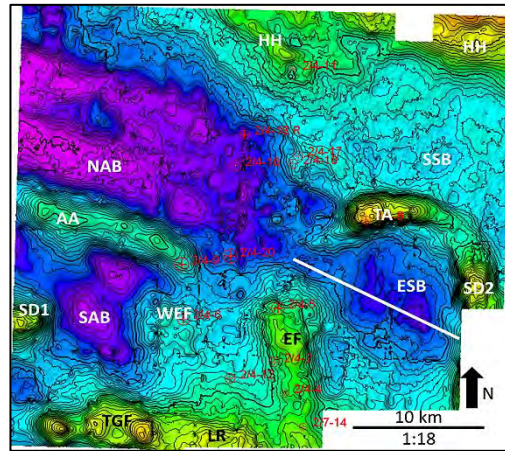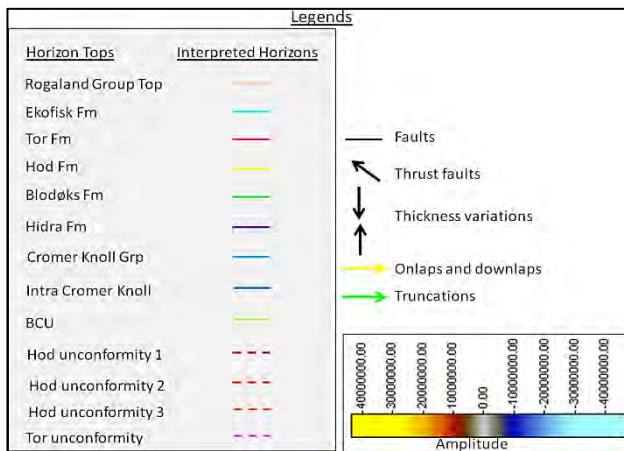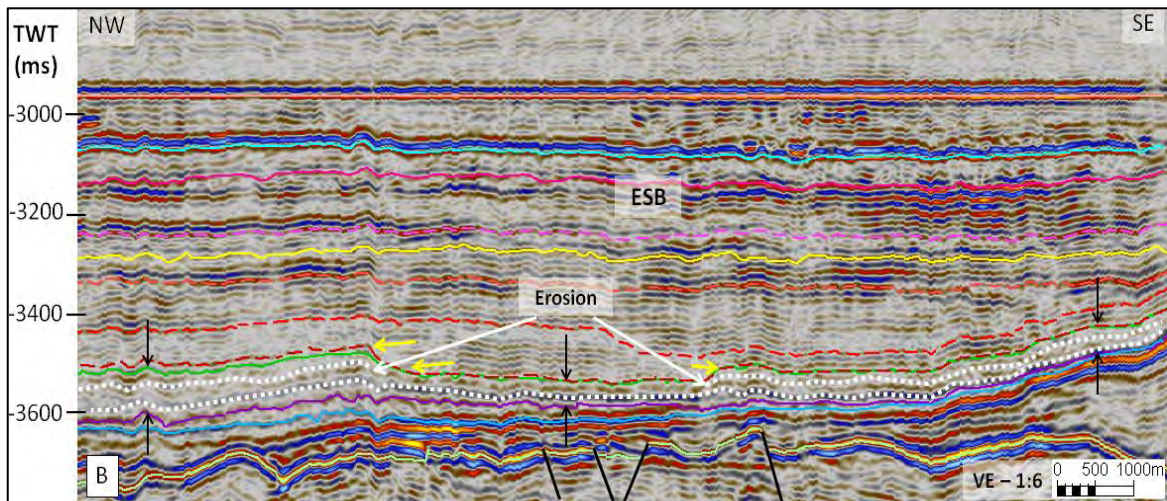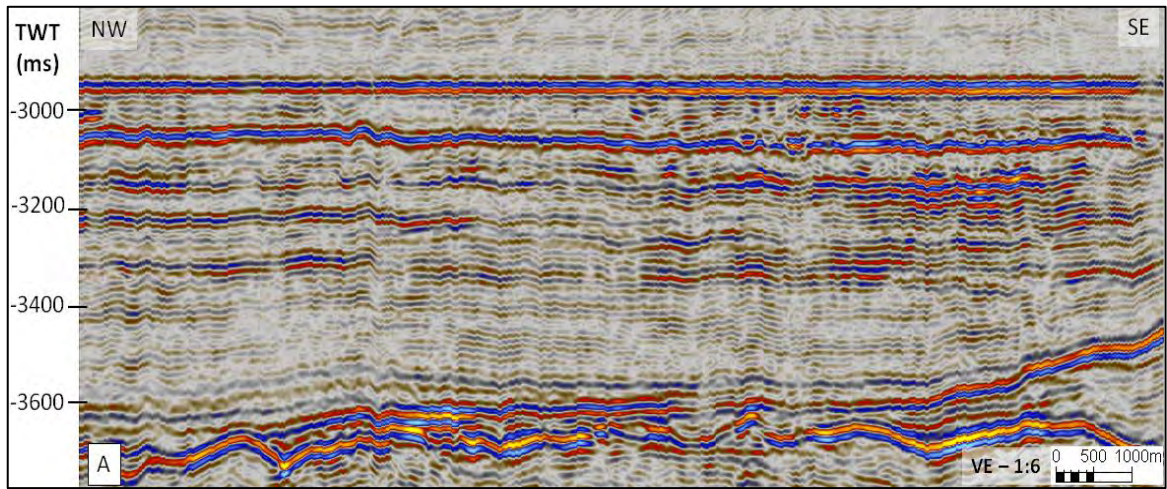
Figure 212: (A) Uninterpreted and (B) Interpreted 3D seismic line flattened on Rogaland Group top in the ESB. The Blodøks Formation is overall thin in the ESB as shown by the black arrow pairs. In the NW the thickness is higher compared to that in the SE indicating more sediment input from the NW. The center of the basin shows a possible eroded area (the area between the white arrows). The reflectors show parallel draping behavior in this basin also. The top of the formation represents an unconformity here too as several overlying formation layers terminate at it. The location of the line is shown in the inset TWT map of the top Blodøks Formation.

64
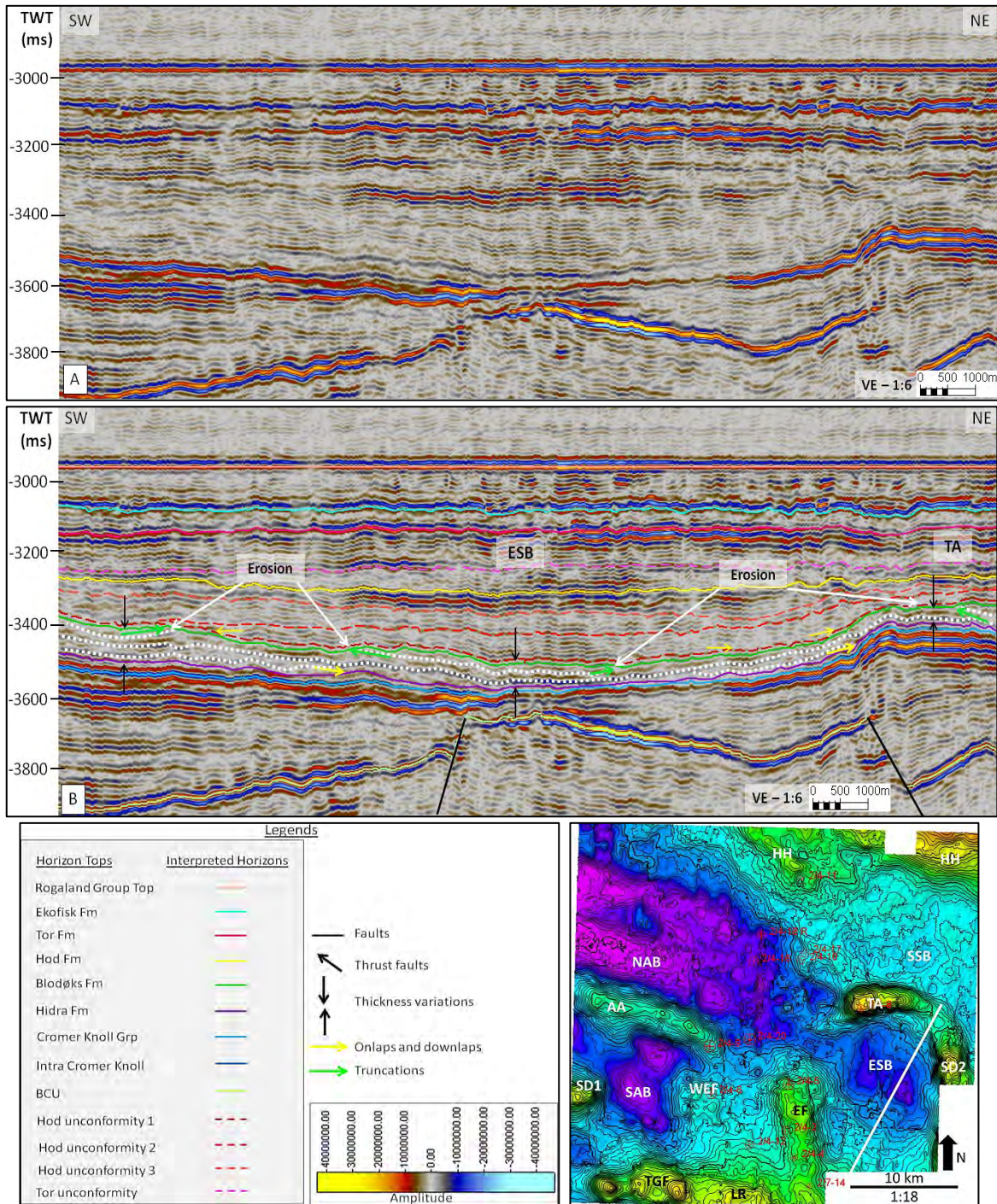
Figure 30: (A) Uninterpreted and (B) Interpreted 3D seismic line flattened on Rogaland Group top in the ESB. The formation is overall thin in this profile in ESB. It is thicker in the SW compared to that near and on top of the TA indicating more sediment input from the SW. Stratal truncations due to erosion as marked in the figure are the possible reasons for a thinner sediment package at the TA. Eroded surfaces are also present in the SW (marked in the figure) but cover a smaller area compared to that near the TA. Reflectors onlap onto the flank of TA (as shown in figure) and few parallel reflectors from the SW downlap towards the center of the basin (as shown in the figure). This also indicates a possible sediment source towards the SW of the basin. The location of this line is shown in the inset TWT map of the top Blodøks Formation.

65
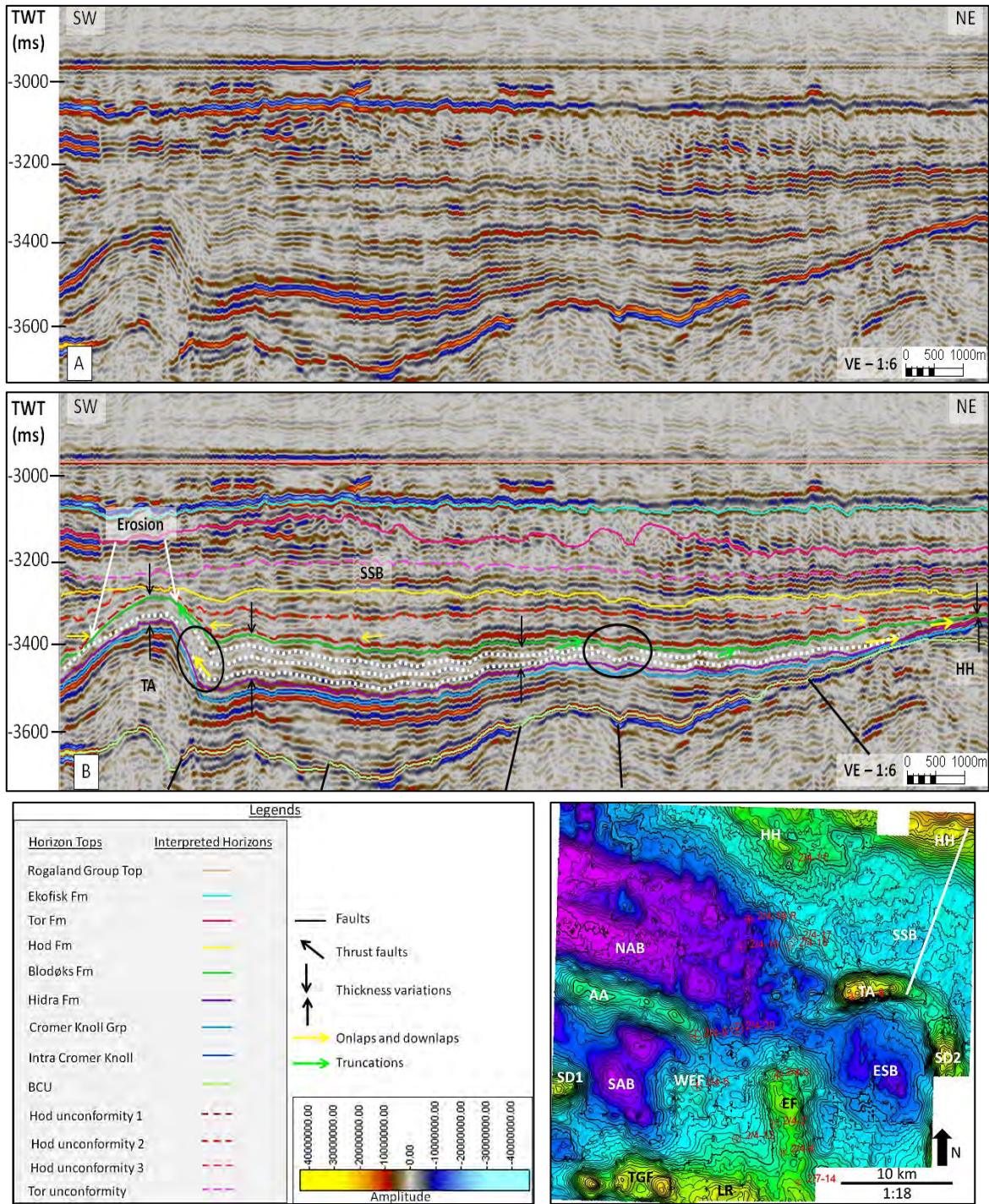
Figure 31: (A) Uninterpreted and (B) Interpreted 3D seismic line flattened on Rogaland Group top in the SSB. The formation clearly pinches out towards the NE as shown in the figure. The formation reflectors onlap on the Hidra Formation top onto the HH and TA flanks. Towards the SW on the top of TA the upper reflectors of the formation are eroded off (as pointed out). On the northern flank of the TA the encircled area shows the chaotic behavior of the reflectors indicating sediment movements. The encircled area towards the NE of the basin shows truncated reflectors due to erosion and forms a small indentation. The location is shown in the inset TWT map of the top Blodøks Formation.
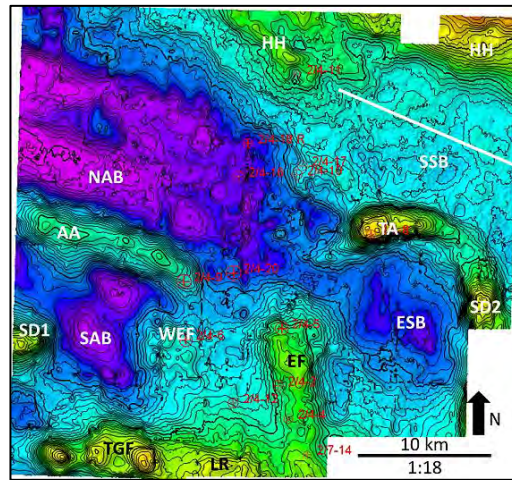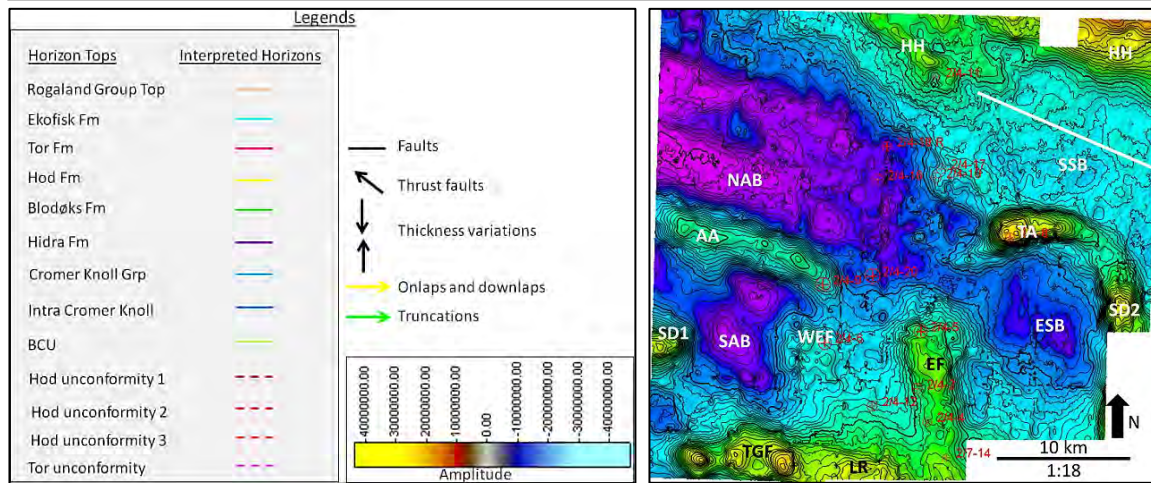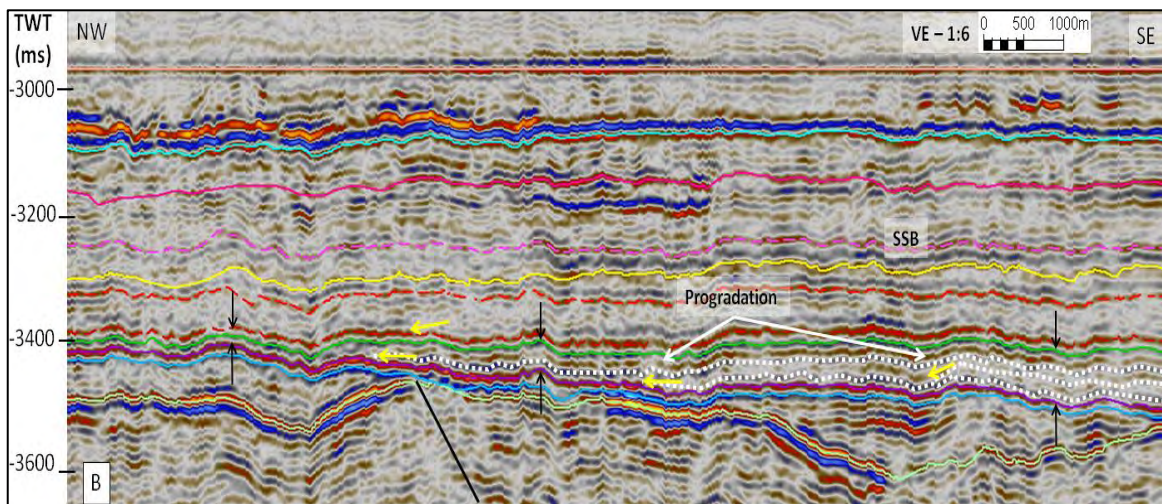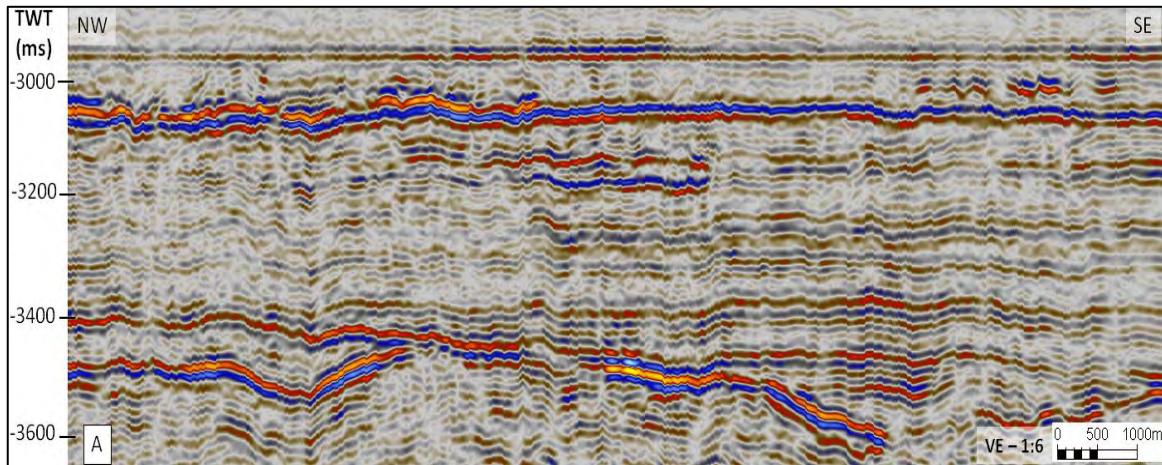
Figure 32: (A) Uninterpreted and (B) Interpreted 3D seismic line flattened on Rogaland Group top in the SSB. The Blodøks Formation has decreasing thickness towards the NW as shown by the black arrow pairs. The internal reflectors of the formation onlap on the Hidra Formation top towards the NW (shown by the yellow arrows). Few overlying formation reflectors downlap on the Blodøks Formation top and thus makes it an unconformity in the SSB. The location is shown in the inset TWT map of the top Blodøks Formation.
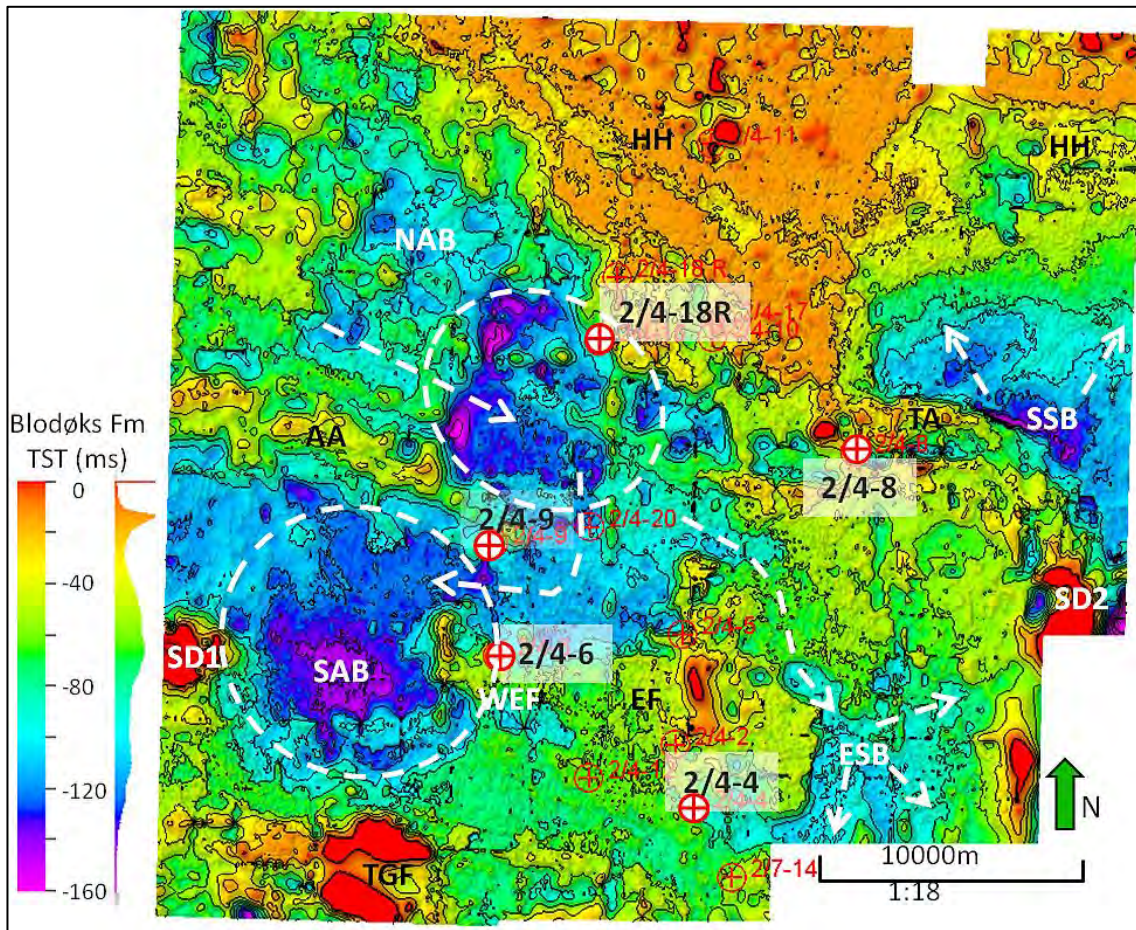
Figure 33: Isochron map of Blodøks Formation in the study area. The thickest sediments are found in the NAB and SAB. A new thick sediment package developed in the SSB. This thins radially outwards towards the HH (marked by arrows). The ESB displays less sediment but shows radial distribution as marked by the arrows. This basin possibly has less sediment flow from the NAB. In the NAB, sediment thickness still trends NW-SE (marked by arrow) and also a shift of the thickest part towards the SE occurred (encircled). SAB now is enclosed by SD1, TGF, WEF and AA (encircled) and has its deepest part at its center. NAB and SAB now have developed connectivity as marked by the arrow indicating NAB as a potential sediment source of SAB. The reduced thickness in the NW of the NAB contradicts the seismic interpretations shown in Figure 25 and thus is considered an area of low confidence for the Blodøks Formation.

5.1.2.4. Interpretations

The Blodøks Formation, similar to the Hidra Formation, shows draping behavior with an overall aggradational stacking pattern and continuous seismic facies in the whole area. This indicates higher accommodation space for deposition in an open marine, pelagic environment. Adding to the parallel and continuous seismic facies, the onlapping of the reflectors onto the flanks of the structural highs of AA, TA and HH, on the flanks of TGF and draping over the WEF and EF confirms a constant sea level rise accompanied with

68

local subsidence creating accommodation space during the latest Cenomanian to early Turonian ages.

The prograding sediments towards the NW of the central NAB (Figure 25) indicate sediment transport direction to be towards the NW. This also implies that the NAB underwent subsidence towards its northwestern part. The patches of discontinuous and chaotic reflectors in the NW and SE indicate possible sediment flows causing redeposition into the basin in different directions from the surrounding structural highs. Across the basin in Figure 24 discontinuities due to erosion confirm sediment transportation in the trough. The sediment reworking mostly took place during the later stages of deposition since the discontinuous seismic facies are commonly observed towards the top of the formation. The formation top in the NAB at some places (Figure 24 and 25) show erosional surfaces as well as stratal terminations of overlying strata suggesting the formation top to be a possible unconformity and a sequence boundary. The shift in sediment thickness in the central NAB towards the SE as observed from the isochron map does not match with the seismic interpretations in the area (Figure 25) and thus is a low confidence zone.

In the SAB the top reflector of the Blodøks Formation shows characteristics of an unconformity with several stratal terminations of the above lying reflectors and truncation of the underlying layers at it (Figures 26 and 27). The general parallel stacking pattern and the continuity of the layers suggest a calm depositional environment during the Blodøks deposition in this basin. The upper layers exhibit a slight waviness and discontinuous nature in the flanks of the SD1 and TGF suggesting sediment flows in the later depositional stages of this formation. The erosion on the tops of the AA, TGF and WEF also indicate that they were active and uplifting in the later stages. The salt structures below the TGF and the SD1 possibly became active in the later depositional stages making these highs as local sources of reworked sediments in the SAB as well as increased the accommodation space. The isochron map (Figure 33) shows the thickest deposits to be in the center of SAB where the sediment sources are possibly the uplifting AA, TGF WEF and the SD1 (Figures 26 and 27).

69

Figure 28 shows sediment slides lying on top of one another along the WEF and EF flanks indicating uplift of these structural highs in phases. The gravity flows along the eastern flank of EF towards the ESB shown in this figure also gives a reason for the presence of thicker sediment packages in the west and NW of the ESB as observed from the isochron map (Figure 33). This basin has a wider distribution of sediments towards the SE and NE as shown in Figures 29, 30 and 33, possibly indicating a rise in sea level accompanied by a local subsidence in the basin. In these figures, again the basal layers show continuity and higher amplitudes indicating calmer depositional environment in the early depositional stages. The formation top is eroded and represents an unconformity as the overlying layers onlap and terminates on it (Figures 29 and 30). The thickness relatively stays uniform in the basinal area with slight thinning towards the outer edges of the basin suggesting low accommodation space towards the basin edges possibly along with low sediment feed. At some places in the basin center the thickness is also less due to erosion as shown in Figure 29.

In the SSB the sediment package deposited (Figure 33) possibly due to deepening of the region by subsidence as seen in the TWT map (Figure 11C) leading to a bigger accommodation space. Stratal truncations indicating erosion on the top of the TA (Figure 31), also indicates that it was active and uplifting during this time and behaved as a sediment source to the SSB. Figure 32 provides two possibilities, firstly the onlapping nature at the base of the formation indicates uplift in the HH, secondly the progradational features in the upper part suggests subsidence of the western and NW margin of the SSB. It is inconclusive at this stage and is discussed in the subsequent chapters.

5.1.3   Hod Formation

The Hod Formation is bounded by the Blodøks Formation below and the Tor Formation above (Figures 5 and 7) and was deposited during the Turonian to Campanian ages (Isaksen et al., 1989).

5.1.3.1. Well Logs and cores

Lithology from cores: This formation dominantly consists of white, light grey to light brown, soft to hard chalk which may alternate with crypto-microcrystalline limestones at places and occasionally contain calcareous clay/shale laminae (Isaksen et al., 1989).

GR, DT, RHOB characteristics: The wireline logs at the base of this formation shows a distinct fall in the gamma ray values along with a rise in acoustic impedance compared to the underlying Formation. Towards the upper boundary the gamma ray values slightly decrease with increased acoustic impedance from Hod to the overlying formation (Figures 7 and 13).

5.1.3.2. Seismic observations

The top of the Hod Formation is represented by a relatively strong peak while the base of the formation is marked by the weak trough representing the top Blodøks Formation (Figures 5 and 7). The top reflector of the formation is irregular to straight in nature and is also relatively continuous throughout the study area (Figures 34-42).

Several reflector terminations occur at the top reflector of the Hod Formation (Figures 34-37, 40 and 41) and thus represent an unconformity. In several places the formation top also shows clear erosional features (Figures 36, 40 and 41). The Hod Formation can be generally divided into three stratigraphic packages in the study area except for the one package in the SSB and in the WEF and EF area where the formation is divided into two packages. These packages are bounded by unconformities (Figures 34-42). The reflectors mostly lie parallel and show aggradational pattern in all the basins.

In the NAB, across the basin, in Figure 34, the basal and the middle subunits have mostly continuous, slightly wavy to straight reflectors onlapping on the flanks of AA and HH. They show infilling characteristics by lying parallel to each other. The top subunit has very discontinuous reflectors (Figures 34 and 35). Along the basin (Figure 35), the reflectors on the basal subunit show progradation towards the NW of the basin while in the middle subunit no such feature is clear. Discontinuous patches in the middle subunit are observed towards the SE of the basin. The top subunit is generally discontinuous but towards the SE it shows some continuity as observed in Figure 35. The formation is

71

bounded by an unconformity at the top identified by overlying onlaps (Figure 34). The formation is thickest in the center of the basin and thinner towards the flanks of AA and HH (Figure 34). On the top of the AA, reflector truncations are observed. Few onlaps of the reflectors can also be seen in the south eastern direction in the basal subunit where the formation tends to thin again.

In the SAB (Figure 36), the basal subunit has parallel seismic facies onlapping on the AA and TGF showing infilling characteristics. The reflectors of the middle subunit also onlap on the TGF and AA and have several reflectors truncated by the above lying unconformity. These truncations show the pockets of eroded areas similar to that in the basal subunit in Figure 36. The very discontinuous nature of the top subunit is also observed from this figure. In Figure 37 it is observed that the basal and top subunits have discontinuous reflectors while the middle subunit has relatively continuous reflectors onlapping on the SD1 and WEF. The discontinuities in the basal and top reflectors increase towards the flanks of the highs compared to that in the center of the basin. The top of the formation in this basin is identified as an unconformity where several stratal terminations of overlying layers occur. The thickness of sediments is highest in the center of the basin and decreases towards the flanks of the SD1 and WEF.

Figure 38 shows the area around WEF and EF where the formation is divided into two subunits. The basal subunit shows discontinuities and the top subunit onlaps onto the flanks of the highs in this seismic profile. On the eastern flank of the EF, in the ESB, the reflectors onlap and they show aggradational stacking pattern. In this basin the reflectors also onlap onto the TA in the north, and the highs in the south and SE as shown in Figures 39 and 40. The reflectors of all the three subunits in this basin show good continuity but are truncated towards the center of the basin most likely due to erosion (Figures 39 and 40). Some patches of chaotic reflectors are also present towards the western part of the basin as shown in Figure 39. The overall thickness of the formation is highest in the center of the basin and reduces towards the south, SE and on the top of the TA where the formation reflectors are truncated by the unconformities at the top reflector of the formation (Figure 40).

In Figure 41 the truncation of the formation reflectors at the top of Hod is prominent especially at the crest of the TA. In the SSB, in the TA area, both the subunits of the Hod Formation have relatively continuous and parallel seismic facies which onlap onto the HH and on the flank of TA. The seismic facies is relatively discontinuous immediately to the north of TA on its flank. Several truncations of the reflectors also occur at the top of the formation in the basin as observed in Figure 41. Figure 42 also shows parallel and continuous reflectors in both the subunits of the formation which onlap on the HH in the west of the basin. The overall thickness of the sediments in the basin reduces towards the north and NW while it is thickest immediately north of the TA (Figure 41). Towards the NE, the formation is also generously thick as shown in Figure 42.

5.1.3.3. *Maps and observations*

TWT structure map: The time structure map of this formation (Figure 11D) shows the same basins as the preceding formations. The deepest parts of the Hod Formation are the central NAB and SAB (~3940-4200m or ~3500-3600ms) while the ESB and the SSB basins are comparatively less deep (~3650-3870m or ~3400-3475ms). A slight deepening of the formation top is observed between the WEF and the EF (~3790m or ~3450ms) (Figure 11D).

TST isochron map: The isochron map of the Hod Formation (Figure 43) shows an increased thickness of sediments in the SE of the NAB which now is connected with the ESB sediments trending NW-SE. A shift in depocenter is also prominent in the SE direction in this figure compared to that in the Blodøks Formation. The thickness of the NAB sediments varies significantly from the edges (~325m or ~130ms) to the center (~688m or ~275ms) of the basin, the thickest being in the central parts. In the southwest, in the SAB, the thickness of the Hod sediments varies from ~312-563m (~125-225ms), the thickest being at the southern base of the AA (Figure 43). In the NE, in the SSB, sedimentation continued with the thickest sediments immediately north of the TA. The formation thickness decreases towards the north and NW. In the structural highs the thinnest formation thicknesses are observed to vary from ~25-275m (~10-110ms) as observed in the isochron map.

Distribution: The deposits of the Hod Formation are widely distributed in the study area as observed from the isochron map (Figure 43). The structural highs are also draped by the upper formation layers with an average of ~125m (~50ms) thick sediments. The major deposition occurred in the central parts of the NAB and ESB while the deposition in SAB and SSB basins were comparatively low.

5.1.3.4. Interpretations

The overall aggradational stacking pattern and the continuous nature of the basal layers of the Hod Formation in the study area indicate that the onset of the deposition of the Hod sediments were in an open marine, pelagic and in a relatively tectonically calm environment. In the NAB, the northwesterly progradational pattern of the basal subunit in Figure 35 indicates a possible continued subsidence of the basin towards its NW since the early Turonian age. The subsidence took place for a brief period of time since this prograding pattern is not present in the overlying middle subunit. During the deposition of the middle subunit possible gravity flows from different directions occurred towards the center of the basin as indicated by the patches of discontinuous reflectors especially towards the SE of the basin (Figure 35). In this figure, the top subunit is thicker with discontinuous reflectors in the SE of the NAB while it is thinner towards the NW. This potentially indicates uplift towards the NW of NAB leading to concentrated sediment deposition in the SE of NAB. The isochron map (Figure 43) showing increased thickness towards the SE of the basin also back up the possible uplift in the later stages of the Hod deposition leading to sediment transportation and deposition from NW to SE of the NAB. The overall aggradational stacking pattern in this basin seen in Figures 34 and 35 refers to a general increase in the water depth due to the rise in sea level (sea level curve of Figure 5). The truncated reflectors on the top of AA also indicate that AA was active and uplifting leading to the erosion of the sediments on top of it.

In the SAB (Figure 36), the basal and middle subunits have relatively continuous reflectors which onlap on the structural highs of AA and TGF indicating a calm depositional environment with an increasing water depth due to a rising sea level. The top subunit however, shows high discontinuities along the slopes of AA and TGF indicating

74

possible uplifts of these structures during the later stages of the deposition of the Hod Formation, creating debris flows towards the basin center. Again, the subunits are truncated at places within the basin as shown in Figure 36, implying erosion due to possible lobes of debris flows from different directions. Figure 37, a seismic profile crossing Figure 36, displays discontinuous reflectors of the basal and the top subunits on the flanks of the SD1 and WEF indicating debris flows towards the basin center. The middle subunit however, has continuous reflectors onlapping on the flanks of the highs. These facts in turn indicate that the SD1 and WEF were also active and uplifting in the initial and later stages of the formation deposition. It is also possible that these lobes of debris flows eroded the basal and middle layer sediments shown in Figure 36. Overall the SAB underwent an increase in accommodation space due to the halokinetic uplift of the AA, SD1, TGF and WEF highs surrounding the basin. Thus the main sources of sediments of this basin are the reworked sediments from these structural highs.

The uplifting WEF also has gravity flows on its eastern flank as inferred from the discontinuous reflectors of the basal subunit (Figure 38). In western part of the ESB (Figure 39), the presence of progradational wedges towards the basin center in the basal and middle subunits indicate sediment inflow from the NAB in the NW into the basin. Overall the aggradational sedimentation as also identified in Figure 40 indicates a rise in sea level and possible subsidence in the basin creating the required accommodation space for the thick deposits (Figure 43). The clear truncation of the reflectors on the top of TA (Figures 40 and 41) imply that the salt structures below TA were active and uplifting and as a result of which the sediments on top of it were eroded showing less thickness in the isochron map (Figure 43). These eroded sediments mostly flowed down the northern flank of the TA creating a chaotic nature of the reflectors immediately north of TA (Figure 41). This also led to the thickest deposition at the northern side of TA in the SSB (Figure 43).
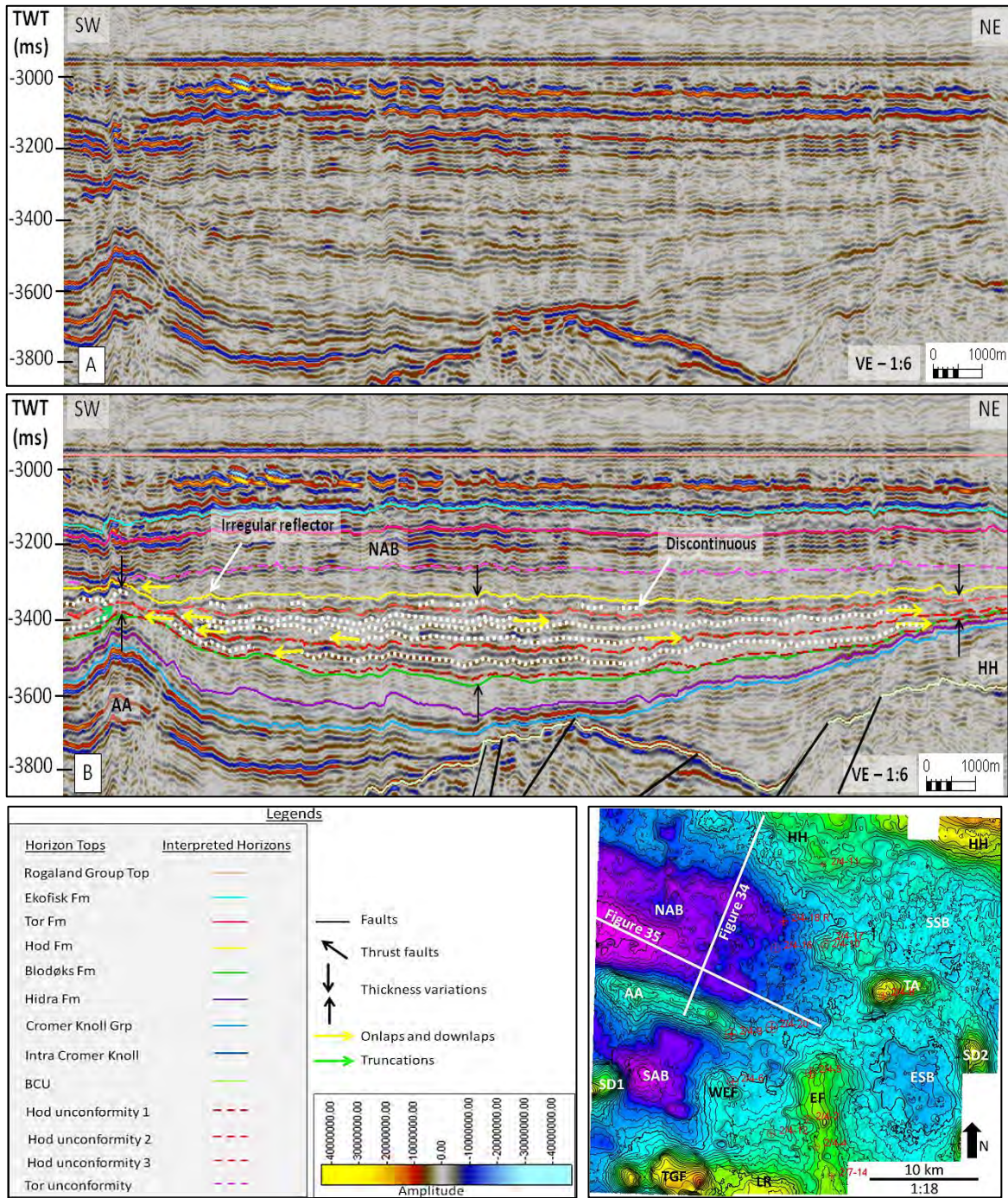
Figure 34: (A) Uninterpreted and (B) Interpreted 3D seismic line flattened on Rogaland Group top in the NAB. The Hod Formation top reflector is straight to slightly irregular in nature. Several overlying reflectors onlap on the formation top indicating it as an unconformity. The internal reflectors throughout the formation onlap onto the flanks of both AA and HH as shown in the figure. Reflector truncations occur on top of the AA (green arrow) indicating erosion and uplift of AA. Two unconformities within the formation divide it into three subunits. The bottom two units show infilling characteristics while the top unit is very discontinuous and thin which is eroded near the crest of AA. The overall thickness of the formation is the highest in the basin center while towards the flanks it is thinner. The location is shown in the inset TWT map of the top Hod Formation.
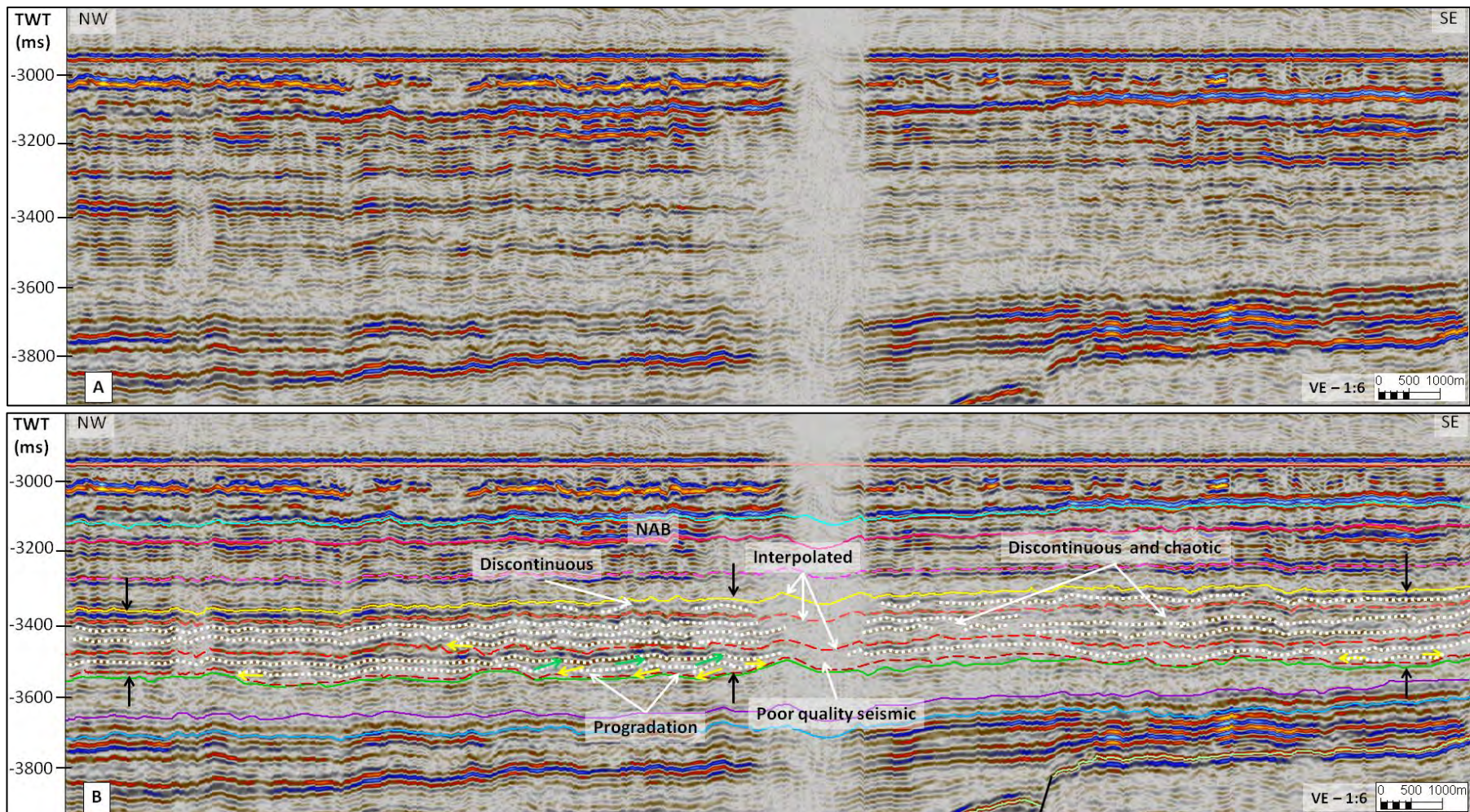
Figure 35: (A) Uninterpreted and (B) Interpreted 3D seismic line flattened on Rogaland Group top in the NAB. The formation shows uniform thickness throughout the section. Two unconformities divide the formation into three subunits. The basal subunit shows small northwesterly prograding units in the central area as shown. Few onlaps towards the NW is also observed. Otherwise the reflectors show good continuity in the basal subunit. The middle subunit also shows good reflector continuities towards the NW but shows some discontinuities and chaotic behavior towards the SE as shown. The reflectors are mostly parallel but very few onlaps towards the NW is also present (yellow arrow in the middle subunit). The top subunit of the formation is very thin in the NW and has discontinuous reflectors towards the SE where the unit becomes slightly thicker. The location and legends are as given in Figure 33.

77
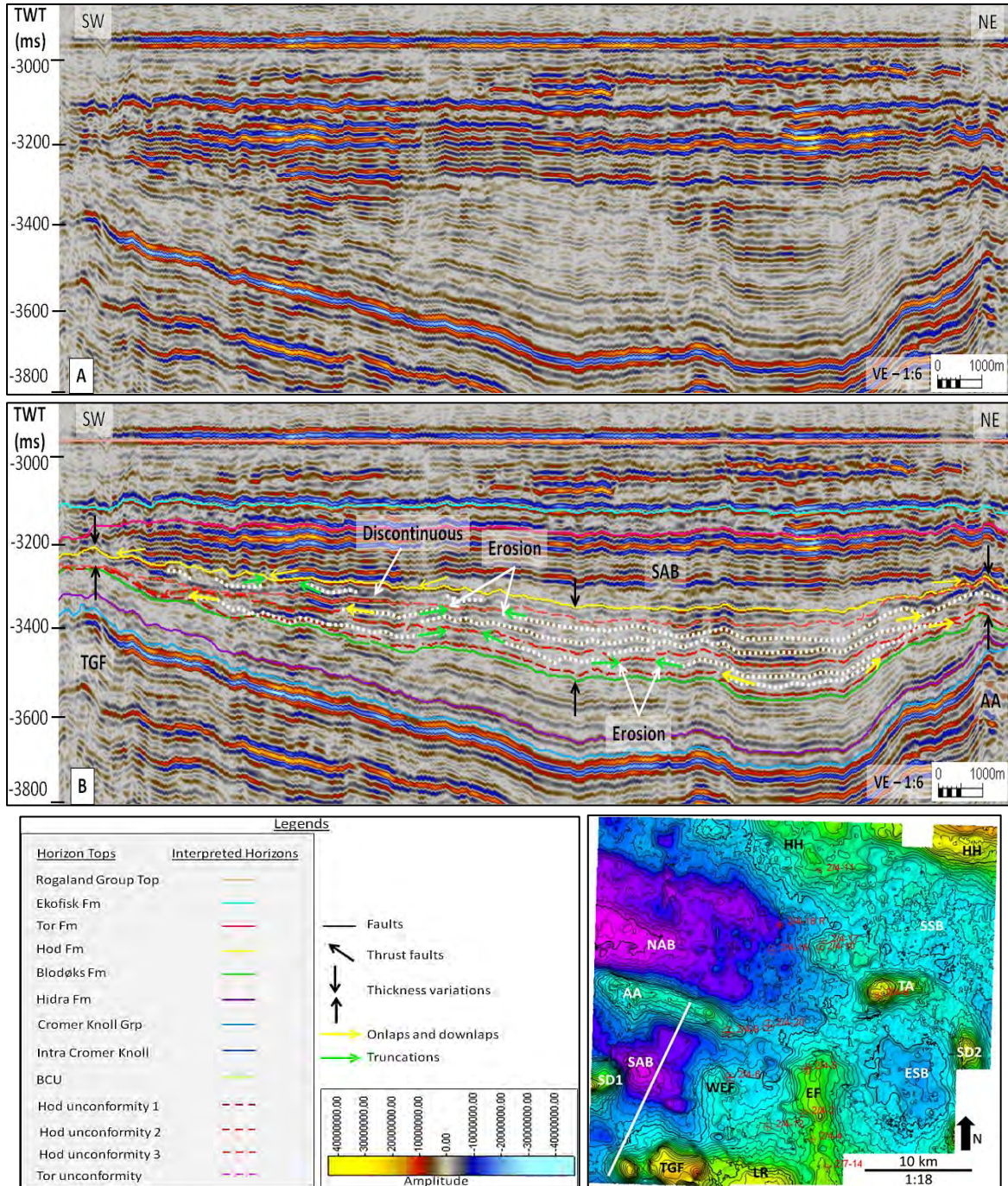
Figure 36: (A) Uninterpreted and (B) Interpreted 3D seismic line flattened on Rogaland Group top in the SAB. The Hod Formation is divided into three subunits by the two unconformities in this basin also. The basal subunit shows infilling characteristics and onlap on the flanks of both the TGF and AA. Reflector truncations occur at the overlying unconformity as shown by the green arrows. These indicate pockets of eroded areas. Similarly, the middle subunit reflectors show onlapping features onto the flanks of the structural highs on the Hod unconformity 2 as shown. Several pockets of eroded sediments are also present in this subunit as shown. Both the subunits show medium continuity of the reflectors. The top subunit shows discontinuous seismic facies at the TGF indicating gravity flows on its flanks. Towards the center of the basin and near the AA the reflectors are not clear since the subunit becomes very thin. Overall the thickness of the formation is highest in the basin center while at the top of the highs it decreases most likely due to erosion. . The location is shown in the inset TWT map of the top Hod Formation.

78
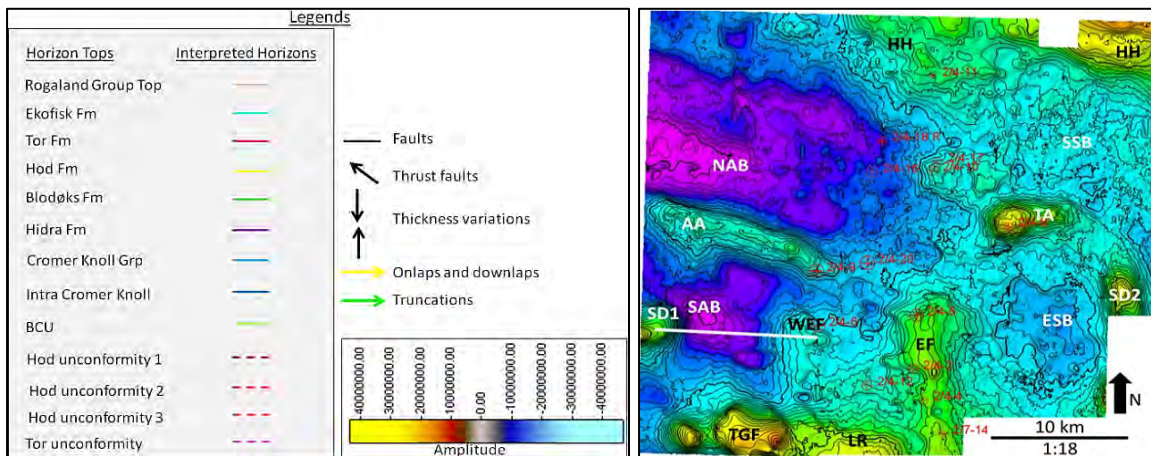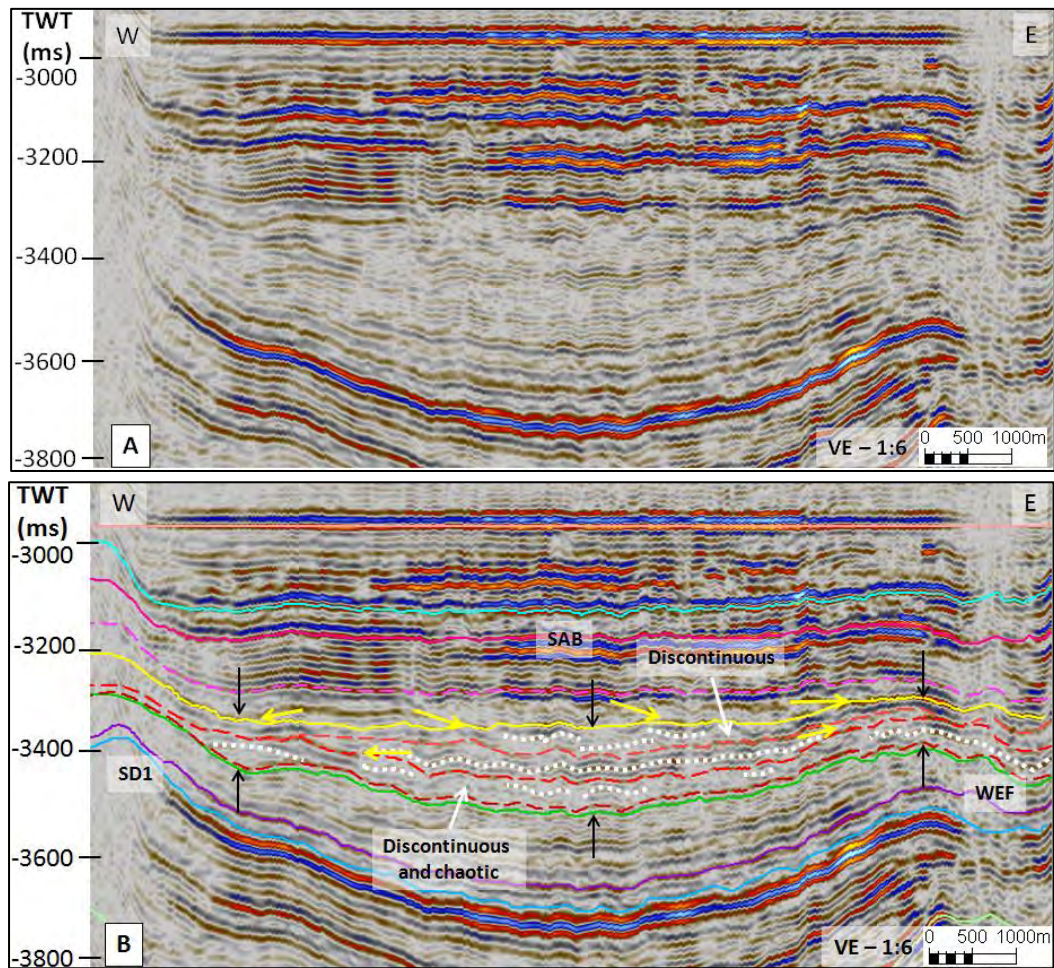
Figure 37: (A) Uninterpreted and (B) Interpreted 3D seismic line flattened on Rogaland Group top in the SAB. The basal subunit show discontinuous and chaotic nature while the middle subunit shows generous continuity in the reflectors. On the other hand the top reflector shows high discontinuity. The basal subunit is more discontinuous along the flanks of the highs which become more continuous towards the basin center. Stratal terminations are not prominent in this subunit. The reflectors of the middle subunit show onlapping on the flanks of SD1 and WEF. The top subunit is thin and stratal terminations are not clear here either. The overall thickness of the formation becomes thinner towards the structural highs while it becomes thicker towards the center of the basin. . The location is shown in the inset TWT map of the top Hod Formation.

79
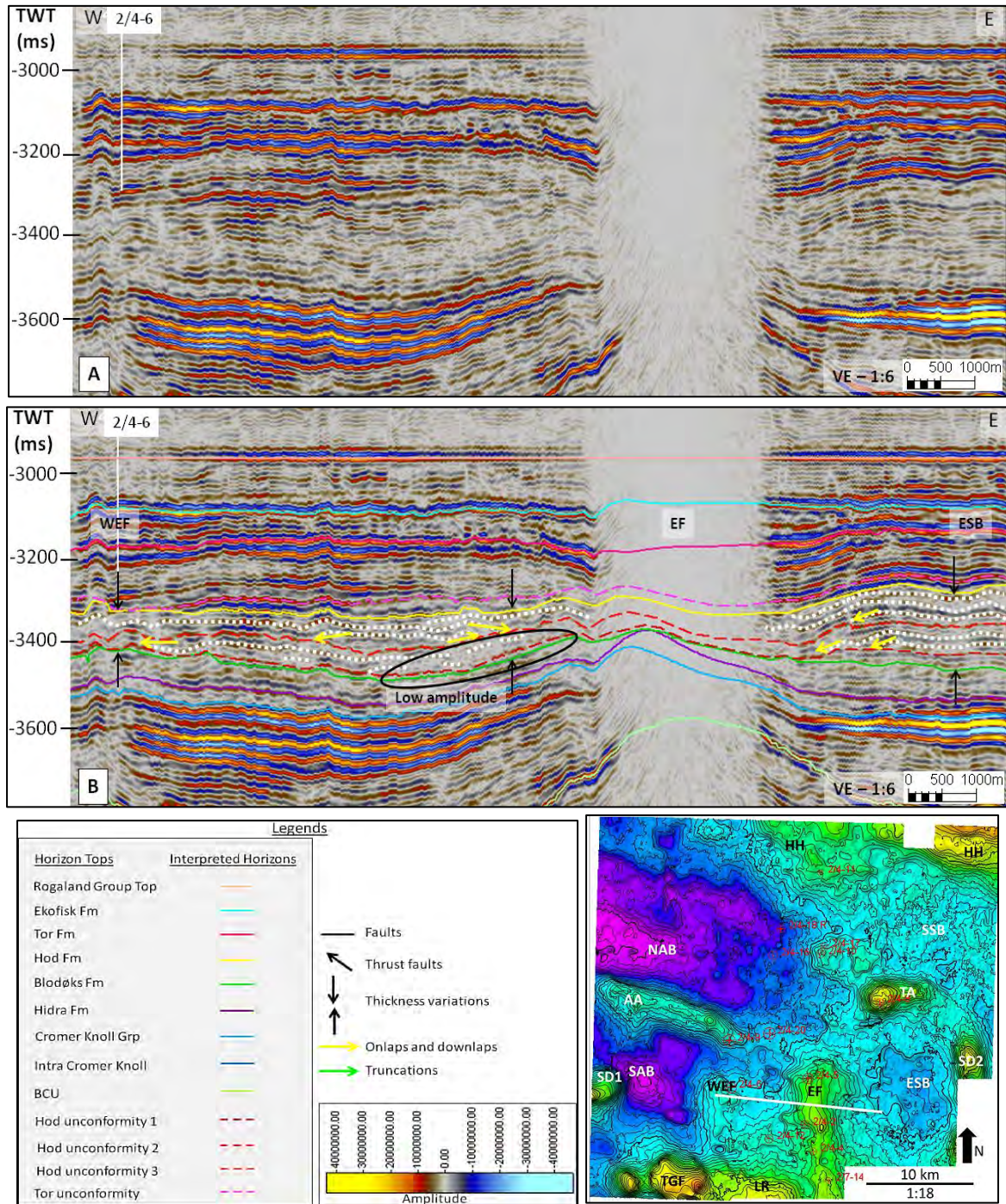
Figure 38: (A) Uninterpreted and (B) Interpreted 3D seismic line flattened on Rogaland Group top in the area between WEF and EF as shown in the inset TWT map of the top Hod Formation.. The formation here has just two subunits created by unconformities within the formation. On the western flank of EF the basal subunit shows chaotic reflectors while on the eastern flank of the WEF the reflectors onlap as shown in the figure. The top subunit has continuous seismic facies where the reflectors onlap on the western flank of EF and on the eastern flank of WEF. The formation is not very thick between the WEF and EF compared to the other basins. In the east of the EF, in the ESB, the formation is thick with continuous reflectors in both the subunits. The reflectors onlap on the unconformities and on the eastern flank of the EF. The concave nature of the formation in the ESB possibly is due to Inversion in the later stages. In the EF the interpretations are interpolated.

80
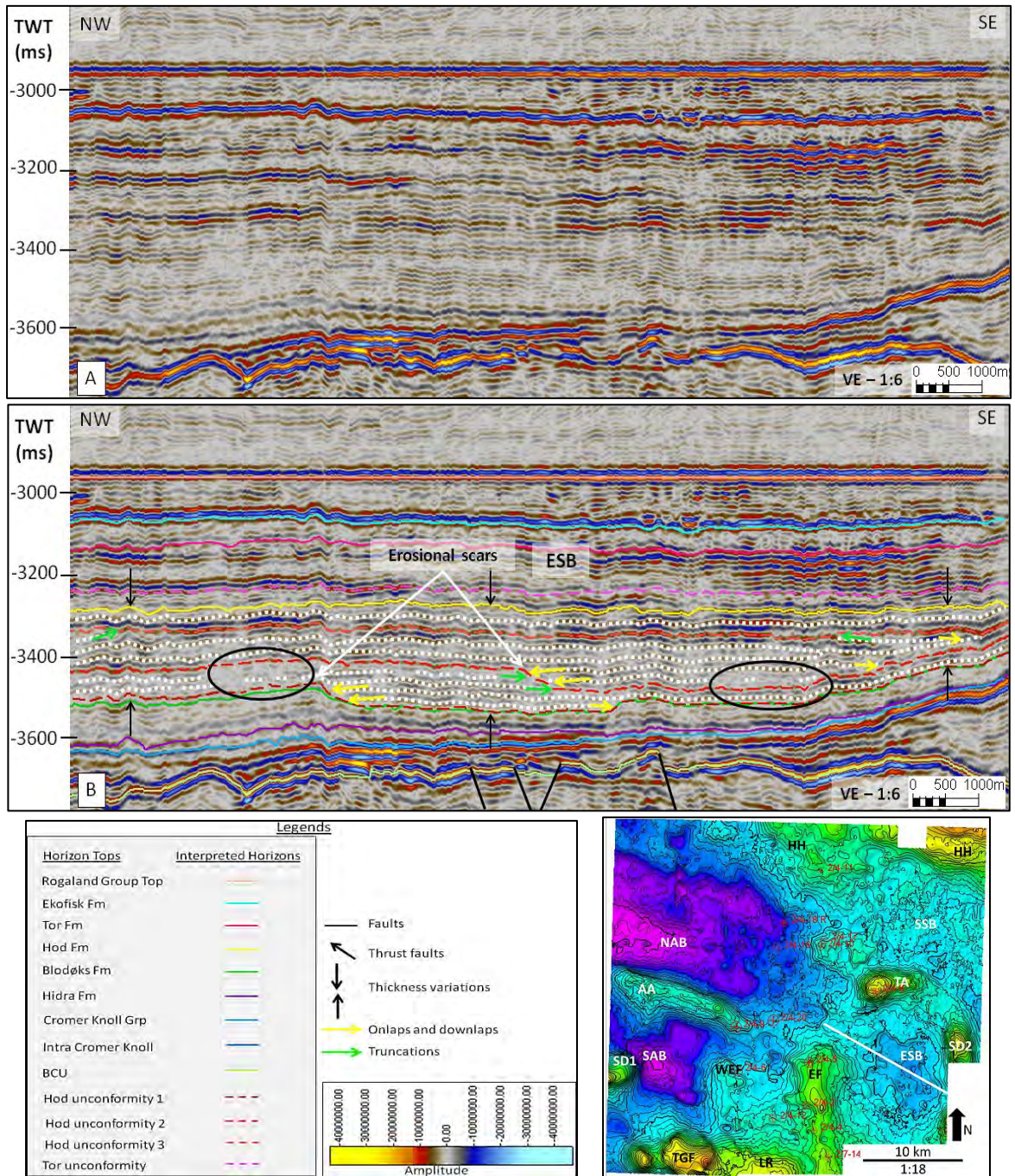
Figure 39: (A) Uninterpreted and (B) Interpreted 3D seismic line flattened on Rogaland Group top in the ESB. The two unconformities within the Hod Formation are clearly visible and divide the formation into three subunits. The basal subunit is thin toward the SE while it is thick in the center of the basin. It contains continuous reflectors which onlap on the Blodøks Formation top in the center of the basin creating erosional scars as shown in the figure. The reflectors are chaotic in the basal subunit towards the NW (encircled). Some of these reflectors are truncated by the overlying unconformity due to erosion in the basin center creating scars as pointed out. The middle subunit is thicker towards the SE and onlap on a structural high. Some reflectors also onlap on the eroded surface of the basal subunit in the center of the basin shown. Towards the top the middle subunit is truncated by the above lying unconformity as shown by the green arrows. The top subunit is thin but shows uniform thickness and has continuous seismic facies. The location is shown in the inset TWT map of the top Hod Formation.

81
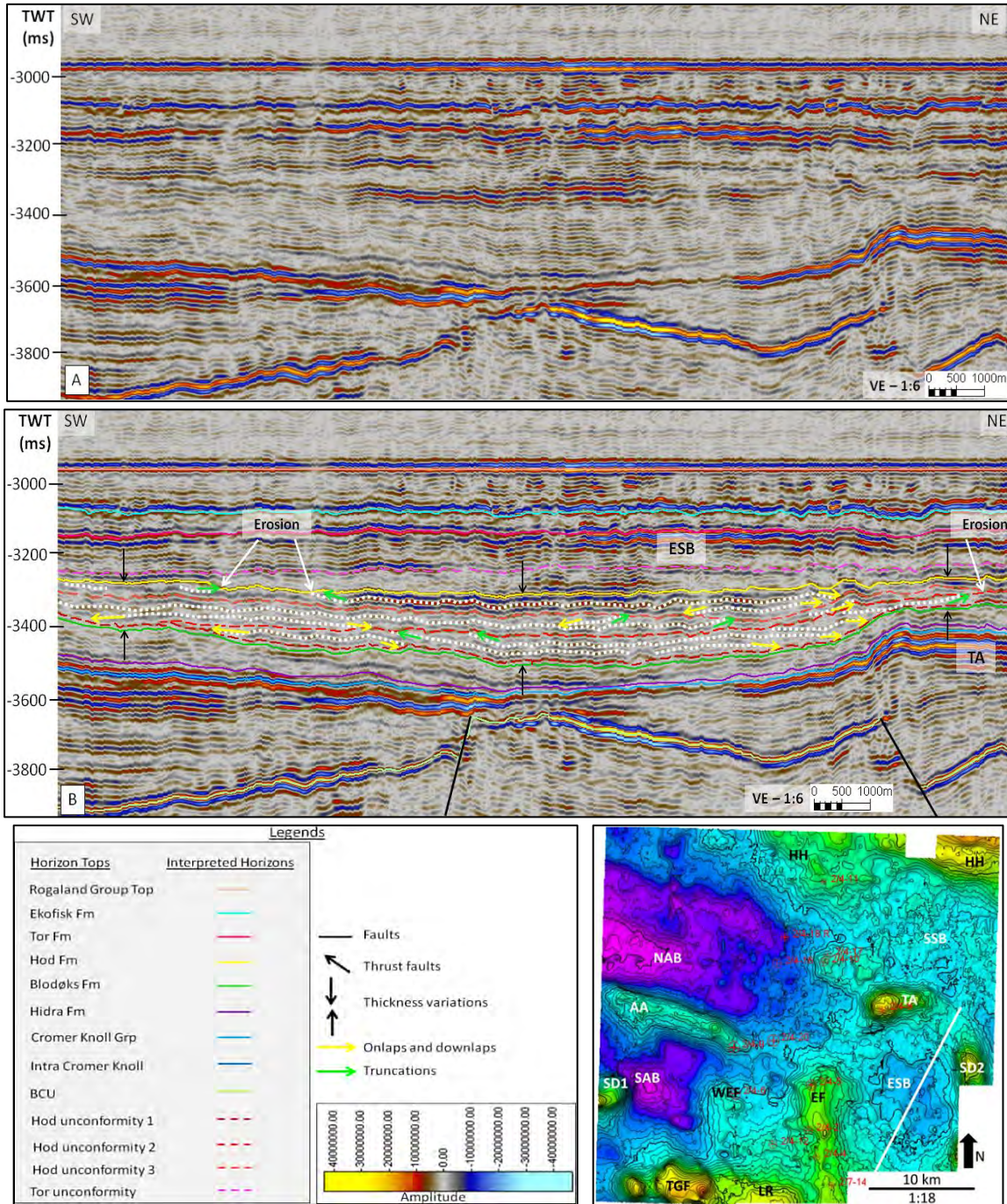
Figure 40: (A) Uninterpreted and (B) Interpreted 3D seismic line flattened on Rogaland Group top in the ESB. The basal subunit reflectors onlap onto the TA and towards the high in the south. The sediments show a basinwards progradation in the SW. The above lying unconformity truncates several reflectors indicating an erosional surface. In the middle subunit the reflectors onlap on the TA and on the high in the south. Towards the SW, the Hod unconformity 2 merges with the Blodøks Formation top which is also an unconformity and thus the reflectors of the middle subunit onlap on the Blodøks Formation top further towards the SW. Several truncations of reflectors are also observed in the middle subunit at the overlying unconformity above which the top subunit of the formation deposited. The top subunit reflectors also truncate at the Hod Formation top indicating it as an unconformity also. The overall thinkness is highest in the basin center while at the TA and further SW the thickness reduces. The location is shown in the inset TWT map of the top Hod Formation.

82
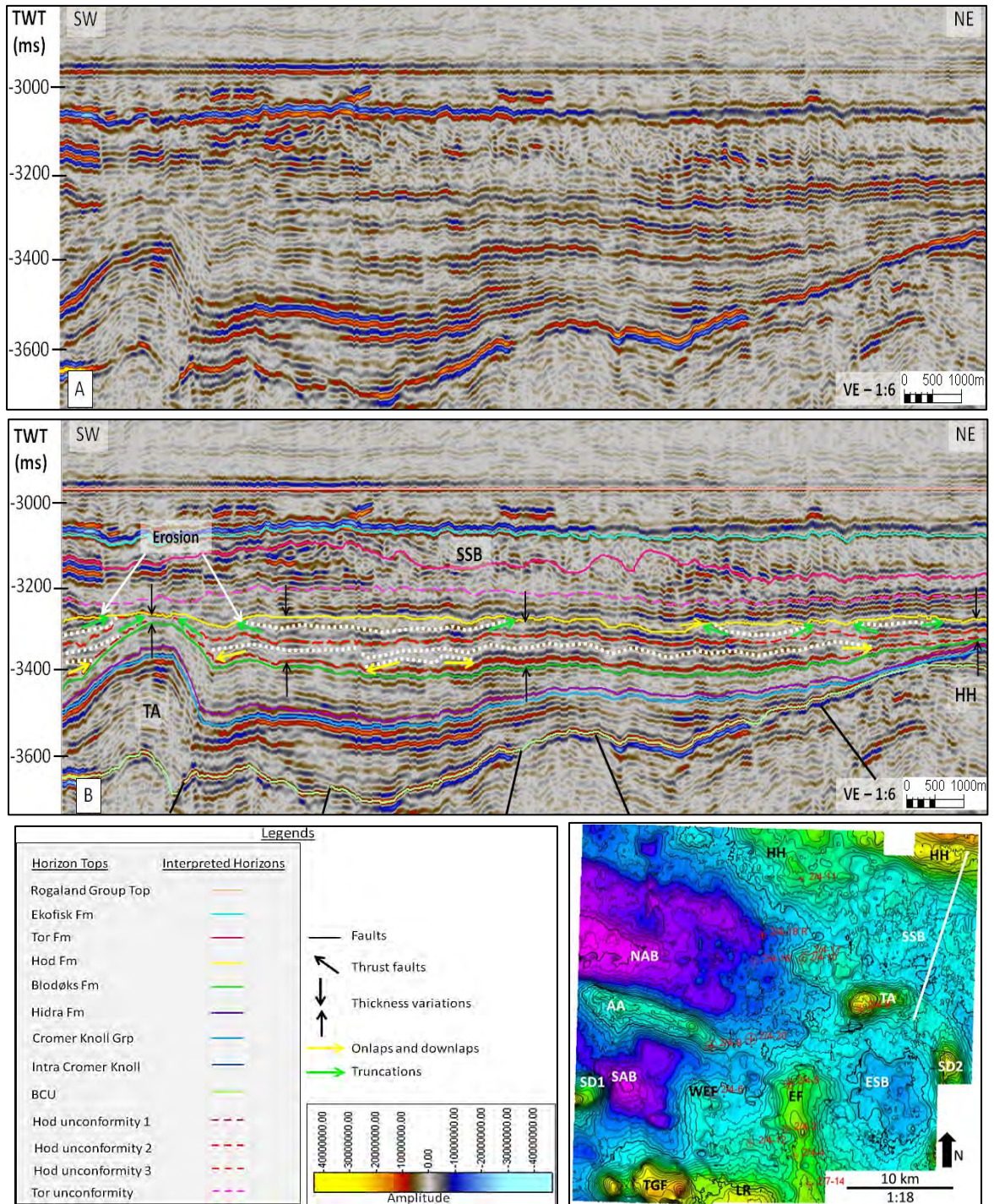
Figure 41: (A) Uninterpreted and (B) Interpreted 3D seismic line flattened on Rogaland Group top in the SSB. The Hod Formation in this basin is divided into two by an unconformity in between. The top reflector of the formation represents an unconformity since several upper reflectors of the formation truncate at it. On top of the TA, erosion of sediments is prominent indicated by the reflector truncations. Reflectors of both the subunits onlap onto the TA and HH as shown in the figure. The overall thickness of the formation is less compared that in the other basin and it is very thin on top of the TA due to the erosion. The formation thins out towards the HH in the NE. The location is shown in the inset TWT map of the top Hod Formation.

83
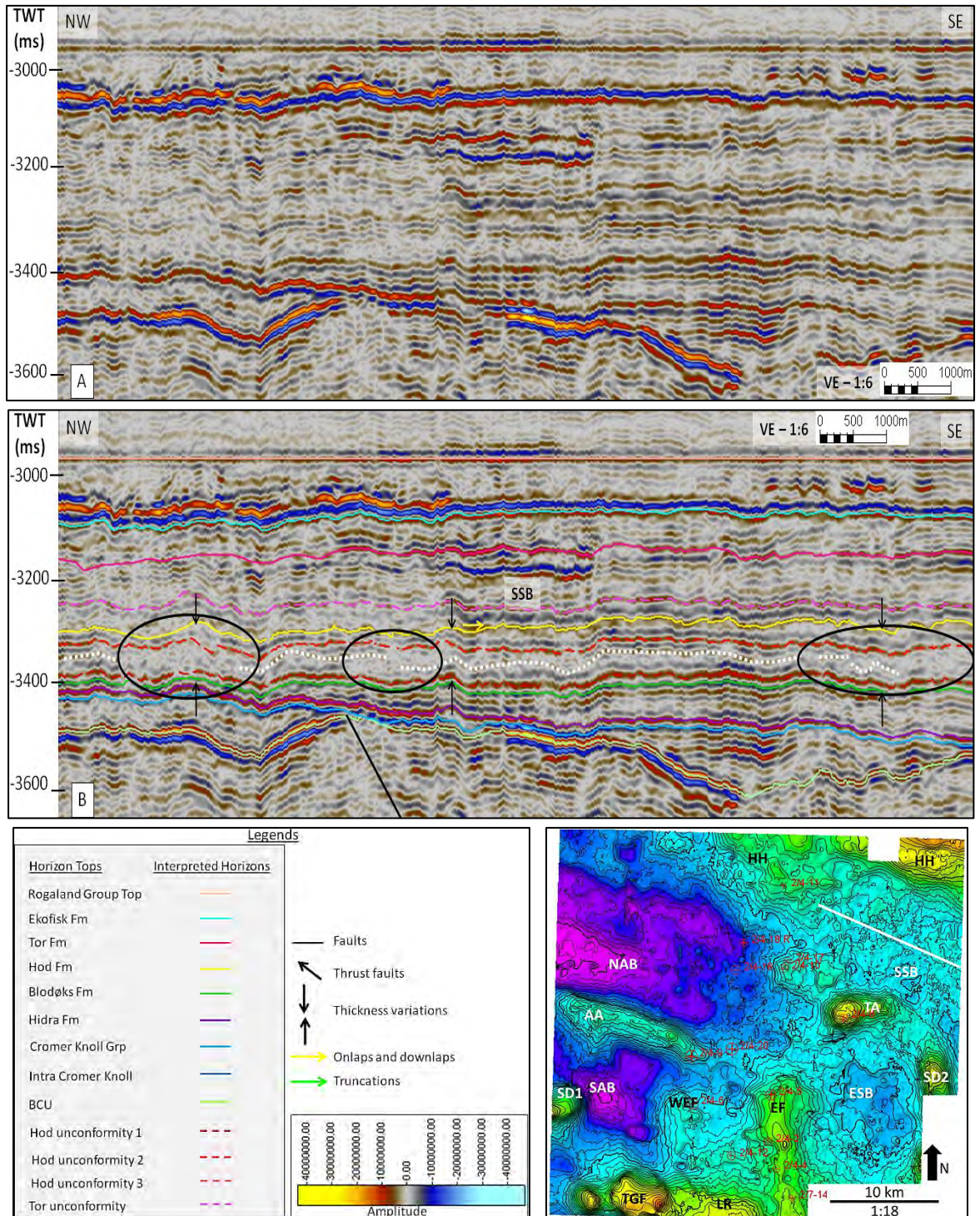
Figure 42: (A) Uninterpreted and (B) Interpreted 3D seismic line flattened on Rogaland Group top in the SSB. The basal subunit is thicker than the upper subunit of the Hod Formation in this profile. The reflectors in the base show patches of discontinuous nature as shown in the encircled areas indicating possible lobes of gravity flows from different directions. The overall thickness of the formation is uniform throughout this seismic section. No specific stratal terminations are prominent here. The location is shown in the inset TWT map of the top Hod Formation.
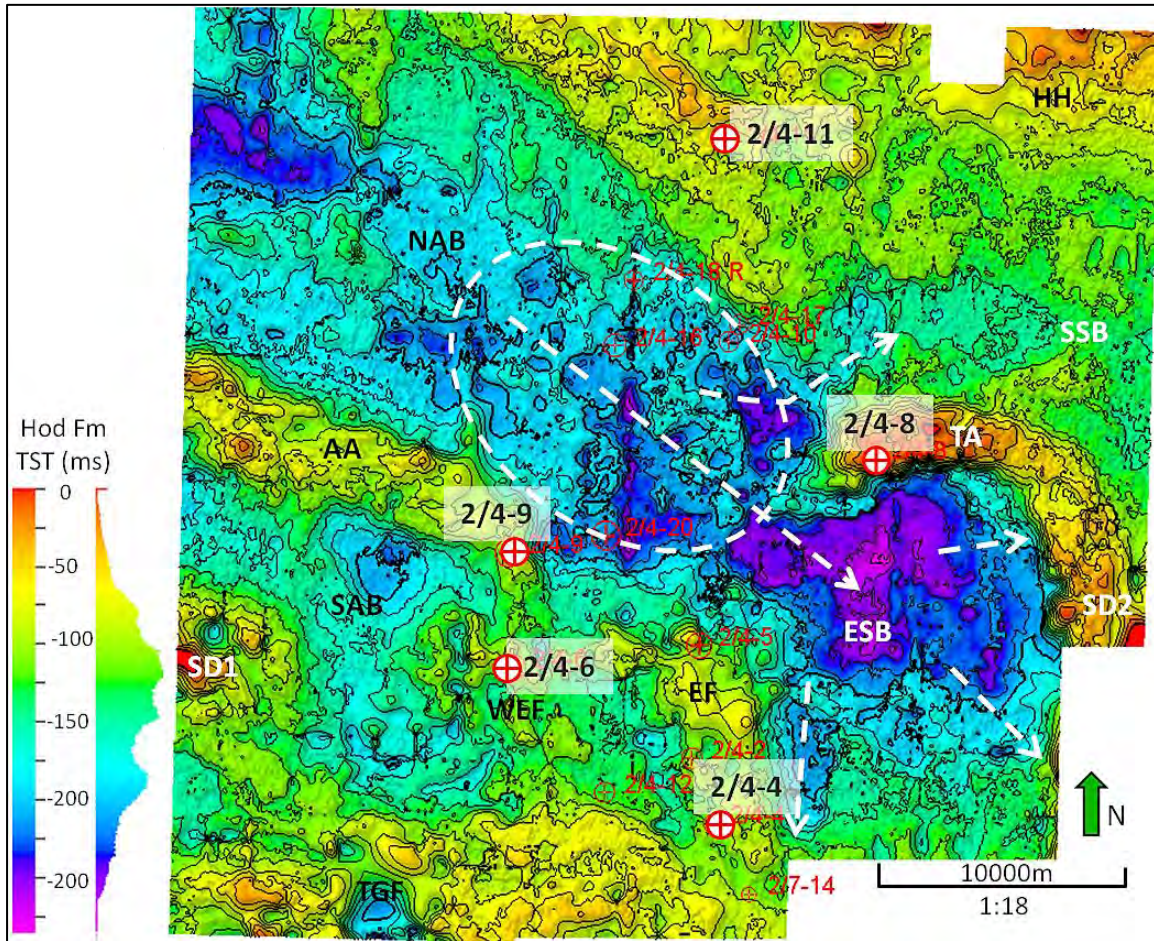
Figure 43: Isochron map of the Hod Formation in the study area. The NAB and the ESB display the thickest sediment deposits and are well connected now. The sediment thickness in NAB further shifted towards SE (encircled). The NAB acts as a major sediment source to ESB making it larger in size as shown by the arrows in the ESB. A possible connectivity developed between the NAB and SSB during this time (shown by the arrow from NAB to SSB). The sediment flow from NAB to SAB possibly reduced compared to that in the Blodøks Formation. The depocenter on the TGF is due to interpolated interpretation and is a low confidence area.

5.1.4   Tor Formation

The Tor Formation is bounded by the Hod Formation at the base and the Ekofisk Formation above. The Tor Formation was deposited during Late Campanian to Maastrichtian age (Isaksen et al., 1989) (Figures 5 and 7).

5.1.4.1. Well Logs and cores

Lithology from cores: This formation is generally homogenous in nature with white to light grey, tan to pink, hard chalky limestones with occasional fine layers of soft grey-green-brown marl and rare stringers of grey-green calcareous shales (Isaksen et al., 1989).

85

GR, DT, RHOB characteristics: The gamma ray values show a slight fall in the Tor Formation compared to that in the underlying Hod Formation as shown in Figures 7 and 13. The acoustic impedance also shows slight fall within the formation. The logs show constant low values throughout the formation which ends towards the upper boundary where the gamma ray values increase in the Ekofisk Formation.

5.1.4.2. Seismic observations

The top of Tor Formation is represented by a strong peak reflector and its base is marked by the strong peak of the top Hod reflector (Figures 5, 7 and 44-52). This reflector is mostly planar in nature except in the NE of the study area (Figure 51). The reflectors within the formation lie parallel to each other in majority of the area. The formation is divided into two subunits by an unconformity in the entire study area (Figures 44-52). The basal subunit generally has a transparent and discontinuous seismic facies bounded by the unconformity on the top, while the top subunit has strong, parallel and continuous seismic facies in the entire study area except for in the northeast.

In the NAB, the reflectors of the basal subunit of the formation are transparent and discontinuous (Figures 44 and 45). In Figure 44, the basal subunit reflectors onlap on the flanks of TA while the top subunit reflectors drape over the structure. The basal subunit has patches of chaotic reflectors towards the HH as shown in this figure. The thickness of the formation in this basin is uniform except for on the top of the TA where it decreases. Along the basin (Figure 45), the thickness is very uniform. The basal subunit contains extensive chaotic patches towards the SE of the basin while the top subunit has similar features towards the NW of the basin as shown in Figure 45. Few truncations occur at the top reflector of the formation, otherwise no stratal terminations are observed in the top subunit.

In the SAB (Figure 46), the reflectors of both the subunits onlap on the TGF while only the basal subunit reflectors onlap on the AA and the top subunit reflectors drape the structure. The unconformity dividing the formation runs over the AA and it merges with the top reflector of the Hod Formation on the top of the TGF. The overall thickness of the formation decreases on the highs while it is thickest in the basin center. Figure 47 displays that the WEF is draped by both the subunits with few basal reflectors onlapping on it. On the

86

flank of the SD1 the basal subunit reflectors display prograding features as shown in the Figure 47 while the top reflectors are transparent on the flanks of SD1.

Figure 48 displaying the area around the WEF and EF shows uniform thickness of the formation with very thin basal subunit. Few stratal truncations are observed near the WEF flank and to the east of EF in the ESB to the west. In the ESB, both the subunits show chaotic seismic facies in Figure 49. The basal subunit also shows discontinuities towards the SE in this profile. Figure 50 displays discontinuities in both the subunits towards the flank of TA in the north. Few basal reflectors near the TA also show some prograding features towards the basin center. The Tor Formation completely drapes the TA. The overall thickness of the formation in both Figures 49 and 50 is observed to be quite uniform while the basin center might be slightly thicker.

In the SSB, (Figure 51), distinctive overriding features in a NE-SW direction, with small thrust faults is present in the top subunit. The deformed sediments are truncated at the top of the formation near the TA as shown in the Figure 51. The formation has varying thickness over the section as a result of these thrust faults. Figure 52 shows a relatively uniform thickness of the formation. The basal subunit displays discontinuous seismic facies while the upper subunit contains prograding features towards the NW near the HH flank.

5.1.4.3. *Maps and observations*

TWT structure map: The time structure map (Figure 11E) shows the preexisting basins and the main structural features. The deepest areas are still in the NAB and SAB centers (~3460-3650 m or ~3325->3400ms), while the deepest of the SSB and ESB areas are comparatively at a shallower level (~3233-3400m or ~3200-3300ms). A new depression connecting the NAB and the SSB is observed to the east and north of wells 2/4-18R and 2/4-17 respectively.

TST isochron map: The isochron map (Figure 53) of the Tor Formation shows the relative thickness of the formation to be ~125-500m (~50-200ms), which is well distributed over the entire study area. The thickest sediments are in the centers of the NAB, SAB and between the West Ekofisk and Ekofisk Fields (~400-500m or ~160-200ms). In the NAB, the NW part shows very thick deposits (~450-500m or ~180-200ms) which relatively thins towards the

SE (~400-450m or ~160-180ms). The ESB and the SSB also show thick deposits (~300-400m or ~120-160ms). The thinnest deposits are observed in the NE and in the TGF area (<275m or <110ms).

Distribution: In Figure 53 the Tor Formation deposits are uniformly distributed in the entire study area, except towards the south and SW. The formation covers and drapes the whole area even over the structural highs (Figures 44-52). A shift in sediment thickness is again observed in the NA, and this time the deposits thin towards the SE from NW.

5.1.4.4. Interpretations

The overall aggradational pattern of the reflectors onlapping on the flanks of the structural highs of the area indicates an open marine and pelagic depositional environment. During the late Maastrichtian the sea level fall lead to the erosion of the sediments and in turn made the formation top an unconformity. Several reflector truncations observed at the top reflector confirms the erosional event (Figures 45, 48, 51 and 52)

In the NAB (Figure 44), the presence of chaotic and discontinuous basal subunit reflectors on the HH flank indicates sediment flows towards the basin center. This again implies uplift of HH which initiated the mass flows in the early stages of the deposition of the Tor Formation. Similar chaotic reflectors are also seen in the top subunit in the same area implying that the uplift of HH continued until the later stages of the deposition of the formation. In Figures 44 and 53, the slight decrease in thickness on the top of AA indicates small amount of erosion, which imply small uplift of AA. The patches of chaotic facies observed in Figure 45 indicate possible lobes of gravity flows towards the basin center deposited in different directions from the surrounding highs.

In the SAB gravity flows were common at the onset of the Tor Formation deposition since the basal subunit is very chaotic and discontinuous as shown in Figures 46 and 47. This implies AA, TGF, SD1 and WEF were active and uplifting during the early stages of the deposition of the formation leading to mass flow deposits towards the SAB center. During the later stages these structures were relatively inactive since the formation drapes over them with an aggradational pattern as observed in these figures. At the onset of the deposition of the formation, not much sedimentation occurred around the WEF and EF since

the basal subunit is very thin here (Figure 48). Here the basal subunit possibly consists of reworked sediments from the WEF. The sedimentation rate in this area, increased in the later stages as indicated by the aggradational pattern draping both the WEF and EF.

In the ESB, the sediments flow in from the NW and is indicated by the presence of the chaotic seismic facies towards the NW (Figure 49). Also, gravity flow sediments from the TA in the north, filled in the basin as indicated by the chaotic facies on the flank of TA in Figure 50. This implies that an active and uplifting TA from the beginning to the mid stage of the deposition of the Tor Formation. During the latest stages TA was possibly inactive since there is no indication of gravity flows and instead, the formation drapes the structure. The SE of the basin possibly lies in a tectonically calm area since the reflectors of both the subunits have good continuity.

In the NE of the SSB, the distinctive overriding features of the reflectors of the top subunit create small thrust faults as shown in Figure 51. This indicates a local compressional force from the NE towards the SW led to a mega slide in the area creating these specific features. The location of the source of this force is outside the study area. Near the TA the top subunit drapes the structure, while few reflectors in the basal subunit onlap and truncate at it. These stratal terminations indicate the aforementioned inactive and active phases of the TA respectively. Figure 52, showing progradational features in the northwestern margin of the SSB indicates a possible local subduction of the HH.
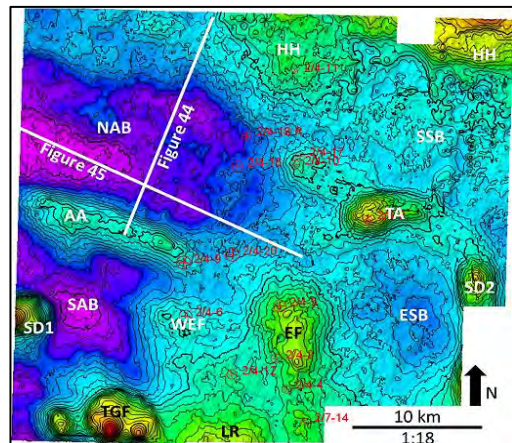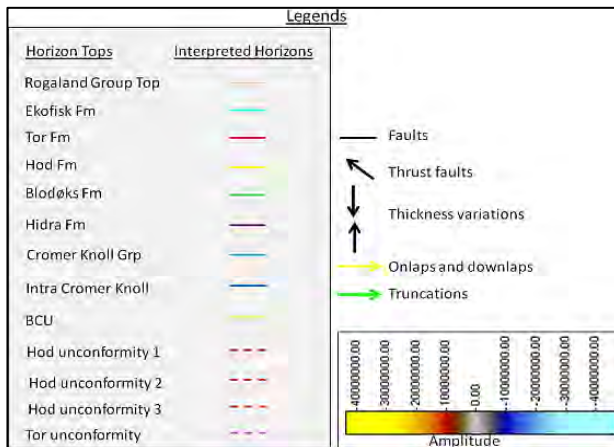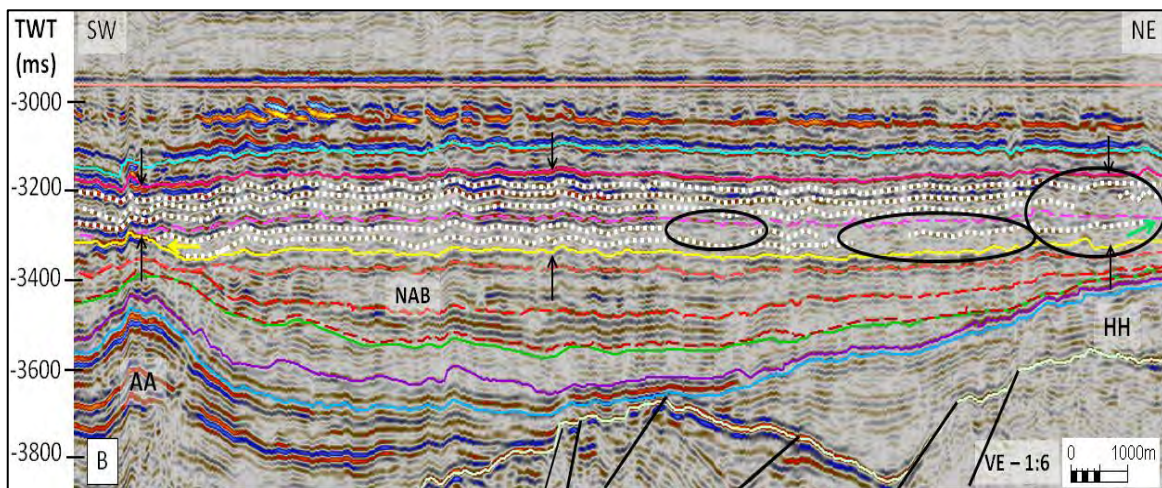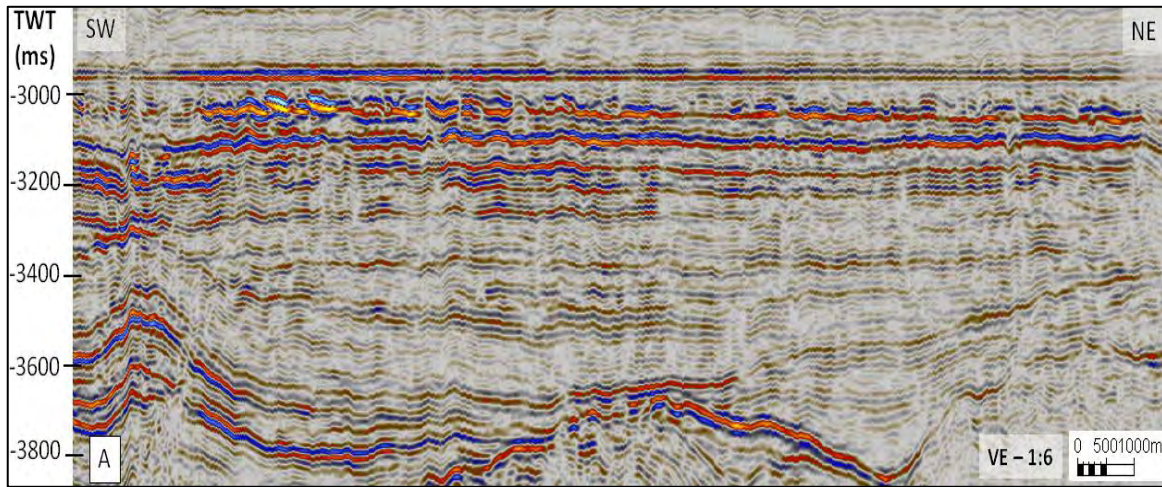
Figure 44: (A) Uninterpreted and (B) Interpreted 3D seismic line flattened on Rogaland Group Top in the NAB. The formation is divided into two subunits by an unconformity. The basal subunit has a clear difference in seismic facies compared to the top subunit. The basal subunit contains slightly transparent facies and shows patches of discontinuities (encircled). Stratal onlaps of the basal subunit occur at the AA while few truncations are also observed towards the HH. The top subunit has parallel and continuous seismic facies which drape over the structural highs of AA and HH. Small chaotic patches in the top subunit are observed towards the HH. The location of the seismic section is shown in the inset TWT map of the Tor Formation top.
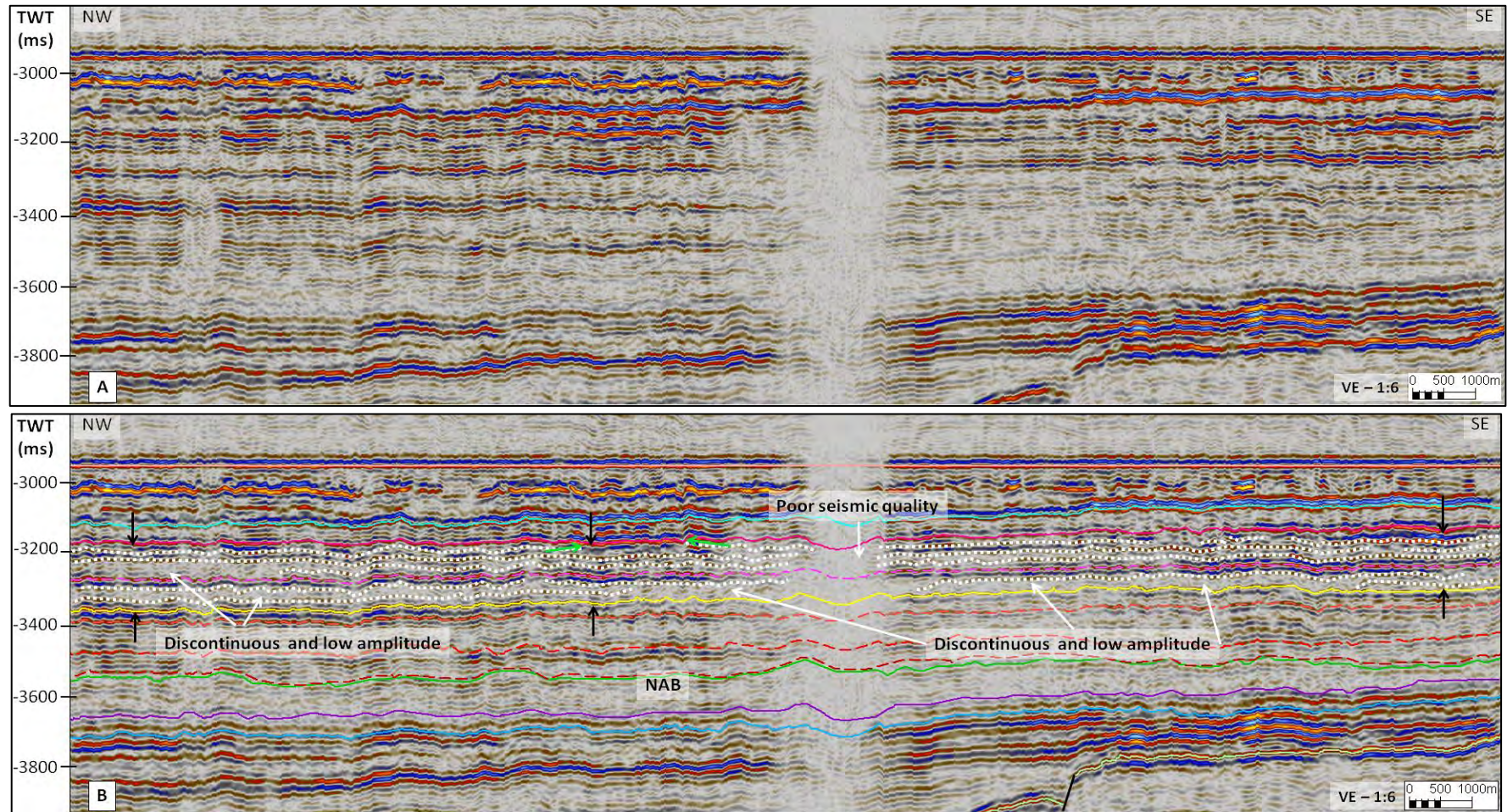
90

Figure 45: (A) Uninterpreted and (B) Interpreted 3D seismic line flattened on Rogaland Group Top in the NAB. The reflectors of both the subunits overall show aggradational stacking pattern and are relatively continuous in nature. However, the basal subunit is generally discontinuous with low amplitudes as shown. Often patches of discontinuous and chaotic seismic facies are observed in both the subunits of the formation as shown. Few truncations also occur at the top of the formation represented by the green arrows indicating that the Tor Formation top is an unconformity in the basin. The interpretations are interpolated in the area with poor seismic quality. The legends and the location of this seismic profile are shown in Figure 44.

91
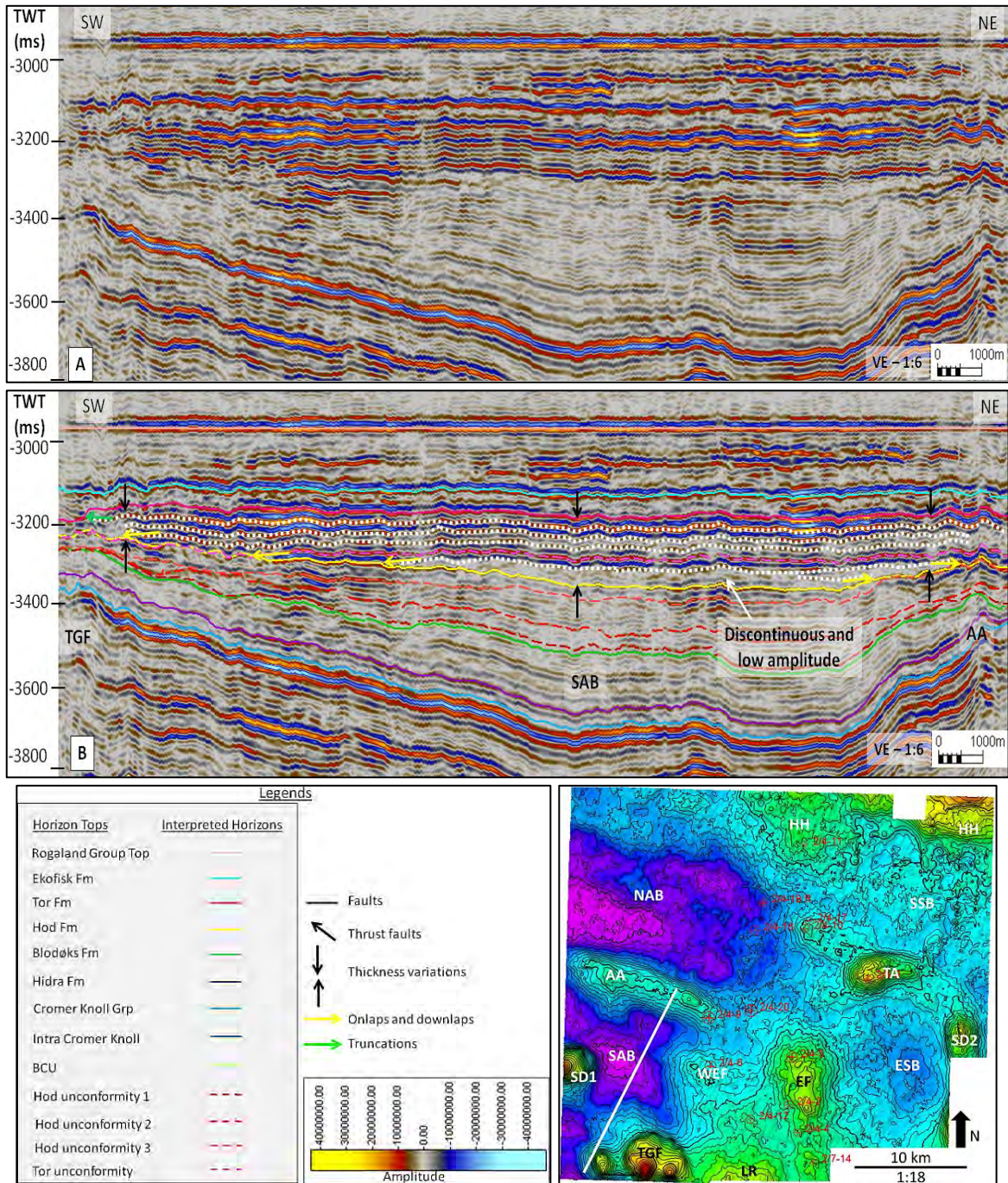
Figure 46: (A) Uninterpreted and (B) Interpreted 3D seismic line flattened on Rogaland Group Top in the SAB. The location of the seismic section is shown in the inset TWT map of the Tor Formation top. The basal subunit clearly has a transparent and discontinuous seismic facies which is different from the overlying parallel, strong and continuous seismic facies of the top subunit. Onlapping features are present on the flank of TGF for both the subunits while only the basal unit onlaps on the AA. The top subunit of the Tor Formation drapes over the AA. The thickness of the formation decreases on the crests of the TGF and AA which possibly is due to erosion although no clear truncations are identified. This also indicates that the TGF was undergoing slow uplift during the Tor deposition and AA underwent uplift during the deposition of the basal subunit of the Tor Formation. The location of the seismic section is shown in the inset TWT map of the Tor Formation top.

92
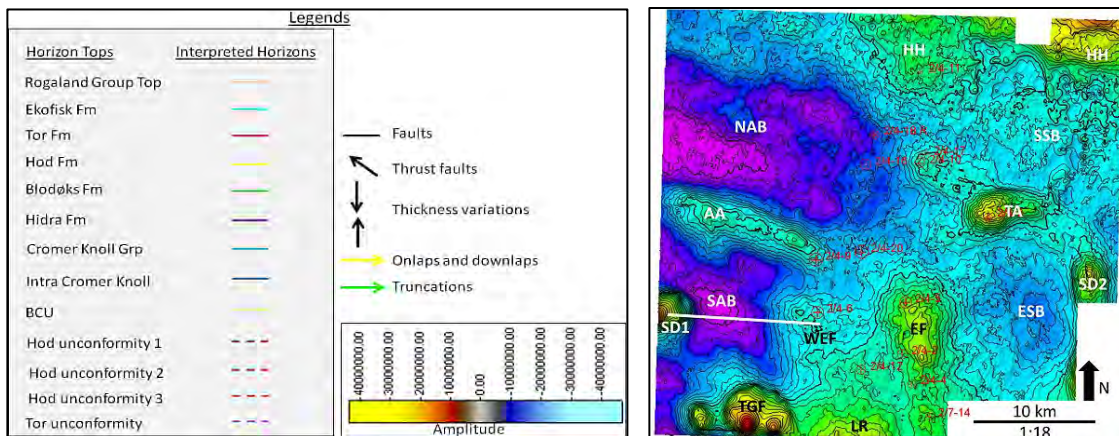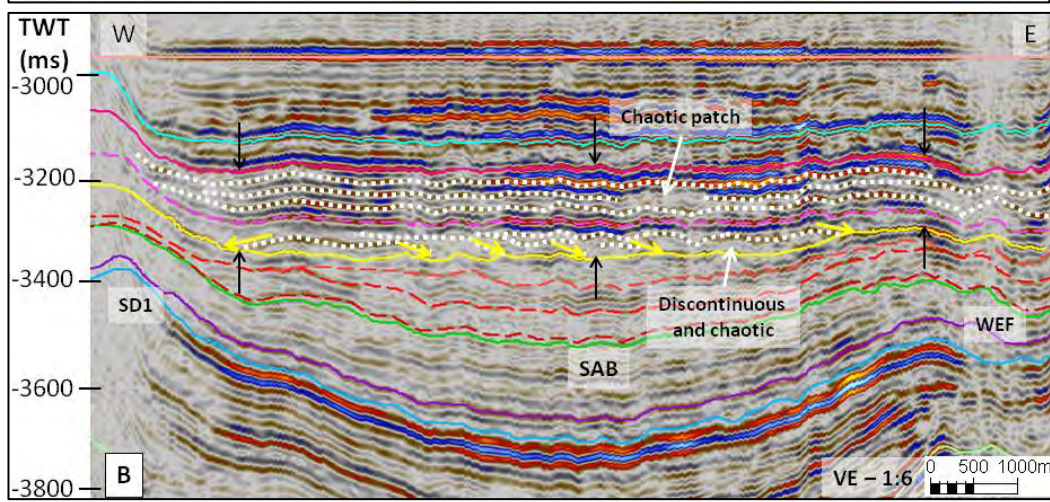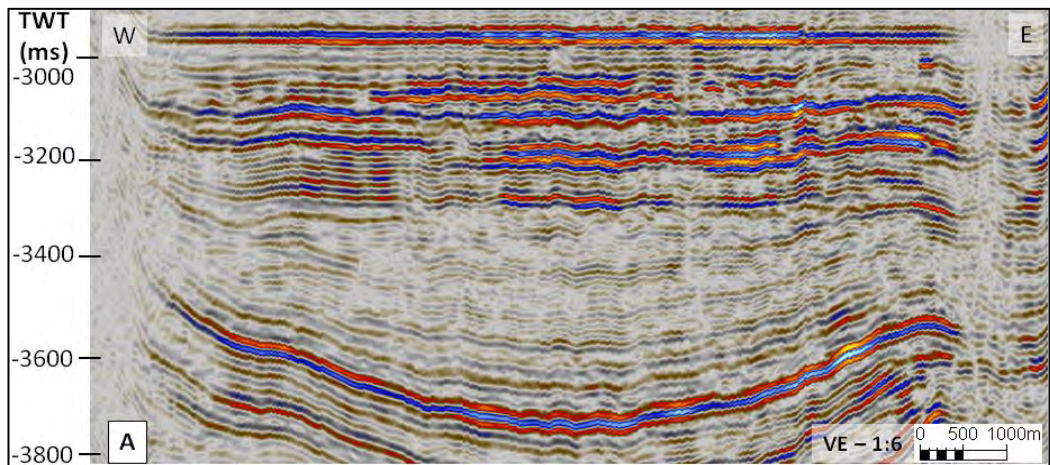
Figure 47: (A) Uninterpreted and (B) Interpreted 3D seismic line flattened on Rogaland Group top in the SAB. The basal subunit is discontinuous with low amplitudes. Progradation of sediment layers towards the basin center from the SD1 flank is observed as marked by the yellow arrows. Onlaps on the WEF flank also occur in the basal subunit. The top subunit has aggradational stacking pattern with strong reflectors. Near the flank of the SD1, the seismic quality becomes poor. The reflectors of the top subunit drape the WEF. Few chaotic patches as shown are also present in this unit indicating gravity flows from different directions. The overall thickness of the formation is uniform in the section apart from in the flank of the SD1 where it is thinner. The location of the seismic section is shown in the inset TWT map of the Tor Formation top.
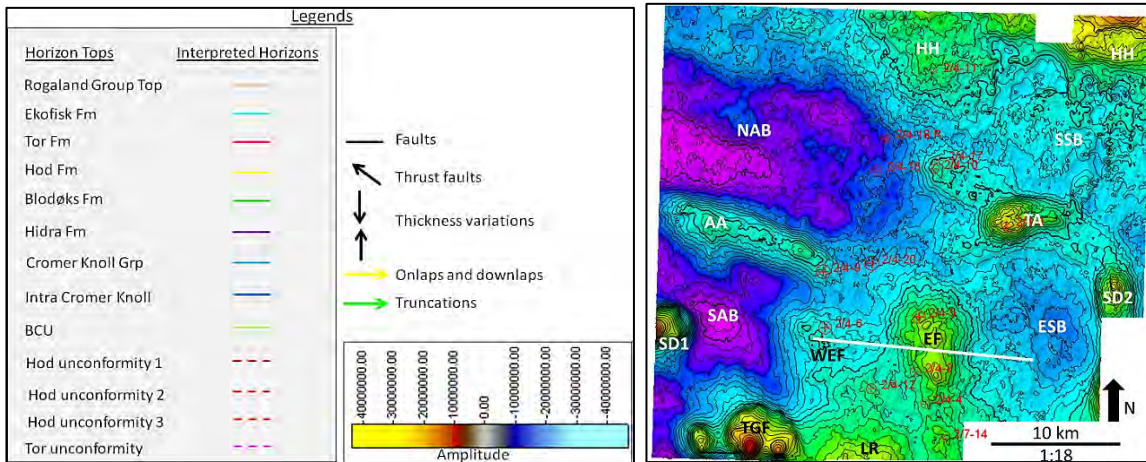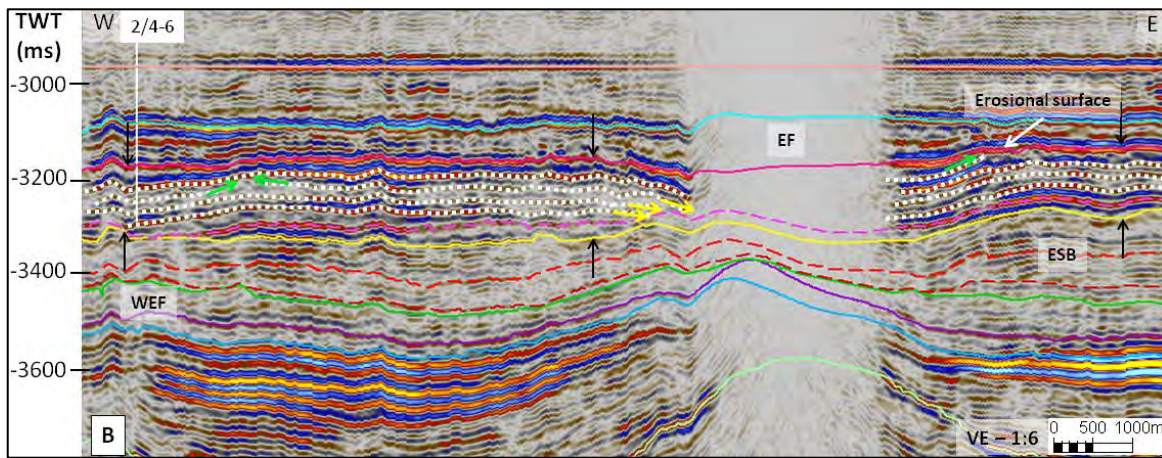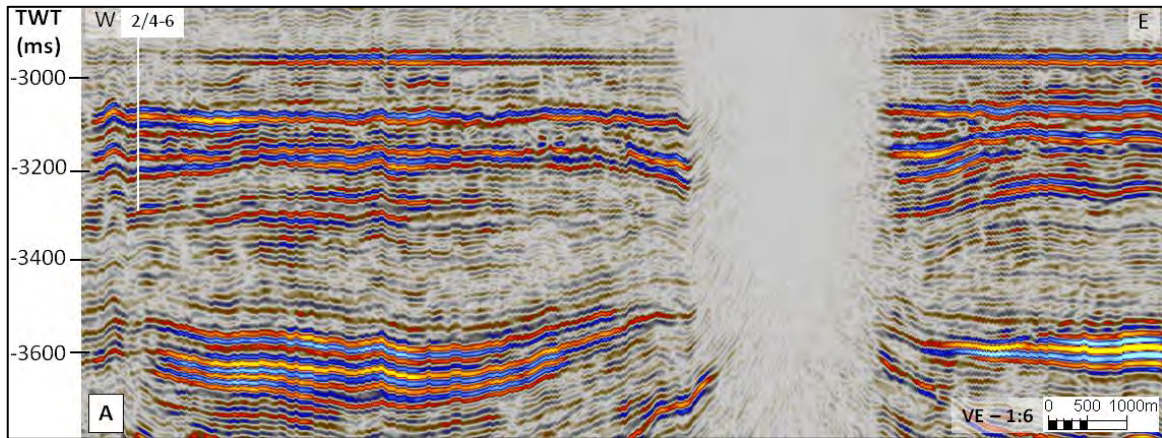
Figure 48: (A) Uninterpreted and (B) Interpreted 3D seismic line flattened on Rogaland Group top around WEF and EF. The basal subunit is very thin in this area. The top subunit displays aggradational pattern with a draping characteristics indicating increase in accommodation space. Few stratal truncations are spotted (green arrows) near the WEF and to the east of EF in the ESB at or near the top of the Tor Formation. The Formation top is an erosional surface in the ESB and represents an unconformity. The thickness of the formation in this profile is relatively uniform. In the EF area the interpretations are interpolated. The location of the seismic section is shown in the inset TWT map of the Tor Formation top.
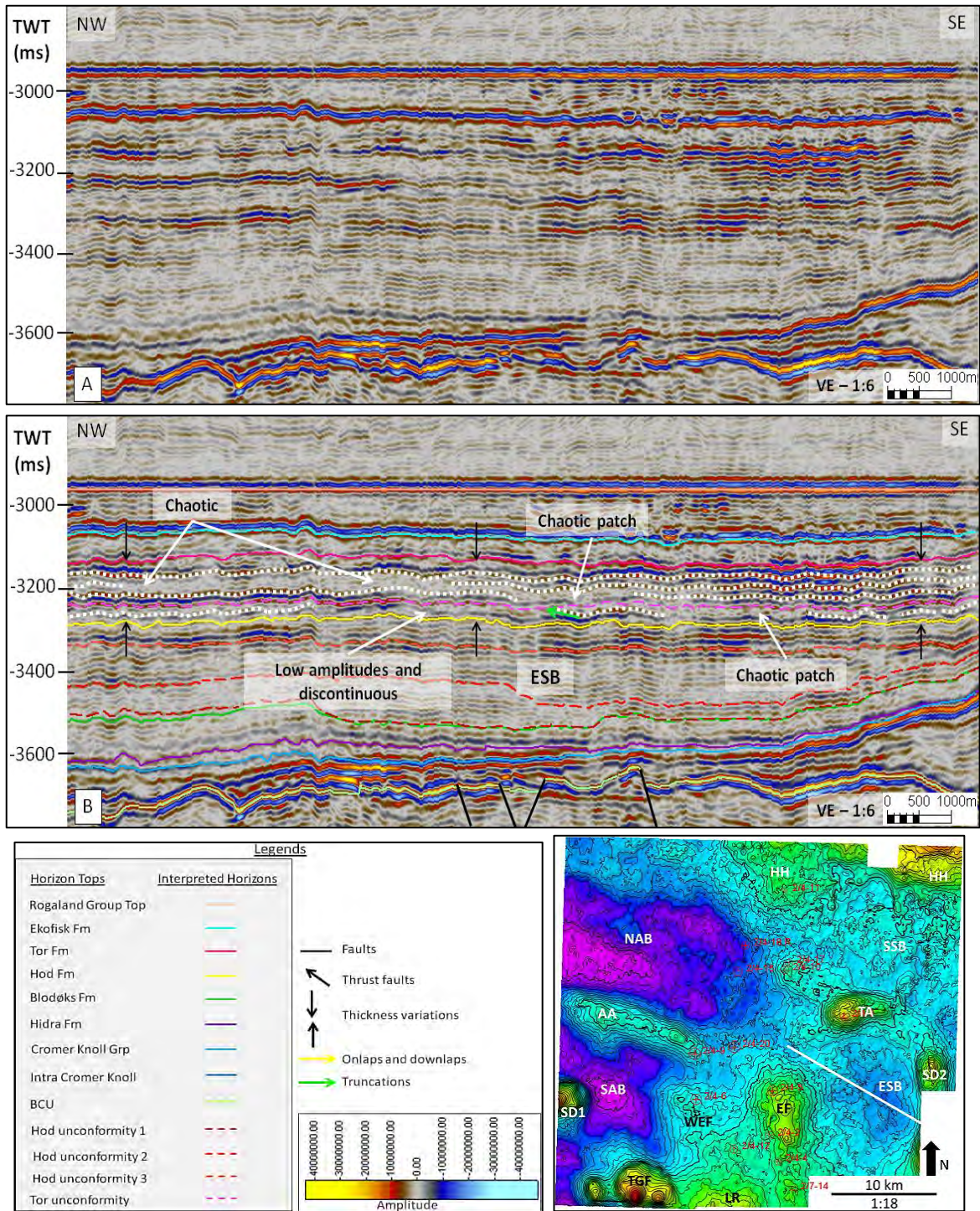
Figure 49: (A) Uninterpreted and (B) Interpreted 3D seismic line flattened on Rogaland Group top in the ESB. Chaotic seismic facies towards the NW of the basin in the top subunit is observed while the basal subunit has an extended chaotic seismic facies towards the SE. These patches possibly represent gravity flows in different directions. In the SE the top subunit displays an aggradational pattern indicating relatively undisturbed deposition. The stratal terminations within the formation are not very clear in this profile except for few truncations at the Tor unconformity as shown by the green arrow. The location of the seismic section is shown in the inset TWT map of the Tor Formation top.
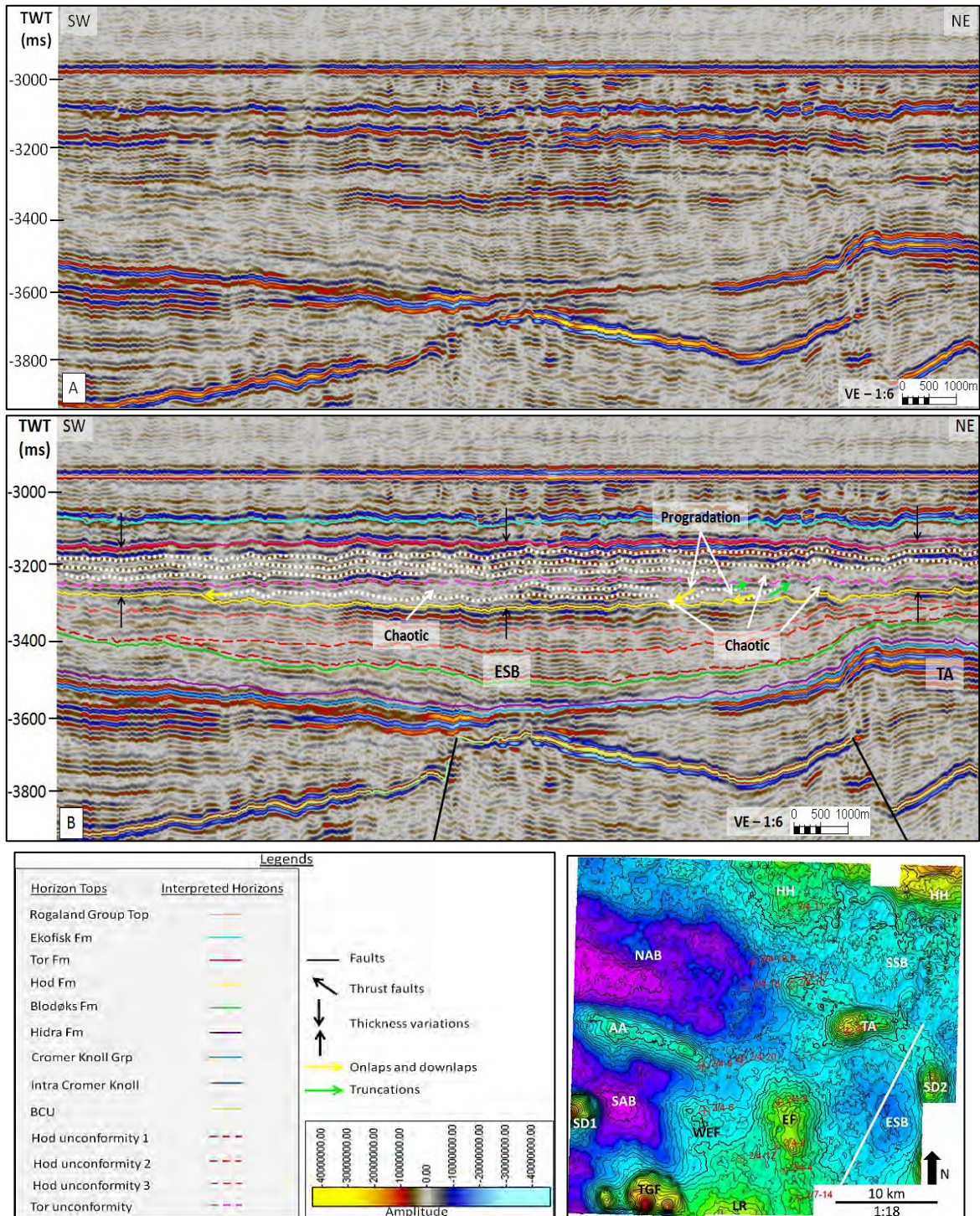
Figure 50: (A) Uninterpreted and (B) Interpreted 3D seismic line flattened on Rogaland Group top in the ESB. The basal subunit shows prograding features on the flank of TA while they onlap towards the SW. This indicates that ESB was a depocenter during the early stages of the deposition of the Tor Formation. Patches of chaotic areas are observed as pointed out in both the subunits especially near TA indicating sediment flows. Overall the formation has an aggradational stacking pattern and display relatively uniform thickness throughout. The location of the seismic section is shown in the inset TWT map of the Tor Formation top.

96
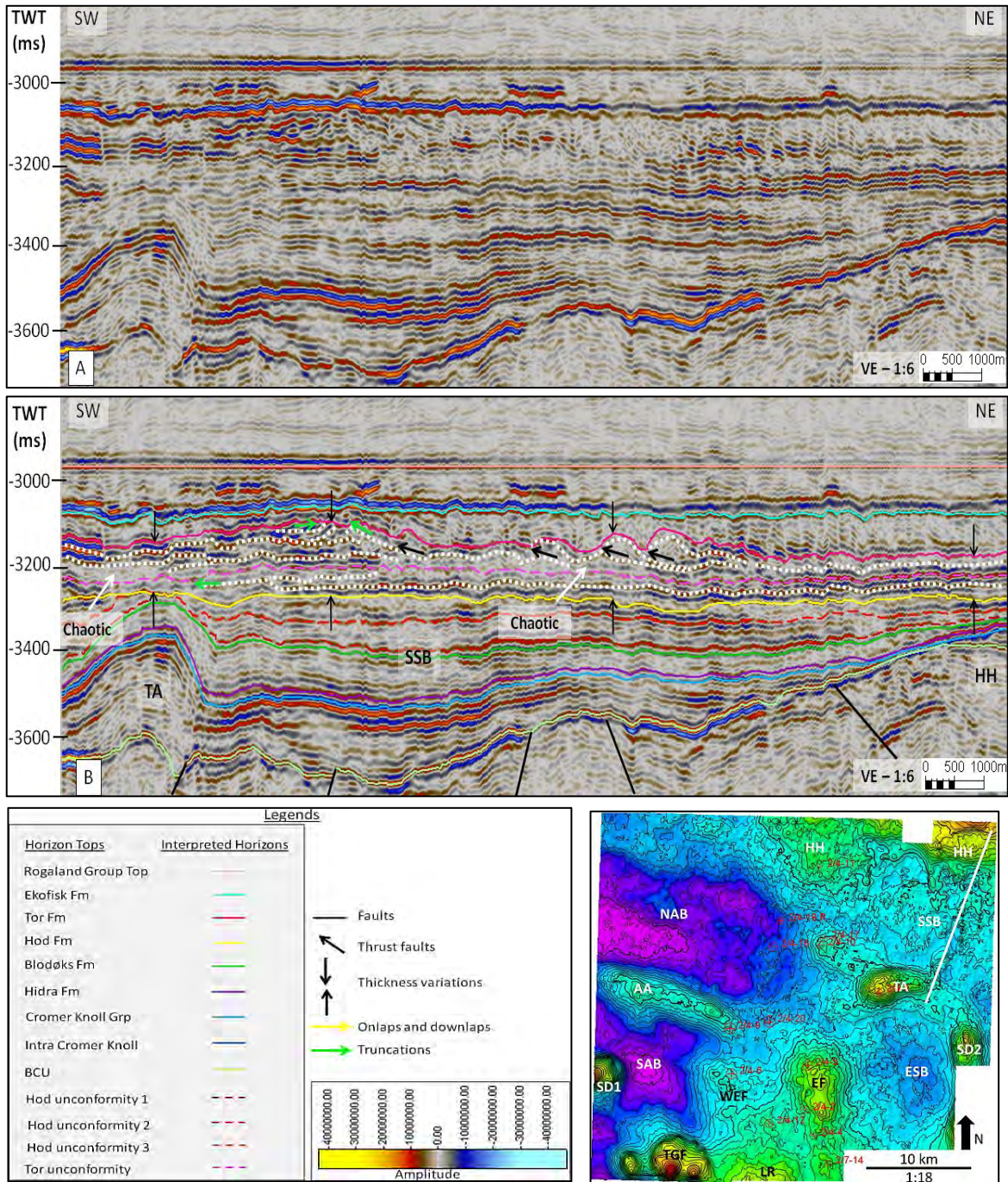
Figure 51: (A) Uninterpreted and (B) Interpreted 3D seismic line flattened on Rogaland Group top in the SSB. The top subunit of the formation has distinctive thrusting features causing several tiny thrust faults as shown indicating a possible local compressional force from NE towards the SW. It is also possible this feature represents a mega slide caused by the NE-SW trending compressional force. Near the TA these displaced sediments are eroded at the top of the formation (green arrows). The formation has varying thickness due to the compressional force creating the thrusting. Some basal reflectors are also truncated at the top of the TA as shown. The location of the seismic section is shown in the inset TWT map of the Tor Formation top.
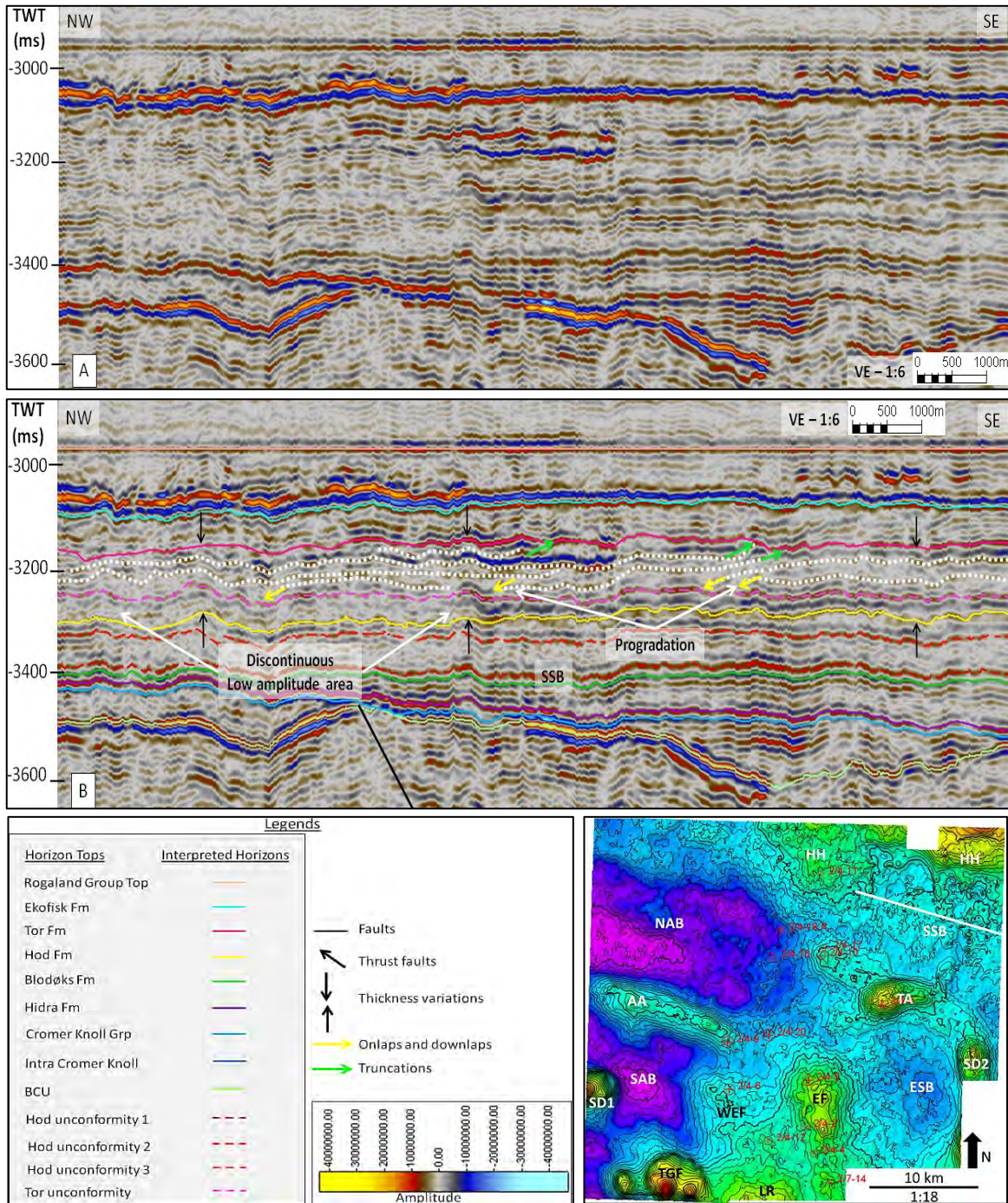
Figure 52: (A) Uninterpreted and (B) Interpreted 3D seismic line flattened on Rogaland Grp. Top in the SSB. The top subunit reflectors show prograding nature of the reflectors towards the NW of the basin as shown by the yellow downlap arrows. The basal unit is quite blurry and chaotic towards the NW. Few reflectors on the top are also truncates by the top reflector of the formation as pointed out. In general the thickness of the formation in this profile is very uniform. The location of the seismic section is shown in the inset TWT map of the Tor Formation top.
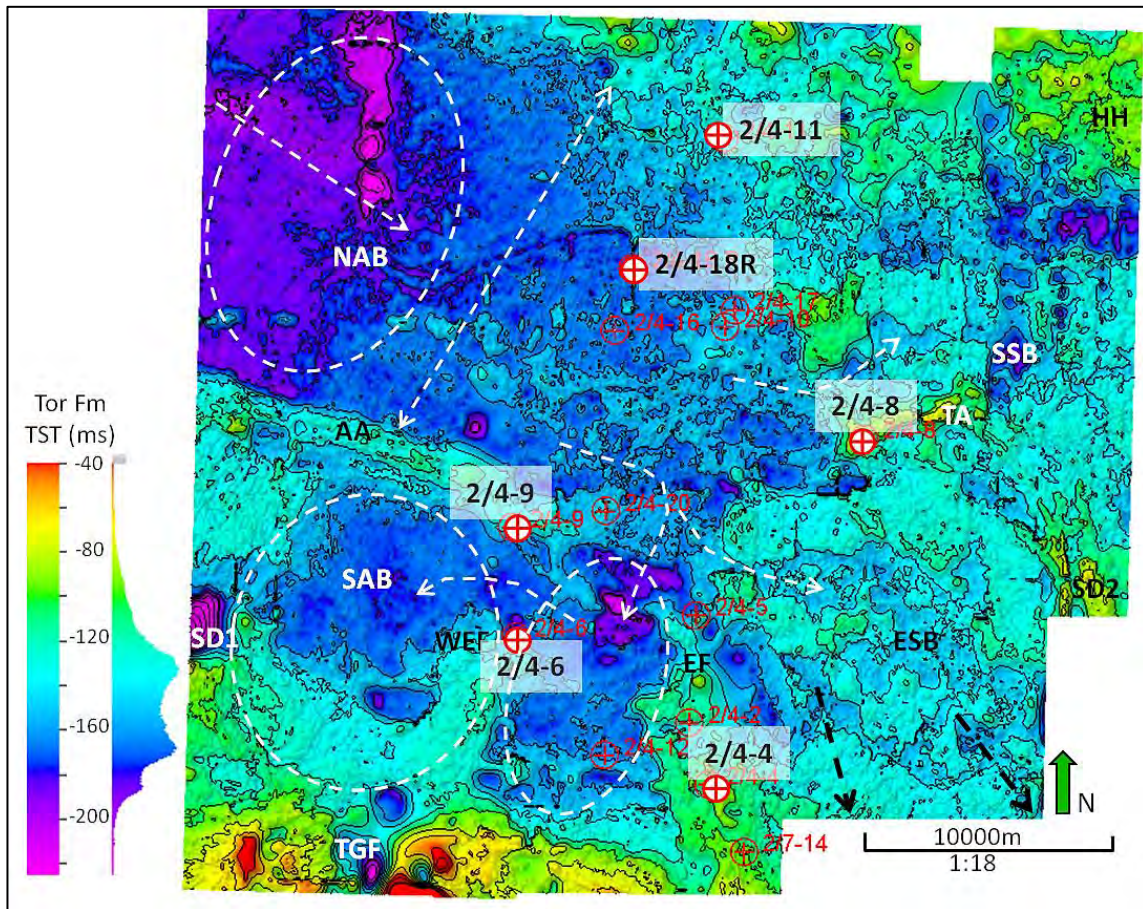
Figure 53: Isochron map of the Tor Formation in the study area. All the initially isolated basins are now connected to each other. A new sediment package developed in the encircled area between WEF and EF whose sediment supply is from the NAB as shown by the arrow coming into the area. NAB displays thicker sediments in the NW (encircled) with a flow direction towards the SE shown by the arrow in this area. This basin now is also wider in the NE-SW direction (shown by the double arrow) than before. The enclosed SAB has the thickest sediments in its center and is indirectly fed by sediments coming from the NAB as shown by the arrow coming into the SAB. ESB is still fed with sediments from the NAB and now extends further towards the SE (indicated by the black arrows). SSB shows narrow connectivity between itself and NAB (arrow going into SSB). The sediment deposition in this basin also expanded further NE.

5.1.5   Ekofisk Formation

The Ekofisk formation is the topmost lithostratigraphic unit of the chalk interval and is bounded by the Tor Formation at the base and Rogaland Group at the top (Figures 5 and 7). This unit was deposited in the Danian (Isaksen et al., 1989).

99

5.1.5.1. Well Logs and cores

<u>Lithology from cores</u>: Hard, dense, white, tan or beige limestones are the basic constituents of this formation. It also contains mudstones with occasional packstones, argillaceous chalks, chalky limestones or clean limestones (Isaksen et al., 1989).

<u>GR, DT, RHOB characteristics</u>: The gamma ray values slightly increase and are more irregular in nature in this formation at the base (Figure 13). The acoustic impedance at the base does not show much difference compared to that in the Tor Formation below. Towards the upper boundary, the gamma ray values jump to high values and the acoustic impedance values fall down as the lithology changes from chalk to marls in the base of the Rogaland Group (Figures 7 and 13).

5.1.5.2. Seismic observations

The top Ekofisk is represented by a strong peak which is planar to occasionally irregular in nature in the study area (Figures 5, 7 and 54-62), while the base of the formation is marked by the strong peak of the top Tor Formation. The formation is thiner in the study area. The seismic facies towards the base of the Ekofisk Formation is generally continuous in nature but also displays occasional discontinuity as shown in Figures 54-62. The facies towards the upper part of the formation is chaotic in the ESB (Figure 59) while in the other basins it is not clearly visible to categorize. The base of the formation also displays relatively higher amplitudes compared to the underlying formations.

In the NAB (Figures 54 and 55,) the formation displays uniform thickness draping over the highs of AA and HH, with a slight thickening towards the SE of the basin. Few truncations at the top of the Ekofisk Formation and downlap on the top Tor Formation is observed near the center of the basin in Figure 54. Figure 55 displays patches of chaotic seismic facies along the basin.

In the SAB (Figures 56 and 57), the thickness of the formation is overall uniform, may be slightly thicker towards the WEF. Chaotic facies is present around the crests of the TGF and AA (Figure 56) while the facies is relatively continuous between SD1 and WEF in Figure 57. The reflectors might display truncation near the flank of SD1. In Figure 58, the seismic facies around WEF and EF is clearly continuous and parallel in

nature with few local pockets of erosion. The thickness of the formation here is slightly less between the highs WEF and EF compared to that towards the highs.

In the ESB (Figures 59 and 60), the basal seismic facies of the uniformly thick Ekofisk Formation is continuous in nature with few discontinuities. A chaotic nature of the facies is observed near the upper part of the formation in Figure 59 while in Figure 60 the reflectors are often truncated at the top of the formation prograding towards the basin center.

The Ekofisk Formation displays varying thickness in the SSB (Figure 61), predominantly due to the highly undulating top of the Tor Formation. Similar to that in the Tor Formation in this area, the Ekofisk formation shows layers overriding each other with presence of small thrust faults between them in the NE representing the mega slide. The reflectors are usually truncated at the top of the formation here. In Figure 62, prograding features towards the HH in the NW are observed within the formation. The layers downlap onto the top Tor Formation and are truncated at the top of the Ekofisk Formation. This thickness of the formation is relatively uniform in the Figure 62 and the layers display progradation towards the NW margin of the SSB.

5.1.5.3. *Maps and observations*

TWT structure maps: Ekofisk Formation top (Figure 10 and 11F) shows a general depth of ~3171m (~3150ms) on an average while the deepest areas (~3400-3940m or ~3300-3500ms) are in the NAB and SAB. The shallowest areas (~2881-2993m or ~2900-3000ms) are at the EF, TA, TGF and HH in the north east. The SSB and the ESB are at depths of ~3171m (~3150ms) and ~3316m (3250ms), respectively.

TST isochron map: The isochron map of the Ekofisk Formation (Figure 63) shows an average of ~138m (~55ms) sediments deposited during the Danian period in the study area. Although the sediment thickness is relatively uniform in the area, the thickest sedimentation (~175-250m or ~70-100ms) is identified in the SSB area. Thick sediment packages are also present in the area between WEF and the EF. In the SE of the NAB a small area also shows thick deposition. Otherwise, in the NAB, SAB and the ESB the

sediment thickness is lower and averages ~113m (~45ms). Figure 63 displays the discussed points in details.

Distribution: The isochron map (Figures 63) of the Ekofisk Formation shows that the sediment distribution of the formation is relatively uniform with a slightly higher rate towards the west and NE of the SSB, in the southeastern part of central NAB and in the area between the WEF and the EF. Otherwise, the formation drapes the whole area including the NAB, SAB and ESB. Figure 63 displays no specific sediment transportation direction in this formation.

5.1.5.4. *Interpretations*

The relative sea level fall during the late Maastrichtian until the early Danian lead to an aggradational environment when the Ekofisk formation was deposited. The gamma ray logs showing slightly higher values and a higher serrated nature (Figures 7 and 13) compared to that in Tor Formation along with decreased sonic log values imply an increase in clay particles in the Ekofisk Formation. The sonic logs showing slightly lower values compared to that in the upper part of the Ekofisk Formation and the underlying Tor Formation (Figure 7) imply that this is a comparatively compact zone with low porosity as also mentioned in the studies by Bramwell et al., (1999) and Gennaro et al., (2013). According to these studies, from the core data, the basal part of the formation consists of clay-rich chalks with abundant flint, marl beds and hardgrounds and is informally referred to as the Ekofisk dense zone or Ekofisk tight zone.

The patches of chaotic seismic facies within the Ekofisk Formation in the NAB and at the crest of the AA indicate possible gravity driven flows from different directions towards the basin center (Figure 54-55). Several downlaps on the flanks of AA and HH prograding towards the basin center also indicate sediment flows from the structural highs into the basin. This also refers to a continued uplift of the AA and HH. The truncations of the reflectors at the top of the formation also indicate that the Ekofisk Formation represent an unconformity in the NAB.

Figures 56-57 show exceptions to a generally continuous seismic facies in the SAB at the TGF and AA crests. The chaotic facies present near the highs restrict themselves in

a smaller area indicating small uplifts of TGF and AA leading to smaller gravity flows along their flanks. The WEF and the SD1 structures were possibly inactive during the Danian period since they display continuous facies on their flanks in Figure 57. The discontinuity created in the center of the SAB in Figure 57 represents an erosional patch caused most likely by the gravity flows from the AA and TGF.

The Ekofisk Formation is thickest between the WEF and EF as shown in the Figure 58 and shows relatively undisturbed deposition of chalk as indicated by the parallel and continuous seismic facies. Few truncations present refer the formation top as an unconformity in the area. It is evident from Figure 60 that the prograding pattern of the truncations towards the basin center represents possible slumps and slides from the NW of the ESB. These slumps and slides create discontinuities representing erosional patches as shown in the Figure 59. In SSB, to the NE (Figure 61), the overriding characteristics of the layers creating small thrust faults indicate a possible compressional force acting in NE-SW direction from further NE of the study area leading to a mega slide mass transport system. The deformed sediment layers due to sliding were then eroded away as indicated by the truncations at the formation top. This in turn implies that the Ekofisk Formation top is an unconformity in the area. The progradational pattern towards the HH in SSB observed in Figure 62 reflects a possible depocenter in the WNW SSB during the Danian which might have been inverted in later stages.

The upper reflectors of the formation showing slight lowering sonic log values implies on possible decrease in clay content in the formation as also mentioned in Isaksen et al., (1989). The overall seismic facies in the upper Ekofisk Formation in the whole area also shows a change from the basal reflectors and are generally discontinuous with medium amplitudes indicating the end of the tight zone (Figure 59). The Ekofisk Formation is mostly dominated by gravity and turbidity flows and thus is interpreted to consist of allochthonous sediments from different basins and sub basins in and around the study area.

The time-structure map of the top of the formation (Figure 10A) shows similar features as before but the relief differences between the structural highs and the basins are not as sharp as before. This implies on a basin infilling process in the area. The isochron

map (Figure 63) showing a widespread chalk deposition in entire area also implies the infilling behavior of the sediments. The SE of the central NAB, west and NE of SSB and the area between WEF and EF has the highest sedimentation rate since they have the thickest sediments (Figures 55, 58 and 61-63). The WEF and EF show very high thickness values in Figure 63 but in the seismic these areas have very low resolution and thus the map in these areas has a higher uncertainty and is an artifact of gridding of the interpreted horizons.

Figure 54: (A) Uninterpreted and (B) Interpreted seismic cross section in the NAB, flattened on Rogaland Group Top. The thickness of the formation is uniform across the basin as shown by the black arrow pairs. The formation top is slightly irregular in this profile. Few truncations and downlaps present are shown. The areas inside the rectangles are towards the basin flanks and have chaotic and discontinuous in seismic facies indicating possible sediment redeposition processes.). The location of the seismic section is shown in the inset TWT map of the Ekofisk Formation top.
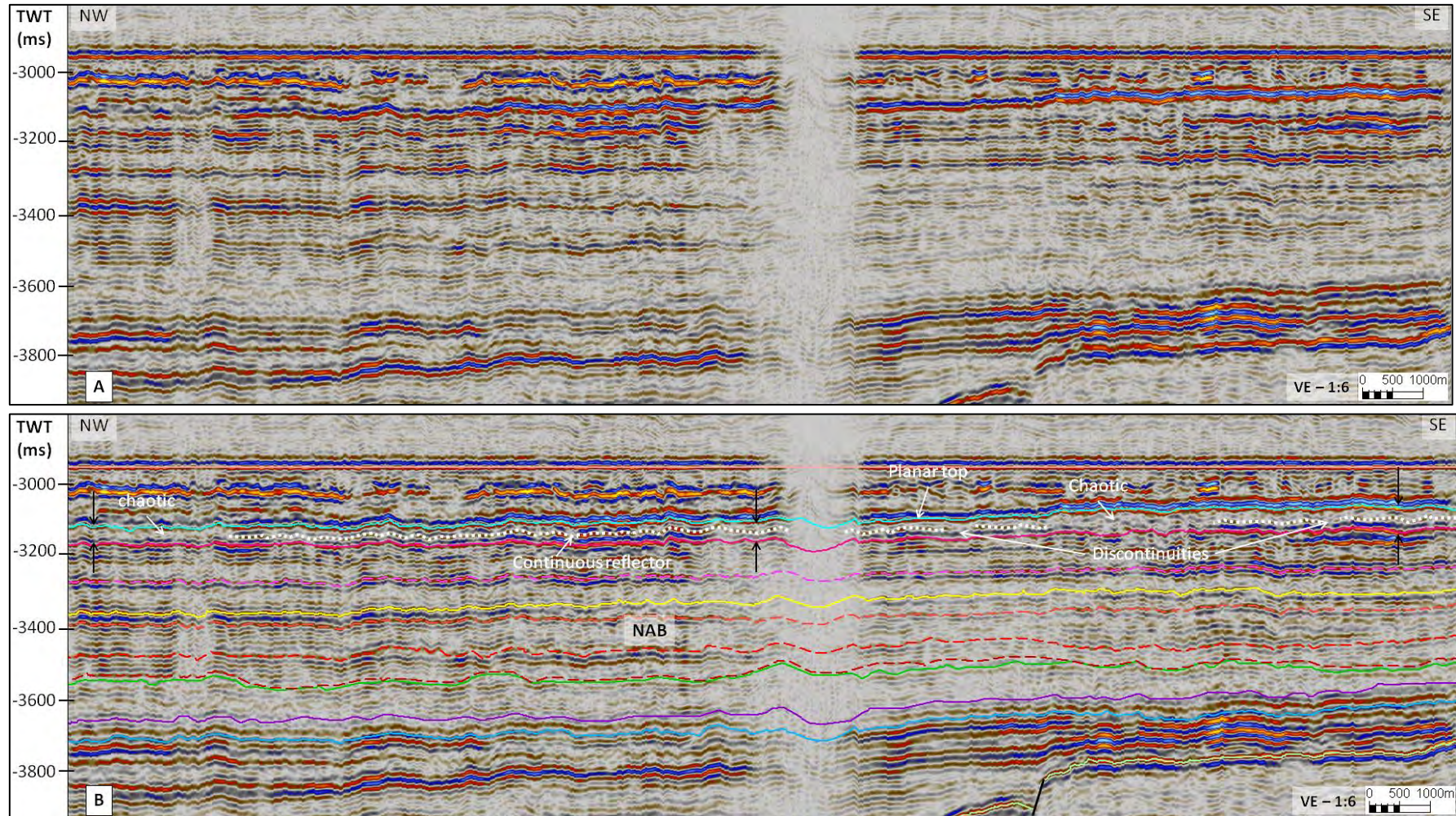
Figure 55: (A) Uninterpreted and (B) interpreted seismic cross section in the NAB, flattened on Rogaland Group Top. The Ekofisk Formation top often shows a planar to slightly irregular nature in this basin. The overall thickness of the formation increases towards the SE as shown by the increasing distance between the black arrow pairs. The formation contains irregular and chaotic seismic facies towards the NW and also towards the SE as shown. Small discontinuities in the reflectors are also observed. Stratal terminations are not clear in this section. The location and the legends are as shown in Figure 54.

106
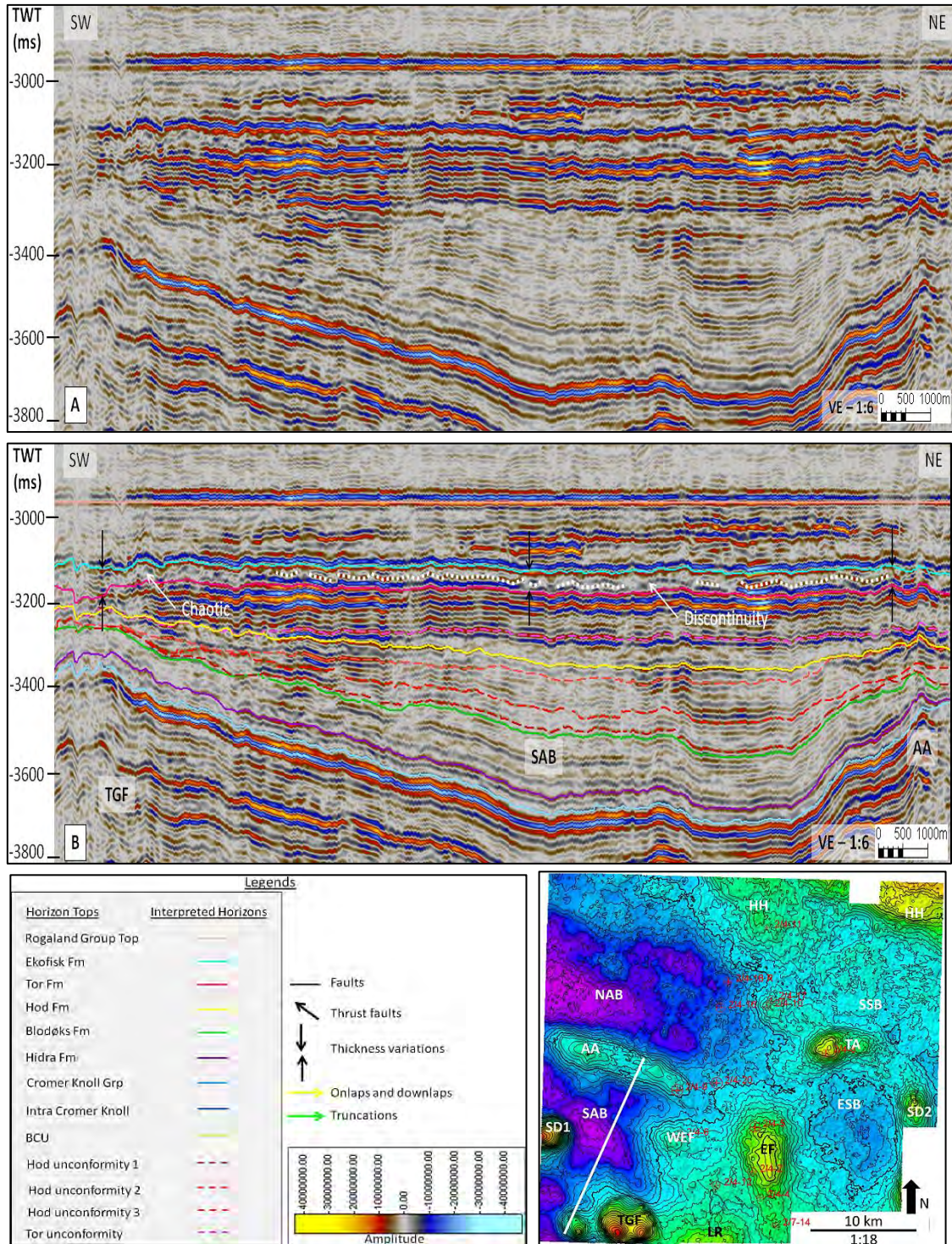
Figure 56: (A) Uninterpreted and (B) interpreted seismic cross section in the SAB, flattened on Rogaland Group Top. The formation displays uniform thickness in this section shown by the black arrow pairs. Near the TGF the seismic facies is chaotic while towards the basin center the reflectors show discontinuity as shown. However, on the flanks of the TGF and AA the seismic facies is relatively continuous. It is possible that redeposition of sediments and turbidity flows from different directions disrupt the continuity of the layers. The location of the seismic section is shown in the inset TWT map of Ekofisk Formation top.

107
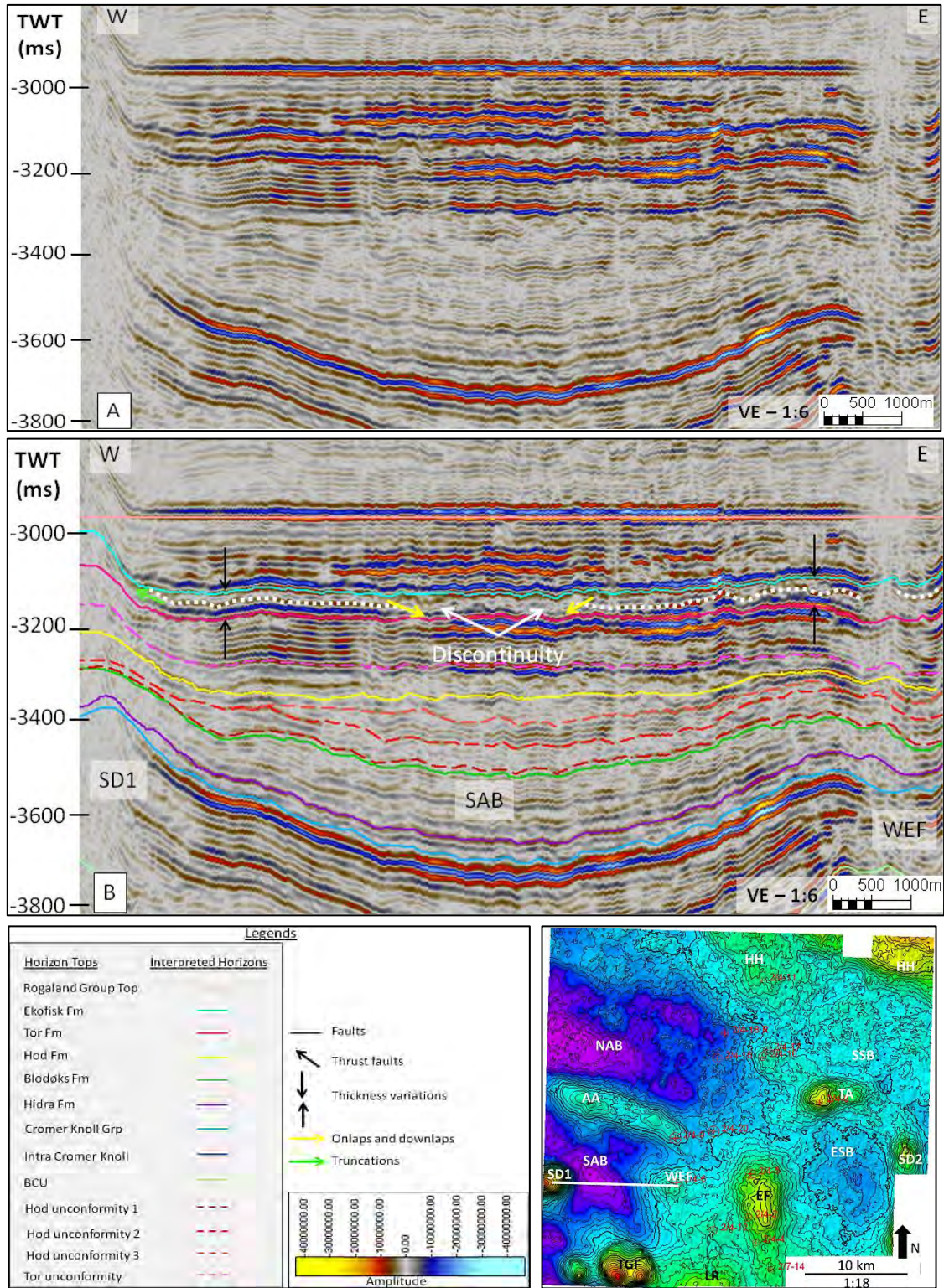
Figure 57: (A) Uninterpreted and (B) interpreted seismic cross section in the SAB, flattened on Rogaland Group Top. The formation top shows straight to wavy nature. The thickness of the formation is uniform in the section (shown by the black arrow pairs). Few reflector truncations at the Ekofisk Formation top and downlaps on the top Tor Formation are identified. Discontinuities in the basal layers are also present as shown. The location of the seismic section is shown in the inset TWT map of Ekofisk Formation top.
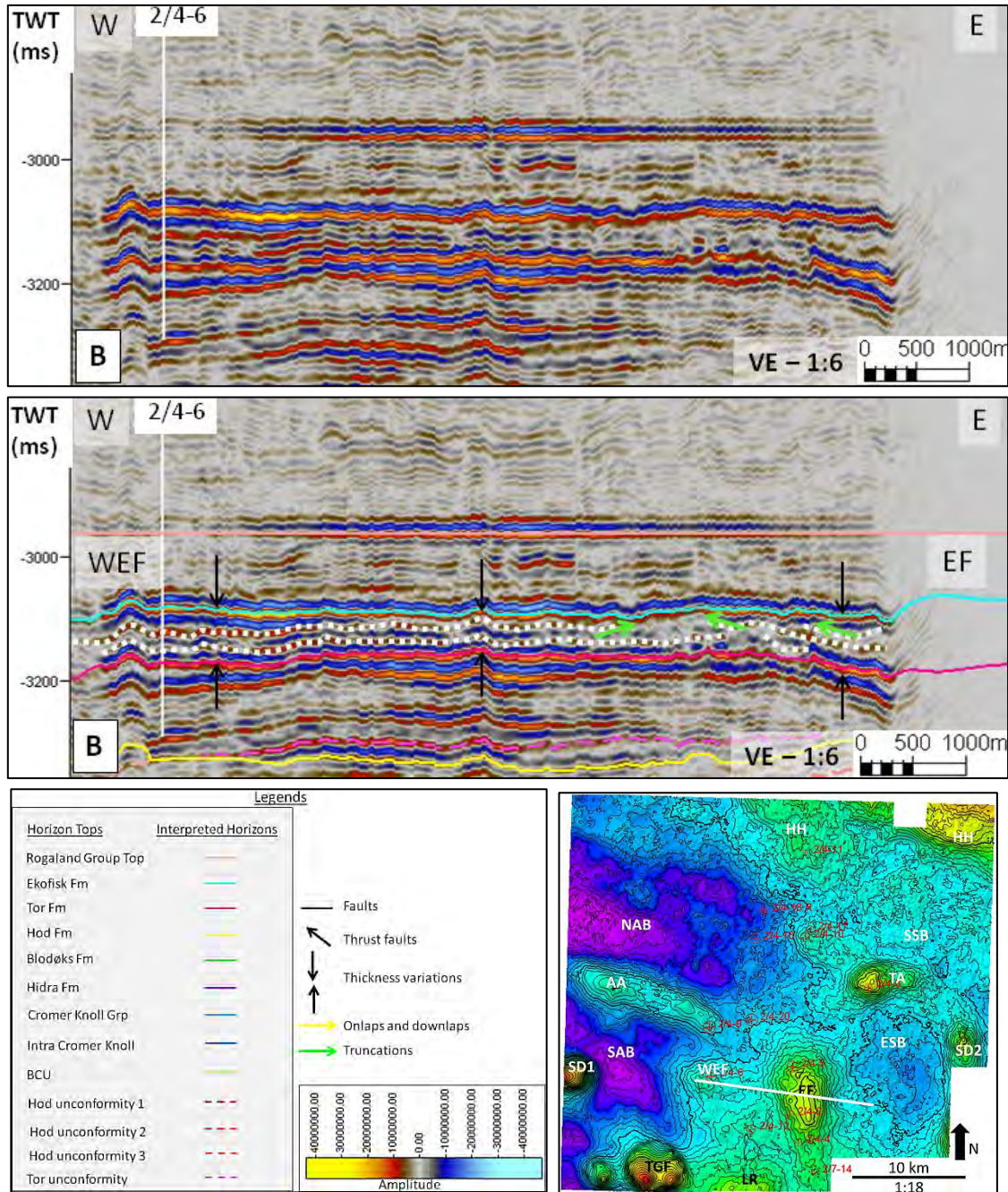
Figure 58: (A) Uninterpreted and (B) interpreted seismic cross section between WEF and EF, flattened on the Rogaland Group Top. The formation thickness slightly increases towards the highs of the WEF and EF compared to that in the middle area. The thickness of the deposits in this area is also more compared to the other basins in the study area. Both the basal and the upper reflectors of the formation show good continuity. Small discontinuities and erosional areas are also identified (marked by the green arrows). The location of the seismic section is shown in the inset TWT map of Ekofisk Formation top.
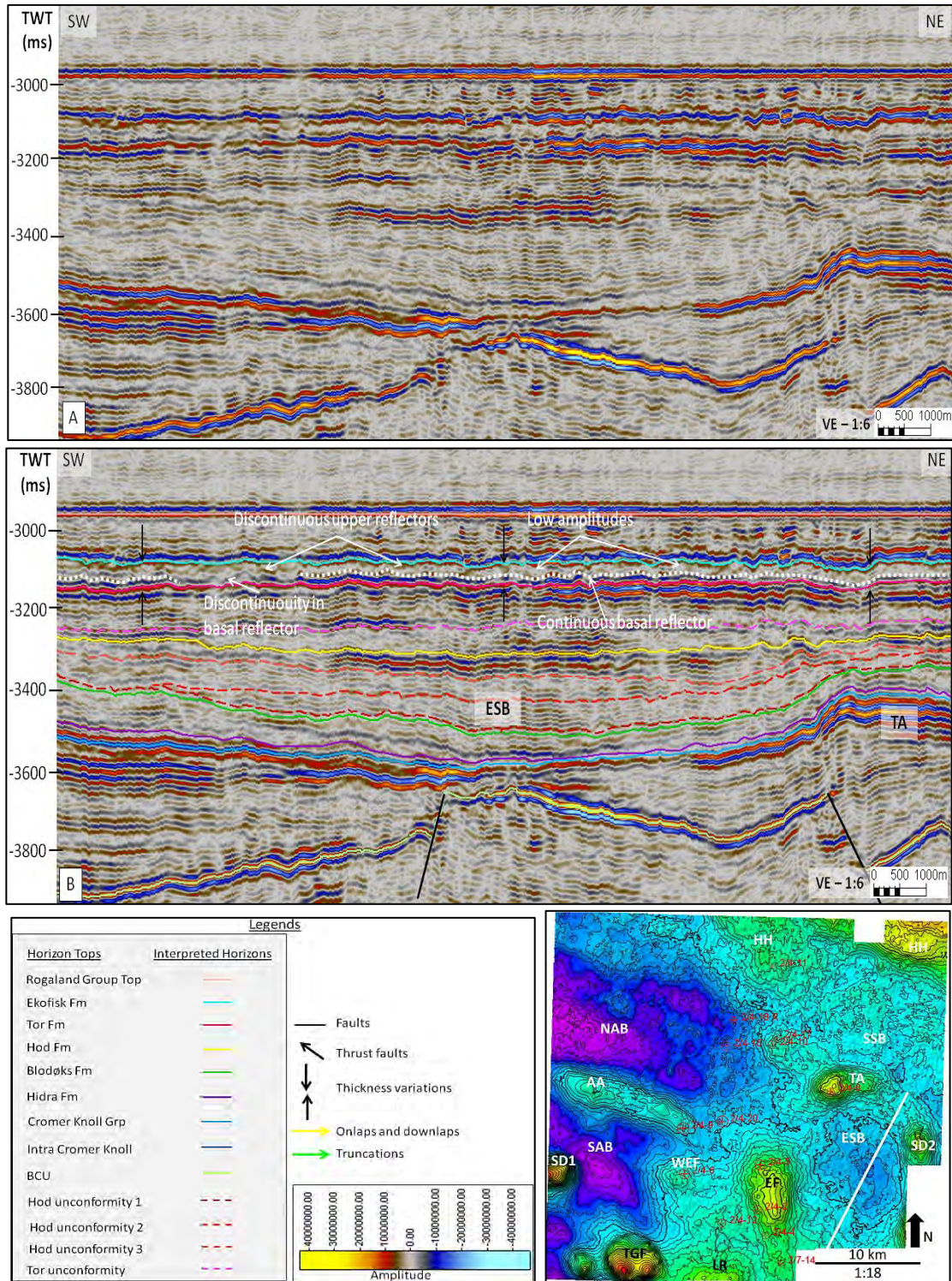
Figure59: (A) Uninterpreted and (B) interpreted seismic cross section in the ESB, flattened on top of the Rogaland Grp. The basal reflectors display good continuity (white dotted line) in general but are sometimes discontinuous with low amplitudes as shown. The reflectors in the upper part of the formation are generally discontinuous and have low amplitudes. The formation thickness in the ESB is uniform as shown by the black arrow pairs. The location of the seismic line is shown in the inset TWT map of Ekofisk Formation top.
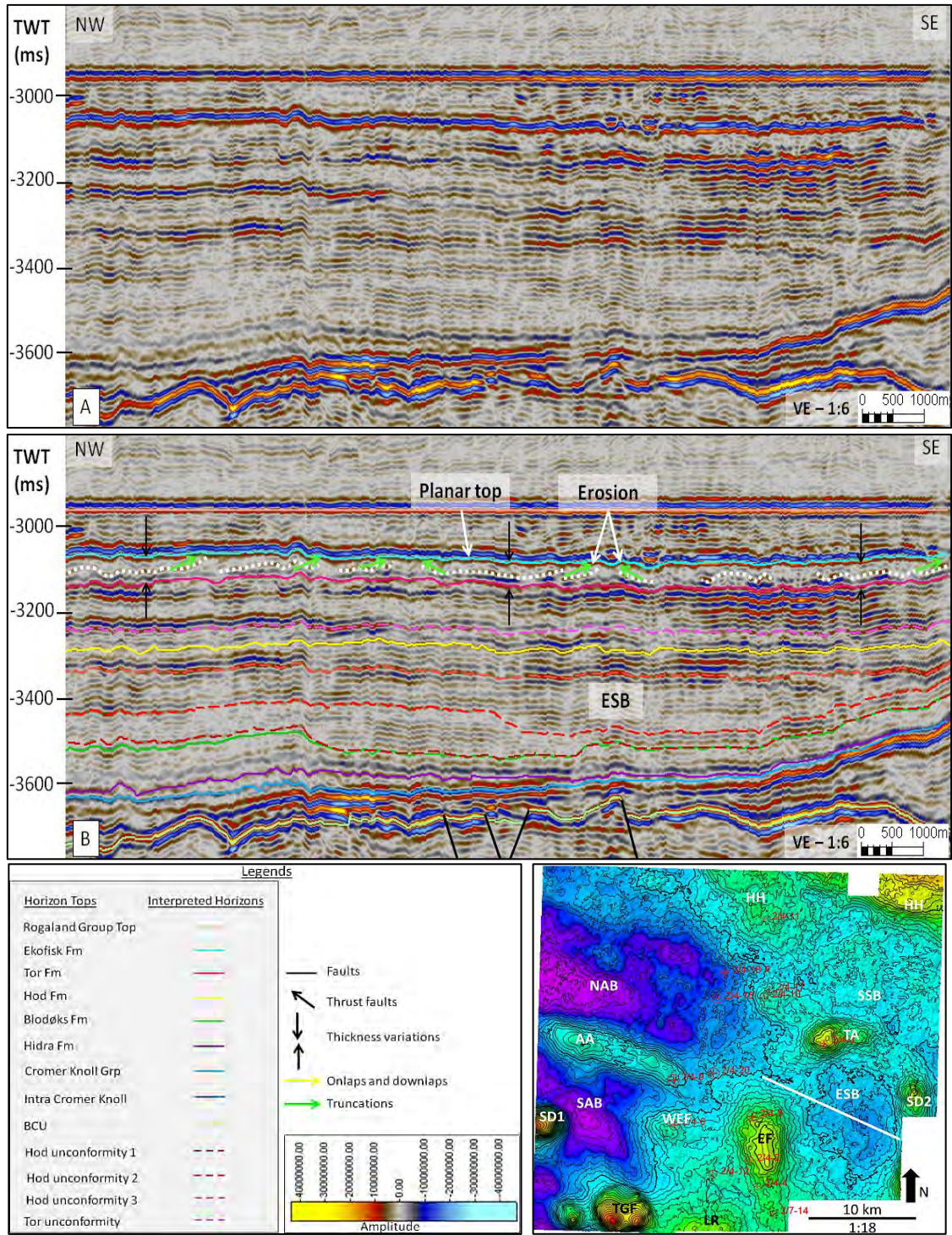
Figure 60: (A) Uninterpreted and (B) interpreted seismic cross section in the ESB, flattened on the top of the Rogaland Grp. The location is shown in the inset TWT map of Ekofisk Formation top. The Ekofisk Formation top shows planar nature often as shown. Several truncations occur at the formation top as shown by the green arrows which indicates that the formation top is an unconformity in ESB. The onlaps and downlaps are not clearly identifiable in this seismic profile. The basal reflectors show discontinuity as shown by the break in the white dotted lines. The formation displays a uniform thickness throughout the seismic profile.

111
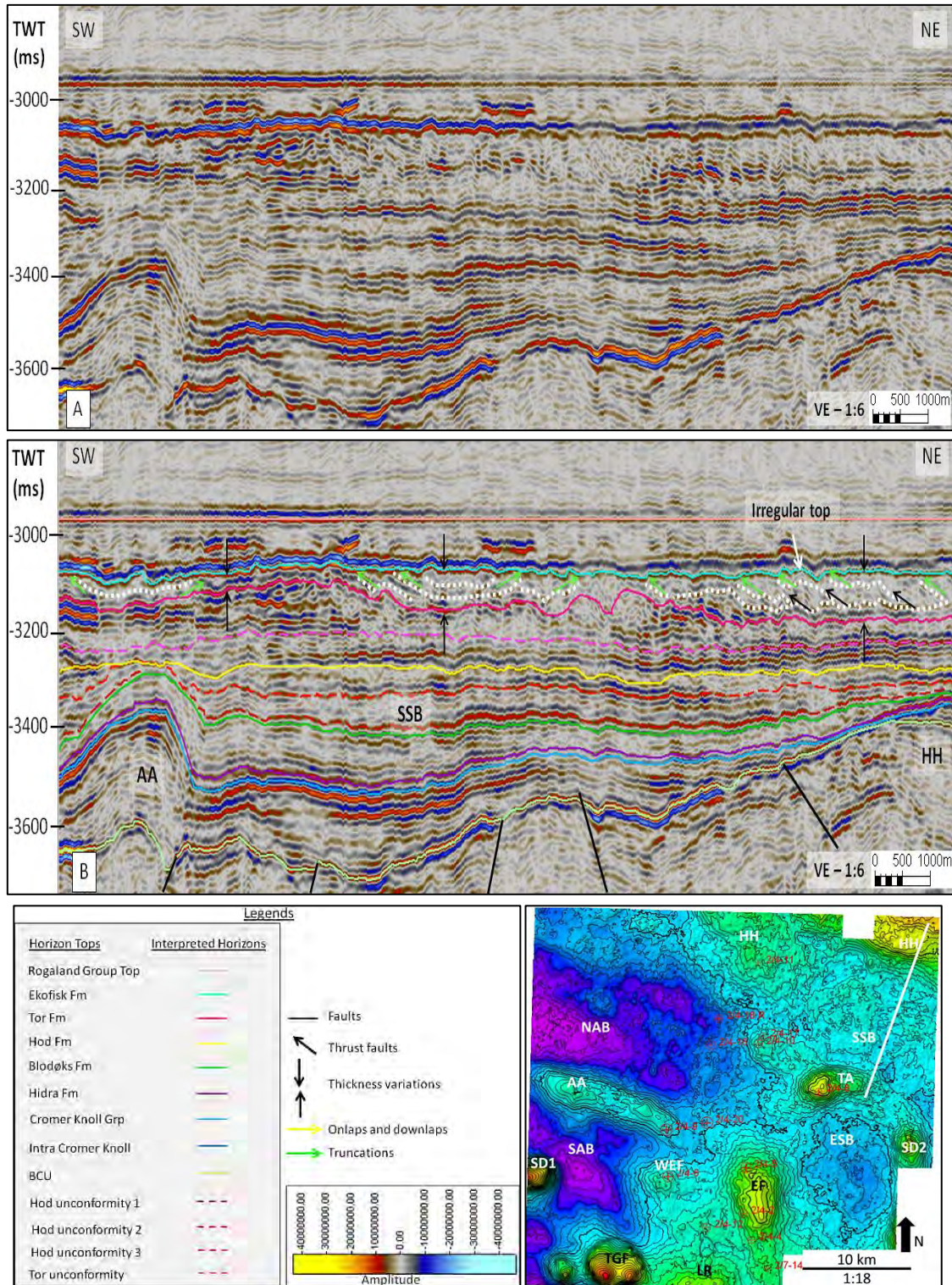
Figure 61: (A) Uninterpreted and (B) interpreted seismic cross section in the SSB, flattened on the Rogaland Grp. Top, showing several reflectors truncating at the Ekofisk Formation Top. This implies that the Ekofisk Formation top represents an unconformity in SSB. In the NE, the reflectors override on top of each other creating tiny thrust faults (black arrows). This feature could potentially be a megaslump system in the basin. The thickness of the formation varies throughout the section as pointed out by the black arrow pairs due to the presence of the megaslump. The location is shown in the inset TWT map of Ekofisk Formation top.

112
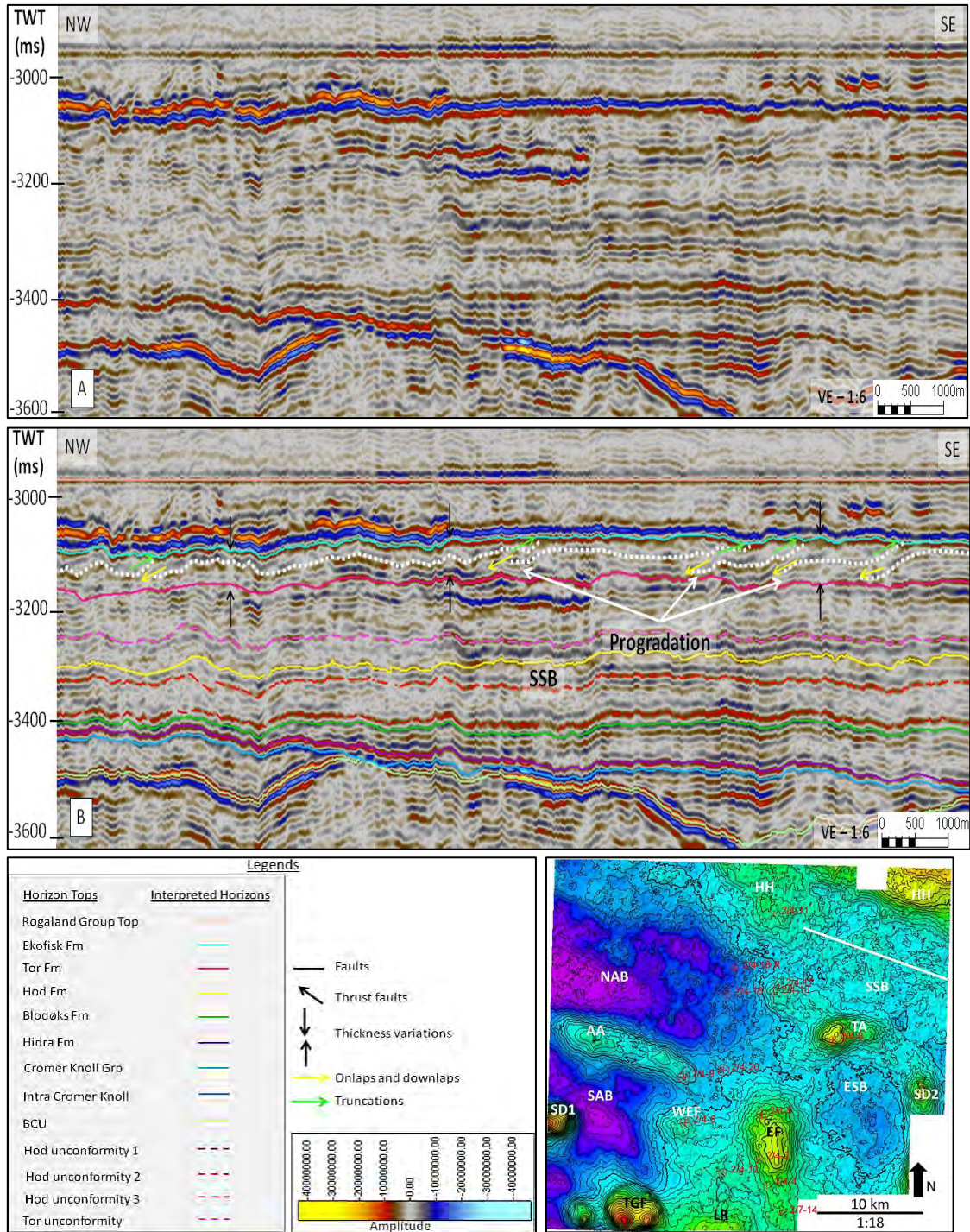
Figure 62: (A) Uninterpreted and (B) interpreted seismic cross section in SSB flattened on the Rogaland Grp. Top showing uniform thickness of the Ekofisk Formation in the SSB shown by the black arrow pairs. The internal reflectors truncate at the top of the Ekofisk Formation indicating it as an unconformity. A progradation pattern of the sediment layers can be noted (indicated by the downlap arrows) towards the HH, west of SSB. This indicates that the western and the north western margins of the SSB were a depocenter during the Danian period. The location is shown in the inset TWT map of Ekofisk Formation top.

113
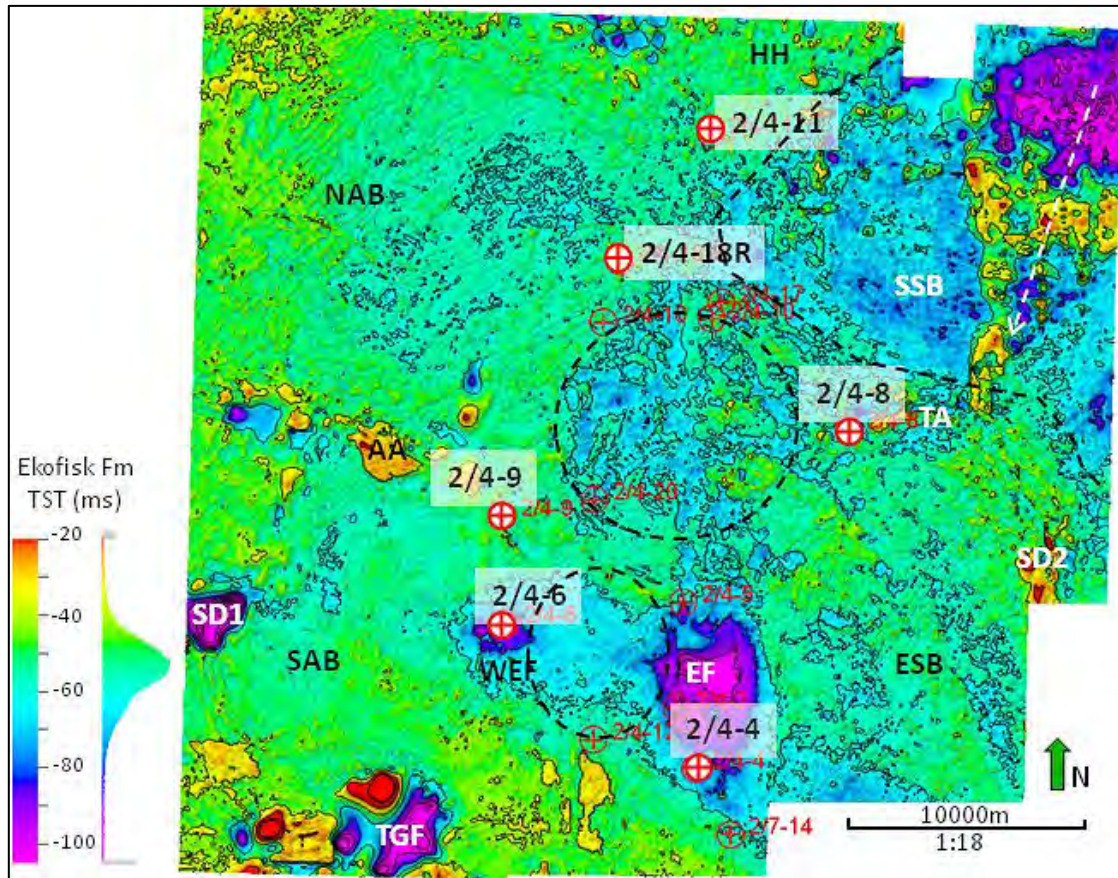
Figure 63: Isochron map of the Ekofisk Formation in the study area. The sediment thickness is approximately uniform in the whole area except in the NW. The SSB displays thicker sediments to its west and the NE as shown by the bounding line in the area. The white arrow running NE-SW shows alternating thick and thin sediments. The thickest parts of the NAB lies to its SE (encircled). Another thick sediment package lies between the WEF and the EF (encircled). No specific sediment flow direction can be identified at this stage and thus it is possible that the sediments infilled the entire study area.

5.2. GEOMORPHOLOGY

5.2.1 Hidra Formation

The attribute maps in Figure 64 show variance (A) and amplitude (B) variations of the entire Hidra Formation aiding in identification of the developments of specific geomorphological features in the study area. This figure display several erosional escarpments in the main depocenter of NAB. Figure 65 is a zoomed in variance map along with seismic profiles VV' and WW' of the escarpments which are most likely formed due sediment transportation. The southern flanks of these escarpments are more scoured as shown in the profiles VV' and WW' in Figure 65. This is possibly due the deflection of the flows towards the south as an effect of the earth's corriolis force in the northern hemisphere.

Few channel like features are identified in the HH area in the north as highlighted in Figure 64. Figure 66 gives a closer view and the seismic characteristics of the channel area. These channels preexisted in the area as indicated by their presence below the Chalk Group as shown in Figure 66 and they flow in a NNW-SSE direction. They might originate from the HH in the north and flow into the SSB. The existence of these channels in the same positions through time might indicate a confined flow in this area.

In the ESB, again, few channel like features are identified as highlighted in Figure 64. Figure 67 is a zoomed in variance map of the area along with its seismic characteristics. These channel like features overlie a faulted high as evident from the seismic profile ZZ'. It is most likely that this area experienced a local uplift leading to creation of these channel like features through which sediments were redistributed in every direction to a lower relief.
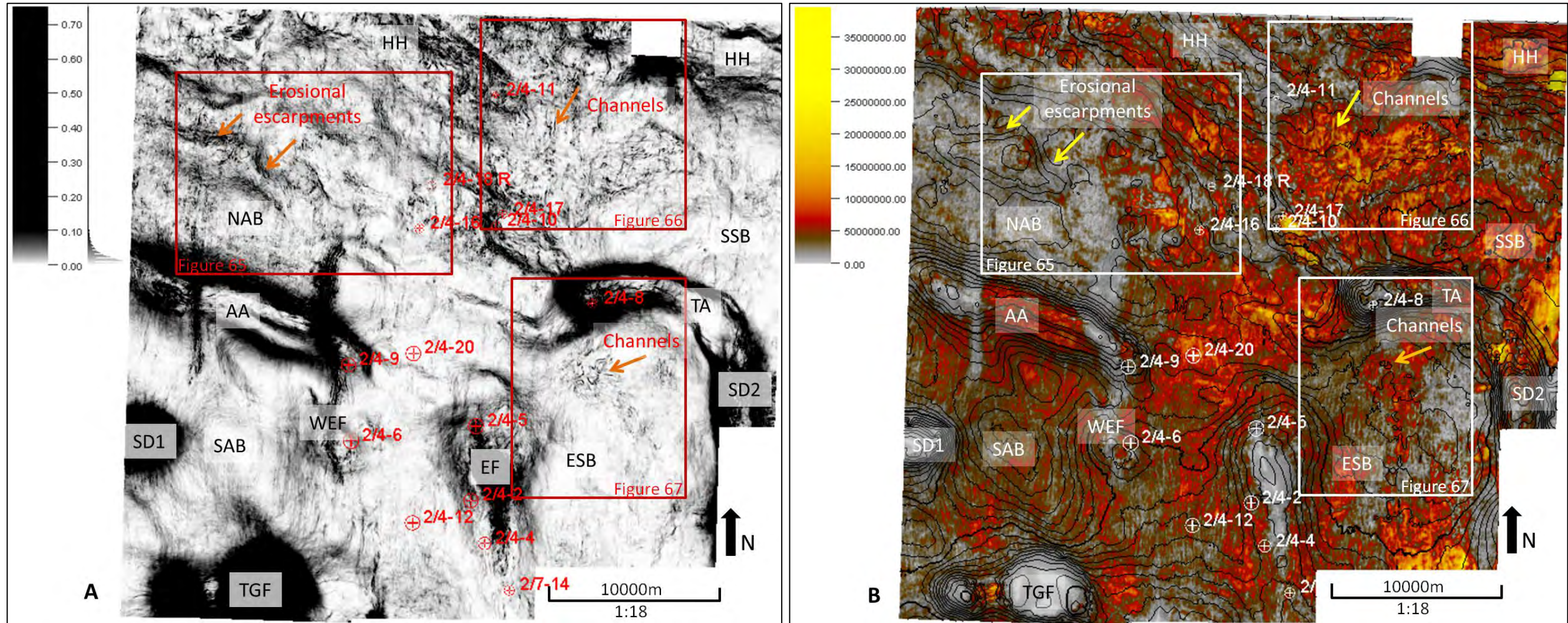
Figure 64: **(A)** Variance and **(B)** Amplitude attribute Maps of the Hidra Formation interval with top Hidra time contours overlain in map B. Both the maps show erosional escarpments in the NAB in the NW as pointed out. The channels are identified in the north in the HH area in the both the maps A and B. In map B the channels show higher amplitude within themselves trending relatively N-S. In the SE, in the ESB, the map A shows several channel like features while map B does not display much variation in amplitude in the channel area. Zoomed in figures with seismic characteristic of the highlighted areas are shown in Figures 65-67. In map B higher amplitudes are observed mostly concentrated in the east and NE part of the study area.
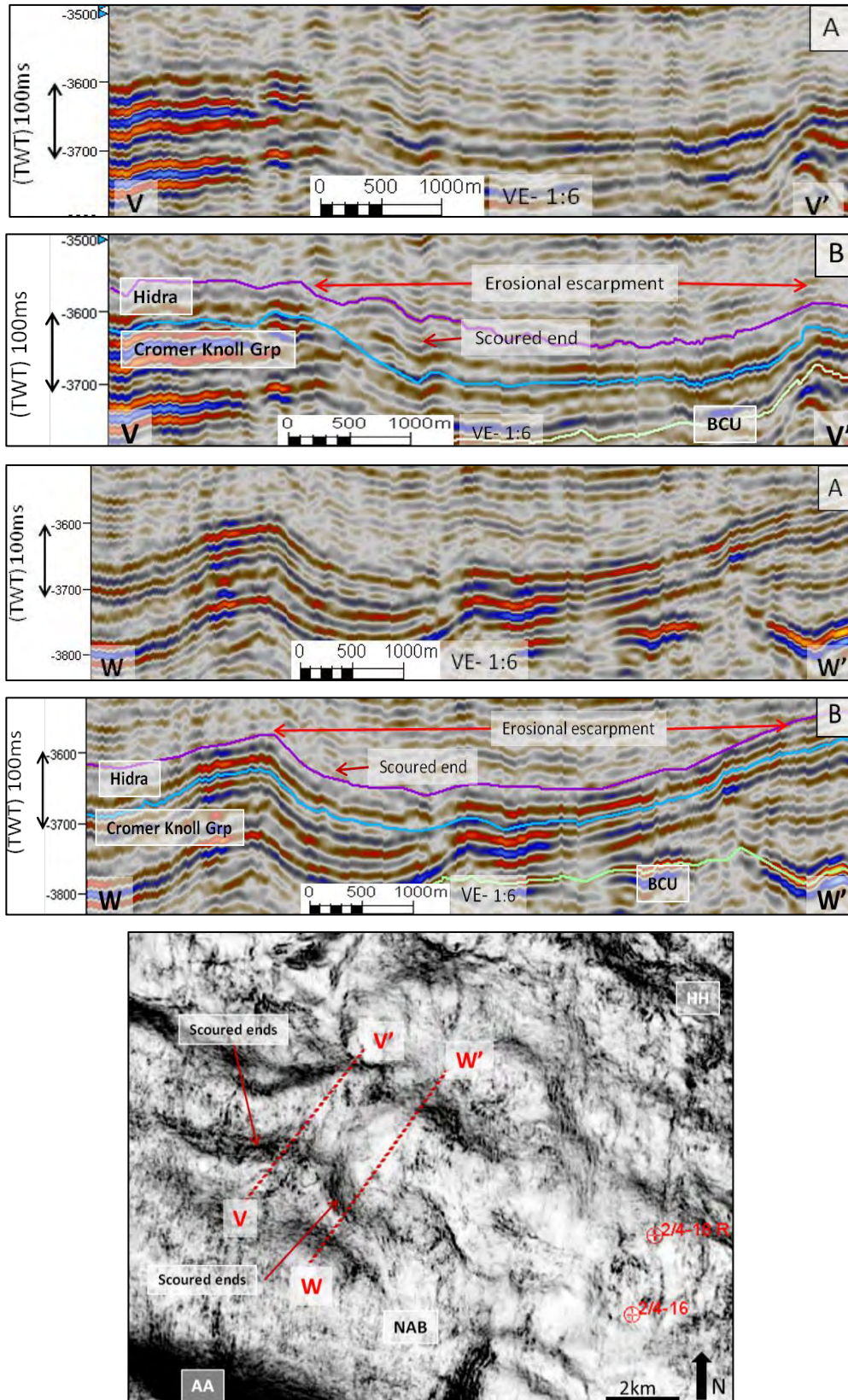
Figure 65: **(A)** Uninterpreted and **(B)** Interpreted **c**ross sections flattened on Rogaland Group top showing erosional escarpments developed in the NAB in the NW potentially caused by sediment transportation. The more scoured ends are towards the southern part of these features due to the deflection of sediment flows caused by the corriolis force of earth in the northern hemisphere. The inset variance map shows the locations of the seismic profiles and is an enlarged view of the area highlighted in Figure 64.

117
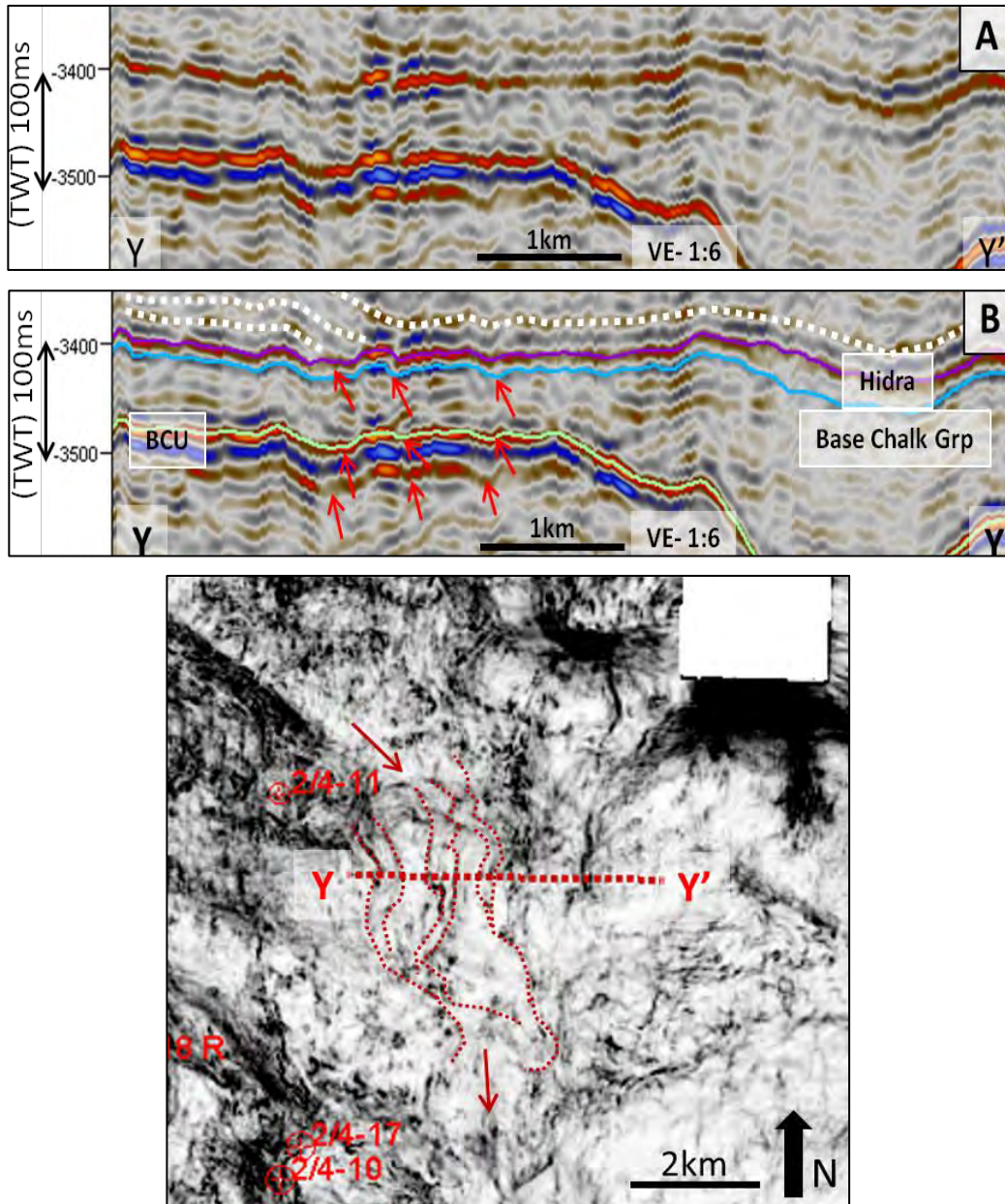
Figure 66: **(A)** Uninterpreted and **(B)** Interpreted **c**ross sections flattened on Rogaland Group top showing the channels present in the north of the study area (red arrows) in the Hidra Formation. The channels are preexisting features in the area and are shown by the red arrows below the Base Chalk Grp. The inset variance map shows the location of the seismic profile and is an enlarged view of the area highlighted in Figure 64. The channels are highlighted by the stipulated lines and their possible flow direction of NW-SSE is shown by the red arrows.
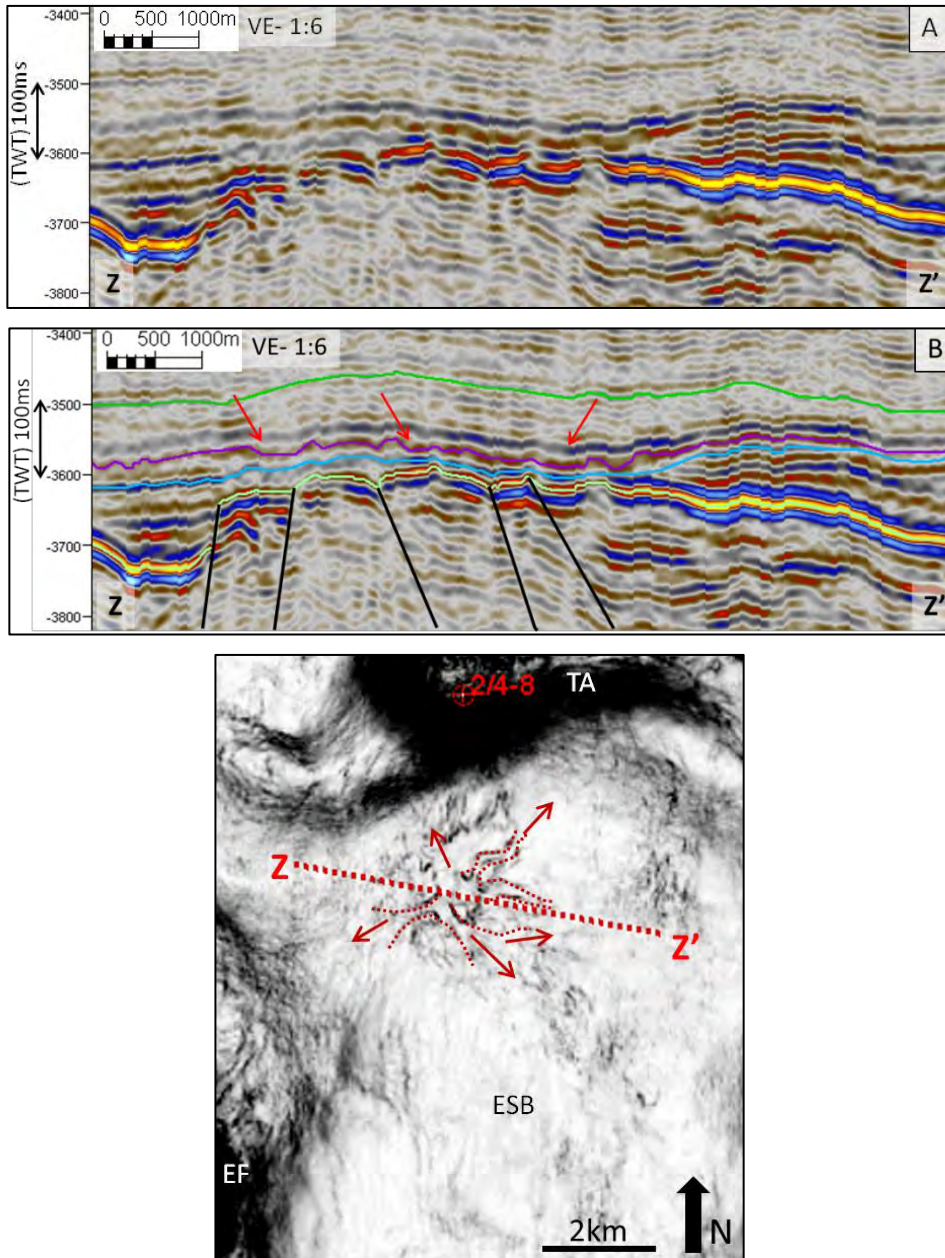
Figure 67: **(A)** Uninterpreted and **(B)** Interpreted **c**ross sections flattened on Rogaland Group top showing the presence of channel like features on top of a faulted high area in the ESB. The inset variance map of the Blodøks Formation shows the location of the seismic profile and is an enlarged view of the area highlighted in Figure 64. The possible channel pathways are indicated by the red arrows. It is possible that this part of the basin underwent a local uplift leading to creation of these channels through which sediments were redistributed in different directions to a lower relief.

5.2.2 Blodøks Formation

The attribute maps in Figure 68 shows variance (A) and amplitude (B) variations of the entire Blodøks Formation. They help identifying different geomorphological features in the area. The preexisting channels possibly originating from the HH are still present as shown in Figures 68 and 69 and trend NNW-SSE. This channel system in the HH has grown in size with increased number of channels and their lengths compared to that in the Hidra Formation (Figure 69). Few of these channels might have experienced scouring by inflowing sediments as shown in this figure.

In the ESB a cluster of isolated depressions developed as marked in Figures 68 and 70, which were absent in the Hidra Formation. These depressions do not show any amplitude variations in Figure 68B but are prominent in the variance map (Figure 68A). These depressions are located just above a faulted area as shown in Figure 70 by the black arrows. They are circular to sub-circular in shape and are possibly pockmarks formed by the expulsion of biogenic or thermogenic fluids (Masoumi et al., 2014). In Figure 70, the expulsion of fluids is interpreted to originate from below the Base Chalk and the possible expulsion pathways make their way upto the top of the Chalk Group in the study area. These possible pathways are marked by the white arrows in this figure.

In the SAB, at the foot of the AA (Figure 68) a sediment onlapping line is identified which was absent in the Hidra Formation indicating infilling processes. In the ESB, the preexisting channel features are absent at this stratigraphic level in the Blodøks Formation. The Figure 68A also shows an overall smoothing in the NAB especially around the erosional escarpments compared to that in the Hidra Formation. These observations together indicate an overall infilling nature of the Blodøks Formation in the study area.

.
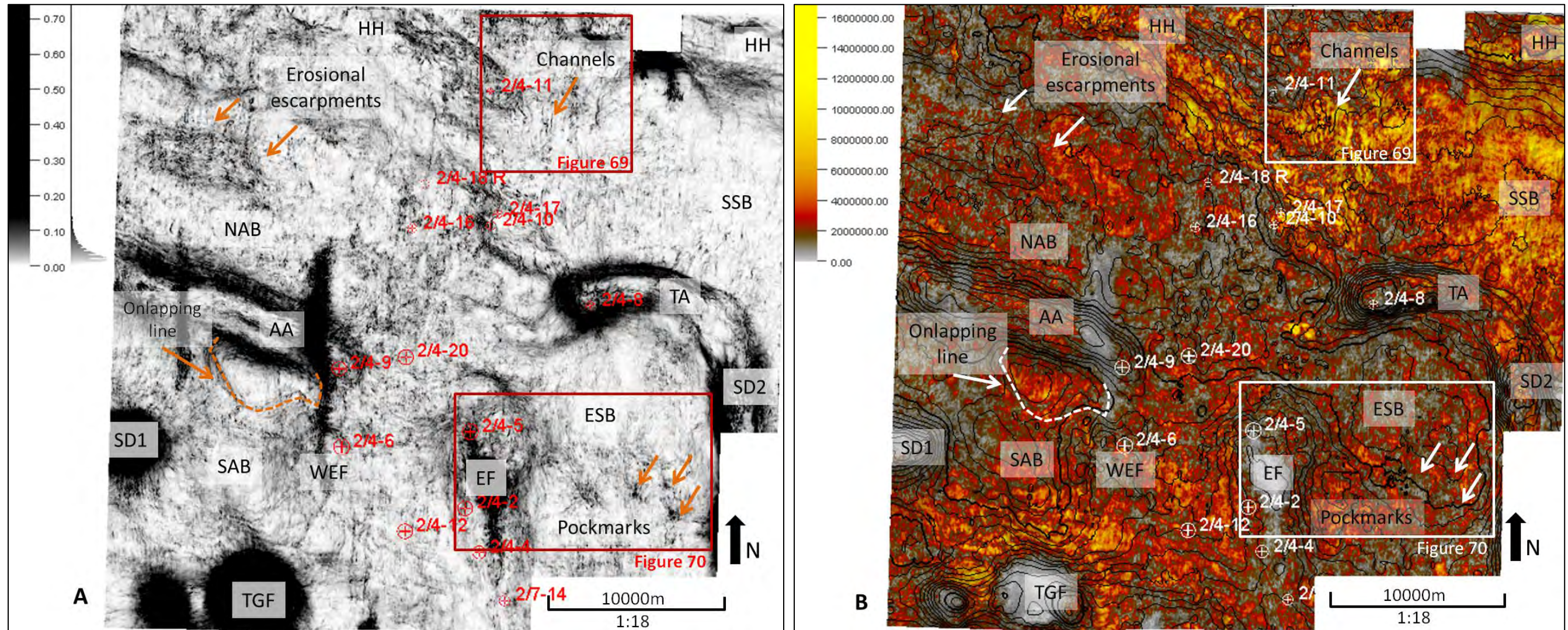
Figure 68: (**A**) Variance and (**B**) Amplitude attribute Maps of the entire Blodøks Formation with top Blodøks time contours overlain in map B. Map A shows development of new features like the pockmarks in the ESB and a sediment onlapping line in the SAB. The preexisting channels in the HH are still flowing in the NNW-SSE direction. In Map A the erosional escarpments in the NAB are less observable and smooth in the Blodøks Formation indicating infilling. The preexisting channels over the faulted area in the ESB is absent in this formation and indicate complete draping. The map B also shows very low amplitude variations in these two areas. The areas highlighted within the rectangles area shown in Figures 69 and 70. In the SSB, in the north, the map B displays high amplitudes. High amplitudes are also present in the HH trending NW-SE near Well 2/4-11 and around the TGF in the south.
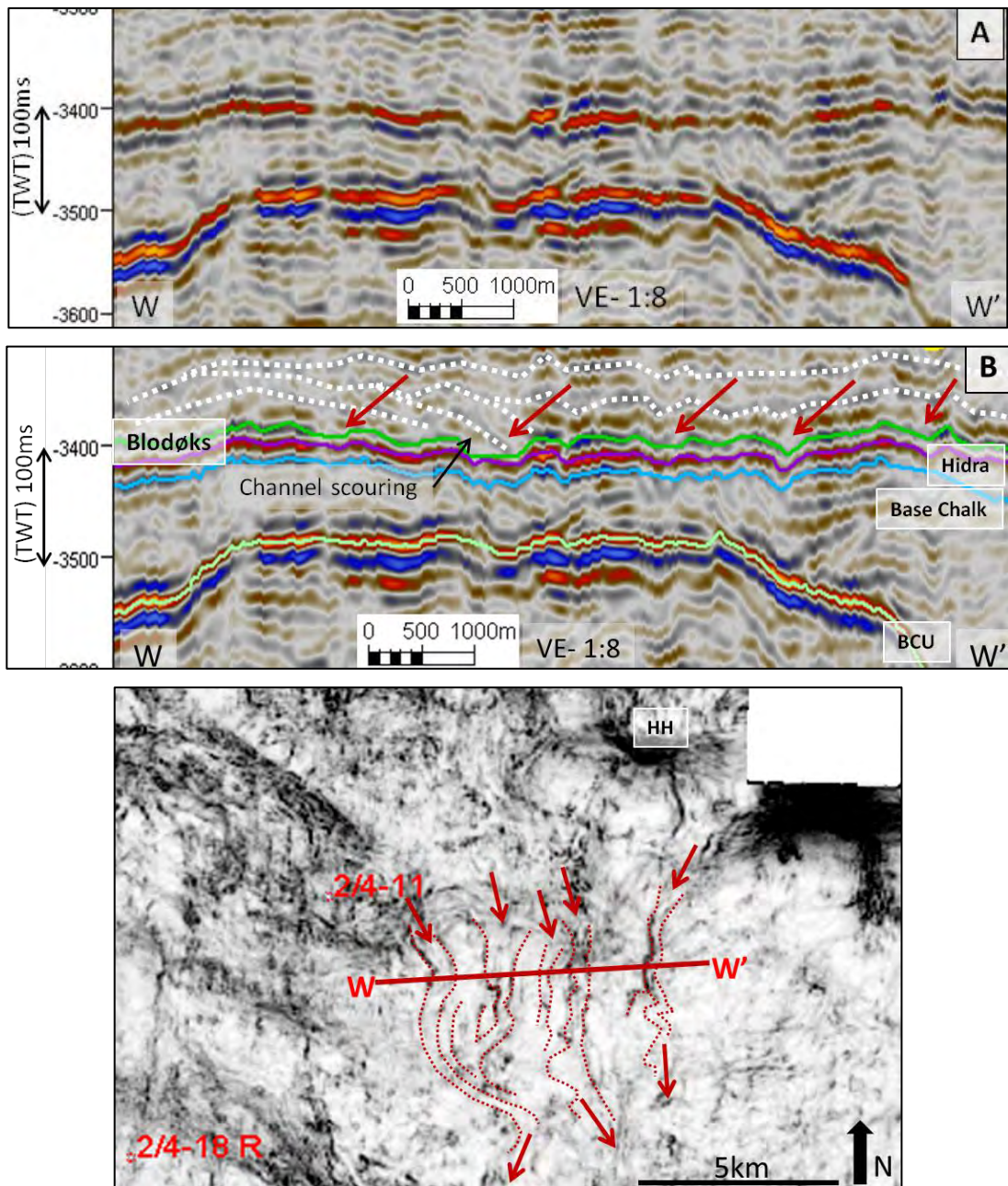
Figure 69: **(A)** Uninterpreted and **(B)** Interpreted **c**ross sections flattened on Rogaland Group top showing the channels in the north of the study area. The channels are pointed out in the seismic section by the red arrows. The channels might have experienced some scouring process as mentioned in the figure. The inset variance map shows the location of the seismic profile and is an enlarged view of the area highlighted in Figure 68. The stipulated lines in the map marks the potential channels in the area. The red arrows indicate the flow directions from the NNW towards SSE.
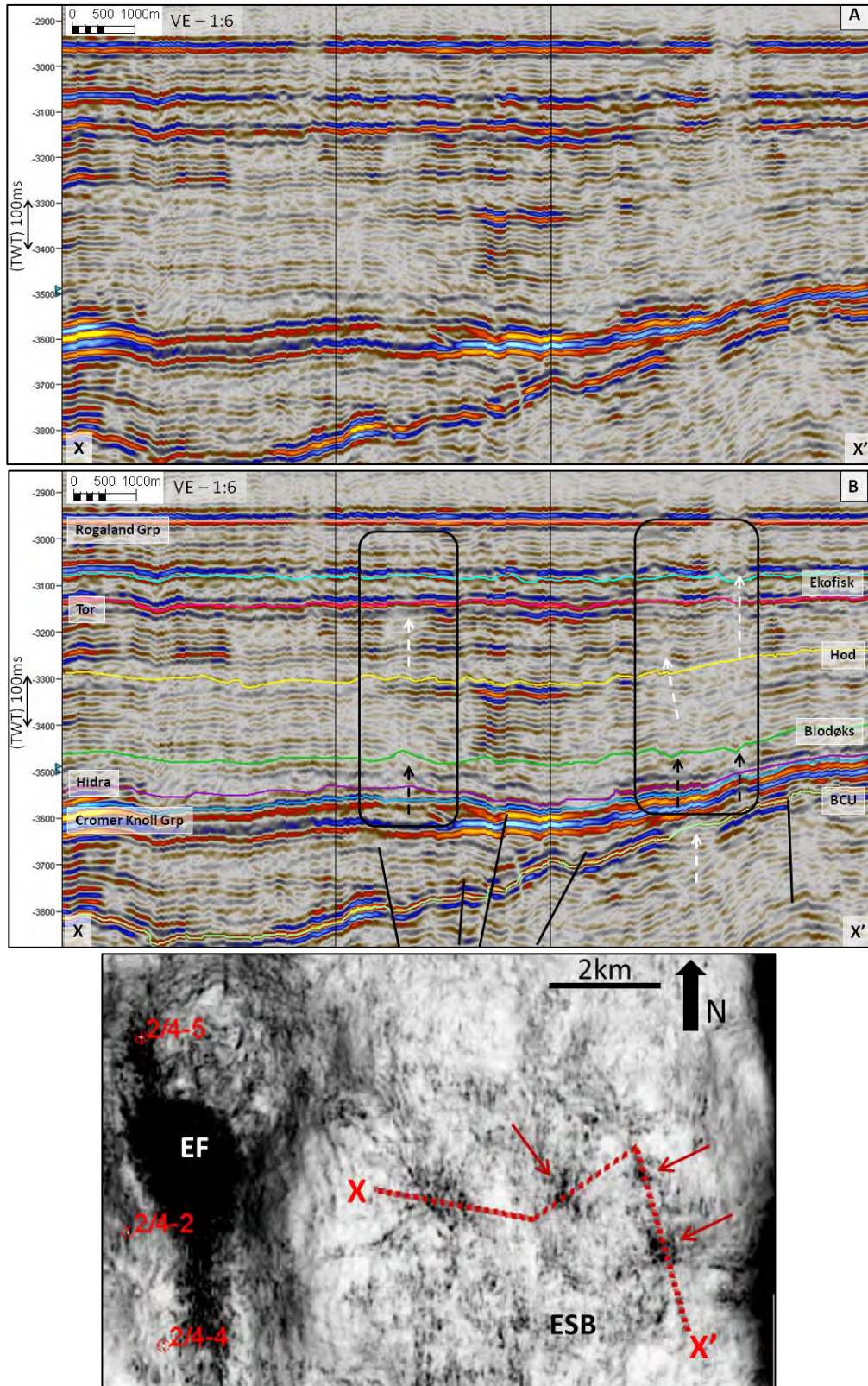
Figure 70: **(A)** Uninterpreted and **(B)** Interpreted **c**ross sections flattened on Rogaland Group top showing the pockmarks in the ESB. The black arrows in the seismic point out the pockmarks present in the inset map. The white arrows indicate the possible expulsion of fluids from below till the top of the Chalk Group. The inset variance map shows the location of the seismic profile and is an enlarged view of the area highlighted in Figure 68. The pockmarks are indicated by the red arrows.

123

5.2.3   Hod Formation

The attribute maps in Figures 71-73 show proportional stratal slices of the Formation from the base to the top. Studying the variance (A) and the amplitude (B) attribute maps the developments of several geomorphological features through time is observed. Figure 71 displays the attribute maps of the basal part of the Hod Formation. Comparing Figure 71 to Figure 68, the preexisting erosional escarpments in the NAB are absent in the basal part of the Hod Formation. The onlapping line in the SAB and the pockmarks in the ESB still exist in this stratigraphic level as shown in Figure 71. The preexisting channels in the HH area are observed to have developed into a larger channel system with increased number of channels and their increased lengths compared to that in the Blodøks Formation. This area is highlighted in Figure 71. Figure 74 is an enlarged view of this channel system in the HH. The channels are relatively straight in nature and flow in a NNW-SSE direction from the HH into the SSB.

Figure 72 shows the attribute maps of the middle part of the Hod formation. In this stratigraphic level, in the ESB, the number of pockmarks is observed to have increased and they also seem to be present in a cluster as shown. The preexisting HH channels still flow from the NNE towards the SSE into the SSB. Figure 72 also displays several gravity flows in the study area. These gravity flows mostly originate from the TA and flow into the ESB and NAB. A few also originate from the northern flank of the EF and flow into the ESB. A high in the central NAB also displays gravity flows flowing towards the SE of the basin as shown in Figure 72. Gravity flows from the LR is also observed flowing towards the north in this figure. In the southern part of the study area in the SAB, few small channels are identified near the TGF. An enlarged variance map of this area highlighted in Figure 72 is shown in Figure 75. This enlarged map displays clearly that the channels flow NNW into the SAB center and they potentially originate from the TGF. These channels in Figure 75 also display branching but are relatively straight in nature.

In the upper part of the Hod Formation (Figure 73), several preexisting gravity flows have disappeared but also several more developed especially in the SSB and in the SAB. In the SSB the gravity flow identified originates from the TA while in the

SAB it originates from the SD1 as shown in Figure 73. Figure 73 display development of a channel network in the central NAB. A zoomed in variance map of this area highlighted in Figure 73 is shown in Figure 76. This enlarged map displays that channels from different directions join to form a single channel in the NW which branches again towards the SE of the basin. The stipulated lines indicate the channel network prevailing in the NAB in Figure 76. The channels possibly originate from further in the west and from the HH in the north and flow towards the SE in the NAB. Figure 76 also shows debris flows (marked by the red dashed curves) near these channels. It is most likely that that the channels here led to destabilization of the sediments and these destabilized sediments created the debris flows in phases.

The pockmarks are still present in clusters in their previous positions in the ESB as shown in Figure 73. The preexisting HH channels are also present in the upper part of the Hod Formation.
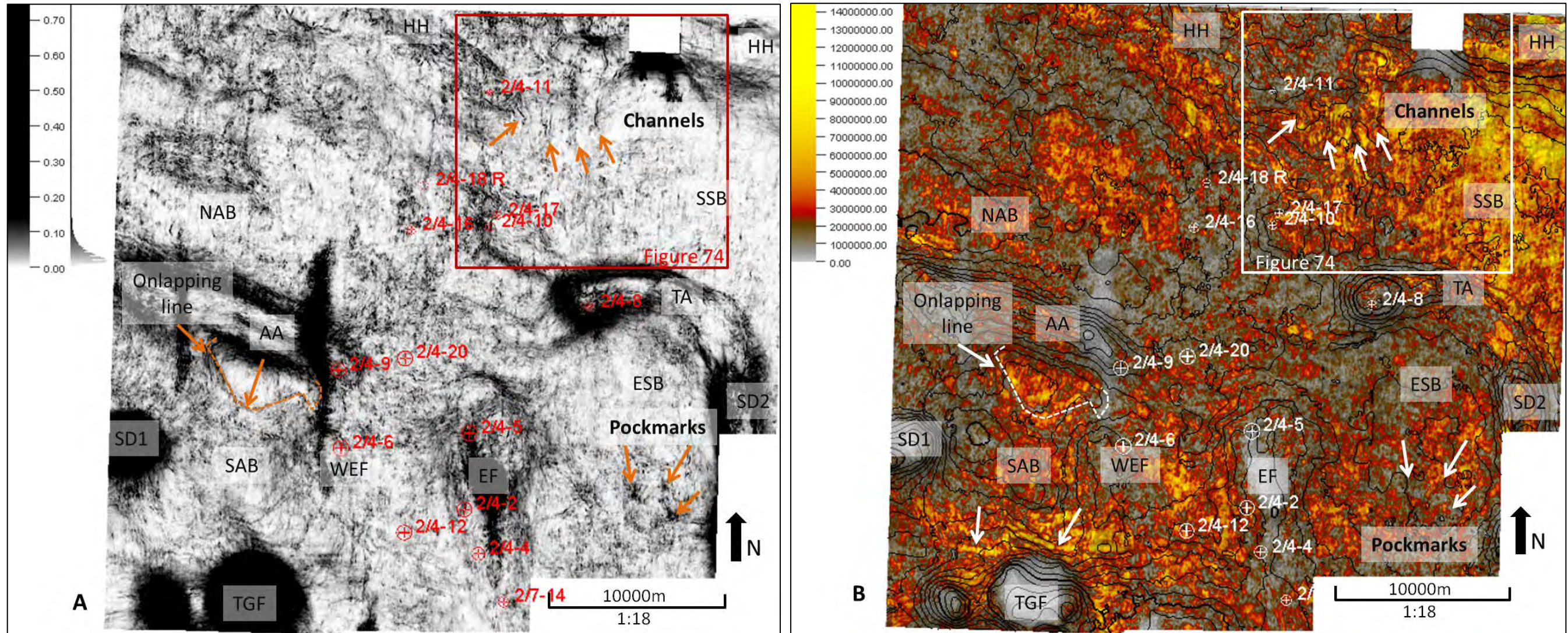
Figure 71: (**A**) Variance and (**B**) Amplitude attribute Maps of the basal part of the Hod Formation with top Hod time contours overlain in map B. The preexisting pockmarks are clearly visible in map A while they are not very prominent in map B. The preexisting channels in the HH in the north and the onlapping line at the foot of AA in the SAB are prominent in both the maps of the basal Hod Formation. The channels in the north have grown in to a channel system and is shown in detains in Figure 74. In the NAB, the erosional escarpments are not prominent anymore in both the maps. In map B very high amplitudes are present in the SSB area and around the TGF while moderately high amplitudes are in the center of the NAB and in the east of the ESB. In the SAB at the foot of the AA moderate amplitudes are also observed. Around the TGF few striations are pointed out in map B and could be possibly some channels. However, these are not clearly observed in the map A.
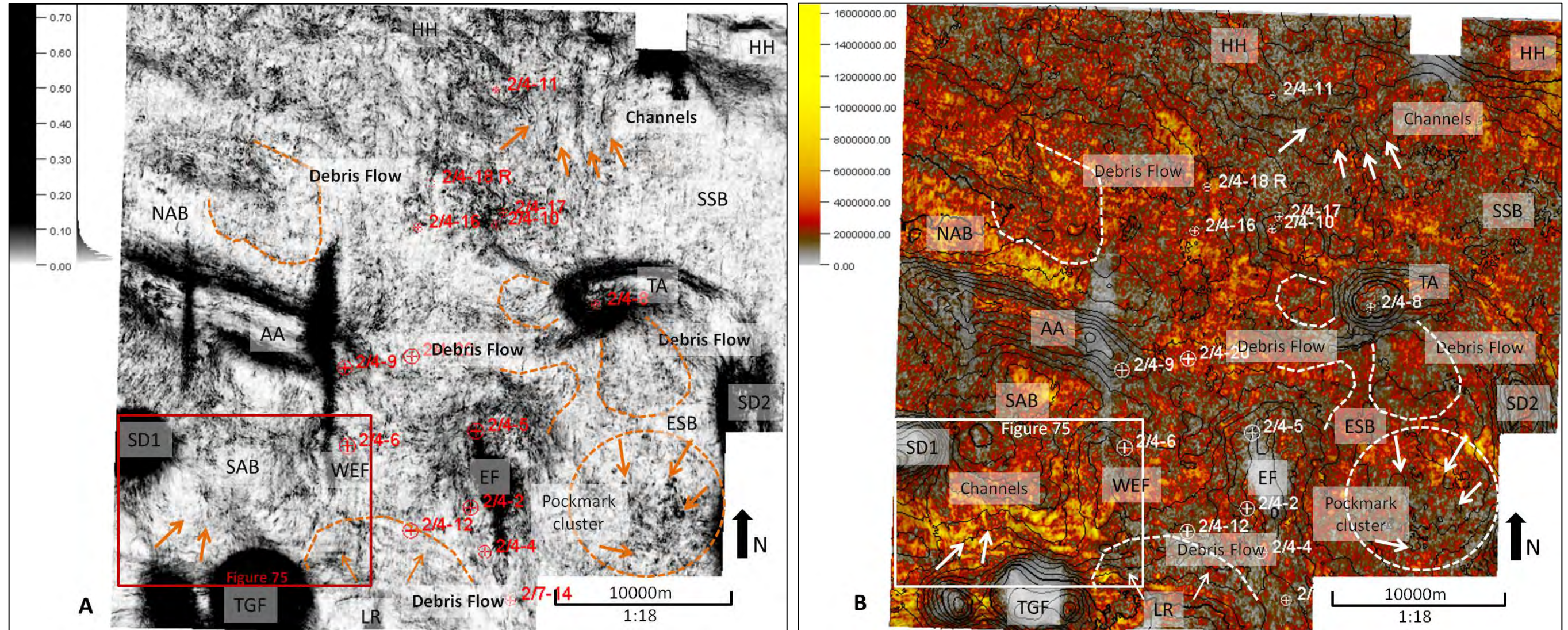
Figure 72: (**A**) Variance and (**B**) Amplitude attribute Maps of the central part of the Hod Formation with top Hod time contours overlain in map B. Several debris flows developed and are visible in both the maps (marked by the dashed curves). The pockmarks increased in number and are present as a cluster shown by the dashed circle in both the maps. The preexisting channels in the north in HH are still present and are clearly visible in map A but are unclear in map B. New channels developed in the SAB possibly originate from the TGF and are shown by the arrows in both the maps. An enlarged variance map of this area with more details of the channels is shown in Figure 75. In map B high amplitudes are in the NAB immediately north of AA and to the north of the TGF while moderate amplitudes are observed in the SSB and in the ESB.

127
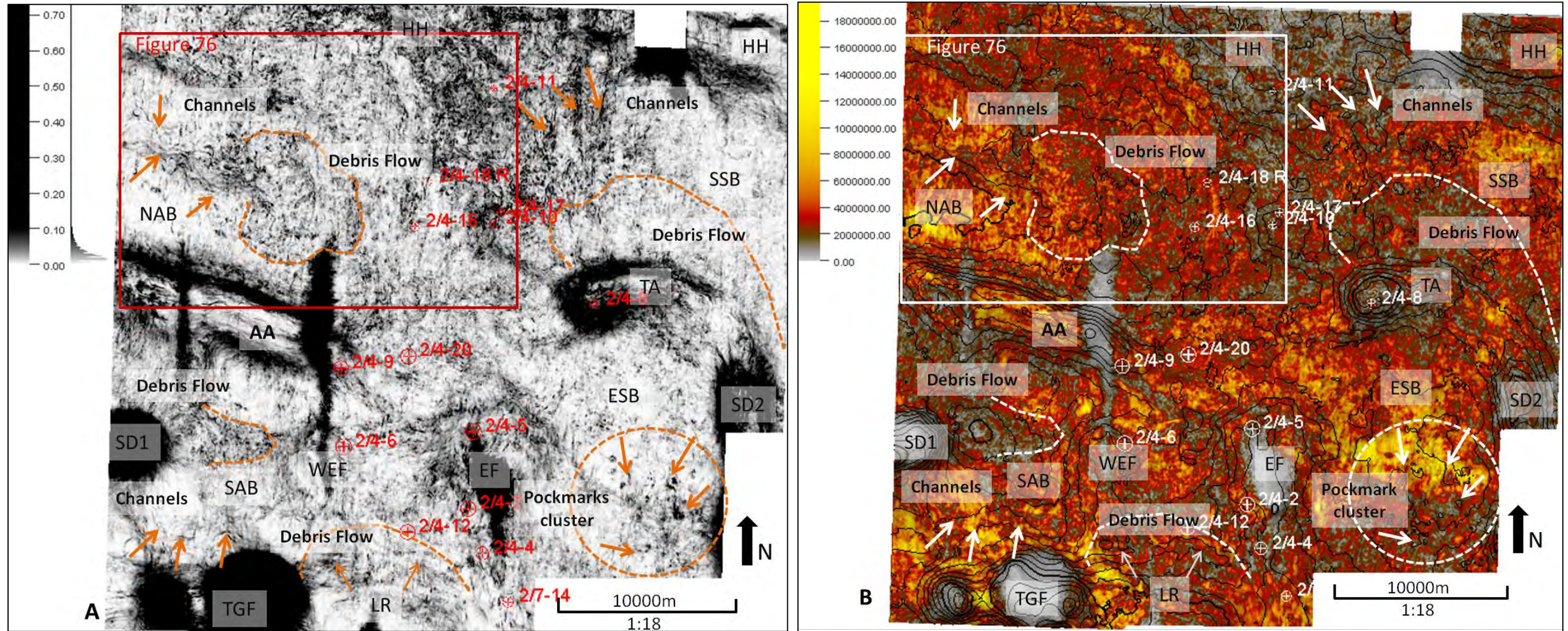
Figure 73: (**A**) Variance and (**B**) Amplitude attribute Maps of the upper part of the Hod Formation with top Hod time contours overlain in map B. Few preexisting debris flows are no more identifiable but new debris flows developed in the SSB and on the flank of the SD1 as shown by the dashed curves in both the maps. The debris flow shown in the NAB distributed more towards the SE compared to that in the Figure 72. New channels also developed around this area in the NAB as shown by the arrows in both the maps. A closer view with more details of this area is shown in Figure 76. The preexisting pockmarks increased in number and are still present in a cluster in the upper Hod Formation as shown in both the maps. The preexisting channels in the north are clearly visible in map A but are unclear in map B. Again the preexisting channels in the SAB area are also clearly visible in both the maps as shown. In map B high amplitudes are in the NAB immediately north of AA, around the TGF, in the ESB around the pockmarks and to the east of the SSB.
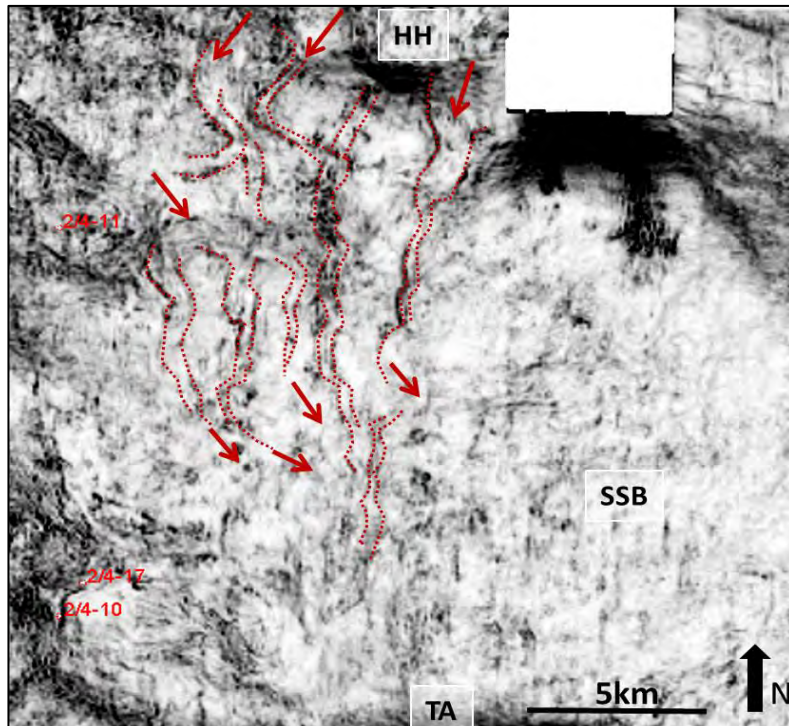
Figure 74: The variance map of the basal part of the Hod Formation displays an enlarged view of the area highlighted in Figure 71. It shows that the channels in the HH in the north of the study area, has developed into a larger channel system. New channels have developed in the area which originates from further north in the HH and a few might also flow from the NW part of the HH. They generally flow SSE into the SSB. A few channels in the north also merge together to form a single channel. These channels display relatively straight nature. The channels are indicated by the stipulated lines and their flow directions are shown by the red arrows.
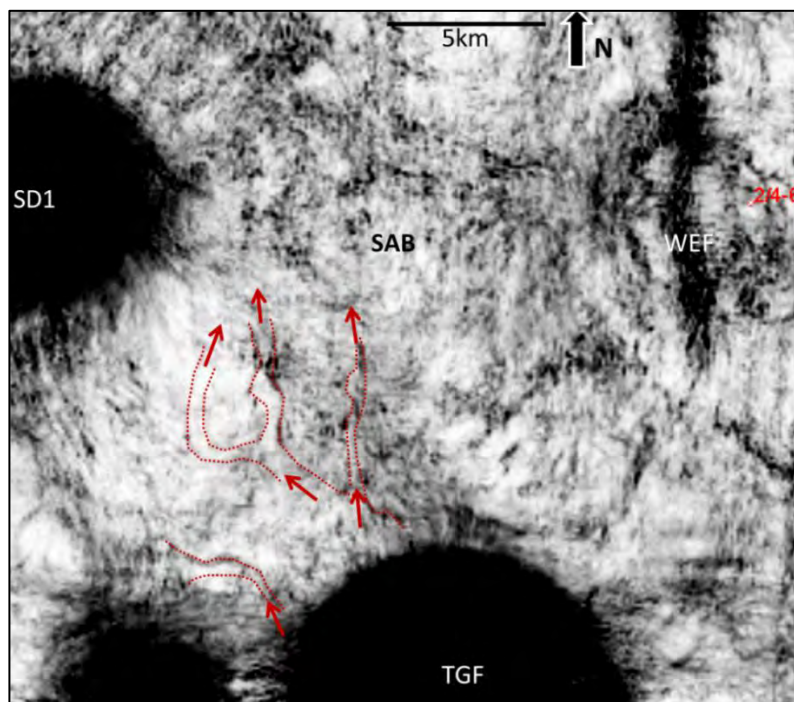
Figure 75: The variance map of the middle part of the Hod Formation displays an enlarged view of the area highlighted in Figure 72. The stipulated lines indicate the possible channels originating from the TGF which flow towards the SAB center. Branching of channels is also observed in the area although they show a relatively straight nature. The flow directions are shown by the red arrows.

129
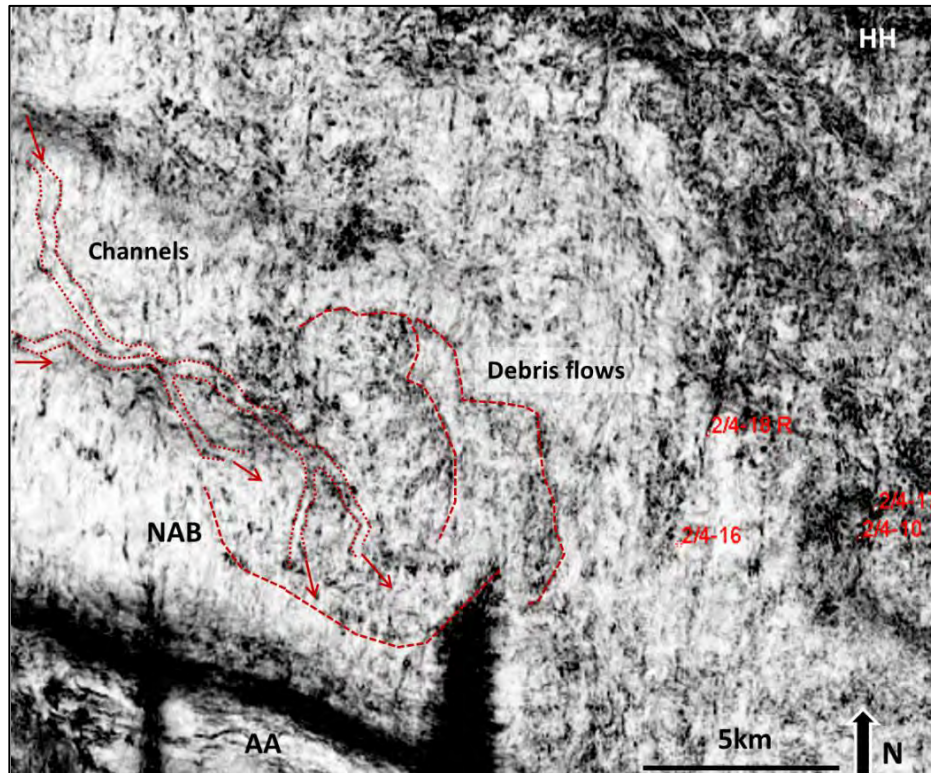
Figure 76: The variance map of the upper part of the Hod Formation displays an enlarged view of the area highlighted in Figure 73. The stipulated lines indicate the channel network prevailing in the NAB. The channels possibly originate from further west and from the HH in the north and flow towards the SE in the NAB. The figure also shows that debris flows (marked by the red dashed curves) are also common in this part of the study area. It is possible that the channels led to destabilization of the sediments and as a result the debris flows were initiated. It also seems like the debris flows occurred in phases as shown by the curved lines.

5.2.4 Tor Formation

Figures 77-80 show several proportional slices of the Tor Formation from the base to the top. They show the variance (A) and the amplitude (B) map of these proportional slices representing the stratigraphic levels from the base to the top.

Figure 77 displays the geomorphology of the basal part of the Tor Formation. It shows the reduction in number of the preexisting pockmarks in the ESB. The size of the cluster thus seems smaller compared that in the underlying upper Hod Formation. The HH channels in the north persistently flow towards the SSE into the SSB as before. The NAB channel network also exists in the same location and is more prominent in both the Figures 77A and B. The majority of the debris flows are absent in Figure 77 compared to that in Figure 73. A smaller debris flow is observed originating from the TA and flowing into the NAB as shown in Figure 77. The preexisting channels in the SAB originating from the TGF also exist in the basal part

130

of the Tor Formation. To the NNE of the EF a few fractures are also noted to appear in this stratigraphic level as shown in Figure 77.

Figure 78 displays the attribute maps of a stratigraphic level above the one shown in Figure 77 in the Tor Formation. The preexisting features like the HH channels, the TGF channels in the SAB, the pockmarks in cluster in the ESB, the fractures in the NNE of the EF and the debris flow from the TA are clearly present in Figure 78 as shown. Apart from them, the NAB channel network has grown in size with addition of many channels from the HH in the north and from the AA in south. The area is highlighted in Figure 78 and an enlarged variance map of this area is shown in Figure 81 with a detailed illustration of the channels. The stipulated lines represent the channels while the arrows indicate their flow directions. The channels mostly trend south and SE except the ones flowing from the AA. The channels from the AA flow north. Figure 78 also displays a new feature like an onset of a mega slide in the NE of the study area trending NE-SW. This mega slide flows into the SSB as shown. Few faults are also observed to appear to the south of the mega slide on the top of the TA and in the ESB as pointed out in Figure 78. It is possible that a compressional force from further NE acting towards the SW caused the mega slide as well as the faults.

Around the middle of the Tor Formation the attribute maps are shown in Figure 79. All the preexisting features from the underlying stratigraphic level like the enlarged NAB channel network, the TGF channels in the SAB, the pockmark cluster, the TA debris flow, the HH channels, the faults in the ESB and the mega slide in the NE still exist as shown in Figure 79. The mega slide is more prominent in both the Figure 79 A and B indicating an ongoing active process. The preexisting fractures in the NNE of the EF are absent in this map. However, new features developed to the WSW of the EF as highlighted in the Figure 79. Figure 82 a zoomed in variance map of the highlighted area clearly shows that a couple of faults have developed in the area. A channel originating from the EF flows to the SSE crossing the faulted area. This channel also displays branching and is moderately straight in nature. The arrows show the possible flow directions of the channels. Seismic profiles AA' and BB' show the faults and BB' also shows the channel.

The upper Tor Formation geomorphological features are displayed in Figure 80. In this figure the preexisting channels like the NAB channel network, the HH channel system, the channels in the TGF and in the WSW of the EF are active and are prominent in Figures 80A and B. The pockmarks in the ESB are very few in number and thus do not form a cluster any more.

Prominent changes are observed in the NAB channel network and in the HH channel system. Along with this, a new debris flow is observed in the central part of the study area and the mega slide in the NE is a pronounced featured in this stratigraphic level. An enlarged view of the highlighted area of the upper half of the study area is shown in Figure 83. A seismic cross section AA', taken across the mega slide displays presence of small thrust faults. This is due to due to the active slides leading to sediment layer overriding each other as shown. The thick red arrow on the variance map indicates the compressional force direction causing the slides.

Figure 83 also displays the changes NAB channel network. Several channels represented by the stipulated lines flow from the WNW and SW and join together to form a potential channel valley. The channels in this valley flow towards the ENE and then fan out at the southern end of the NAB. It is also possible that several channels from the HH and from the south join the channels in the valley. The seismic cross sections CC' and DD' show the channel incisions increasing in number from the west to the east. To the south and center of the Figure 83 a debris flow is identified and the seismic profiles II' and JJ' display the prograding nature of the sediment in the feature is towards the south. This figure also clearly shows channel scouring developed in the north as a result of a confined channel flow in this area since the Cenomanian period. The channels flow towards the south originating from the HH. Few channels also originate from the NW of the HH. They all mostly flow into the ESB.

It is noteworthy that most of the geomorphological features appear on the northern half of the study area. The southern half of the study area is relatively quiet with respect to formation of new geomorphological features apart from developments of few channels. This might lead to a favourable condition of the hydrocarbons to mature around the TGF and EF which is also indicated by the presence of higher amplitude anomalies here.
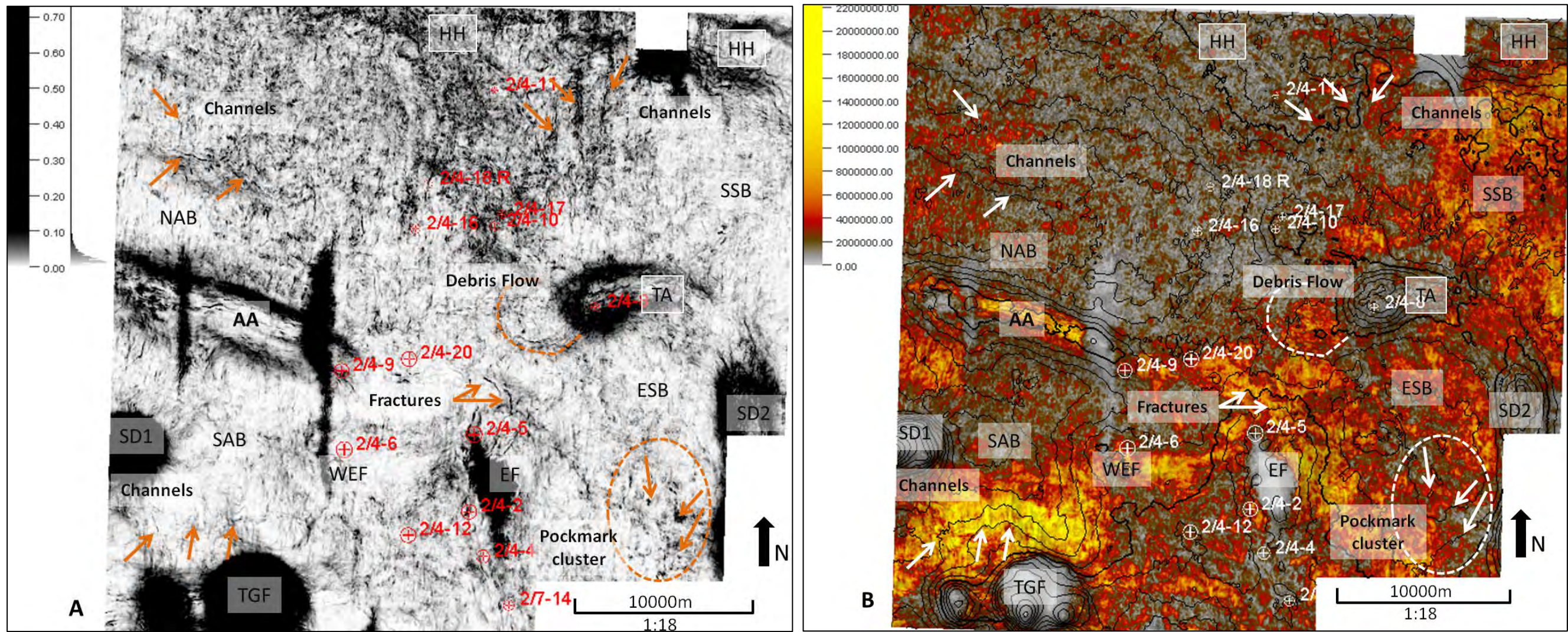
Figure 77: **(A)** Variance and **(B)** Amplitude attribute Maps of the basal part of the Tor Formation with top Tor time contours overlain in map B. Several preexisting features like the Channels in the HH, NAB and SAB still exist. Few new features like the fractures to the north of the Ekofisk developed and a new debris flow from the TA towards the NAB is also observed. Several preexisting debris flows are absent in the basal Tor Formation. The pockmark cluster has shrunk in size and the number of pockmarks also reduced in the ESB as shown in both the figures. In map B high amplitudes are located on the northern flank of the TGF and on the eastern flank of the EF. The crest of the AA also displays high amplitudes. Moderate amplitudes are observed in the SSB and to the north of the ESB while NAB shows very low amplitudes.

133
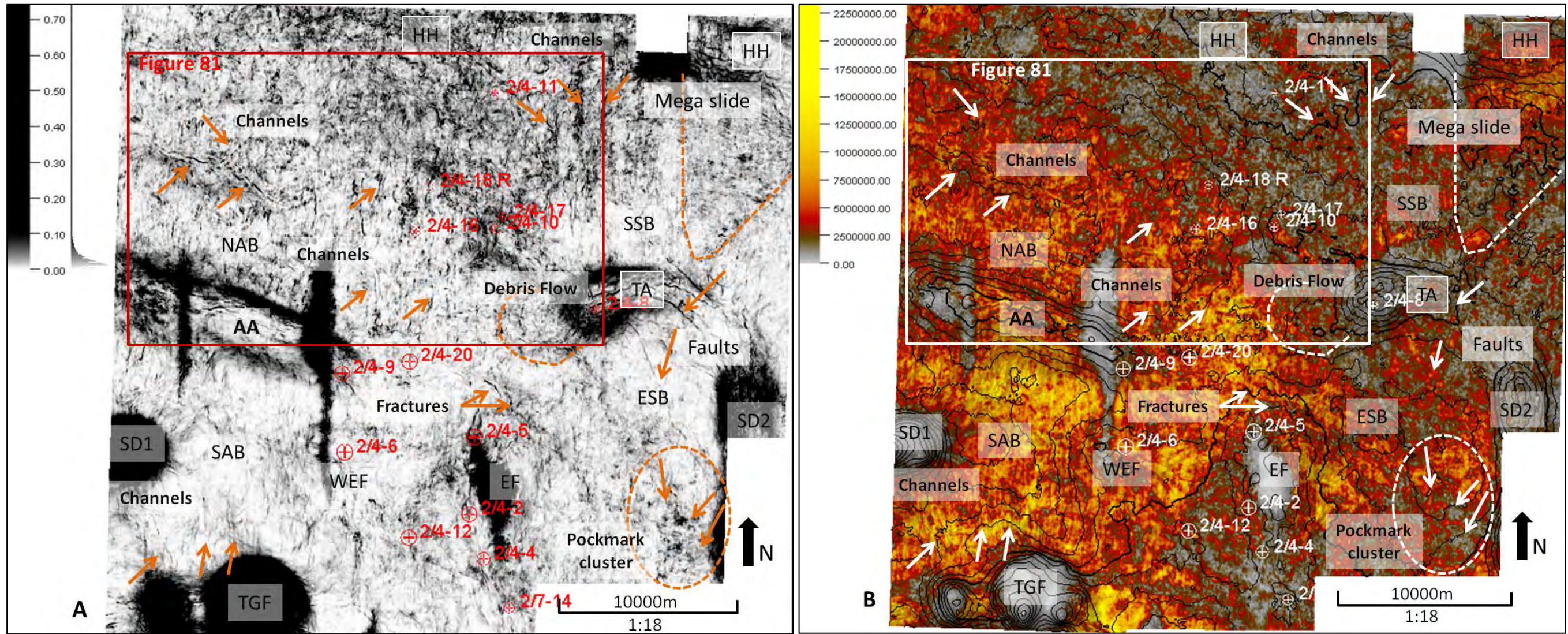
Figure 78: (**A**) Variance and (**B**) Amplitude attribute Maps of the Tor Formation stratigraphically above the previous slice in Figure 77 with top Tor time contours overlain in map B. Both the maps show generation of a mega slide in the NE of the study area. New faults on the TA and in ESB are clearly visible in map A but in map B they are not very clear. In the NAB a network of channels is formed. The area is highlighted by the red rectangle and a closer view to the area is shown in Figure 81 with more details. Preexisting features like the HH and the TGF channels, the pockmark cluster and a debris flow still exists in this stratigraphic level of the Tor Formation. High amplitudes are located in the SAB, around TGF and in the SE of NAB. Moderate amplitudes are observed in central NAB and ESB while in the SSB in the NE, the amplitudes are relatively lower.
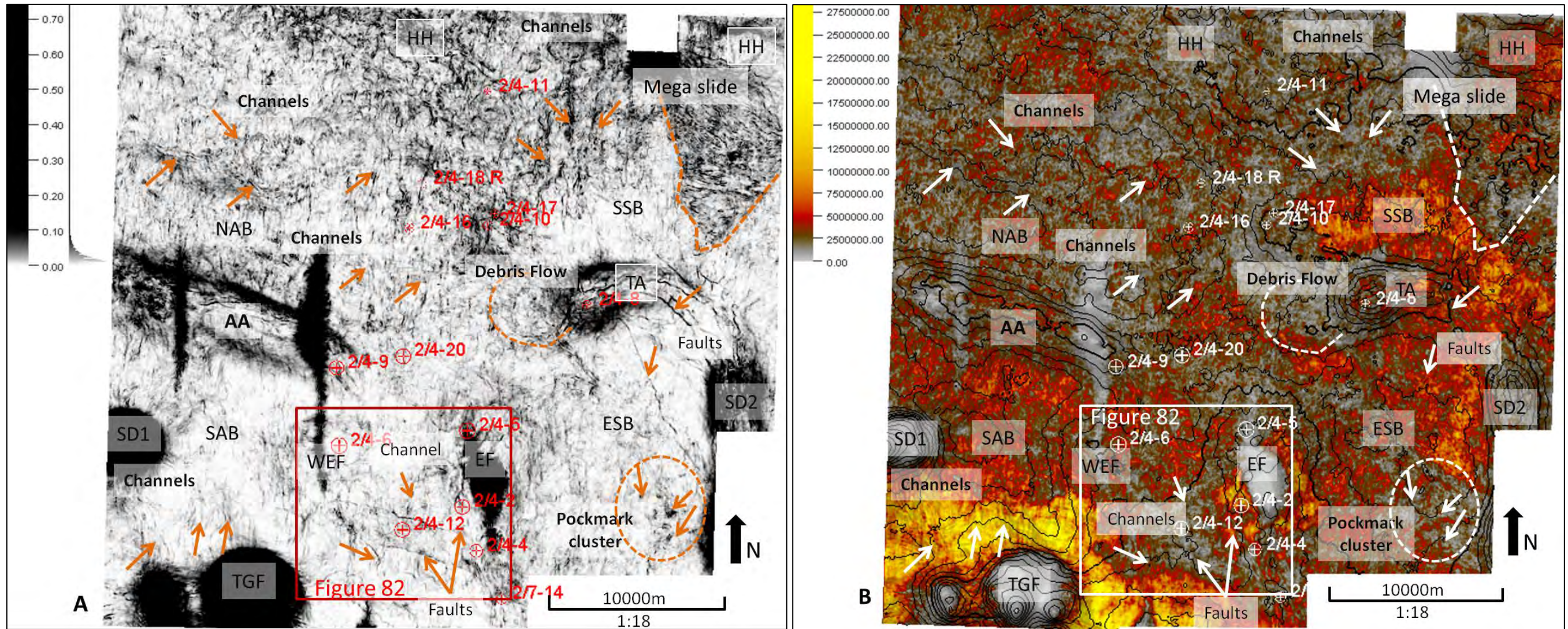
Figure 79: **(A)** Variance and **(B)** Amplitude attribute Maps of the Tor Formation overlying previous stratigraphic level shown in Figure 78 with top Tor time contours overlain in map B. New channel network along with a couple of faults developed in the SW of the EF as highlighted by the rectangle in both the maps. A zoomed in variance map of this area is shown in Figure 82. Both the maps in this figure display very prominently the mega slide in the NE of the study area in this stratigraphic level. The preexisting channel systems in the NAB, SAB and HH still exist as shown. The preexisting faults on the TA and in ESB are much clear in both the maps. The pockmark cluster is much smaller in size compared to before. High amplitudes are located specifically around TGF, south of the SAB and moderate amplitudes are observed in the SSB and NE of ESB. The NAB displays very low amplitudes.

135
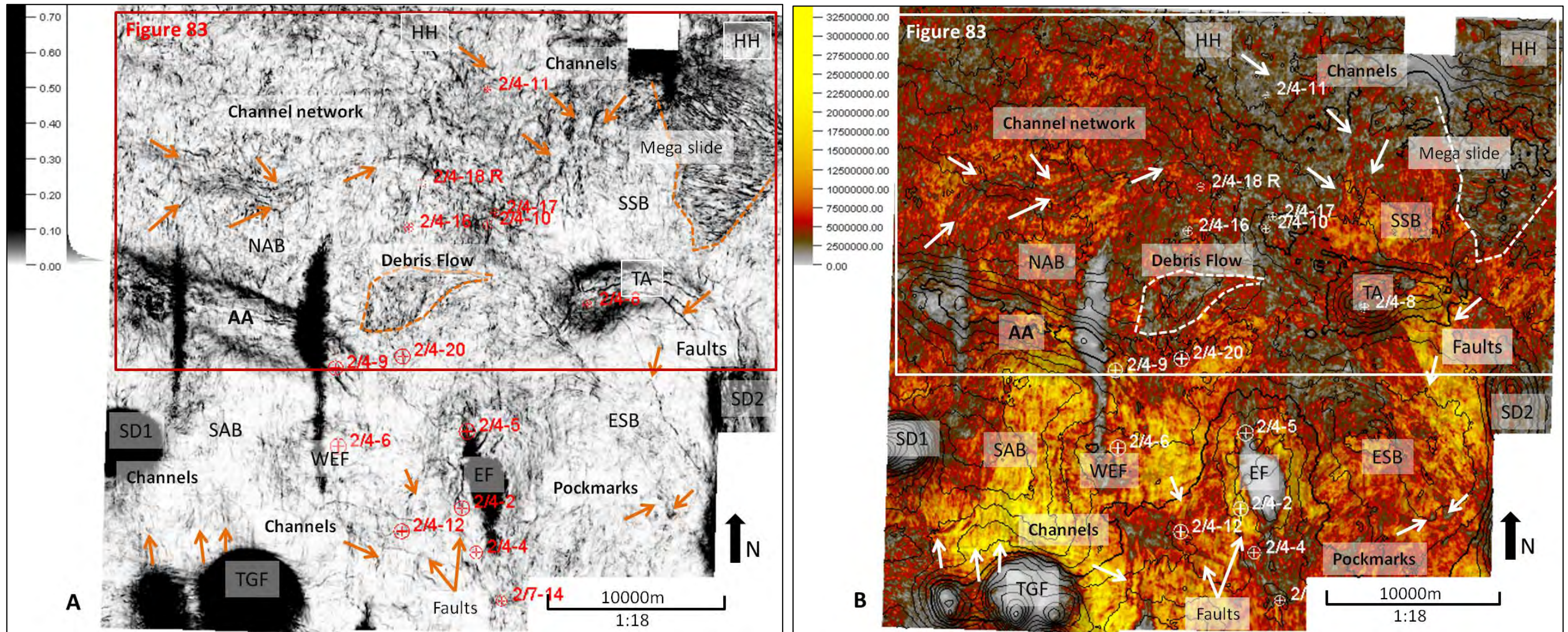
Figure 80: (A) Variance and (B) Amplitude attribute Maps of the upper part of the Tor Formation with top Tor time contours overlain in map B. The channel network in the central NAB is very prominent in both the maps. It is also possible that several other channels from the HH and the south join this channel network. A new debris flow is identified in the central part of the study area as shown in both the maps. Both the maps also show the mega slide prominently in the NE of the study area. The HH channels also show scouring effect in map A. The highlighter area covers all these features and a zoomed in variance map with details of this highlighted area is shown in Figure 83. The preexisting faults on the TA and in ESB are clear in both the maps. High amplitudes are located around TGF, in the SAB and around the WEF and EF while moderate amplitudes are observed in the NAB.

136
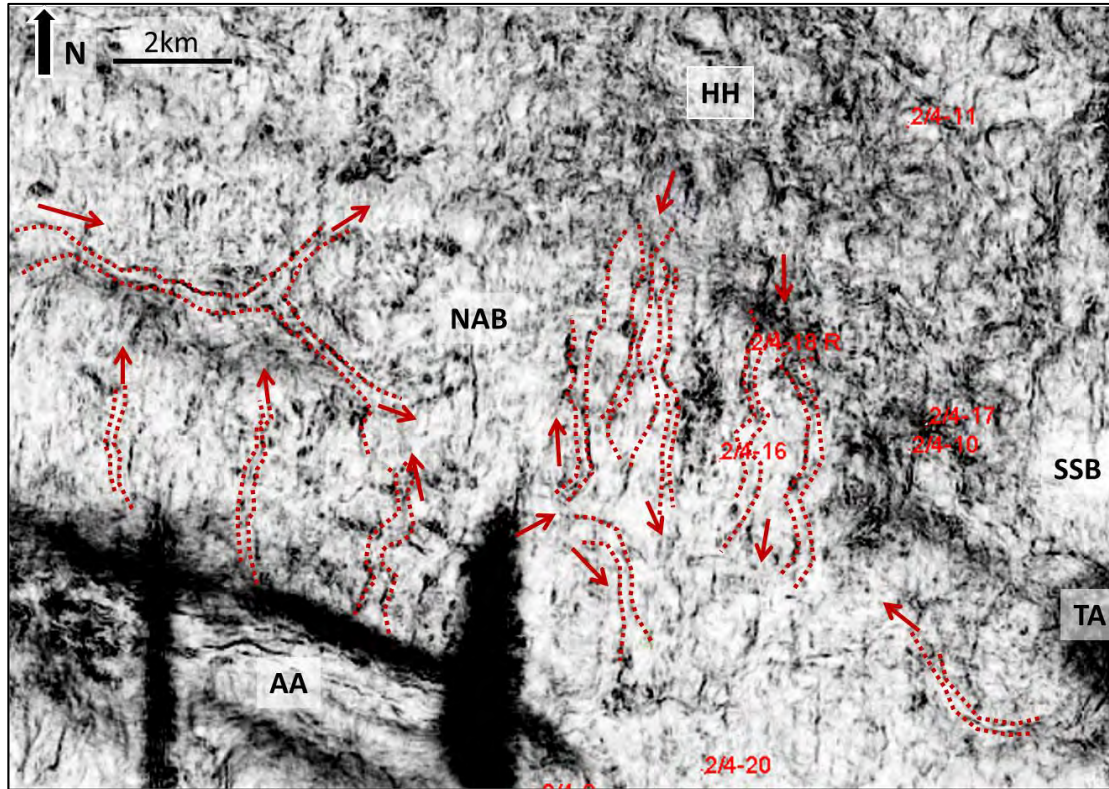
Figure 81: The variance map in the lower middle part of the Tor Formation is the enlarged version of the highlighted area in Figure 78. This figure clearly shows that the NAB channel network increased in size with addition of new channel to the system. Many channel flow from the HH towards the south while a few also flow from the AA towards the north as shown. The general trend of the channel network is from the NW towards the SE but many flow from north to south and vice versa. All the channels are relatively straight in nature.
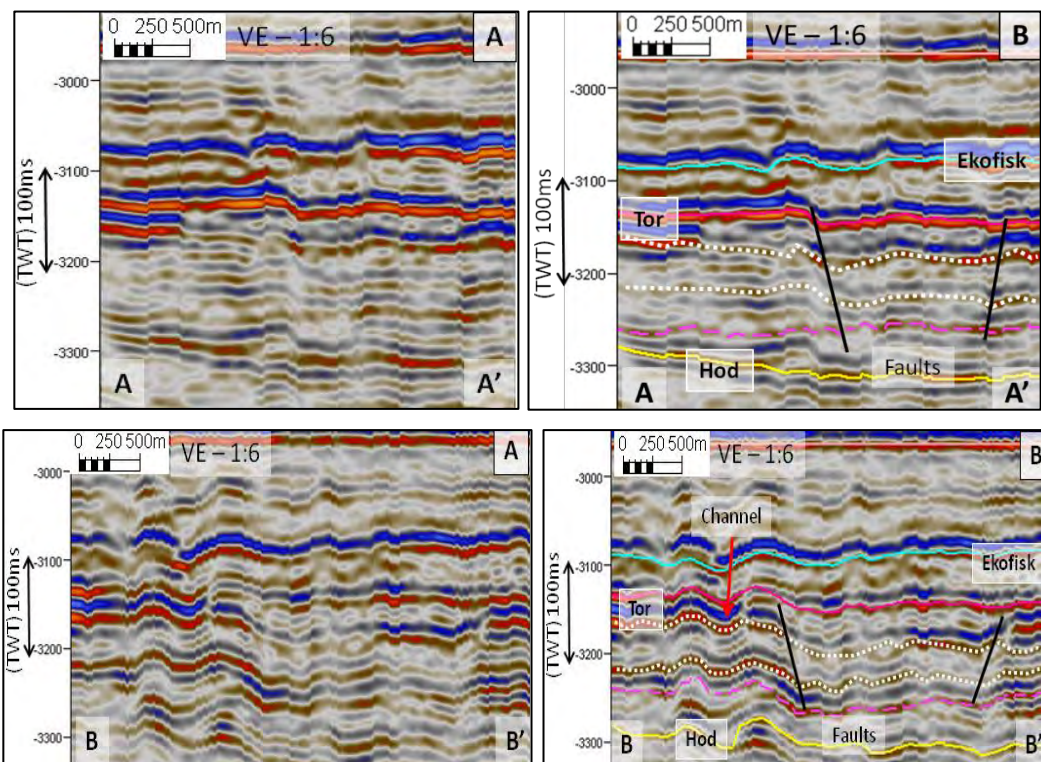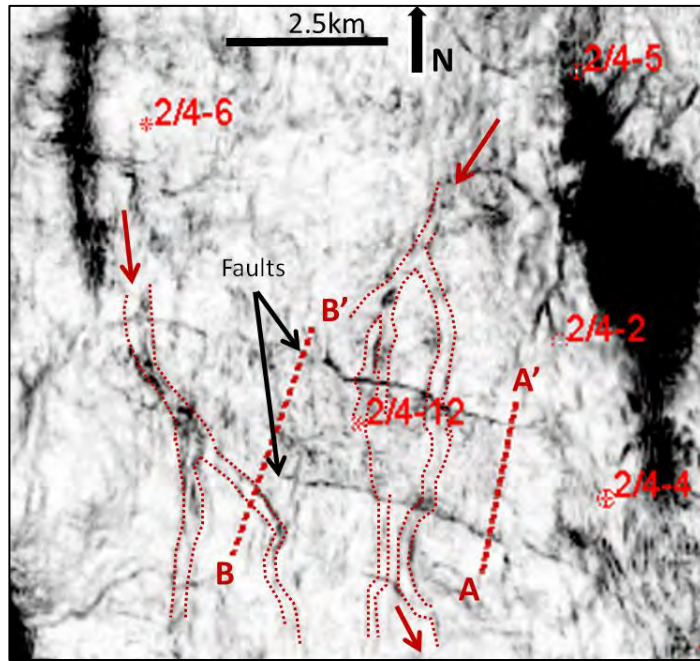
Figure 82: **(A)** Uninterpreted and **(B)** Interpreted **c**ross sections flattened on Rogaland Group top showing faults and a channel in the SW of the EF. The red arrow in the seismic profile BB' point out the channel. The faults are shown by the black lines in both the profiles AA' and BB'. The inset map shows the locations of the seismic profiles and is an enlarged view of the area highlighted in Figure 79. It is clear that the channels originating from the EF branches out and flow towards the south crossing the faulted area.

138
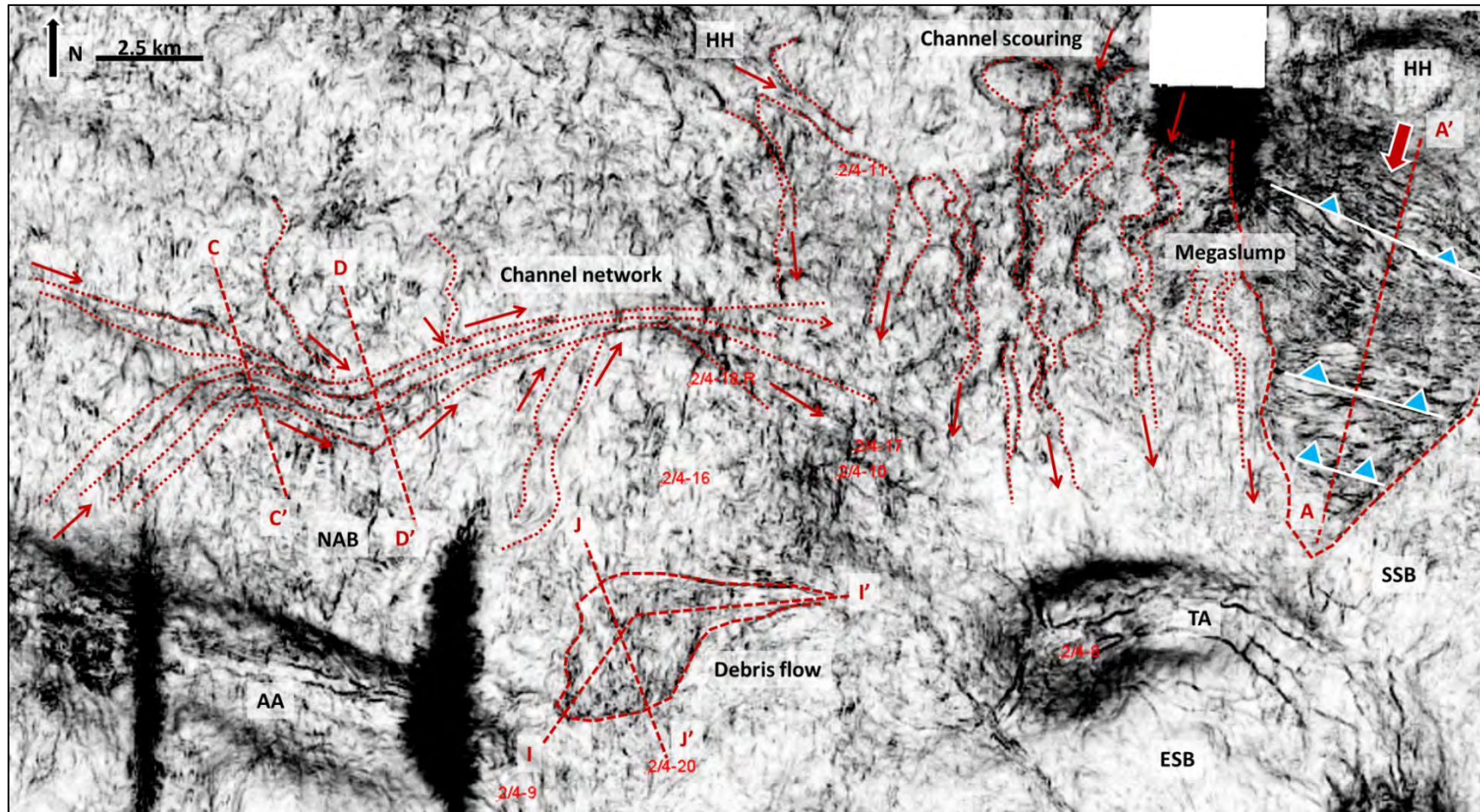
Figure 83: The variance map in the upper part of the Tor Formation is the enlarged version of the highlighted area in Figure 80. This shows that the megaslump in the NE of the study area is developing through time. The direction of the force causing the sliding is oriented NE-SW as shown by the thick red arrow. The seismic cross section AA' through this feature is also shown below. In the NAB a huge channel network has developed as shown by the stipulated lines. The red arrows indicate the potential inflow and outflow directions of the channels. The seismic cross sections CC' and DD' crossing the channel system are shown below. A debris flow also developed in this stratigraphic level as shown and the seismic cross section II' and JJ' are also shown below. In addition the channel system in the HH has grown in size with respect to number of channels and the area covered. Few channels also flow from the NW part of the HH as shown. They all flow SSE into the SSB as shown. The channels in this area are confined and thus they create channel scours as shown.
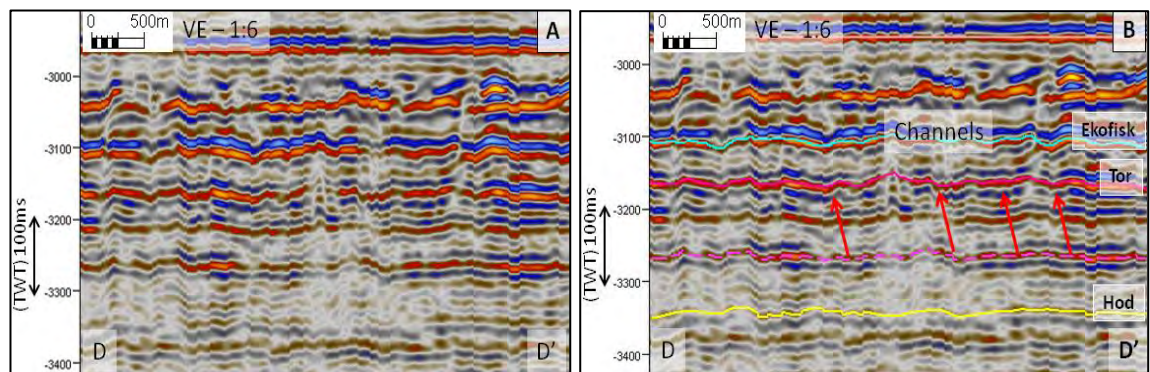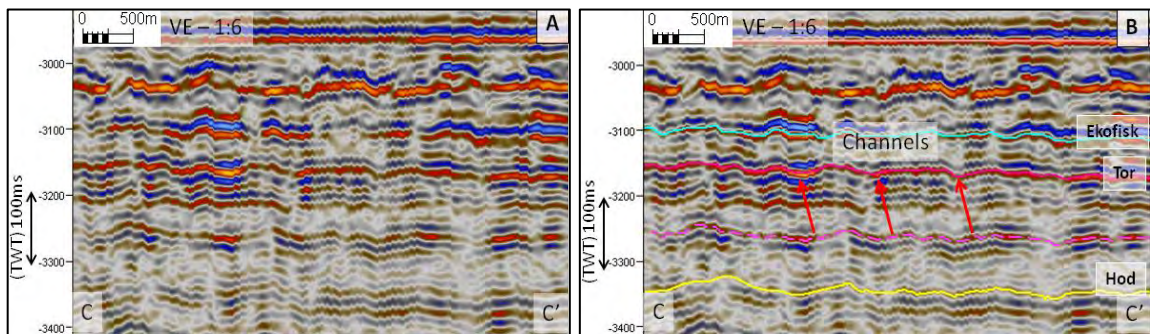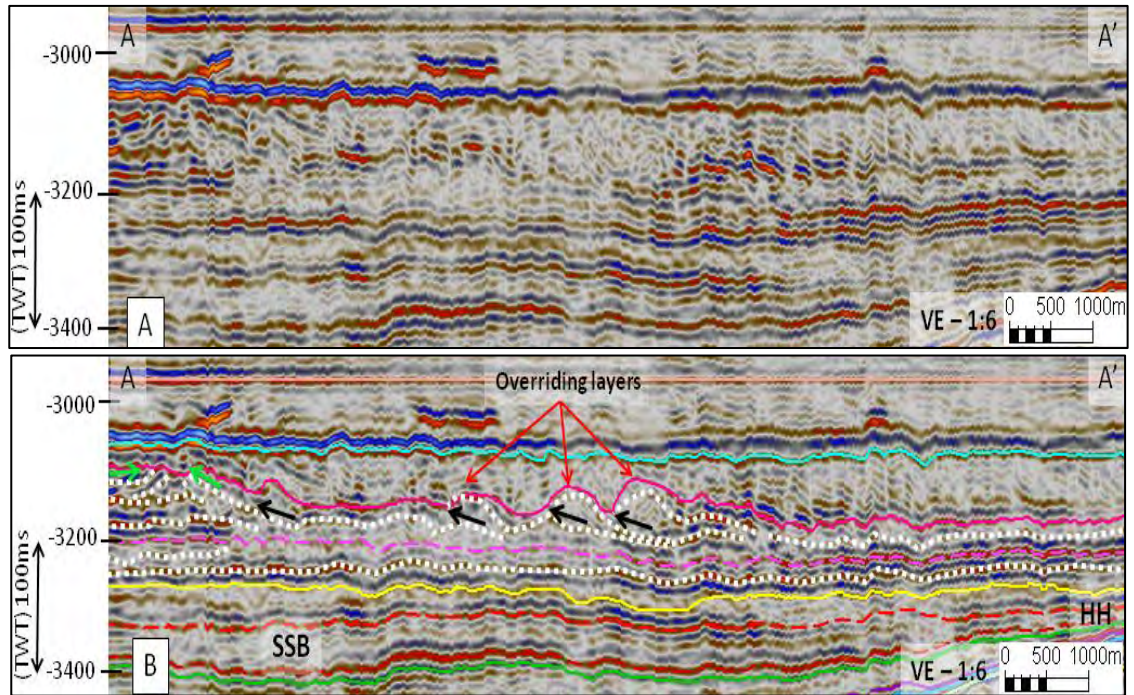
139

Figure 83 continued: **(A)** Uninterpreted and **(B)** Interpreted cross sections flattened on Rogaland Group top. The profile AA' show the seismic characteristics of the mega slide in the NE where the layers show overriding characteristics. Small thrust faults are also created as a result of the sliding marked by the black arrows. The green arrows indicate reflector truncations at the formation top. The profiles CC' and DD' show a new channel network that developed in the central NAB. The profile CC' shows the at least three channels while there is an increase in the number of channels to at least four in the seismic profile DD' as shown by the red arrows. This possibly indicates that shifting of the channels or splitting of channels into several distributaries. The locations of these profiles are shown in the enlarged variance map of the upper part of the Tor Formation in Figure 83.
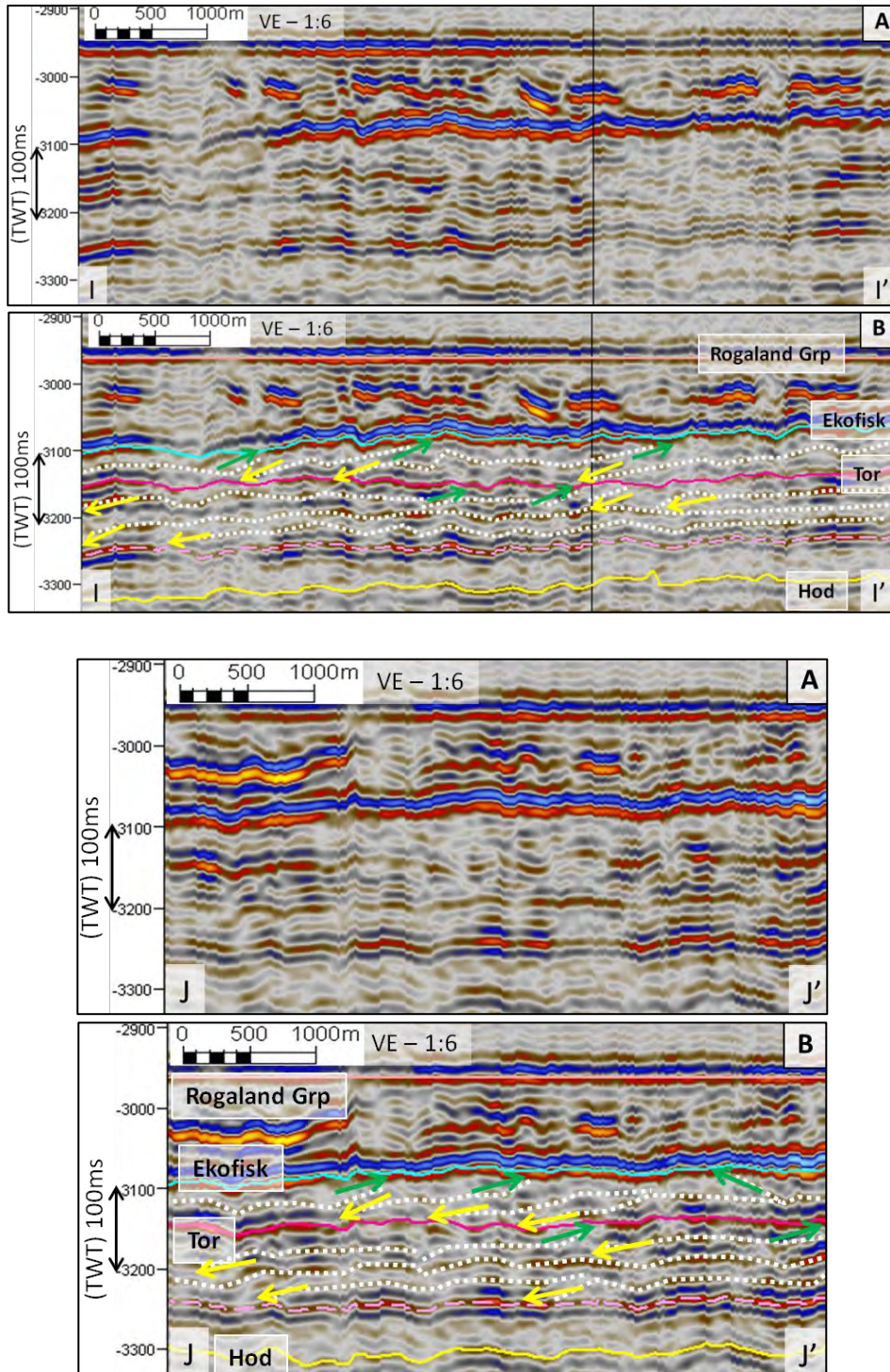
140

Figure 83 continued: **(A)** Uninterpreted and **(B)** Interpreted **c**ross sections flattened on Rogaland Group top showing the seismic characteristics of the debris flow originating from near the TA and flowing into the NAB. Prograding features in profile II' and JJ' indicate an overall southern flow direction. The low amplitudes and presence of discontinuities in the JJ' profile also indicates flows oriented from different directions. The yellow and green arrows represent downlaps and truncations respectively. The location of these profiles is shown in the enlarged variance map of the upper part of the Tor Formation in Figure 83.

5.2.5   Ekofisk Formation

The attribute maps in Figures 84 and 85 show two proportional slices of the Ekofisk Formation taken towards the base and the top respectively. They show the variance (A) and the amplitude (B) maps of the two stratigraphic levels. Figure 82 in the basal parts of the formation displays the presence of the preexisting features like the mega slide in the NE, the faults to the south of the mega slide on top of the Tor and in the ESB, the NAB channel network forming a valley, the gravity flow into the NAB in the central part of the study area, the channels from the TGF and in the SW of the EF. The pockmarks in the ESB have increased in number and seem to be present in clusters. Two such clusters are identified as marked by the dashed circles. The channel system in the HH show scouring features as pointed out in the highlighted area in Figure 82. A zoomed in variance map of this highlighted area is shown in Figure 86. This figure shows the seismic cross sections AA' and BB' where the red arrows show the corresponding scoured parts as shown in the variance inset map. The channels in this area has been flowing N-S since or before the Cenomanian period. This indicates that they flow in a very confined area for a very long time. As a result, the scouring of the channel pathways occurred.

Figure 83 displays the geomorphological features in the upper Ekofisk Formation. Here the preexisting NAB channel network and the gravity flow disappeared. A new channel originating from the EF is identified to flow NNW towards the NAB. This new channel area is shown in the enlarged variance map in Figure 87. Figure 87 clearly shows that the channel originating from the EF splits into several branches flowing north in the NAB. Although the original channel is relatively straight, its branches are very meandering in nature as shown by the stipulated lines. The profiles CC', DD' and EE' show the splitting of a single channel into at least 3 branches. The mega slide area in the NE shows smoothing in map A while the faults lying to its south have also disappeared. Instead three clusters of pockmarks are identified in the area trending NE-SW. This pockmark area highlighted in Figure 83 is shown in Figure 88 which is the enlarged variance map of the highlighted area. Figure 88, in the ESB show rounded to sub-rounded depressions which are interpreted to be the pockmarks. Similar features are also found in the top Chalk Group of the North

Sea of the Danish basin as mentioned in the study by Masoumi et al., (2014). These depressions appear around the area where the faults were present before. These pockmarks also lie very near to the flanks of the salt cored TA and the SD2. The seismic profiles FF' and GG' taken across the pockmarks show that they are generally V-shaped in nature. These pockmarks are a mixture of symmetrical and asymmetrical V-shapes. Few of them also display U-shaped nature.

In the NAB, the preexisting channels network with the valley trending E-W is no more active and thus is not visible in Figure 83. Instead a new feature with mounds and depressions trending NW-SE developed as highlighted in this figure. Figure 89 shows an enlarged variance map of the area and also displays the seismic along the profile HH'. The seismic section HH' shows presence of folded layers with asymmetrical limbs. The thick red arrow indicates the possible direction of a compressional force causing the folding to be NW-SE. The reflectors above and below the Ekofisk Formation also show this folding nature and possibly indicate a later local compressional force.

Figure 90 shows attribute maps of all the slices discussed above. These maps are a combination of the variance and the amplitude maps. The amplitude map is overlaid by the variance map to identify the geomorphological features and to understand the combined variations shown by the morphological features through time. In Figure 90, the maps A-Hidra Formation, B-Blodøks Formation, C-Basal Hod Formation, D-Middle Hod Formation, E-Upper Hod Formation, F-Basal Tor Formation, G-Lower Middle Tor Formation, H-Upper Tor Formation, I-Top Tor Formation, J-Basal Ekofisk Formation and K-Upper Ekofisk Formation.

The Figures A–C show higher amplitudes in the NE of the study area, D and E shows patches of higher amplitudes distributed in the whole study area while F shows concentration of the higher amplitudes towards the south SW and NE of the study area. The figures G-H mostly shows higher amplitudes concentrated in the SW and south of the study area. The maps I-K also shows concentration of higher amplitudes around the EF especially on its flanks.
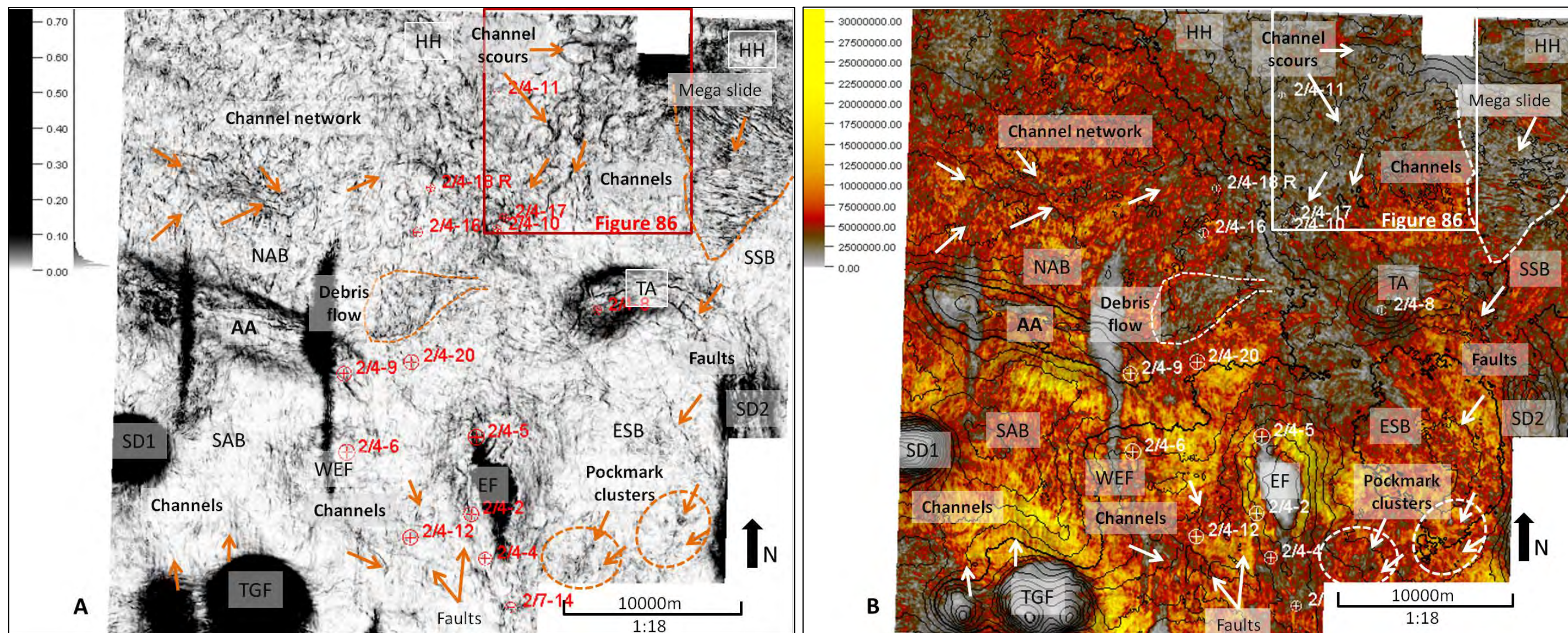
Figure 84: **(A)** Variance and **(B)** Amplitude attribute Maps of the basal part of the Ekofisk Formation with top Ekofisk time contours overlain in map B. In the figure the channel scours are very prominent in the HH area in the north. This area is highlighted and a zoomed in variance map of this area is shown in Figure 86 with more details. The NAB channel network forming a valley still exists but is slightly smooth in the map A compared to that in Figure 80A. This possibly indicates that the channel currents reduced with an increase in sediment infilling process. The preexisting debris flow is present but is also smoother in map A compared to before. The channels in the TGF, SW of EF and in the HH also are present in this stratigraphic level. The pockmarks have reappeared increasing in numbers and are now present in two clusters as shown. High amplitudes are located on the flanks of AA and TGF in the SAB and around the EF. Moderate amplitudes are observed in the NAB and ESB.

144
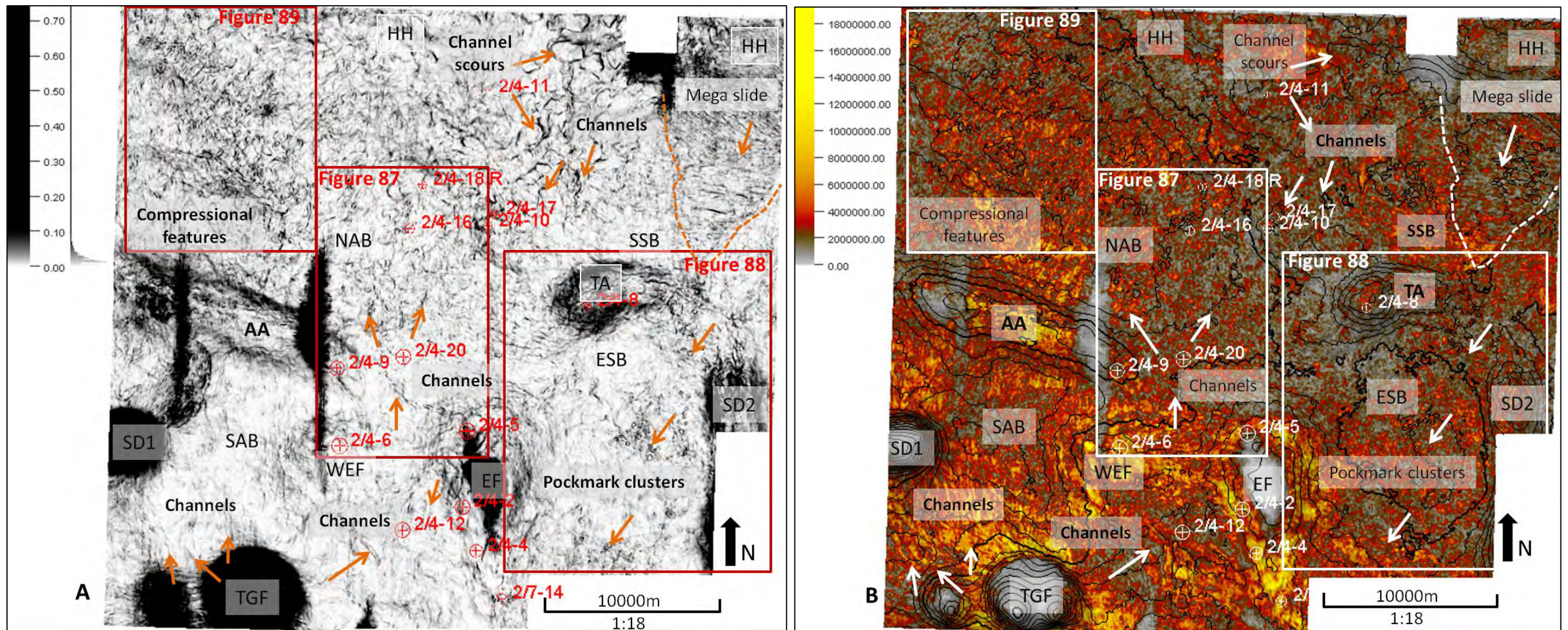
Figure 85: (**A**) Variance and (**B**) Amplitude attribute maps of the upper part of the Ekofisk Formation with top Ekofisk time contours overlain in map B. The previously developed NAB channel network valley is absent in this figure. The preexisting channels in the SW of EF exist also the channels from the TGF are still flowing towards the NNW. The faults in the SW of the EF are although not clearly visible in either of the maps. The channel scours have become more prominent in the upper Ekofisk Formation. New channel originating from the EF is identified to flow towards the NW which divides into few branches in the NAB as pointed out. This area is highlighted as its enlarged variance map is shown in Figure 87 with more details. In the ESB, many pockmarks appeared and they seem to lie in three clusters. These clusters trend in NE-SW direction. The pockmark area is also highlighted and its zoomed in variance map is given in Figure 88 with more details. In the NAB, alternating features of mounds and depressions are identified in the highlighted area, which possibly formed due to a compressional force acting NW-SE. An enlarged variance map of this highlighted area with the seismic characteristics is shown in Figure 89. High amplitudes are located in the SAB and around the EF while moderate amplitudes are observed in the NAB. The ESB and SSB have lower amplitudes.
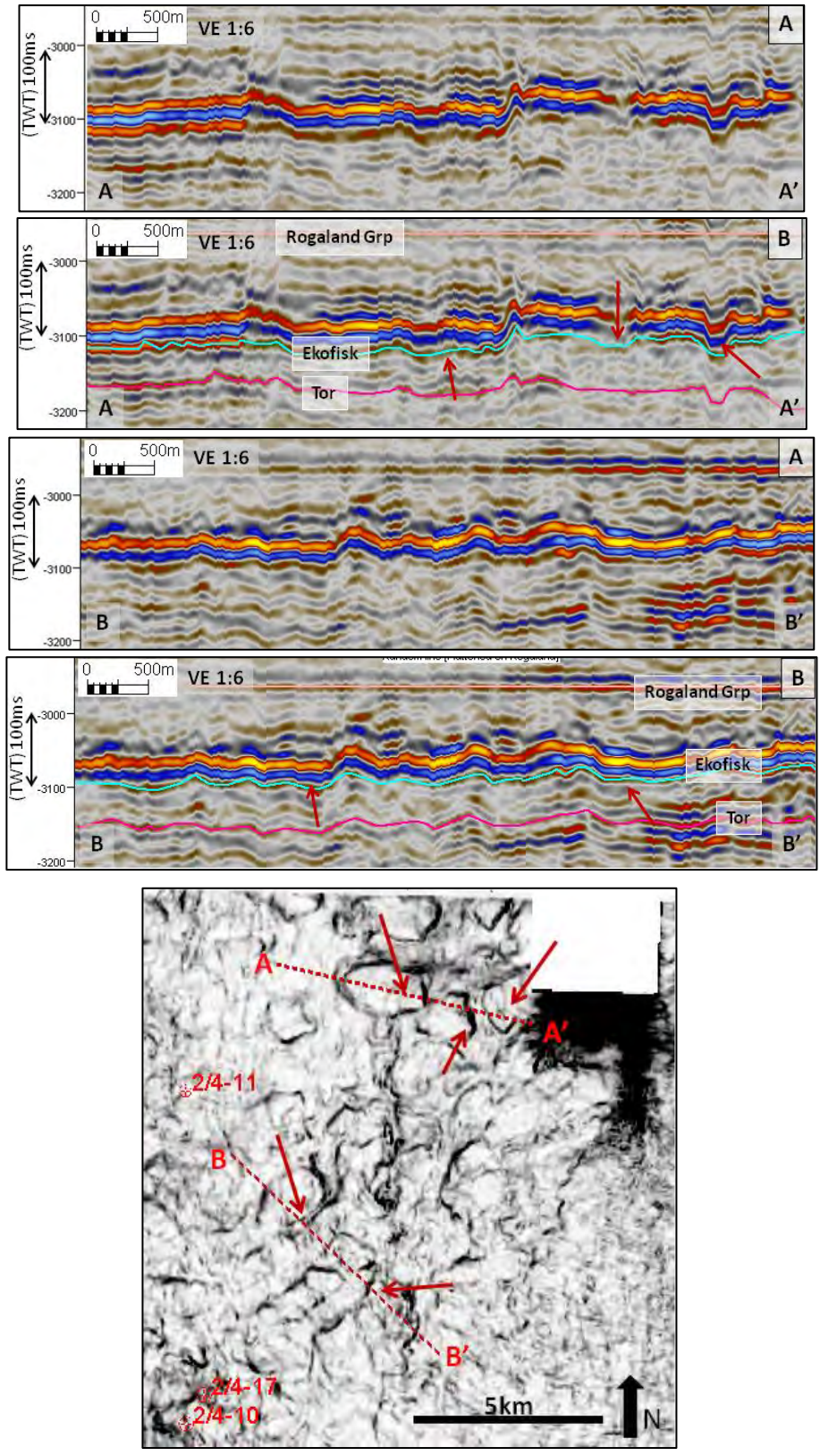
Figure 86: **(A)** Uninterpreted and **(B)** Interpreted **c**ross sections flattened on Rogaland Group top showing the seismic characteristic of the channel scours in the north in HH. The red arrows point out the scours in the seismic profiles AA' and BB'. The inset map shows the location of the seismic profile and is an enlarged view of the area highlighted in Figure 84. These scouring appear here due a confined flow of the channels in this area since the Cenomanian period.

146
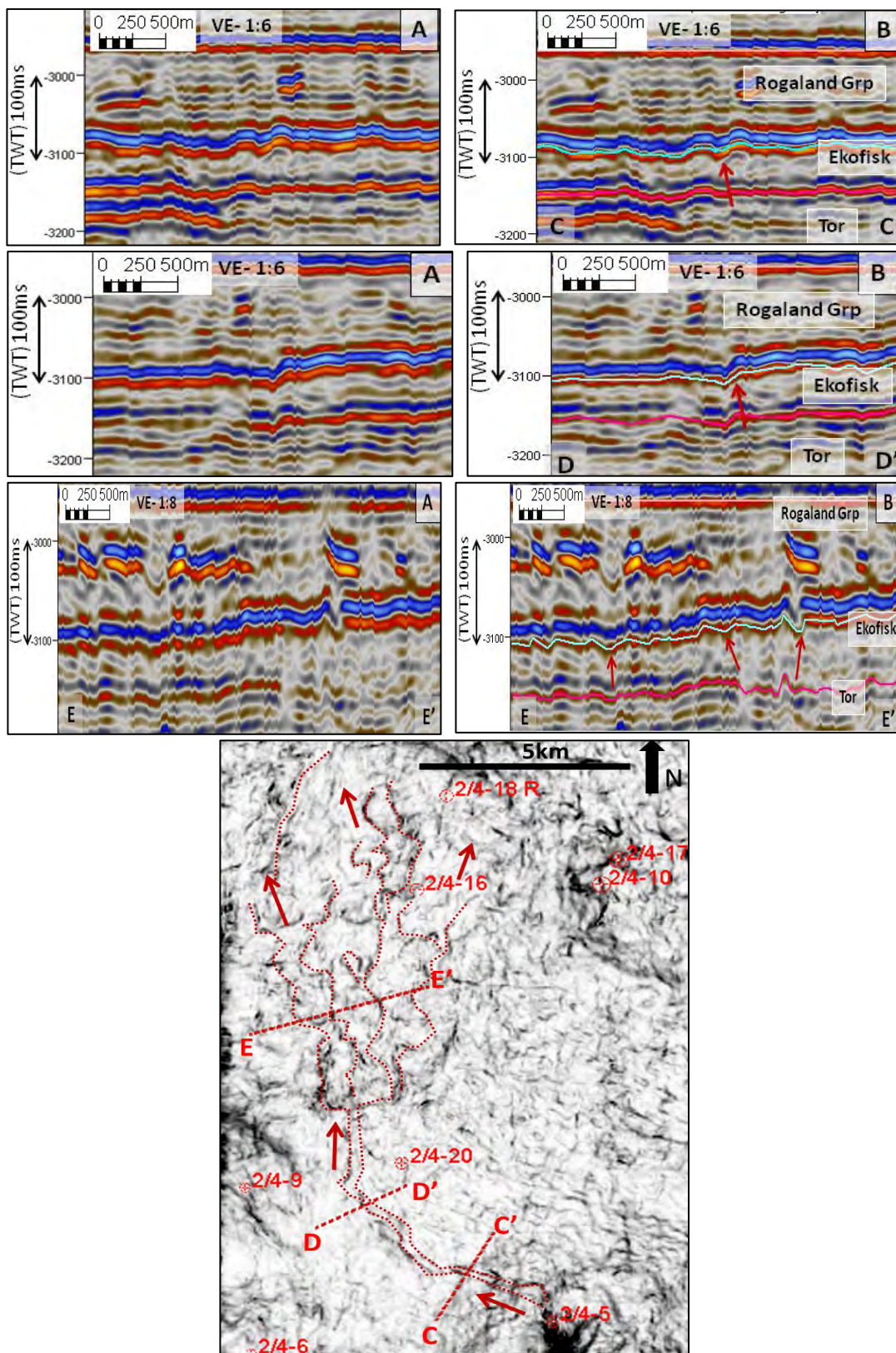
Figure 87: **(A)** Uninterpreted and **(B)** Interpreted **c**ross sections flattened on Rogaland Group top showing the seismic characteristic of the new channel system originating from the EF and flowing into the NAB in the north. The channel splits into three meandering distributaries as it enters the NAB. The red arrows point out the corresponding channels. The inset map shows the location of the seismic profile and is an enlarged view of the area highlighted in Figures 85

147
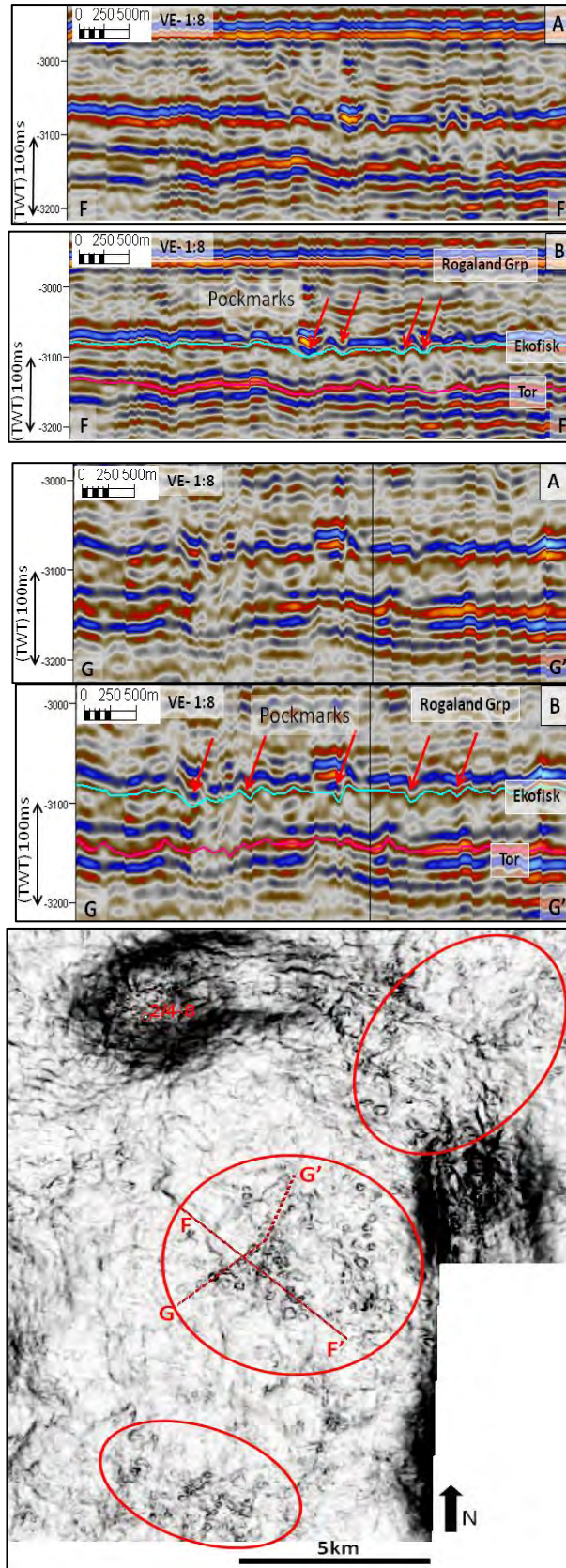
Figure 88: **(A)** Uninterpreted and **(B)** Interpreted cross sections flattened on Rogaland Group top showing the seismic characteristic of the pockmarks developed in the ESB. The red arrows point out the rounded to sub-rounded pockmarks in the seismic profiles FF' and GG'. The inset map shows the location of the seismic profile and is an enlarged view of the area highlighted in Figures 85.

148
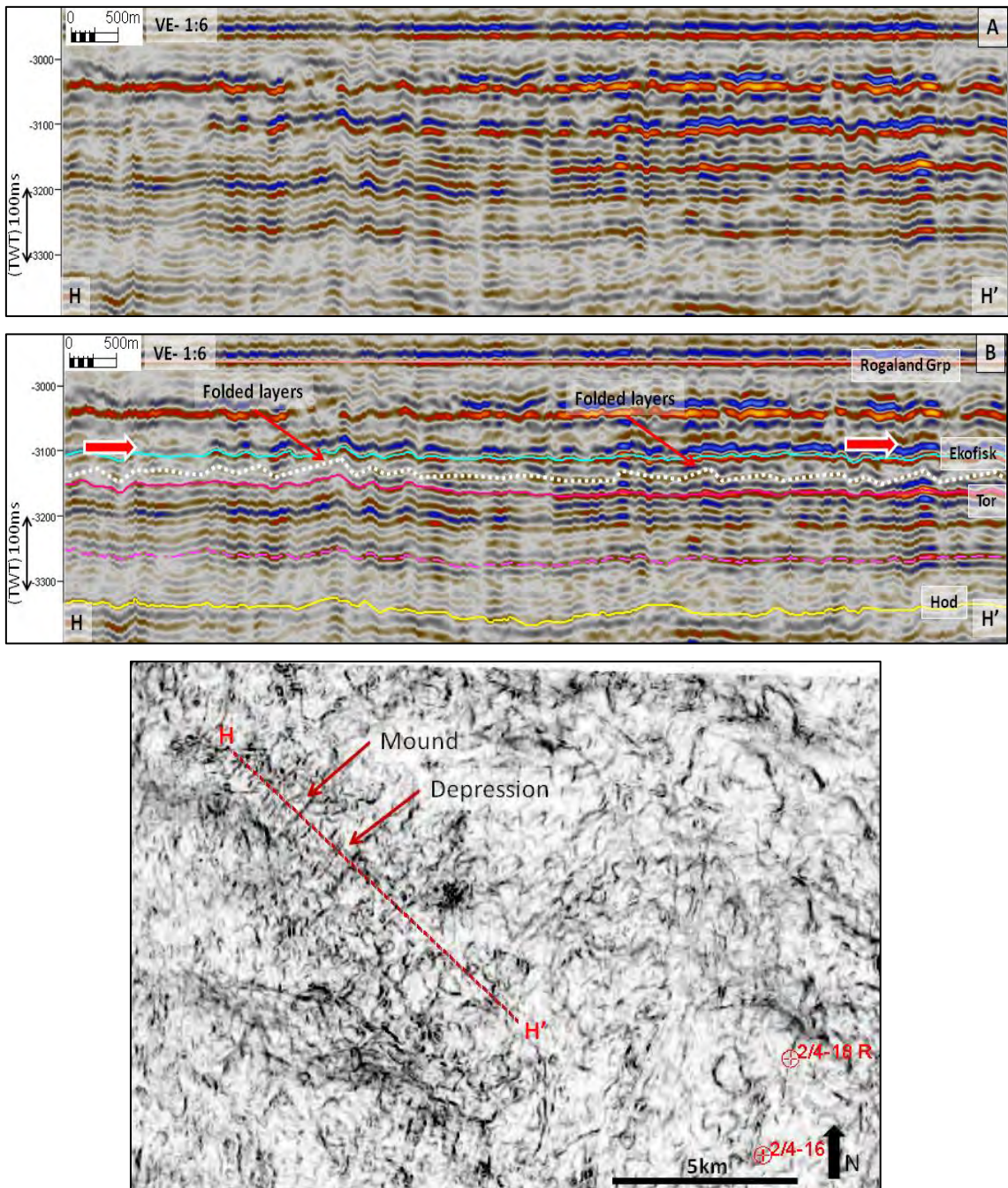
Figure 89: (A) Uninterpreted and (B) Interpreted cross sections flattened on Rogaland Group top showing the seismic characteristic of the compressional force in the NAB. The seismic profile HH' shows folded layers indicating the direction of the force to be from NW to SE. The red arrows show the force direction. The inset map shows the location of the seismic profile and is an enlarged view of the area highlighted in Figures 85.
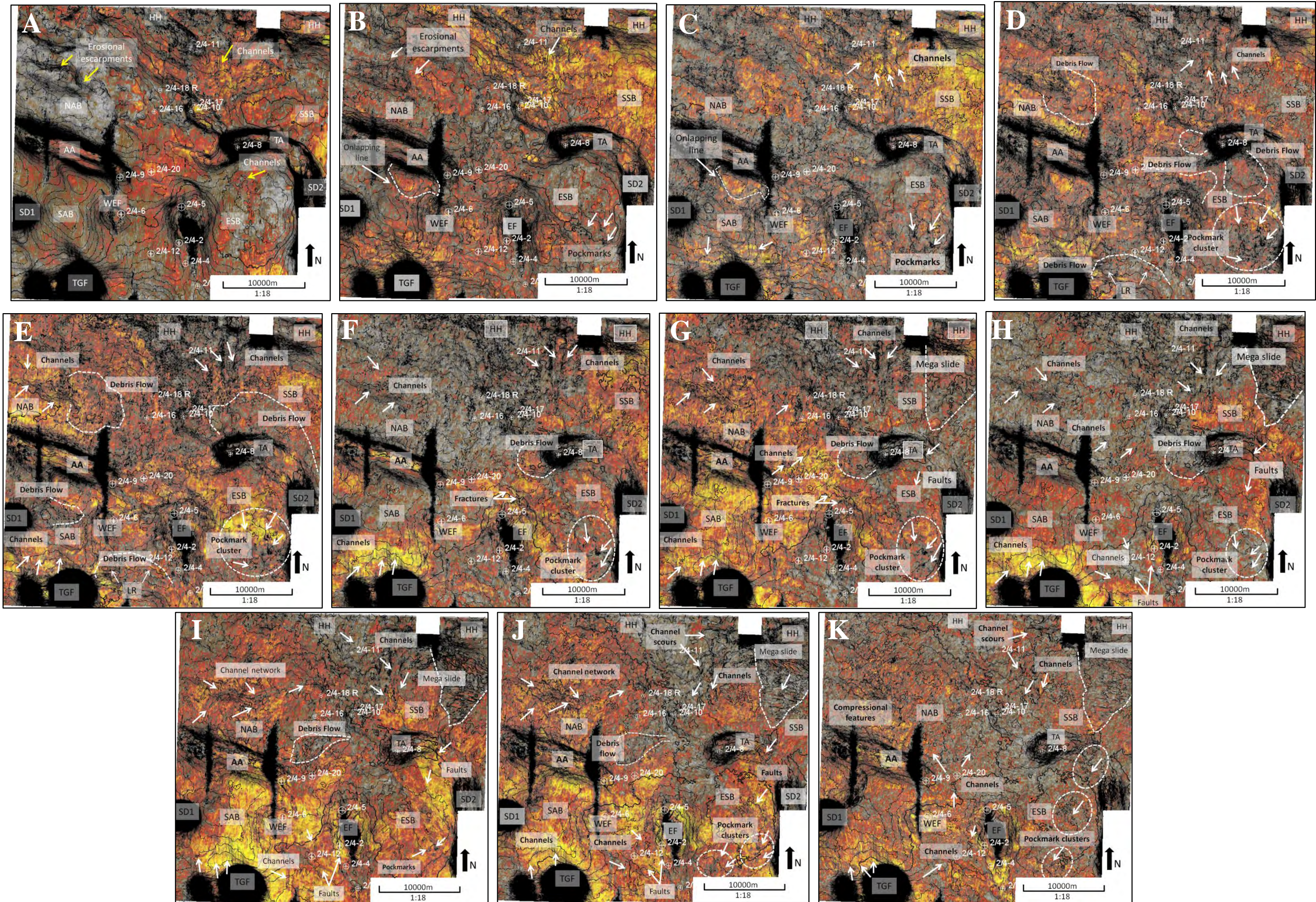
Figure 90: The attribute maps of all the slices discussed above are displayed. These maps are a combination of the variance and the amplitude maps. The amplitude map is overlaid by the variance map to identify the geomorphological features and to understand the combined variations shown by the morphological features through time. The colour legends are as given in Figures 64 for A, 68 for B, 71 for C, 72 for D, 73 for E, 77 for F, 78 for G, 79 for H, 80 for I, 84 for J and 85 for K. The Figures A–C show higher amplitudes in the NE of the study area, D and E shows patches of higher amplitudes distributed in the whole study area while F shows concentration of the higher amplitudes towards the south SW and NE of the study area. The figures G-H mostly shows higher amplitudes concentrated in the SW and south of the study area.

6. Discussions

The Chalk Group of the Central Graben in the Norwegian Continental Shelf is divided into five major seismic sequences bounded by six sequence boundaries. The seismic sequences of the Hod and Tor formations have been further divided into three and two subunits respectively by the presence of unconformities within these formations. The available well data integrated with the interpreted seismic sequence characteristics led to a better understanding of the depositional environments prevailing during the deposition of each seismic sequence and the tectonic activities leading to generation of specific geomorphological features. The results led to identification of three different phases in the evolution of the study area during the Late Cretaceous as discussed below which is also in accordance with the study by Gennaro et al., (2013).

6.1. THE PRE-TECTONIC PHASE

The Hidra, Blodøks and the basal subunit of the Hod Formation were deposited during the pre-tectonic stage in the study area. The Hidra and Blodøks formations constitute the basal part of the Chalk Group and show an overall draping behavior (Figures 14-22) indicating a relatively tectonically calm period during the Cenomanian till the early Turonian ages. The basal subunit of the Hod Formation has onlapping features on the flanks of the structural highs (Figures 34-42) and thus shows infilling behavior. Studying the distribution and the increasing thickness of the sediments in the NAB, SAB, ESB and SSB from the isochron maps of Hidra and Blodøks formations (Figures 23 and 33), the infilling and draping nature of the sediments during this phase is evident.

The flanks of the structural highs of AA, SD1, TGF and WEF surrounding the SAB contain small amounts of turbidites and redeposited sediments in the Hidra and the Blodøks formations (Figures 16 and 17) and in the basal subunit of the Hod Formation (Figure 37). Thus suggest that the mentioned highs were uplifting at a very slow rate during this relatively tectonically calm period. The onlapping of the reflectors of the basal subunit of the Hod Formation on the flanks of AA and TGF in Figure 36 indicate infilling

characteristics while the presence of the erosional pockets also indicate sediment flows from SD1 and WEF. This in turn indicates SD1 and WEF were active.

The presence of the erosional escarpments in the Hidra Formation in the NAB (Figure 64) suggests that density currents trending NW-SE were common in the basin during the Cenomanian age. The more scoured southern bank of the erosional escarpments is due to the deflection of the flows to their south caused by the earth's corriolis force in the northern hemisphere. However, these currents gradually diminished with the beginning of the deposition of the Blodøks Formation and these erosional escarpments were infilled by the Blodøks sediments (Figure 68). The presence of the small channel like features in the ESB (Figure 67) over a faulted high indicates that this area underwent a local uplift leading to formation of these channels through which the sediments escaped to a lower relief. The infilling nature of the Blodøks formation is also clearly observed in the SAB, SSB and ESB in Figures 24-32 and 68. Later when the basal subunit of the Hod Formation began depositing, the NAB was also undergoing a subsidence as evident from the prograding features shown in the Figure 35.

The appearance of pockmarks over a faulted area in the ESB on the top of the Blodøks Formation and in the basal subunit of the Hod Formation (Figures 68, 70 and 71) also indicates a slightly active fault system leading to ascension of aggressive fluids along the underlying fault network. The expulsions of these fluids are as thermogenic fluids from below till the top of the Chalk Group (Figure 70). Similar features are also found to be present near the top Chalk surface in the Danish North Sea as presented in a study by Masoumi et al., (2014).

Figures 64, 68 and 71 all show the presence of the channels in the HH. Comparing the Figures 66, 69 and 74 the development of these channels to a bigger channel system is observed. This indicates that HH possibly experienced slow uplifts during the Blodøks and basal Hod deposition time increasing the accommodation space in the SSB area.

The top of the Blodøks formation is also an unconformity and a sequence boundary in the study area as indicated by the sharp fall in GR in Figure 7 and 13 and a fall in DT in Figure 7. The seismic sequence interpretations in Figures 14-22 also support this fact. The Figures 68 and 71 of Blodøks and basal Hod formations respectively display calm

and infilling nature. It is possible that there was a period of non-deposition after which the deposition of the Hod formation began. Since there is no evidence of any gravity flows in the Figure 71, it is also interpreted that the basal Hod Formation deposited during the pre-tectonic phase.

6.2. THE SYN-TECTONIC PHASE

The deposition of the middle and the top subunit of the Hod Formation occurred while the study area was undergoing tectonic uplifts due to halokinesis and inversions leading to the formation of onlapping features on the flanks and erosions at the crests of the structural highs in the study area (Figures 34, 36-38, 40 and 41). On the other hand the basal subunit of the Tor Formation also deposited during this phase while the rate of the tectonic uplifts were culminating. This is indicated by the combination of relatively continuous – parallel and chaotic seismic facies which show onlapping on some of the flanks of the highs, draping of the highs and also erosion at the crests of the highs (Figures 44, 46, 50 and 51).

The unconformities overlying the basal, middle and top subunits of the Hod Formation indicate gravity driven erosional surfaces formed by uplift during the late Coniacian and Santonian intense tectonic inversions (Bailey et al., 1999; Gennaro et al., 2013; Hampton et al., 2010). The unconformity overlying the basal subunit of the Tor Formation marks the culmination of the inversion phase.

Several debris flows dominating the middle subunit of the Hod Formation as shown in Figures 72 reflects the high intensity of the tectonic inversions and halokinetic uplifts during the Santonian and early Campanian ages leading to destabilization of the slopes causing slope failures. The continuing inversion and halokinesis during the Campanian is evident from the wider spread of the existing debris flows and formation of new such mass transport systems as shown in Figure 73. The presence of active faults below the ESB is indicated by the increase in the number of the pre-existing pockmarks as pointed out in both the Figures 72 and 73 compared to that in Figure 71.

The channels in the north, in the HH area as shown in Figures 72 and 73 also indicate presence of bottom and turbidity currents generated in this area during the

153

Santonian and the Campanian due to gradual uplifts of the HH. The unchanged locations of the channels also indicate a confined flow. Figure 74 shows relatively straight channels in the area indicating strong currents. Figure 75 also shows generation of relatively straight channels from the TGF indicating relatively fast uplift in the TGF. Figure 76 also shows several channels from the west merging together to flow towards the SE. A preexisting debris flow very near to the channel system shows evidences of sediment flow in phases. It is possible that the debris flows in the later stages were due to the destabilization of the slope sediments by the SE flowing channels nearby.

During the early Maastrichtian period the deposition of the basal subunit of the Tor Formation displays existence of most of the preexisting features like the NAB, HH and the TGF channels in Figure 77. Very few gravity flows are observed in Figure 77 compared to that in the Figure 73 indicating culminating tectonic activities in the study area. The reduction in the number of pockmarks and the cluster size indicates deactivation of the underlying faults leading to reduced expulsion of thermogenic gases.

6.3. THE POST-TECTONIC PHASE

The top subunit of Tor Formation and the Ekofisk Formation were deposited during the post tectonic phase during which the existing structural highs were the source of allochthonous sediments as indicated by the presence of discontinuous and chaotic seismic facies around them in Figures 44, 45, 46, 50, 54 and 56. Figures 51 and 61 during the mid-Maastrichtian and the Danian ages show development of a mega slide feature in the NE of the SSB trending NE-SW. Figure 78 shows the initial appearance of this feature in the Tor Formation and indicates a localized compressional force originating further to the NE of the study area trending NE-SW. Destabilization of the slope sediments in the HH caused by this force led to the formation of the mega slide. The seismic cross sections in Figures 51 and 61 and AA' in Figure 83 show the formation of several small thrust faults as a result of continuous slides occurring through time. Along with this feature also appears to its SSW, few faults on the TA and in the ESB trending approximately NW-SE as pointed out in the Figure 78. It is interpreted that the same compressional force creating

the mega slide might be the cause of these faults. It is also possible that this compressional force is a small part of a larger event occurring further to the NE of the study area which is beyond the scope of this study.

Figures 79 and 80 are stratal slices taken towards the upper part and top of the Tor Formation respectively. They display developments of new channel systems in the NAB trending E-W and to the SW of the EF trending approximately N-S. A couple of faults also appear to the SW of the EF in both these figures. The channel from the EF flows crossing these faults. The developments of such channel systems indicate that the late Maastrichtian period was dominated by bottom currents which in turn were influenced by the relative fall of sea levels. Figure 83 shows the increase in number of channels in the NAB and HH indicating the relative fall in sea level leading to increased and strong bottom and turbidity current effects. This sea level fall gradually narrowed the existing sea-pathways and intensified the circulation of the bottom currents in the study area as also mentioned in the study by Gennaro et al., (2013). The channels are also formed when the bottom currents are sufficiently strong enough to erode the sea bed and takes place mostly along the slopes (Esmerode et al., 2008; Faugères et al., 1993). This also indicates the presence of turbidity and density flows which accelerated to become fully turbulent (Back et al., 2011). The presence of the overlying unconformity of the basal subunit of the Tor Formation marks the change in sedimentation from a non-current oriented to current dominated depositional system (Faugères et al., 1993; Faugères et al., 1999; Faugères et al., 1998; Gennaro et al., 2013; Nielsen et al., 2008). In the mean while the compressional force from the NE became stronger during the late Maastrichtian as the mega slide is more pronounced and prominent.

Localized uplifts of the HH (Figure 54) and TGF (Figure 56) still continued during the Danian period leading to small scale topographic highs; while a localized part of the HH adjacent to the west of the SSB underwent subsidence as indicated by the prograding seismic facies shown in Figure 62. The northeastern compressional force was still active during the early Danian period as indicated by the presence of the mega slide and the faults to its south in Figure 84. In the early Danian the presence of the pre-existing channel features along with newly developed channel scours in the north and debris flows

155

(Figure 84) reflect the increased intensity of the bottom current circulation in the study area. These intense bottom currents lead to destabilization of the slope sediments by increasing the slope inclination and thus triggered gravity driven redeposition and emplacement of allochthonous units in the basin (Esmerode et al., 2008; Hansen et al., 2004) as shown by the presence of the debris flow in Figure 84. The N-S flowing channels in the HH in the north experienced increased erosion forming the prominent scoured features as pointed out in the Figures 84 and 85.

The late Danian period (Figure 85) experienced the culmination of the northeastern compressional force as indicated by the draping and smoothing of the mega slide and the absence of the faults. Several clusters of pockmarks appeared trending NE-SW as pointed out by the arrows. These trend perpendicular and lie on the top of the underlying faults in the ESB. They also lie very near to the salt cored TA and the SD2. It is possible that aggressive fluids were ascending along the underlying fault network forming these depressions as mentioned in the study by Masoumi et al., (2014). However, the attribute maps show their continuously diminishing presence till ~65ms above top chalk indicating increased inactivity of the pockmarks. The presence of similar pockmarks is also observed on the top chalk in the Danish basin which continuously diminishes above as mentioned in the study by Masoumi et al., (2014). These pockmarks however, are present in the area since the deposition of the Blodøks Formation and the expulsions of thermogenic gases originate from below the Chalk group as shown in Figure 70.

The pre-existing channel systems in the NAB is inactive as indicated by the draping and infilling by the sediments of the late Danian period as observed in Figure 85. The channel system to the west of the EF is also nearly draped and inactive. This indicates decrease in bottom current activities in the NAB as well as in the west of EF. A new channel system originating from the EF developed approximately trending N-S as shown in this Figure 85. This channel system splits into several sinuous branches near the NAB (Figure 87) indicating the decreasing velocities of the currents and increasing infilling characteristics during the late Danian times. However, this also indicates renewed redistribution system creating large amounts of allochthonous sediments into the NAB. In the NW of the study area in the NAB as highlighted in Figures 85 and 89, lineation like

features showing alternating mounds and depressions indicate slight folding of the layers with asymmetrical limbs (seismic profile HH' in Figure 89). This reflect generation of a new local compressional force trending NW-SE in the area which might have participated in continuing sediment reworking and redistribution.

Overall during the late Danian the Ekofisk seismic sequence was influenced by relatively reduced and weak bottom currents. The rate of sedimentation was also more than the rate of erosion leading to an infilling and draping behavior observed in Figures 54-62.This indicates that the bottom current activities waned off gradually from the early to late Danian periods. This is in accordance with the findings of the studies by Esmerode et al., (2008) and Gennaro et al., (2013).

Figure 90 displays the overlaid variance and amplitude attribute maps of all the stratigraphic slices considered in Figures 64, 68, 71-73, 77-80, and 84-85. The clear shifting of the higher amplitude anomalies towards the south and SW of the study area through geological time in Figure 90A-K is observed. The higher amplitudes are often observed in the locations where relatively undisturbed deposition occurred. Therefore comparing the maps A-K of Figure 90, relatively undisturbed depositional environment prevailed towards the south and SW during the Tor and Ekofisk formations. This also creates a favourable environment for hydrocarbon maturation. Higher amplitude anomalies are observed around the EF with several drilled wells and it is well known that this field has been producing hydrocarbons since its discovery in 1969. Similar or higher amplitude anomalies are observed in the SW on the TGF and in the SAB and might indicate hydrocarbons. However, the lack of wells in this area restricts the investigation regarding the trap and seal quality and conditions.

7.   Conclusions

i. The Chalk Group in the Norwegian Central Graben in the study area has been subdivided into five major seismic sequences namely, Hidra (Cenomanian), Blodøks (latest Cenomanian – early Turonian), Hod (Turonian - Campanian), Tor (late Campanian – Maastrichtian) and Ekofisk (Danian). These are also the names of the formations identified in various previous studies. The Hod and the Tor seismic

sequences have been further subdivided into three and two subunits by the identification of the presence of two and one unconformities respectively within the Chalk Group in the study area.

ii. The seismic sequences are organized into three groups, namely pre-tectonic phase, syn-tectonic phase and post-tectonic phase with respect to their depositional timing and pattern. The Hidra and Blodøks formations along with the basal subunit of the Hod Formation represent the pre-tectonic depositional phase during the Cenomanian – Coniacian. The middle and top subunits of the Hod Formation along with the basal subunit of the Tor Formation represent the syn-tectonic depositional phase during the Santonian – late Campanian and finally the top subunit of the Tor Formation and the Ekofisk Formation represent the post-tectonic depositional phase during the Maastrichtian – Danian.

iii. The study area in the Norwegian Continental shelf, in the pre-tectonic phase underwent an overall initial draping combined with infilling processes in the later stages. This was a relatively tectonically calm period which still experienced some small uplifts in the structural highs of AA, SD1, and TGF surrounding the SAB. In the NAB the presence of bottom currents creating erosional escarpments during this phase indicates some extent of reworking of sediments by bottom currents.

iv. During the syn-tectonic phase the study area underwent several uplifts due to halokinesis and tectonic inversions. The structural highs of AA, TA, SD1, WEF, TGF and HH were especially uplifted increasing the accommodation space in the NAB, SAB, ESB and SSB. This also led to several gravity-driven mass flows in the area which aided in creation of the erosional surfaces representing the within formation unconformities. The halokinesis and the inversion had a direct impact on the chalk depositional environment in the post-tectonic phase.

v. The post-tectonic phase experienced a reduction in tectonic activities although still few localized activities were identified. The study area also experienced an overall increase in bottom current circulation as an aftereffect of the tectonic uplifts. Overall the depositional environment changed from the preexisting pelagic to an environment dominated by bottom currents creating gravity driven mass transport systems

especially near the flanks of the structural highs as also documented by Gennaro et al., (2013).

vi. The contour parallel bottom currents dominating the upper Tor and Ekofisk formations in the post-tectonic phase became stronger during the late Maastrichtian times leading to erosions along the slopes. These erosions destabilized the already unstable slopes due to inversion, further to cause slope failures creating slumps and slides. The sediments from the slumps were picked up again by these bottom currents creating turbid and density flows. Channels were then created by these turbid and density flows due to friction and erosion with the sea bed. Channel scours were also created by these circulating strong bottom currents possibly in an entrapped and confined condition. Overall sediment reworking and redistribution was at its peak during this period.

vii. A mega slide feature displaying overriding characteristics of the sediment layers in the NE of the study area during the Maastrichtian times indicate a compressional force trending NE-SW from further NE of the study area. The appearance of few faults in the same stratigraphic level to the south of this mega slide, running perpendicular to the force direction possibly hints on a small part of a larger event located outside the study area and is out of scope of this study.

viii. During the late Danian times, the diminishing relatively straight channel features indicate that the effects of bottom currents were waning off due to increased infilling characteristics and reduced current velocities. This is also evident from the events of single channels splitting into several sinuous branches in the study area.

ix. On the top Chalk surface in the latest Danian times, the appearance of clusters of pockmarks showing some extent of lineaments with a NE-SW trend in the ESB is just above the pre-existing fault network and in the vicinity of the flanks of SD2 and a salt cored TA. This situation leads to a conclusion that aggressive fluids possibly from the matured main Jurassic source rocks below, ascended along the fault network. These aggressive fluids were expelled at the surface thermogenic fluids creating the pockmarks. This similar process is present in the top chalk in the Danish Central Graben of the North Sea as documented by Masoumi et al., (2014). In the same stratigraphic level a development of a compressional force trending NW-SE in the

NAB prove that this tectonically calm period also had some localized activities which might have imparted to sediment reworking and redistribution.

x. The higher amplitude anomalies present in the SW of the study area on the TGF and in the SAB during the Tor and Ekofisk Formation might indicate hydrocarbon. However, further information on the petroleum system is required to understand the trap and seal quality and conditions to confirm hydrocarbon presence.

8. Further scopes of the study

i. A detailed study on the pockmark geometries, orientation, density and distribution in the study area might throw an insight upon the prevailing current flow directions, acceleration or deceleration of the currents and the sea floor morphology created by the contour current interactions.

ii. An in-depth study regarding the changing channel patterns, sinuosity, branching of the channels might help explain more about the mass transport systems and their dependence on the changing sea level and tectonic activities.

9. References

Back, S., et al. (2011). 3D seismic geomorphology and sedimentology of the Chalk Group, Southern Danish North Sea. *Journal of the Geological Society, 168*(2), 393-406.

Bailey, H., et al. (1999). Joint Chalk Research Phase V: A Joint Chalk Stratigraphic Framework. *Norwegian Petroleum Directorate (NPD), Stavanger*.

Bramwell, N., et al. (1999). *Chalk exploration, the search for a subtle trap.* Paper presented at the Geological Society, London, Petroleum Geology Conference series.

Deegan, C. t., et al. (1977). *A standard lithostratigraphic nomenclature for the Central and Northern North Sea* (Vol. 1): HMSO.

Esmerode, E. V., et al. (2008). Interaction between bottom currents and slope failure in the Late Cretaceous of the southern Danish Central Graben, North Sea. *Journal of the Geological Society, 165*(1), 55-72.

Faugères, J.-C., et al. (1993). Bottom-current-controlled sedimentation: a synthesis of the contourite problem. *Sedimentary Geology, 82*(1), 287-297.

Faugères, J.-C., et al. (1999). Seismic features diagnostic of contourite drifts. *Marine Geology, 162*(1), 1-38.

Faugères, J., et al. (1998). Seismic patterns of a muddy contourite fan (Vema Channel, South Brazilian Basin) and a sandy distal turbidite deep-sea fan (Cap Ferret system, Bay of Biscay): a comparison. *Sedimentary Geology, 115*(1), 81-110.

Fontaine, J. M., et al. (1987). SEISMIC INTERPRETATION OF CARBONATE DEPOSITIONAL ENVIRONMENTS. *American Association of Petroleum Geologists Bulletin, 71*(3), 281-297.

Gennaro, M., et al. (2013). Seismic stratigraphy of the Chalk Group in the Norwegian Central Graben, North Sea. 1-31.

Gennaro, M., et al. (2013). Seismic stratigraphy of the Chalk Group in the Norwegian Central Graben, North Sea. *Marine and Petroleum Geology, 45*, 236-266. doi: 10.1016/j.marpetgeo.2013.04.010

Gennaro, M., et al. (2013). Characterization of dense zones within the danian chalks of the Ekofisk Field, Norwegian North Sea. *Petroleum Geoscience, 19*(1), 39-64.

Hallam, A., et al. (1999). Mass extinctions and sea-level changes. *Earth-Science Reviews, 48*(4), 217-250.

Hampton, M., et al. (2010). *A holostratigraphic approach to the chalk of the North Sea Eldfisk Field, Norway.* Paper presented at the Geological Society, London, Petroleum Geology Conference series.

Hansen, J., et al. (2004). 3D seismic analysis reveals the origin of ambiguous erosional features at a major sequence boundary in the eastern North Sea: near top Oligocene. *Geological Society, London, Memoirs, 29*(1), 83-90.

Isaksen, D., et al. (1989). *A revised Cretaceous and Tertiary lithostratigraphic nomenclature for the Norwegian North Sea*: Norwegian Petroleum Directorate.

Jones, G. A., et al. (2014). Characterization of fractures and faults: A multi-component passive microseismic study from the Ekofisk reservoir. *Geophysical Prospecting, 62*(4), 779-796.

Kominz, M., et al. (2008). Late Cretaceous to Miocene sea-level estimates from the New Jersey and Delaware coastal plain coreholes: An error analysis. *Basin Research, 20*(2), 211-226.

Masoumi, S., et al. (2014). Buried pockmarks on the Top Chalk surface of the Danish North Sea and their potential significance for interpreting palaeocirculation patterns. *International Journal of Earth Sciences, 103*(2), 563-578.

Neal, J., et al. (2009). Sequence stratigraphy hierarchy and the accommodation succession method. *Geology, 37*(9), 779-782.

Nielsen, T., et al. (2008). Seismic expression of contourite depositional systems. *Developments in Sedimentology, 60*, 301-321.

Rossland, A., et al. (2013). Permian–Holocene tectonostratigraphic evolution of the Mandal High, Central Graben, North Sea. *97*(6), 923–957. doi: 10.1306/12031212093

Surlyk, F., et al. (2003). Upper Cretaceous. In D. Evans, et al. (Eds.), *The Millennium Atlas: Petroleum Geology of the Central and Northern North Sea* (pp. 222-242): The Geological Society of London.

Back, S., et al. (2011). 3D seismic geomorphology and sedimentology of the Chalk Group, Southern Danish North Sea. *Journal of the Geological Society, 168*(2), 393-406.

Bailey, H., et al. (1999). Joint Chalk Research Phase V: A Joint Chalk Stratigraphic Framework. *Norwegian Petroleum Directorate (NPD), Stavanger*.

Bramwell, N., et al. (1999). *Chalk exploration, the search for a subtle trap.* Paper presented at the Geological Society, London, Petroleum Geology Conference series.

Deegan, C. t., et al. (1977). *A standard lithostratigraphic nomenclature for the Central and Northern North Sea* (Vol. 1): HMSO.

Esmerode, E. V., et al. (2008). Interaction between bottom currents and slope failure in the Late Cretaceous of the southern Danish Central Graben, North Sea. *Journal of the Geological Society, 165*(1), 55-72.

Faugères, J.-C., et al. (1993). Bottom-current-controlled sedimentation: a synthesis of the contourite problem. *Sedimentary Geology, 82*(1), 287-297.

Faugères, J.-C., et al. (1999). Seismic features diagnostic of contourite drifts. *Marine Geology, 162*(1), 1-38.

Faugères, J., et al. (1998). Seismic patterns of a muddy contourite fan (Vema Channel, South Brazilian Basin) and a sandy distal turbidite deep-sea fan (Cap Ferret system, Bay of Biscay): a comparison. *Sedimentary Geology, 115*(1), 81-110.

Fontaine, J. M., et al. (1987). SEISMIC INTERPRETATION OF CARBONATE DEPOSITIONAL ENVIRONMENTS. *American Association of Petroleum Geologists Bulletin, 71*(3), 281-297.

Gennaro, M., et al. (2013). Seismic stratigraphy of the Chalk Group in the Norwegian Central Graben, North Sea. 1-31.

Gennaro, M., et al. (2013). Seismic stratigraphy of the Chalk Group in the Norwegian Central Graben, North Sea. *Marine and Petroleum Geology, 45*, 236-266. doi: 10.1016/j.marpetgeo.2013.04.010

Gennaro, M., et al. (2013). Characterization of dense zones within the danian chalks of the Ekofisk Field, Norwegian North Sea. *Petroleum Geoscience, 19*(1), 39-64.

Hampton, M., et al. (2010). *A holostratigraphic approach to the chalk of the North Sea Eldfisk Field, Norway.* Paper presented at the Geological Society, London, Petroleum Geology Conference series.

Hansen, J., et al. (2004). 3D seismic analysis reveals the origin of ambiguous erosional features at a major sequence boundary in the eastern North Sea: near top Oligocene. *Geological Society, London, Memoirs, 29*(1), 83-90.

Isaksen, D., et al. (1989). *A revised Cretaceous and Tertiary lithostratigraphic nomenclature for the Norwegian North Sea*: Norwegian Petroleum Directorate.

Jones, G. A., et al. (2014). Characterization of fractures and faults: A multi-component passive microseismic study from the Ekofisk reservoir. *Geophysical Prospecting, 62*(4), 779-796.

Kominz, M., et al. (2008). Late Cretaceous to Miocene sea-level estimates from the New Jersey and Delaware coastal plain coreholes: An error analysis. *Basin Research, 20*(2), 211-226.

Masoumi, S., et al. (2014). Buried pockmarks on the Top Chalk surface of the Danish North Sea and their potential significance for interpreting palaeocirculation patterns. *International Journal of Earth Sciences, 103*(2), 563-578.

Nielsen, T., et al. (2008). Seismic expression of contourite depositional systems. *Developments in Sedimentology, 60*, 301-321.

Rossland, A., et al. (2013). Permian–Holocene tectonostratigraphic evolution of the Mandal High, Central Graben, North Sea. *97*(6), 923–957. doi: 10.1306/12031212093

Surlyk, F., et al. (2003). Upper Cretaceous. In D. Evans, et al. (Eds.), *The Millennium Atlas: Petroleum Geology of the Central and Northern North Sea* (pp. 222-242): The Geological Society of London.

van der Molen, A. S., et al. (2005). The influence of tectonic regime on chalk deposition: Examples of the sedimentary development and 3D-seismic stratigraphy of the Chalk Group in theNetherlands offshore area. *Basin Research, 17*(1), 63-81.

van der Molen, A. S., et al. (2007). Towards an improved lithostratigraphic subdivision of the chalk group in the Netherlands North Sea area - A seismic stratigraphic approach. *Geologie en Mijnbouw/Netherlands Journal of Geosciences, 86*(2), 131-143.

van der Molen, A. S., et al. (2005). The influence of tectonic regime on chalk deposition: Examples of the sedimentary development and 3D-seismic stratigraphy of the Chalk Group in theNetherlands offshore area. *Basin Research, 17*(1), 63-81.

van der Molen, A. S., et al. (2007). Towards an improved lithostratigraphic subdivision of the chalk group in the Netherlands North Sea area - A seismic stratigraphic approach. *Geologie en Mijnbouw/Netherlands Journal of Geosciences, 86*(2), 131-143.

Ziegler, P. A. (1990). Tectonic and palaeogeographic development of the North Sea rift system. *Tectonic evolution of the North Sea rifts*, 1-36.